2020-09-11

Fine-tuning blood vessel development

Watterston, Charlene

UNIVERSITY OF CALGARY

Fine-tuning blood vessel development

by

Charlene Watterston

A THESIS
SUBMITTED TO THE FACULTY OF GRADUATE STUDIES
IN PARTIAL FULFILMENT OF THE REQUIREMENTS FOR THE
DEGREE OF DOCTOR OF PHILOSOPHY

GRADUATE PROGRAM IN BIOCHEMISTRY AND MOLECULAR BIOLOGY

CALGARY, ALBERTA

SEPTEMBER, 2020

Abstract

Blood vessel development is typically characterized by stages marking the growth and gradual refinement of vascular networks. Understanding how these stages integrate is essential to our understanding of how the early signals which control vessel growth can influence later stages of vessel stabilization. In this thesis, I use a zebrafish model (*Danio rerio*) to explore the roles of two negative regulators that modulate key signaling pathways controlling vessel growth. At the early stages, the initial growth of vessels is carefully controlled by distinct gene expression patterns. As a vessel forms, in response to the attractive Vascular endothelial growth factor (Vegf) pathway, its sprouting is often opposed by repulsive Semaphorins (Semas) which limit directional growth. I investigated the role of semaphorin3fb (sema3fb) which I found to be expressed within developing endothelial cells of the zebrafish embryo. I found that sema3fb likely acts through auto-secretory feedback to modulate Vegf responses to promote appropriate vessel growth. At later stages, a supportive layer of vascular smooth muscle cells (vSMCs) is recruited to form the contractile layer of the vessel wall. Bone morphogenic protein (Bmp) signaling is implicated in cellular crosstalk from the underlying endothelium to vSMCs which is critical to the structural integrity of a blood vessel. I investigated the microRNA26a (miR26a), which I found enriched in the endothelial lining of the blood vessel. I identified a non-autonomous role for miR26a in regulating Bmp signaling through its effector Smad1 to control vSMC maturation. Together my work offers mechanistic insight into the cellular communication pathways that regulate blood vessel formation and focuses on how both internal and external signaling pathways communicate to promote vessel formation.

Preface

Chapter Two of this thesis is based on the manuscript: ‘Endothelial Semaphorin 3fb regulates Vegf pathway-mediated angiogenic sprouting’. All writing, experiments, quantifications, images, and figures are my own. This work was in collaboration with the laboratory of Dr. Sarah McFarlane (University of Calgary).

The appendix of this thesis is based on a manuscript: ‘Semaphorin 3f controls ocular vascularization from the embryo through to the adult’. Halabi, R., Watterson, C., Mori-Kreiner, R., Childs, S.J., McFarlane, S. My contributions to this publication are as follows: I conceptualized and performed all whole-embryo confocal images, and retinal flat mounts for Figures 2, 3, 4, and 6.

Chapter Three of this thesis was published on May 15, 2019, in PLOS Genetics as Charlene Watterston, Lei Zeng, Abidemi Onabadejo, Sarah J Childs. "MicroRNA26 attenuates vascular smooth muscle maturation via endothelial BMP signaling." PLoS genetics 15.5 (2019): e1008163. All writing, experiments, quantifications, images, and figures are my own with the following exceptions: Lei Zeng provided some *in situ* hybridization, histology images and performed knockdown or overexpression experiments for Figure 3.1, Figure 3.4, Figure 3.8, and Figure 3.10. Abidemi Onabadejo conceptualized the experimental design for Figure 3.7

Acknowledgments

I would firstly like to express my deepest appreciation to my supervisor Sarah Childs for her continued support and guidance over the last 6 years. I'm extremely grateful to you and I admire your passion for science. You taught me to have a flexible and optimistic approach to research and encouraged me to explore multiple interests both in and out of the lab. I feel very lucky to have had the opportunity to develop my skills in a workspace that allows free and creative thinking.

I'm very grateful to Sarah McFarlane, you opened a space for me to explore and collaborate on work that allowed me to widen my research. Your feedback, support, and encouragement have been invaluable, especially in these final stages. I would also like to extend my deepest gratitude to my committee members Peng Huang and William Brook for your time, understanding, and advice over the years which has been invaluable to my growth as a researcher. Thank you to Shirin Bonni and Deborah Yelon for your readiness to be part of my examination committee.

I thank all members of the Childs Lab, past and present, for your support, guidance, and contributions. To Jae-Ryeon Ryu, you are an excellent teacher and I thank you for all your service to maintain our happy lab. Thank you to Michela Goi, Corey Arnold, and Tom Whitesell for welcoming me into the lab so warmly and for our continued friendships. Thank you to Jasper Greysson-Wong and Nabila Bahrami for being wonderful lab mates and travel companions, we have shared so many adventures. Thank you to Suchit Ahuja and Danielle Blackwell for your advice and help in the last stretch of my time in the lab.

I would also like to thank members of the McFarlane lab – Carrie Hehr, Gabriel Bertolesi, and Paula Cechmanek for all your feedback and valuable advice. I also extend my thanks to members of the Brook Lab, Lindsay Phillips, and Pia Svendsen, for being a great support, and celebrating my accomplishments however big or small. Thank you to Leslie McGill and Theresa Connolly, for all you do and always checking in to have a chat. Thank you to Lian Willets, Dierdre Lobb, and Vincent Chiang for being a wonderful

teaching team to work with. Thank you to Jonathan Viola and Morgan Guo for your mentorship and the opportunity to explore and prepare for my next steps post Ph.D.

Special thanks to all my dear friends who have made Calgary my second home. To Ramy Halabi, your unwavering support has guided me through every milestone of grad school, and I am very lucky to count you as a friend. To Rami Abu Zeinab you are a wonderful friend, thank you for all your support and encouragement. Thank you to Katie Greene, Sophie Briggs, Rhiannon Campden, Nikita Burke, and Teja Klančič for always being there for me. We all arrived here around the same time and formed steady friendships that got us all through all the ups and downs together.

To my family thank you for making home such a hard place to leave but such a wonderful place to return to. To Maria and Michael, I cannot begin to express my thanks to and there aren't enough words to describe how your love and support have given me the strength to keep pushing forward.

Lastly, I would like to thank the Department of Biochemistry and Molecular Biology, ACHRI, Eyes High, and NSERC for the support and opportunities to develop as a researcher. Thank you to all those mentioned here and all others I have not directly mentioned without all of you I would not have had such a wonderful experience of graduate school.

Dedication

To my Mother, without your love and support, none of this would be possible

Nothing in life is to be feared, it is only to be understood. Now is the time to understand more, so that we may fear less - Marie Curie

Table of Contents

List of Figures and Illustrations

List of Symbols, Nomenclature or Abbreviations

Symbol	Definition
° C	degrees Celsius
%	percent
μM	micromolar
aa	amino acid
acta2	alpha smooth muscle actin
Alk	activin-like kinase
Ang	angiogenin
BCIP	5-bromo-4-chloro-3-indolyl-phosphate
BBB	blood brain barrier
BMP	bone morphogenetic protein
bp	base pair
CArG	CC(A/T)6GG rich motif
Cas9	CRISPR associated protein 9
CNC	cardiac neural crest
CNV	choroidal neovascularization
CVP	caudal vein plexus
CRISPR	clustered regularly interspaced short palindromic repeats
CRISPRi	CRISPR interference
Cxcl12	C-X-C motif chemokine 12
Cxcr4	C-X-C chemokine receptor 4
DA	Dorsal Aorta
dpf	days post fertilization
ECM	extracellular matrix
EGFP	enhanced green fluorescent protein
FACS	fluorescence-activated cell sorting
Flk	fms-like tyrosine kinase-1
GAP	GTPase activating proteins
h	hour
hpf	hours post-fertilization
HUVEC	human umbilical vein endothelial cells
ISH	In Situ Hybridization
ISA	Intersegmental Artery
ISV	Intersegmental Vein
kdrl	kinase insert domain receptor-like
L	Liter
mCherry	monomeric red fluorescent protein
mg	Milligram
ml	Milliliter
MLCP	myosin light chain phosphatase
MO	morpholino
mRNA	messenger RNA

Myh	Myosin heavy chain
n	number
NBT	nitro blue tetrazolium
NCC	neural crest cell
nls	nuclear localization sequence
ng	nanogram
Nrp	neuropilin
obd	out of bounds
PCR	polymerase chain reaction
PCV	Posterior Cardinal Vein
PDGF	platelet derived growth factor
PDGF-BB	platelet derived growth factor ligand BB
PDGFRβ	platelet derived growth factor receptor β
Plxn	plexin
RNA	ribonucleic acid
RPE	retinal pigment epithelium
PTU	1-phenyl-2-thiourea
qRT-qPCR	quantitative real-time quantitative PCR
Sema	Semaphorin
sFlt1	soluble fms-like tyrosine kinase-1 (sVegfr1)
Shh	sonic hedgehog
sgRNA	single guide RNA
ss	somite stage
TGFβ	transforming growth factor β
Tg	transgenic
TL	Tupfel Long Fin
RTK	receptor tyrosine kinase
Vegf	vascular endothelial growth factor
Vegfr	vascular endothelial growth factor receptor
VE-cadherin	Vascular endothelial VE-cadherin
Wnt	Wingless-related integration site
WT	Wild type
ZO-1	zona-occludens 1

Guideline for gene names across species using the example of smooth muscle actin

Organism	Gene and RNA Symbol	Protein Symbol
Human	*ACTA2*	ACTA2
Mouse	*Acta2*	ACTA2
Zebrafish	*acta2*	Acta2

Note: Zebrafish nomenclature is used when the same findings are shared in multiple organisms including zebrafish. It is also used when talking in general terms about signaling pathways unless noted.

Chapter One: Introduction

Signals are an essential form of communication. In developmental biology, cellular signals communicate information to control and coordinate cell actions. The ability of a cell to both receive and respond to signals is key to regulating responses and to shaping its microenvironment. During blood vessel development, signaling networks function to regulate various physiological functions such as regulation of the proliferation, migration, and differentiation of the cells that form vessels. The inner lining of a blood vessel termed the endothelium, is made up of endothelial cells and the surrounding vessel wall is comprised of a supportive layer of vascular smooth muscle. As an interface between circulating blood and the vessel wall, the endothelial cell is an important signaling hub and responsible for perceiving signals from both mechanical stimuli such as blood flow, and biochemical stimuli such as hormones and gases. These stimuli can be interpreted and used to signal within the cell, between cells, or passed to the vessel environment. In this thesis, I have worked to identify genes that influence blood vessel development and to further understand the dynamic processes that regulate pattern formation and vessel integrity. In Chapter 2 I investigate how the coordination of opposing signaling pathways promotes vessel growth. In Chapter 3, I demonstrate that fine-tuning endothelial signals influences the differentiation of smooth muscle cells.

1.1. Forming a vessel network

The blood vessel networks that make up the vertebrate circulatory system have a vital function to supply and perfuse tissues throughout life. As the major delivery system, vessels carry a variety of molecules including hormones, cytokines, and immune cells. The integration of vessels into tissues and organs is essential to respond to internal and external stimuli such as temperature, pH, and pressure which can be translated into signals. Vascular development begins with vasculogenesis (de novo blood vessel formation) and is initiated when angioblasts (endothelial cell precursors) are specified and migrate to form the major axial vessel structures. These primary vessels act as scaffolding from which new vessels sprout through a process termed angiogenesis. Angiogenesis depends on the proliferation, migration, and assembly of endothelial cells (ECs) into vessels which are gradually refined to form hierarchically patterned vessel beds (reviewed in Betz *et al*., 2016).

Current models of angiogenic growth establish sprout formation to be dependent on two distinct 'states' of the angioblast which control the balance between migration and proliferation. The *tip cell* of a forming sprout guides the migration in a specific direction using filopodia to scan the environment for attractive and repulsive cues. The cells behind the tip cell in the sprout are called *stalk cells*, which form the vascular lumen (Geudens and Gerhardt, 2011)

1.1.1. Molecular regulation of angiogenic sprouting

Differentiation of the angioblasts into tip and stalk cells during sprout formation is controlled by a complex feedback loop between Vegf and Notch signaling to maintain cellular states (Figure 1.1). During embryonic development, angioblasts are specified and express Vascular Endothelial Growth Factor Receptor (Vegfr-2, also known as Fetal Liver Kinase 1: Flk1 or Kinase insert Domain Receptor: KDR) which bind the signaling molecule vascular endothelial factor A (VegfA). VegfA functions as a master regulator of ECs dynamics, particularly as a chemoattractant to stimulate angiogenesis (Ferrara, 2002; Adams and Alitalo, 2007). VegfA signaling via Vegfr2 is vital to initiate tip cell formation, where reduced Vegfr2 expression results in decreased vascular density attributed to the disruption of tip cell responses (Gerhardt *et al.*, 2003a; Tammela *et al.*, 2008). In mammals, the function of all three VEGF receptors controls the formation and migration of tip cells. Sprouting behavior has been well characterized in murine retinal angiogenesis, where tip cells require the appropriate expression and location of Vegfr1, Vegfr2, and Vegfr3 to function. For example, reduced Vegfr1 can increase the number of tip cells (Bentley *et al*. 2008) whereas blocking Vegfr3 reduces the number of branch points and endothelial cell proliferation (De Smet *et al*., 2009).

Notch-mediated signaling, on the other hand, is responsible for maintaining stalk cells and repressing tip cell identity (Tammela *et al*., 2008; Zarkada *et al*., 2015). In endothelial cells, Notch ligands include Delta-Like-1 (Dll-1), Dll-3, Dll-4, and Jagged1, 2 which play important but different roles in angiogenesis. Dll4 is expressed in tip cells and signals to Notch2 expressing stalk cells. Under Vegf stimulation, Dll4 expression is indirectly upregulated in the tip cells. In turn, Dll4 ligand activates Notch signaling in the stalk. This cell-cell signaling inhibits Vegfr2 expression suppressing the tip cell phenotype. Notch can also induce Vegfr1 expression and the expression of its soluble protein splice variant isoform sVegfr-1(sFlt1) that sequesters VegfA in the local environment of the sprout (Xu *et al*. 2014; Kangsamaksin *et al*. 2015)

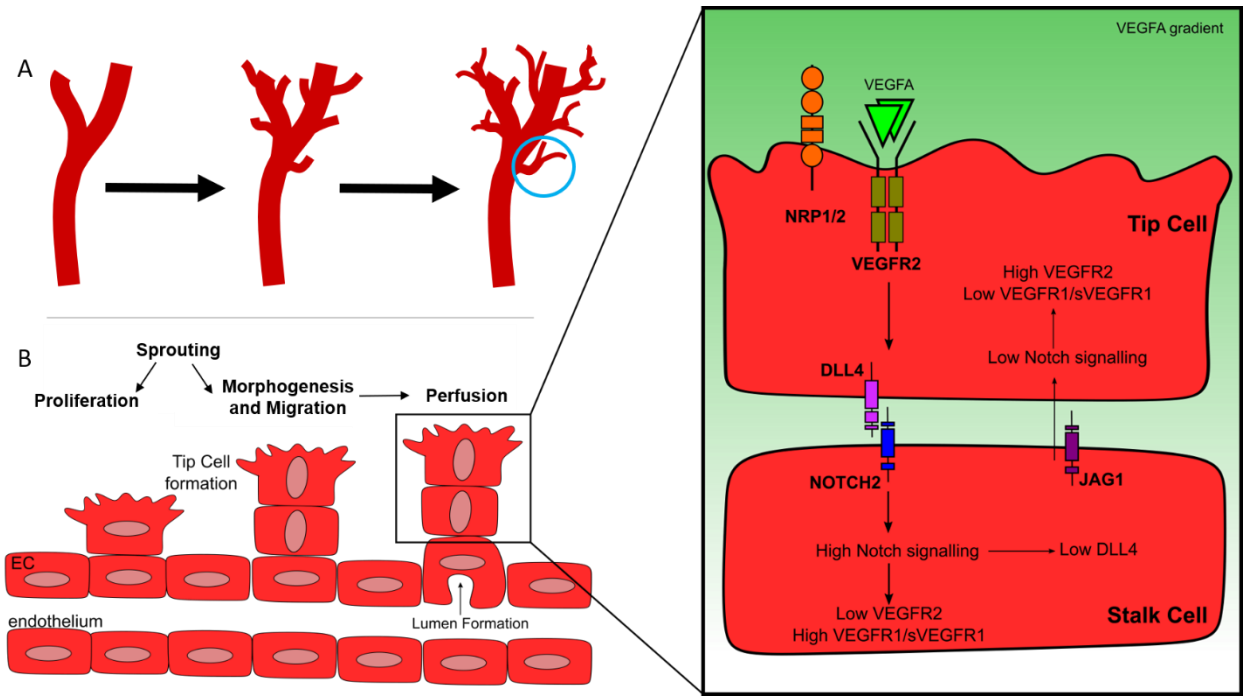

Figure 1.1: Vessel Formation and Angiogenic Sprouting Model

A) Growth of the primary vascular tree occurs by angiogenesis. B) The drawing shows how the angiogenic sprout is led by the tip cell that uses filopodia to scan the environment. The stalk cells proliferate and form a lumen. Here, primary vessels respond to a local environmental stimulus by forming tip cells that can migrate out of the vessel and lead a cellular sprout to form a new vessel. Inset: During sprouting angiogenesis, VEGF interacts with VEGFR2, expressed at the surface of the endothelial cells. NRP1 modulates the VEGF signaling output, enhancing the binding activity and signaling of VEGF through VEGFR2. Under VEGF stimulation, Dll4 expression is up-regulated in tip cells. In turn, Dll4 ligand activates Notch signaling in the stalk, consequently suppressing the tip cell phenotype. Notch signaling activation reduces VEGFR2 expression and increases VEGFR1/sVEGFR1 levels as well as the expression of different Notch target genes (e.g., JAG1) in stalk cells. In contrast, the tip cell receives low Notch signaling, allowing high expression of VEGFR2 and low VEGFR1/sVEGFR1.

1.1.2. Development of vasculature in Zebrafish

As a model of early vascular development, zebrafish (*Danio rerio*) have greatly advanced our understanding and appreciation for the signaling pathways that regulate vessel growth. Zebrafish have proven to be particularly suitable for the study of vascular development *in vivo* as their rapid and external development allows for passive oxygen diffusion even with disrupted vessels or heart formation (Stainier *et al.*, 1996). Both in developmental and functional studies, transgenic zebrafish expressing fluorescent proteins have been essential for the *in vivo* study of specific cell populations during embryo development. In addition to their ease of screening, the use of transgenic zebrafish in forward genetic approaches has been successful in discovering many regulators of vessel formation. (Liu *et al*. 2007; Baldessari and Mione 2008; Avagyan and Zon 2016; Covassin *et al*. 2009). In zebrafish, vasculogenesis begins at around ~10 hours post-fertilization (hpf) (Dooley and Zon, 2000; Davidson and Zon, 2004). Subsequent angiogenic processes result in the formation of a primitive circulatory loop consisting of blood flow from the heart to the major axial vessels - the dorsal aorta (DA) and posterior cardinal vein (PCV) - of the head and trunk by 30 hpf (Fouquet *et al*., 1997; Gore *et al*., 2012; Isogai *et al*., 2001; Isogai *et al*, 2003) (Figure 1.2).

The trunk of zebrafish embryos contains one of the best-studied angiogenic vessel beds, the stereotypically patterned intersegmental vessels which are well conserved across species. At 20hpf, intersegmental arteries (ISAs) sprout from the DA, and then grow toward the dorsal side of the embryo, laterally to the notochord and neural tube. By 30 hpf each sprout consists of three to four endothelial cells. Once the tip cell reaches the dorsal side, it branches along the longitudinal axis, forming a T-branched cell, and individual sprouts connect the paired dorsal longitudinal anastomotic vessels (DLAVs). Once they connect dorsally, the vessel is luminized which allows vessel perfusion and blood flow. The dorsally sprouting ISVs and DLAVs are considered intersegmental arteries (ISAs), as they emanate from the DA, and express arterial-specific markers by 35 hpf (Bussmann, Wolfe, and Siekmann 2011; Xu *et al*. 2014). Sprouts from the PCV connect with the base of some arterial ISAs, and roughly half of the new sprouts form intersegmental veins (ISVs) by around 2.5 dpf (Isogai *et al.*, 2003) (Figure 1.2). At the tail, the Caudal Venous Plexus (CVP) also initiates sprouting ventrally (i.e. away from the ISAs) from the PCV to form a transient venous network.

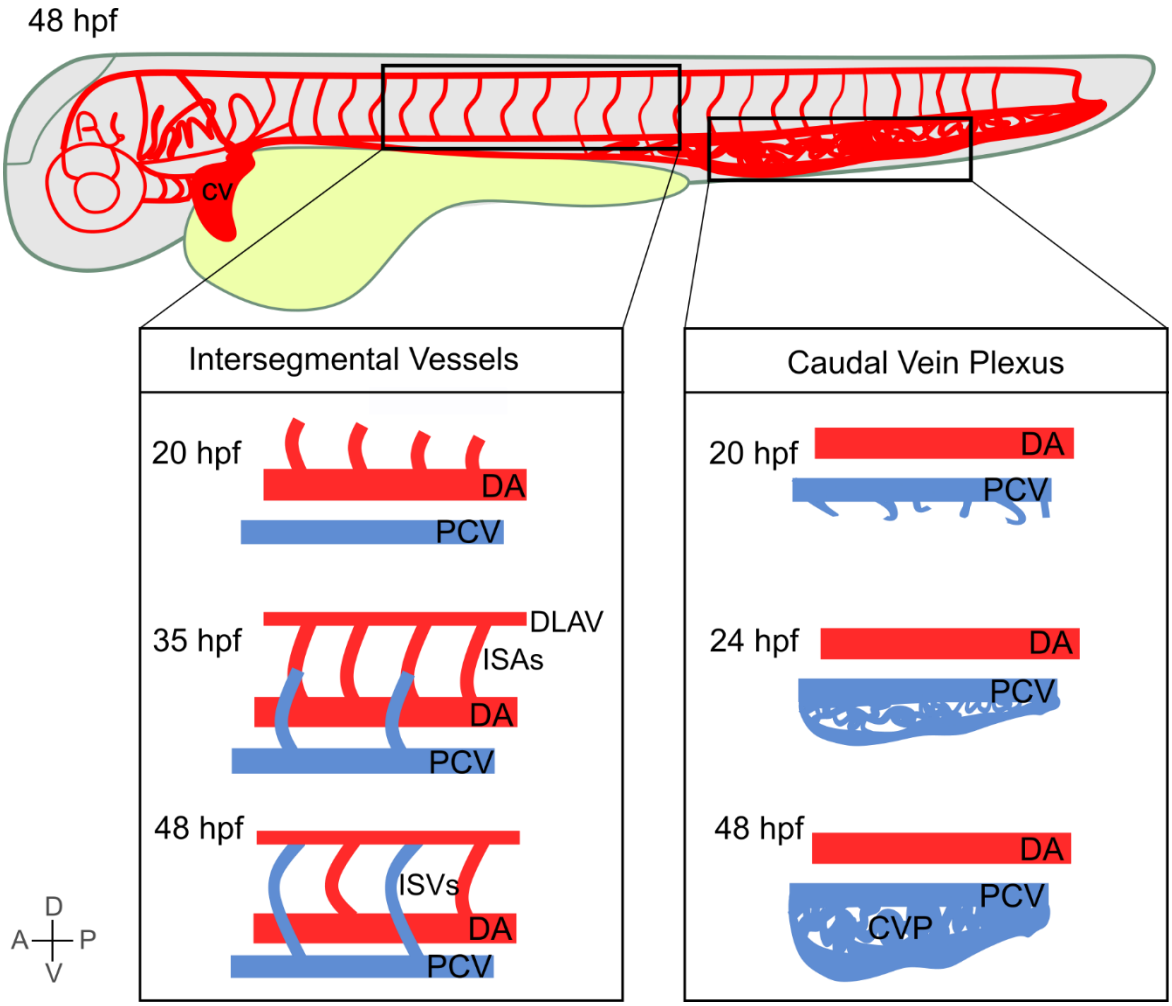

Figure 1.2 Formation of Zebrafish Trunk Vessels

Illustration of vessels in 48 hours post-fertilization (hpf) embryo. A) The intersegmental vessel arteries (ISAs) first sprout from the dorsal aorta and reach the dorsal part of the embryo to connect at the DLAV. Secondary sprouts from the PCV connect with the arterial vessels turning them into intersegmental veins (ISAs). (D) The caudal venous plexus (CVP starts with ventral sprouts from the PCV. The honeycomb-like structure defines and remodels quickly. Hpf: hours post fertilization; DA: dorsal aorta; PCV: posterior cardinal vein; DLAV: dorsal longitudinal vessel. Orientation (A: anterior; P:posterior; D:Dorsal; V:Ventral)

1.1.3. Signaling pathways that promote arterial vs. venous vessel beds in Zebrafish

As an angiogenetic sprouting model, ISAs have contributed an understanding of how vessels are guided in their growth. In Zebrafish, *Vegfa* is released by muscle cells in response to Sonic hedgehog (Shh) secreted from the notochord. This environmental gradient attracts Vegfr2 (Flk1/Kdrl) receptor-expressing angioblasts of the DA to form upward branching sprouts (Bahary *et al*., 2007; Bussmann *et al*., 2010; Yamaguchi *et al*., 1993). In vertebrate and cell culture models, Notch signaling modulates the response of the tip cell to local Vegf thus controlling the direction of migration and limits proliferation (Figure 1.1). However, in contrast to murine and human models, the zebrafish tip cell is proliferative, and as the leading cell migrates, the trailing stalks cells become quiescent and form the vascular lumen and give rise to the phalanx (Gerhardt *et al.*, 2003a; Siekmann and Lawson, 2007; Geudens and Gerhardt, 2011). Unlike ISAs, CVP sprouts grow ventrally from the PCV and migrate in response to Bone morphogenetic protein (Bmp) signaling (Wiley *et al.*, 2011). Similar to murine models of venous vessel growth, as sprouts of the CVP connect to form a venous plexus they are stabilized by Sphingosine-1-phosphate (Sip1) signaling which limits excessive filipodia extensions to allow unique honeycomb-like vessel arrangements (Hisano *et al*., 2015; Wakayama *et al*., 2015; Wei *et al*., 2014).

1.2. Establishing a Vascular Pattern

Establishing an effective vascular plexus or maintaining a pre-existing one involves a coordinated progression of positive and negative signaling events to meet the functional needs of the tissue. Vessel growth can be restricted by spatial cues that limit vascular responses to angiogenic stimuli. Classical axon guidance molecules, such as Ephrin's, Slit's, Netrins, and Semaphorins have emerged as key regulators of angiogenesis (reviewed in Hogan and Schulte-Merker 2017). The function of these molecules is dependent on Vegf-mediated specification of tip and stalk cells to guide and carefully balance vessel growth.

1.2.1. Membrane- localized signaling that regulate vessel pattern formation

Interactions between membrane-bound receptors and their membrane-bound ligands regulate various aspects of angiogenic growth through direct inter-endothelial cell communication. As a lateral inhibition pathway, the interaction between Notch transmembrane receptors (Notch-1-4) and their transmembrane ligands Delta-like (Dll-1, Dll-3, Dll-4) or Jagged (Jag1 and Jag-2) leads

to Notch receptor cleavage, giving rise to the Notch intracellular domain (NICD) that translocates into the nucleus to form an activated transcriptional complex that regulates the expression of target genes, such as hairy and enhancer of split (HES)-1, HES -5, HES -7 and HES-related repressor protein (HERP)-1 to -3. These pathway effectors typically suppress cell proliferation, differentiation, and promote cell survival (reviewed in Iso *et al*., 2003). Human diseases, such as Alagille syndrome (AGS) and cerebral autosomal-dominant arteriopathy with subcortical infarcts and leukoencephalopathy (CADASIL), which show abnormalities in the cardiovascular system, are caused by loss-of-function mutations of Jag-1 and Notch-3, respectively (Joutel *et al*. 1996; Li *et al*. 1997). Similarly in murine models, homozygous null mutations in either the receptor or ligand result in embryonic lethality, with the vascular defects attributed to vascular remodeling and angiogenesis most likely due to disruption in endothelial cell specification (Huppert *et al.*, 2000; Krebs *et al.*, 2000; Gessler *et al.*, 2002).

Ephrins and Eph's are membrane-localized ligand and receptor pairs expressed by ECs and regulate the endothelial response to Vegf in tip and stalk cells. Ephrin ligands (EphrinA1-A5 and EphrinB1-B3) are membrane-bound proteins that typically act to repel vessel growth through bidirectional signaling to endothelial expressed tyrosine kinases Eph receptors (EphA1-8 and B1-B4, B6) (Kullander and Klein, 2002; Kuijper, Turner and Adams, 2007; Pitulescu and Adams, 2010). In murine retinal vessel sprouting, EC EphrinB2 controls tip cell behavior by positively regulating Vegfr2 trafficking to the EC membrane in response to engaging its receptor EphB4, thus influencing vessel guidance. EphrinB2-EphB4 signaling is also important in refining capillary beds into finer arterial and venous networks (Sawamiphak *et al*., 2010; Wang *et al*., 2010). In zebrafish mutation of the Notch effector, Herp1 homolog gridlock (*grl)* results in disordered assembly of the aorta (Fishman *et al*, 2000). The latter effects vessel refinement intersect Ephrin signaling, where the loss of the Notch effector reduces expression of *ephrinb2* in arteries and leads to expansion of *ephB4* expressing venous regions (Zhong *et al*, 2001).

1.2.2. Environmental interactions that regulate vessel pattern formation

Netrins signal through two receptor families, Deleted in Colorectal Cancer (DCC) and Uncoordinated 5 (Unc5). There are three Netrins in mammals (Netrin1/2/4) that are typically expressed in neural tissues, such as the neural tube. In vitro cell culture models have identified

Netrin-1 as a potent regulator of angiogenesis (Kye *et al.*, 2004; Wilson *et al.*, 2006). Disruption of the Unc5b gene in mice, or *netrin-1a* in zebrafish, leads to the aberrant extension of endothelial tip cell filopodia, and abnormal navigation results in excessive vessel branching. The Unc5 receptor is enriched in the endothelial tip cell, and the cells form aberrant filopodia in Unc5b knockout mice (Lu *et al.*, 2004). Netrin1-Unc5 signaling in zebrafish is likely repulsive in that *netrin1* overexpression inhibits vessel invasion (reviewed in Adams and Eichmann 2010).

Slits (Slit1-3) are large secreted glycoproteins that signal through the Roundabout (Robo1-4) family of transmembrane protein receptors (Brose and Tessier-Lavigne, 2000). The interaction of the SLIT2/ROBO1/ROBO4 signaling axis activates an antiangiogenic pathway that counteracts VEGF downstream signaling (Acevedo, Weis, & Cheresh, 2008; Gimenez *et al*., 2015). However, although Robo4 has specific vascular EC expression its function is somewhat controversial. In murine retinal sprouting models, Robo4 is expressed predominantly in the stalk and not tip cells, suggesting that the receptor is not required for vascular guidance (Chen *et al*., 2019; Herbert & Stainier, 2011; Suchting *et al*., 2005). However, it has been suggested that Robo4 may utilize the ligand Unc5b, which is highly expressed on tip cells, to help stabilize adjacent phalanx cells and promote EC quiescence to limit vessel branching (Chen *et al*., 2019; Jones *et al*., 2009; Koch *et al*., 2011; Sheldon *et al*., 2009).

Semaphorins (Semas) comprise a family of more than 20 membrane-bound, transmembrane, and non-membrane bound proteins that have a key role in mediating directional guidance. My work focus on Class 3 secreted Semas, which are capable of establishing long-range diffusion gradients that typically limit vessel growth (reviewed in Zhang *et al*. 2018). Two receptor families mediate Sema signaling; the transmembrane proteins Plexin (Plxn) and the cell-surface glycoproteins Neuropilins (Nrp) (reviewed in Gay *et al*., 2011). Plexin (PlxnA-D) and Neuropilins (NRP1-2) are transmembrane receptors for Semaphorins (Tamagnone *et al.*, 1999; Yazdani and Terman, 2006). Sema3's typically regulate angiogenesis by binding to the endothelial expressed co-receptor Nrp, which then interacts with Plxns to elicit an intracellular signaling cascade that leads to the collapse of EC filipodia projections (Carmeliet, 2003b; Gu *et al.*, 2003; Banu *et al.*, 2006). An exception is Sema3e, which directly binds and activates PlxnD1 to guide vessel growth (reviewed in Oh and Gu 2013). Upon ligand binding, Plxns generally act as guanosine

triphosphatase-activating proteins (GAPs) and downstream interactions with both ERK and MAPK signaling modulates integrin-mediated cell adhesion and cytoskeletal dynamics. PlexinD1 plays a key role in both developmental and pathological angiogenic models inhibiting the growth of vessels into 'forbidden' zones (Gay *et al*., 2011). In tumor progression models, activation of endothelial PLEXIND1 limits vessel invasion (Gay *et al*., 2011; Sakurai *et al*., 2012). Sema3A/E signaling can also act as competitive antagonists to Nrp1 which acts as a Vegf non-kinase co-receptor to modulate Vegfr2 output (Fantin *et al*., 2015, 2013; Herzog *et al*., 2011). Specifically, in the tip cell, low Notch signaling allows high expression Nrp1 and Vegfr2 (reviewed in Blanco and Gerhardt 2013). Nrp1 acts as a positive regulator of tip cells by enhancing the binding of Vegfr2 to modulate the proliferative and migratory response to Dll4 (Hellström *et al*., 2007; Williams *et al*., 2006; Yokota *et al*., 2015). The antiangiogenic effects of PlexinD1 can be further modulated by intracellular endocytic adaptors of the GIPC family and small GTPases belonging to the Ras and Rho family that modulate cytoskeletal proteins. In murine models, GIPC1 promotes arterial branching by associating with the cytosolic tail of NRP1 enhances the trafficking of VEGFR2 to cell membranes to promotes the signaling (Pascoe *et al*, 2015). Following Vegf inhibition, reducing PlexinD1 activity in zebrafish carrying a mutation in GIPC1 binding domains restores vessel formation demonstrating an interaction between the two pathways (Carretero-Ortega *et al.*, 2019).

1.2.3. Controlling pattern formation in Zebrafish

The stereotypic patterning of early blood vessels is well conserved across vertebrate species and relies on similar angiogenic signaling mechanisms. However, there are organ-specific differences in patterning cues to produce different vessel beds. In the zebrafish trunk, *sema3a* is expressed in somite regions and *plexinD1* is expressed in angioblasts. Sema3a signaling via PlexinD1 increases the abundance sFlt1 which sequesters Vegfa to inhibit the Vegfr2 (Flk1/Kdrl) pathway and effectively limits angiogenic sprouting (Bussmann *et al.*, 2008; Zygmunt *et al.*, 2011) (Figure 1.3). In mice, Sema3e is a PlexinD1 ligand in trunk patterning, but in zebrafish, it does not appear to take on this same role (Gu *et al*., 2005; Lamont *et al*., 2009).

Out of bounds (obd), zebrafish genetic mutants have a mutation in the *plexinD1* gene and display extensive vessel patterning defects with precocious ISV sprout migration and aberrant connections among vessels (Childs *et al*., 2002; Torres-Vázquez *et al*., 2004) (Figure 1.3). The

absence of Sema3a-PlexinD1 signaling in *obd* results in increased ECs within sprouts and more tip cells compared to wild-type (Zygmunt *et al.*, 2011) (Figure 1.3). Similarly, mouse embryos lacking either PlexinD1 or Sema3e have similar vascular phenotypes, showing evolutionary conservation (Kim *et al*., 2011; Oh & Gu., 2013).

1.2.4. Sema3f as a regulator of vessel environments

The complex coordination of vascular network establishment during angiogenesis involves tissue-specific regulation of sprouting, migration, and proliferation. How a vessel achieves its refined architecture and what shields against aberrant vessel formation during embryogenesis are key questions in vascular development. Sema3f is one of the best-studied members of the Sema3 subclass, especially in the context of guiding axons in a variety of systems. In mouse, Sema3f is expressed in the caudal midbrain and rostral hindbrain, leaving a non-repellent corridor at the midbrain-hindbrain junction for Nrp2-expressing motor neurons to migrate (Giger *et al*., 2000). During cranial neural crest cell (CNCC) migration in zebrafish, *sema3fb* (and *sema3ga/sema3gb*) are expressed in the neural crest cell (NCC) free zones of hindbrain rhombomeres (r) 3 and r5 which restricts *nrp*-expressing NCC migration into distinct peripheral streams (Yu and Moens, 2005). Similarly, Sema3F deficiency in mice results in the crossing of NCC migratory streams (Gammill *et al*., 2007; Gammill *et al*., 2006).

In vascular systems, Sema3f has anti-angiogenic effects on tumor growth in vitro, and retinal vessels in vivo (Kusy *et al.*, 2005; Buehler *et al.*, 2013; Sun *et al.*, 2017; Nakayama *et al.*, 2018). The zebrafish genome contains duplicated orthologs of SEMA3F - sema3fa and sema3fb (Yu and Moens, 2005) and our labs recently demonstrated an anti-angiogenic role for Sema3fa in control retinal vascularization (Appendix). However, although these studies provide evidence of an anti-angiogenic role for exogenous Sema3F in preventing vessel invasion, the studies did not explore an endogenous function of Sema3F during angiogenesis. In zebrafish, sema3fb is expressed within cardiomyocytes during heart formation and promotes differentiation of the ventricle (unpublished Halabi, 2019). Upon closer examination of preliminary in situ hybridization (ISH) data, *sema3fb* expression was noted within developing ISAs. I, therefore, hypothesized that the specific EC expression of *sema3fb* may be suggestive of a role angiogenic sprouting. In Chapter 2, I investigate the endogenous role of Sema3f as an endothelial regulator of the Vegf-mediated responses to promote the establishment of appropriately patterned growth fronts.

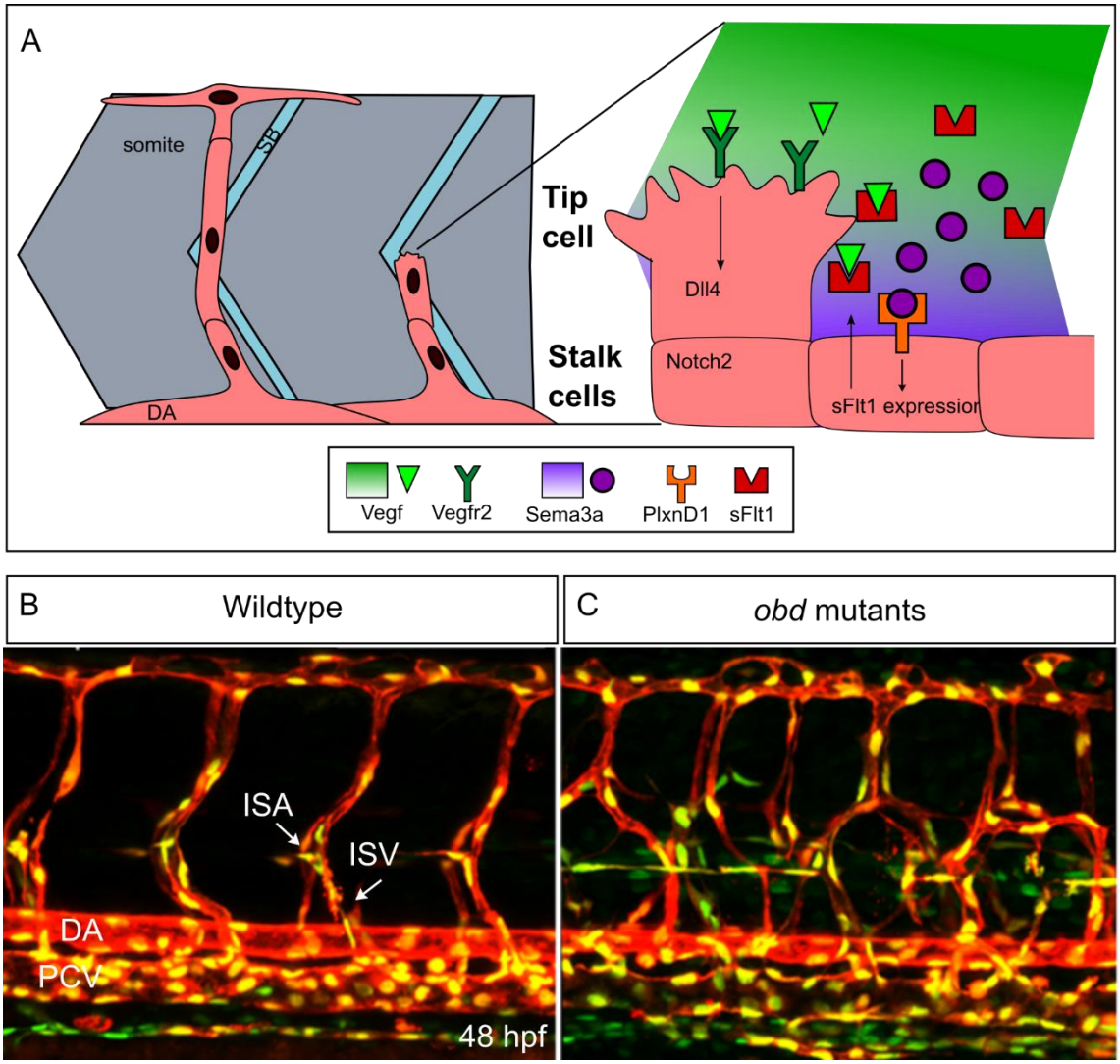

Figure 1.3: Sema3a-PlexinD1 signaling restricts angiogenic sprouts along the dorsal aorta

A) Illustrations of the interactions among Sema3a-PlexinD1, and Vegf-Vegfr2 or sFlt1 (soluble Vegfr1, inhibitory receptor). Sprout formation is directed by the Vegf gradient in the somite boundary (SB). Sema3a and Vegf are expressed in somites and forms a repulsive gradient to limit sprouting into the SB.PlexinD1 expressing angioblasts in the aorta bind their Sema3a ligands and induce sFlt1 production in cells adjacent to the developing sprout. sFlt1 inhibits Vegf availability to prevent new sprouts emerging in the local vicinity. (B-C) Confocal pictures of wild-type and an *obd* mutant at 48 hpf. Fish are double transgenic lines *Tg(fli:nEGFP)y7* (expressing GFP in nuclei of endothelial cells) and *Tg(kdrl:mcherry)ci5* (expressing mCherry in endothelial cells). In *obd* embryos, the absence of PlexinD1 and sFlt1 leads to ectopic sprouts

1.3. Supporting a Vascular Network

Following the establishment of the primary networks, vessels are stabilized through vascular myogenesis, the recruitment of vascular mural cells to endothelial tubes. The processes of mural cell recruitment and differentiation are highly dependent on signals to and from the underlying endothelium. Key pathways such as Notch, Platelet Derived Growth Factor (Pdgf), and Transforming growth factor-β (Tgf-β) play important roles in regulating communication between the components of the vessel wall. These processes are enhanced by physical contact and communication of endothelial cells with mural cells (reviewed in Gaengel *et al*. 2009).

1.3.1. Regulation of mural cell recruitment

During vessel development, the term vascular mural cell refers to both vascular smooth muscle cells (vSMCs) and pericytes. Both cells are in close contact with endothelial cells but have distinct vessel associations; pericytes cover microvessels such as capillaries, while large-diameter vessels like arteries and veins are covered by VSMCs (reviewed in Díaz-Flores *et al*. 2009; Gerhardt and Betsholtz 2003; Geudens and Gerhardt 2011) (Figure 1.4).

Vascular mural cells can be further identified by their morphology and the expression of genes that allow contractile functions. Upon recruitment to vessels, migrating vSMC appear rhomboid and are termed immature or synthetic vSMCs. These express Pdgfrβ and demonstrate increased rates of proliferation, and production of extracellular matrix proteins (Hungerford *et al*., 1996; Mack, 2011; Owens, 1995; Owens, Vernon, & Madsen, 1996; Owens, Kumar, & Wamhoff, 2004) (Figure 1.5). The early migration and attachment of mural cells to vessels and mural cell proliferation are controlled by Pdgfβ and Notch signaling (Figure 1.6). Endothelial cells secrete the ligand Pdgfb while mural cells express its receptor Pdgfrβ (Hellström *et al*., 1999; Hirschi *et al*., 1999; Lindahl *et al*., 1997). During vSMC recruitment, mural cells express the Pdgfrβ and Notch3 receptors and respond to the EC expressed ligands (reviewed in Anderson and Gibbons 2007). The receptor Notch3 is expressed by mural cells while its ligand Jagged1 or Dll4 is expressed by endothelial cells (Liu, Kennard, & Lilly, 2009; Liu *et al*., 2010). In zebrafish and murine mural cell recruitment, Notch3 further integrates the two pathways by enhancing expression of Pdgfrβ and inducing expression of vSMC genes to increase vSMC coverage of trunk vessels (Domenga *et al.*, 2004; High *et al.*, 2007).

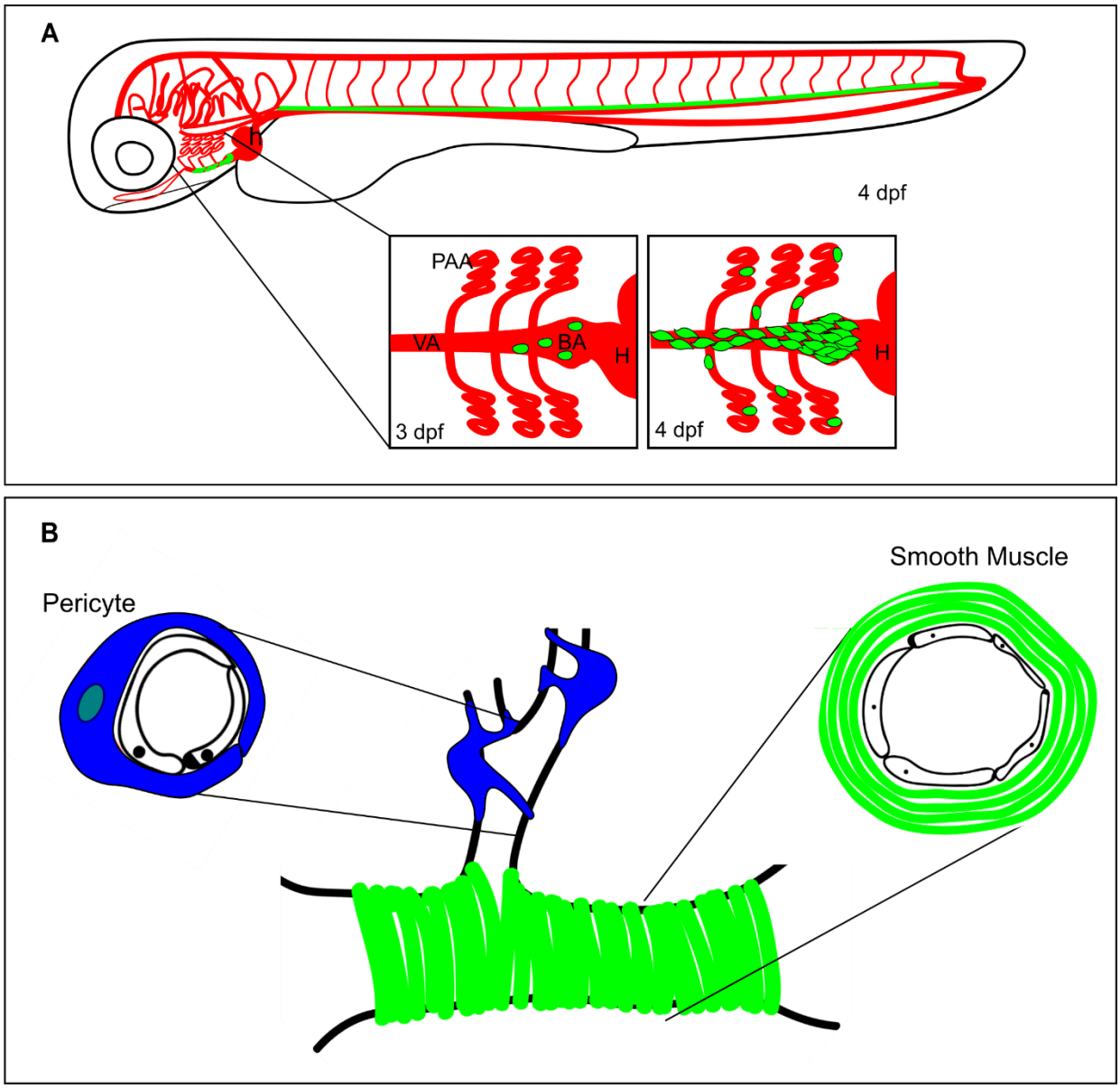

Figure 1.4: Mural cell coverage and function

A) Illustration of progressive vascular smooth muscle (green) coverage of major arterial vessels (red) in a zebrafish embryo. H: heart; VA: Ventral Aorta; BA; Bulbous Arteriosus, PAA: Pharyngeal Arch Arteries (B) vSMCs (green) are found in a continuous sheath around the endothelium of larger vessels, while pericytes (blue) are punctate cells, with individual processes wrapping around the endothelium of smaller vessels.

1.3.2. Mural Cell Function and Differentiation: focus of TGFβ/BMP regulation

Once associated with vessels, vSMCs take on a mature or contractile phenotype which is defined by a change in morphology to an elongated spindle-like shape (Figure 1.5). Mature vSMCs display low rates of proliferation and express SMC specific contractile genes such as smooth muscle myosin heavy chain (Sm-mhc/Mh11a), smooth muscle (α)-actin (α-Sma/Acta2), and *Sm22α* (Manabe and Owens 2001; Miano *et al*. 1994; Mack and Owens 1999; Milewicz, *et al*. 2010; Li *et al*. 1996). This mature vSMC repertoire allows vSMCs to induce vessel contraction and relaxation through the control of the actin-myosin apparatus in response to external stimuli to maintain vascular tone (Somlyo and Somlyo, 2003).

Of relevance to my work in Chapter 3, the TGFβ and BMP pathways have essential roles in regulating vSMC maturation. Mechanistically, induction of mature vSMC marker genes such as ACTA2 can occur through TGF-β responsive control element (TCE) sites located in CArG (CC(A/T-rich)6GG) elements located within vSMC promoter-enhancer regions (Tomasek *et al*., 2005). These motifs are critical in the induction of SMC contractile marker genes (Hendrix *et al.*, 2005). Binding of serum response factor (SRF) to the serum response element (SRE) contained within CArG boxes appears to be the major determinant of steady-state expression levels of SMC contractile marker genes (Li *et al*. 1997; Miano *et al*. 2000; Wang *et al*. 2003). Myocardin is a transcription factor that is considered to be a master regulator of SMC gene expression and is required for the cooperative activation of vSMC genes via SRF–myocardin complexes (reviewed in Mack 2011).

The sustained contractile forces of vSMCs operate under changes in blood flow, the effects of which are in part mediated by TGF-β/BMP non-Smad pathways. The TGF-β inducible Rho-family of small GTP-binding proteins plays a central role in regulating actin dynamics and transcription of vSMC genes (Chen *et al*., 2006; Clements *et al*., 2005; Lagna *et al*., 2007; Sun *et al*., 2006). For example, downstream signaling to Rho-kinase prevents the phosphatase activity of myosin light chain phosphatase (MLCP) and serves as a mechanosensory signal to promote actin-myosin cross-bridge cycling, via myosin-light chain kinase (MLCK), to maintain vascular tone (reviewed in Fang, Wu, and Birukov 2019). The Krüppel-like factor 2 (Klf2) transcription factor is one of the best-known blood flow-regulated genes and (Dekker *et al.*, 2002, 2005; Nayak, Lin and Jain, 2011). Klf2 is heavily expressed by endothelial cells (Ghaffari, Leask and Jones, 2017).

Indeed, *in vitro* models suggest that the EC induction of Klf2 could be a negative regulator of adjacent vSMC migration and cellular differentiation (Mack, 2011; Wang *et al*., 2011). Furthermore, BMP-2, -4, -6, and TGF-β share KLF4 as a common downstream molecule in maintaining the vSMC contractile phenotype. For example, KLF-2/4 binding at SMC marker gene promoters blocks SRF activation and limit transcription factor access through the induction of histone deacetylatase (Sun *et al*., 2011; Wang *et al*., 2011; Yoshida *et al*., 2008)

1.3.3. Zebrafish as a model for myogenesis

During early development, it is difficult to fully distinguish pericytes from immature vSMC as they both express PDGRβ. However, pericytes are readily identified by location and a distinct morphology with a prominent cell body and several long processes that wrap around capillaries (Figure 1.4 B). Pdgfrβ transgenic zebrafish lines have revealed real-time associations between ECs and brain pericytes in angiogenic spouting and stabilizing vessel walls (Davis *et al*., 2011; Stratman & Davis, 2012; Stratman *et al*., 2010; Wiens *et al*., 2010) Although pericytes have a mosaic expression of some of the same markers as vSMCs, differentiated pericytes do not express Acta2 (Alliot *et al*, 1999; Ando *et al*., 2016; Hartmann *et al*., 2015; Whitesell *et al*., 2019). For this reason, it is still controversial whether brain pericytes control blood flow (Fernández-Klett *et al*., 2010; Fernández-Klett & Priller, 2015; Hall *et al*., 2014; Hill *et al*., 2015). Our lab recently provided evidence to support the role of pericytes to restrict vessels in early brain vasculature development (Bahrami and Childs, 2020).

In zebrafish, the contractile vSMC markers *sm22α* and *acta2* are expressed around proximal vessels (bulbous arteriosus and ventral aorta) carrying high-pressure blood exiting the heart starting at late 3 days post fertilization (dpf) (Georgijevic *et al*., 2007; Santoro, Pesce and Stainier, 2009). To visualize vSMCs at the early stages, our lab developed transgenic Acta2 fluorescent reporter lines, in which ~3.5 dpf is the earliest time *acta2* cells are identifiable on the ventral aorta (VA) and pharyngeal arch arteries (PAA) (Figure 1.4 A). Characterization of this line demonstrated that *acta2* expressing cells display little to no proliferation or motility, suggestive of it being a marker of a contractile phenotype (Whitesell *et al*., 2014). In Chapter 3, I use our transgenic smooth muscle (*acta2)* and endothelial lines to assay changes in vSMC coverage at 4dpf.

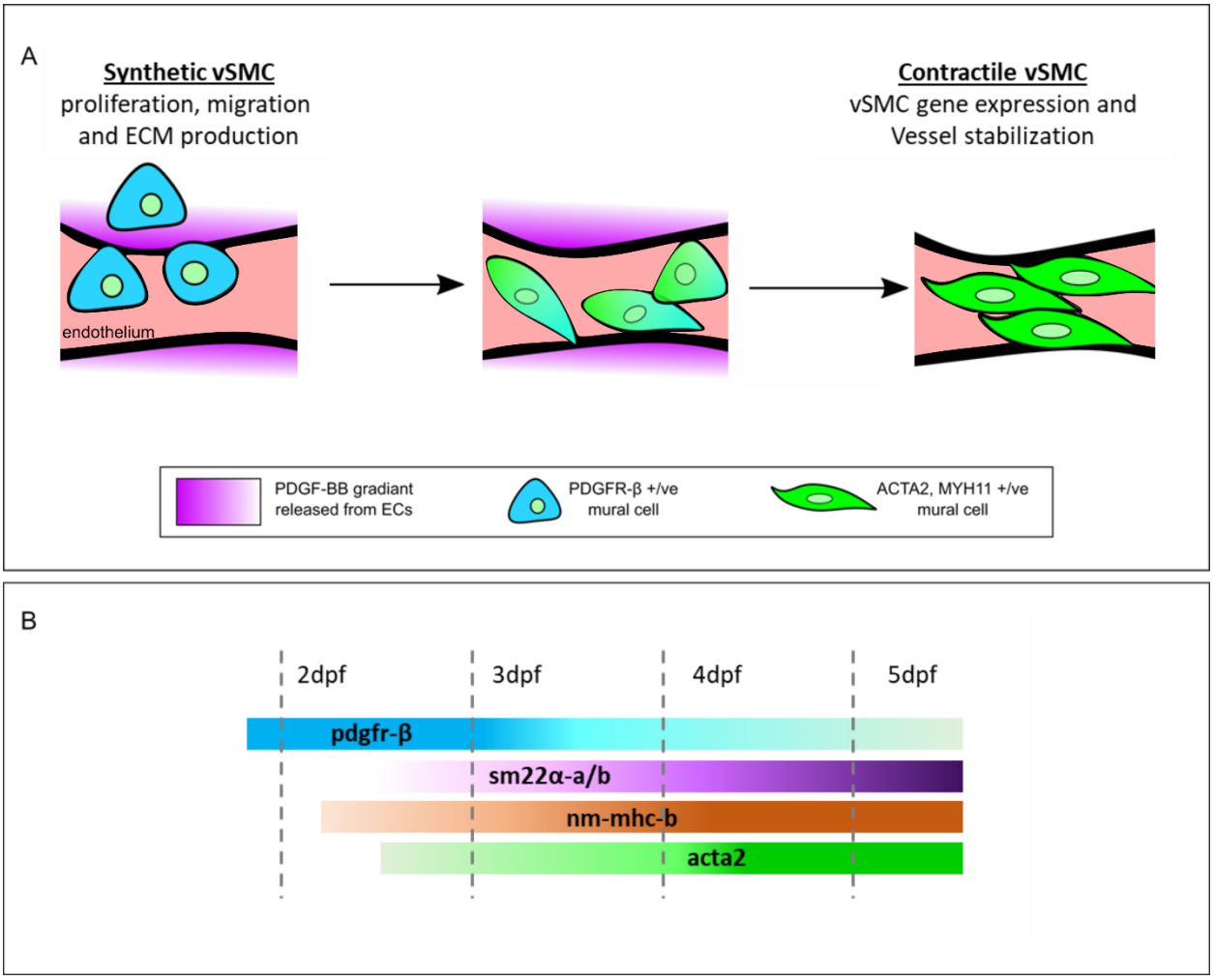

Figure 1.5 Mural cell recruitment and differentiation

A) Pdgfrβ expressing vascular mural cells are attracted Pdgfb ligand expressing endothelium. At this stage, the highly proliferative mural cells are termed synthetic as they synthesize extracellular matrix (ECM) components. Once attached, the mural cells begin to differentiate into contractile vSMCs which support and stabilize the underlying endothelium. B) Timeline of mural marker gene expression in zebrafish. dpf: days post fertilization; pdgfrβ: platelet derived growth factor receptor-β; sm22a/b: smooth muscle myosin 22a/b; nm-mhc-b: non-muscle myosin-heavy chain (myh11); acta2: smooth muscle actin.

1.4. Genetic regulation of endothelial and mural cell crosstalk

Vessel walls have a core function in providing structural integrity. Altered mural-endothelial communication can produce several phenotypes resulting from the loss of mural cell coverage (Gore *et al*., 2012; Owens *et al*., 2004). As an intermediate between circulating blood and supportive vSMCs, the endothelial cell serves as a vital point of communication and interpretation of stimuli during this process (Intengan *et al*., 2001; Lehoux *et al*., 2006; Lindahl *et al*. 1997; Yuan and Jing 2010).

1.4.1. Communication between cells during vascular development

Mature vSMCs are located outside the basement membrane that surrounds endothelial cells, this close association allows communication via small molecules and ions to trigger non-autonomous signaling in both cells (Cuevas *et al*., 1984; Larson *et al*., 1987) (Figure 1.6). During recruitment to vessels, immature vSMC stimulate the formation of the vascular basement membrane by endothelial cells and produce some components of the extracellular matrix. The increased mural cell coverage restricts vessel diameter, which is indicative of vessel stability and myogenic tone (Davis *et al*., 2011; Hellström *et al*., 2001; Hungerford *et al*., 1996; Stratman *et al*., 2010).

In vitro assays using collagen matrices demonstrate that the association of mural cells to vessel walls is vital for tube formation (Hellström *et al*. 2001; Lindblom *et al*. 2003; Xu and Cleaver 2011; Davis *et al*. 2013). Early murine models suggest mural cells promote vessel formation by blocking EC proliferation which promotes the formation of stable intra-endothelial junctions (Hellström *et al*., 2001; Orlidge & D'Amore, 1987). For example, trafficking and activation of the stabilizing N-cadherin adherens junctions facilitate signaling to promote vSMC differentiation and endothelial maintenance (reviewed in Armulik, Genové, and Betsholtz 2011; Li *et al*. 2018). Chemokine signaling also plays a role in directing vessel growth and mural cell recruitment. The C-X-C chemokine receptor 4 (CXCR4) and its associated ligand CXCL12 are expressed on arteries or in tissue directly adjacent to arteries during early development (Busillo and Benovic, 2007; Bussmann *et al*., 2011; Cha and Weinstein, 2012; Corti *et al*., 2011; Fujita *et al*., 2011; Li *et al*., 2013). In zebrafish, cxcr4b/cxcl12 signaling in the arterial endothelium promotes Pdgfb ligand expression, which ultimately drives arterial vSMC recruitment and limits venous coverage in response to changes in flow induction of klf2 (Stratman *et al.*, 2019).

1.4.2. TGF-β/BMP regulation of cell interactions during vessel stabilization

Key to vascular development, TGF-β, and BMP serine/threonine receptors activate distinct and often opposing Smad-dependent signaling cascades that influence vascular stability (David *et al*., 2009; Goumans & Mummery, 2000; Hirschi *et al*., 1999; Korchynskyi & Dijke, 2002). The EC-specific type 1 receptor activin-like kinase 1 (Alk1/Acvrl1) and its co-receptor Endoglin respond to circulating Bmp9 and Bmp10 ligands. Binding activates the Smad1/5/9 axis to promote the expression of genes, such as inhibitor of differentiation 1 (Id1) and Jag1 which induces cell quiescence and vSMC differentiation in response to flow (Massagué and Wotton, 2000; Clark *et al.*, 2016). Mutations in Alk1, Endoglin or co-SMAD4 are causative of Hereditary Hemorrhagic telangiectasia (HHT) which is characterized by dilated cutaneous blood vessels (telangiectases), gastrointestinal hemorrhage, and arteriovenous malformations (AVMs) (Srinivasan *et al*. 2003; Mahmoud *et al*. 2010; Wang *et al*. 2014). Deletion of Alk-1 in mice leads to cranial hemorrhages, AVM-like fusion of micro-vessel plexus, hyperdilation of large vessels, and rescued coverage of vSMCs (Walker *et al.*, 2011). Similarly, in zebrafish Alk1 limits EC proliferation in response to flow-induced Bmp9/10 (Roman *et al.*, 2002; Corti *et al.*, 2011; Laux *et al*., 2011)

In vSMCs, cumulative evidence suggests that autonomous BMP signaling represses proliferation to promote vSMC maturation (Deng *et al*., 2000; Johnson *et al*., 2012; Paul *et al*., 2005). In vSMCs, ALK-3/BMPR1, and ALK2/BMMPR2 phosphorylation of Smad 1/5/9 results in the transcription of target genes such as the inhibitor Smad6 that opposes the effects induced by TGF-β-Smad2/3 signaling (Nakaoka *et al.*, 1997). The anti-proliferative BMP2/4 ligands can be expressed by either vSMCs or ECs depending on the vessel bed. Mutations in ALK2 results in the vascular disease Pulmonary Arterial Hypertension (PAH) which is characterized by aberrant vSMC proliferation and compromised responses to changes in blood flow (Frank *et al*., 2005; Johnson *et al*., 2012; Park *et al*., 2006; Paul *et al*., 2005). Disrupted Pdgf and Notch signaling can also result in defective endothelial junctions and increased permeability which is attributed to a lack of mural cell recruitment. For example, diabetic retinopathies with reduced PDGF signaling are characterized by pericyte detachment and hemorrhage of overgrown retinal capillaries (Geraldes *et al*., 2009; Motiejūnaitė and Kazlauskas, 2008). Aberrant Notch and TGFβ signaling are implicated in Cerebral cavernous malformations (CCM), where decreased Notch3 signaling between mural cells and endothelial cells reduces pericyte coverage which likely results in hemorrhage due to loss of vessel stabilization (reviewed in Winkler *et al*., 2011)

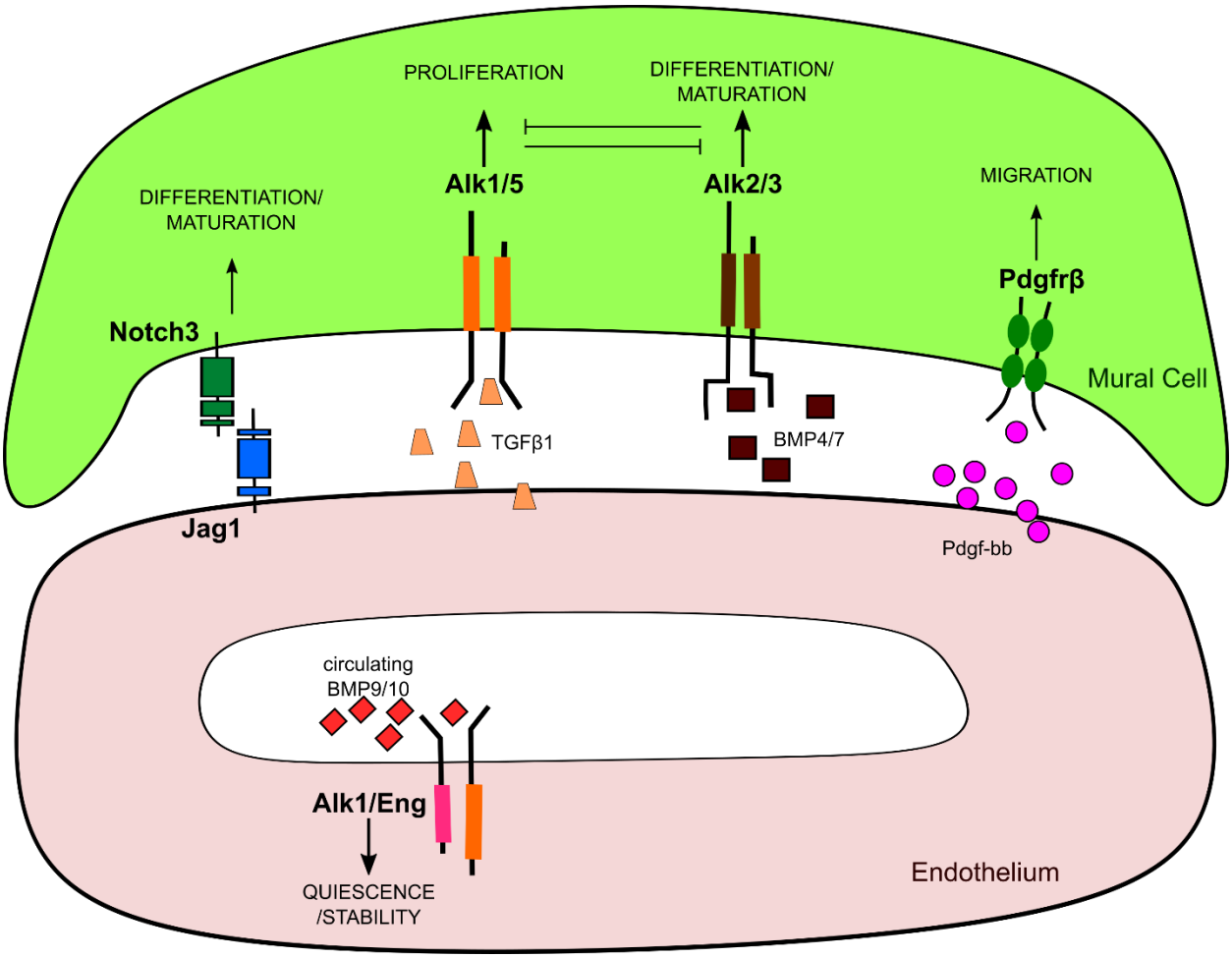

Figure 1.6 Pathways that promote endothelial and smooth muscle cell associations

Signaling pathways involved in vascular mural cell differentiation, recruitment, and vascular maturation. Pdgfbb is secreted and retained by endothelium where it serves as an attractant for migrating mural cells expressing Pdgfrβ. In endothelial cells, Alk1/Eng/Smad1 promotes cell quiescence in response to circulating Bmp9/10 ligands. Jag1 expressing endothelial cells signal to Notch3 expressing mural cells to induce vSMC marker gene expression and promote differentiation. TGF-β produced in endothelial cells induces SMC proliferation in adjacent perivascular cells via Alk5/Smad2/3. The expression of vSMC genes is maintained by Alk2/Smad1/5 in response to BMP4/7 ligands. Alk: Activin-like kinase; BMP: bone morphogenic protein; Eng: Endoglin; PdgfB: platelet derived growth factor receptor-BB; Pdgfrβ: Pdgf receptor-β; Jag1: Jagged1.

These examples highlight the importance of the initial recruitment of mural cells to promote endothelial growth arrest, and to promote vSMC maturation. However as both endothelium and smooth muscle respond to many of the same TGFβ/BMP signals (Figure 1.6), caution must be applied in interpreting results from knockout studies (reviewed in Gaengel *et al*. 2009; Chu *et al*. 2004; Kim *et al*. 2012). For example, endothelial-specific knockout of Bmpr-1a (Alk3) (Mishina *et al*., 1995) leads to embryonic lethality characterized by reduced vSMC coverage on blood vessels. But similar defects also occur with vSMC-specific deletion of Bmpr-1a (Eblaghie *et al*., 2006). In Chapter 3, I explore the effects of an endothelial-derived BMP signal in controlling vSMC differentiation.

1.5. Micro-RNA regulation of vessel growth and stabilization

Intracellular modulation of signaling by microRNAs (miRNAs) play important roles in vascular diseases through their direct targeting of key genes involved in vascular growth and stability (Albinsson *et al.*, 2010; Vidigal and Ventura, 2014; Ali *et al.*, 2015; Conde and Artzi, 2015). As a class of ever-emerging small endogenous RNAs, miRNAs represent a mechanism for tuneable posttranscriptional control of gene expression. From a disease viewpoint, understanding the integration of post-transcriptional mechanisms may offer potential avenues for therapeutics aimed at improving vascular stability (Nebbioso *et al*. 2012; Chamorro-Jorganes *et al*., 2013; Zhou *et al*. 2018).

miRNAs are relatively short RNAs (20-22 nucleotides) that are generated from double-stranded RNA (dsRNA) precursors. miRNA biogenesis is initiated by the transcription of a long (several kb) poly-adenylated primary miRNA (pri-miRNA) transcript. Successive cleavage by the enzymatic proteins Dicer and Drosha results in the production of small miRNA duplex complexes (Bartel, 2004). Once the duplex is formed one of the strands is incorporated into an RNA-induced silencing complex (RISC). Target recognition is achieved via a 7-8 base pair 'seed sequence' in the 5' end of the miRNA, which binds a complementary target site within the 3' untranslated region (UTR) of mRNA targets (Davis-Dusenber *et al*., 2011). Once bound, miRNAs downregulate target genes expression by translational inhibition or degradation of nascent peptides (Fjose and Zhao, 2010).

1.5.1. microRNA control of Vegf dependent pathways in endothelial cells

During vascular growth, many miRNAs have roles in regulating angiogenic sprouting processes that are dependent on VEGF activity. microRNA126 (miR126) is one of the best-characterized examples of an endothelial-specific miR that has a role in regulating VEGF dependent vessel growth. Deletion of miR126 in murine models or knockdown in zebrafish leads to a loss of vascular integrity (Kuehbacher *et al*., 2007; Nicoli *et al*., 2010; Suárez *et al*., 2007). miR-126 targets the negative VEGF regulators Sprouty-related protein (SPRED1) and phosphoinositol-3 kinase regulatory subunit 2 (PIK3R2/p85-β), and functions in a positive feedback loop that promotes angiogenesis in response to activation of the VEGF pathway (Fish *et al*., 2008b; Harris *et al*., 2010; Kuehbacher *et al*., 2007; Suárez *et al*., 2007).

The VEGF inducible miR-17-92 cluster regulates the oncogenic transcription factor c-Myc and its downstream effector E2F and promotes angiogenesis by downregulation of anti-angiogenic proteins such as tissue inhibitor of metalloproteinase 1 (TIMP1) which prevent ECM degradation (Bonauer *et al.,* 2009). Conversely, miR16 and miR424 are induced by VEGF, however, they function in a negative feedback loop to represses VEGFR2 which reduces EC proliferation, migration, and impairs tube formation on *in vitro* (Chamorro-Jorganes *et al.,* 2011). The endothelial expressed miR-23-24-27 cluster has a role in regulating angiogenic sprouting. In particular, miR-27 represses SEMA6A that negatively regulates Ras/MAPK responses downstream of VEGFR2 mediated signaling (Zhou *et al*. 2011; Bang *et al*. 2012). In zebrafish inhibition of both *miR-27a* and *miR-27b* results in the upregulation of *sema6a* which impairs sprouting in ECs in vitro, and embryonic vessel formation (Nicoli *et al.,* 2010). miR function can also be modulated by notch activity, for example, zebrafish *miR-221* expression is downregulated by a notch to limit tip cell behavior (Davis *et al*. 2009; Nicoli *et al*. 2012).

1.5.2. microRNA control of TGFB/BMP pathways in vascular stability

A smooth muscle-specific conditional deletion of Dicer (the enzyme critical for cleavage of miRNAs to their mature form) results in early embryonic lethality in mice due to extensive hemorrhaging implicating miRNA processing in vascular remodeling events (Pan *et al*., 2011). However, overexpression of a single miRNA is insufficient to rescue vascular stability defects suggesting that additional miRNAs promote vascular stabilization (Albinsson *et al*., 2010; Wang & Atanasov, 2019).

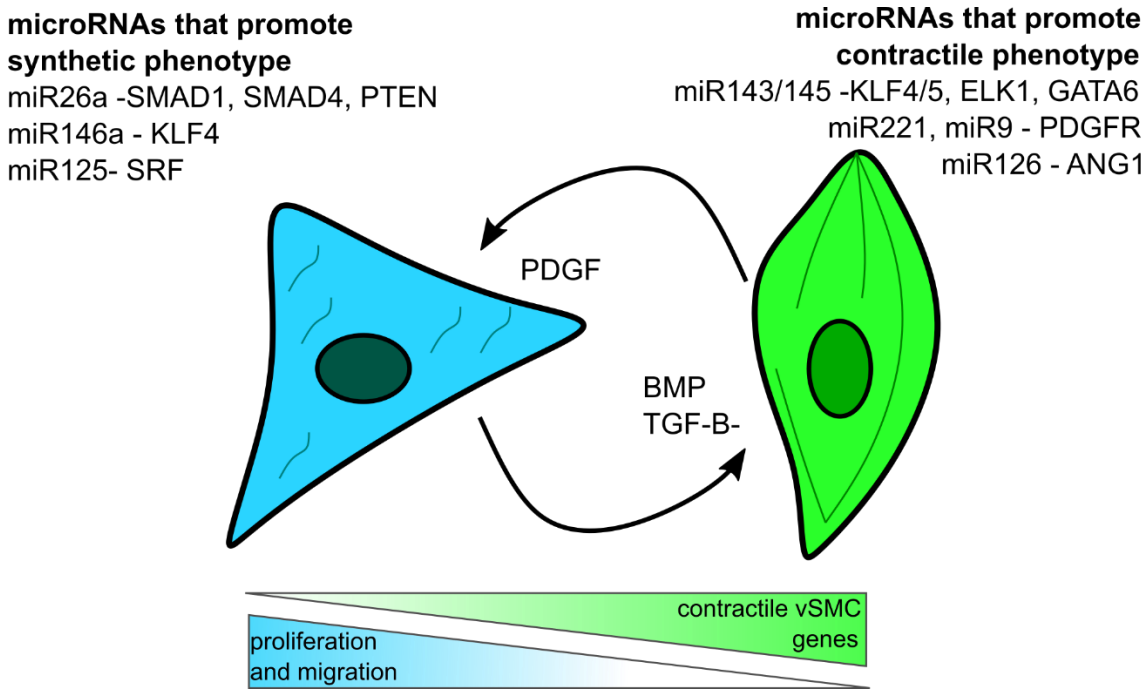

Figure 1.7 microRNA control of vascular smooth muscle maturation

Regulation of vascular smooth muscle cell (vSMC) proliferation/migration and differentiation/maturation by microRNAs (miRs) and their targets. miR-143/145, miR221, miR9, and miR26 inhibit bone morphogenetic protein (BMP) and transforming growth factor-β (TGF-β)-induced differentiation. miR26a and miR146a increase platelet derived growth factor (PDGF)-induced VSMC proliferation and migration. miR125 targets SRF and limits vSMC gene expression. Ang1: Angiopoietin 1; ELK1, ELK1 members of ETS oncogene family; Gata6: GATA Binding Protein 6; KLF4/5: Krüppel-like factor 4/5; PTEN: phosphatase and tensin homolog; SRF: serum response factor.

As one of the best-characterized vSMC regulators, the miR-145/143 family has direct control of contractile morphology through its repression of Klf2/4 (Cordes *et al.*, 2009; Zeng, Carter and Childs, 2009; Albinsson *et al.*, 2010). TGF-β/BMP induction of miR21 promotes cleavage of miR-143/-145 to mediates vSMC differentiation (Davis *et al*., 2010; Ji *et al*., 2007; Rangrez *et al*., 2011). The elevated miR21 expression can more strongly repress apoptosis and promote differentiation to a contractile phenotype in response to TGF-β (Sarkar *et al.*, 2010). Along with its endothelial actions, miR126 also enhances the proangiogenic actions of VEGF in vivo which are key features to trigger vSMC coverage (Jason E Fish *et al.*, 2008; Endo-Takahashi *et al.*, 2014). In addition to TGFβ/BMP pathways miRs also target pathways that promote mural cell proliferation, for example, miR146 targets Klf4 and functions in response to Pdgf ligands to promote cell migration and proliferation (Ham *et al*., 2017; Sun *et al*., 2011) Conversely miR9 directly targets Pdgf receptors to downregulate its downstream effects and promote vSMC differentiation. At the transcriptional level, miRs can downregulate key modulators of vSMC differentiation, for instance, miR125 targets SRF to limit vSMC gene expression (Chen *et al*., 2018) (Figure 1.7).

1.5.3. The role of miR-26a in BMP regulated vessel biology

As a regulator of Smad1, miR-26a has been studied in the context of angiogenesis and vSMC differentiation. In endothelial cells, miR26a is thought to play an anti-angiogenic role. miR26a expression is reduced upon VEGF stimulation and regulates the Id1 signaling axis that inhibits angiogenesis via its target Smad1 (Bai *et al*., 2011; Wang *et al*., 2019). In zebrafish overexpression of *miR-26a* adversely affected physiological angiogenesis by impairing the formation of the CVP, a BMP-responsive region. In vSMCs, miR-26a is thought to function as an inhibitor of vSMC differentiation and can be induced upon Pdgfb stimulation (Yang *et al.*, 2017) (Figure 1.7). However, its role within the vSMC cell is somewhat context-dependent. For example, knockdown of miR-26a accelerates vSMC differentiation, and conversely, overexpression of miR-26a reduces VSMC differentiation in cell culture models (Bai *et al*., 2011; Icli *et al*., 2014). Interestingly, in aortic aneurysm models in mice, although expression of miR-26a is reduced at a time point when VSMC de-differentiation is pronounced, Leeper *et al*. found no differences in the expression of smooth muscle actin expression in hearts compared to controls (Leeper *et al.*, 2011). This raised a question about whether miR-26a regulates vSMCs autonomously in vivo as it did not appear to

affect vSMC differentiation in intact vessel walls. Whilst these studies have shown that miRNAs, including miR26a influence both endothelial cell and vSMC differentiation, most studies are conducted in vitro models. Cell culture systems often fail to adequately recapitulate the complex interplay of intercellular regulatory signals or tissue-specific localizations that are present in vivo (Dzau *et al*., 2002; Koh *et al*., 2008; Milewicz *et al*., 2010). Preliminary ISH data showed punctate expression of miR26s within and around developing vessel walls. I, therefore, hypothesized that miR26a may have a role in promoting vessel maturation. In Chapter 3, I explore miR26a function in controlling endothelial smad1 and its non-autonomous effects on vSMC maturation.

In this thesis, I identify genes that influence blood vessel development and aim to understand the dynamic processes that regulate pattern formation and vessel integrity. The expansion of blood vessels into a hierarchically branched 'vascular tree' is controlled largely via signaling pathways. Several vascular diseases including stroke and hypertension result from abnormal blood vessel structure or behavior deriving from defective growth/maturation cues that lead to the subsequent impaired vascular functions. Together this work offers mechanistic insight into the endothelial-derived pathways that regulate blood vessel formation.

Chapter Two: Endothelial Semaphorin 3fb regulates Vegf pathway-mediated angiogenic sprouting

This chapter is adapted from a manuscript in preparation for publication: 'Endothelial Semaphorin 3fb regulates Vegf pathway-mediated angiogenic sprouting'. Charlene Watterston[1], Rami Halabi[2], Sarah McFarlane[2], and Sarah J Childs[1]

1) Department of Biochemistry and Molecular Biology, Alberta Children's Hospital Research Institute, University of Calgary, 3330 Hospital Dr., NW, Calgary, AB, Canada T2N 4N1. 2) Department of Cell Biology and Anatomy, Hotchkiss Brain Institute, Alberta Children's Hospital Research Institute, University of Calgary, 3330 Hospital Dr. NW, Calgary, AB, Canada T2N 4N1

Thank you to Jae-Ryeon Ryu, Carrie Herr, and Gabriel Bertolesi for technical assistance. Thank you to the members of the Flow Cytometry core facility.

2.1. Abstract

The mechanisms that guide vessel growth rely on the integration of molecular stimuli and cellular responses to shape morphogenesis. The pro-angiogenic effects of Vascular Endothelial Growth Factor (VEGF) must be carefully balanced during angiogenic sprouting. We identified a role for a member of the Semaphorin family, better known for mediating repulsive guidance cues, in promoting vessel growth. The secreted ligand *Semaphorin3fb (Sema3fb)* is expressed within developing endothelial cells. Loss of *Sema3fb* results in abnormally wide and short intersegmental vessel artery sprouts. We find that *Sema3fb* mutants show increased Vegf activity with higher expression of *vegfr2* and *dll4*. However, we also note the increased expression of *soluble flt1/vegfr1* which typically acts to limit Vegf responses. Reducing Vegf activity rescued the angiogenic deficits and suggests that *Sema3fb* balances Vegf signaling. Our data points to a novel feedback mechanism where a cell can utilize a negative cue to modulate growth factor signaling to promote appropriate vessel growth.

2.2. Introduction

Sprouting angiogenesis is a process by which new vessels branch and grow from existing vessels, establishing perfusion of body tissues and organs, and is often dysregulated in disease (Carmeliet, 2003a; Fischer, Schneider and Carmeliet, 2006; Ramasamy, Kusumbe and Adams, 2015; Hogan and Schulte-Merker, 2017). How sprouting angiogenesis is coordinated at the intrinsic and extrinsic levels is one of the most important questions in vascular biology. Vessel growth is highly dependent on Vascular Endothelial Growth Factor (VEGF) signaling, which functions as a master regulator to promote angiogenesis. VEGF gradients within tissues are responsible for the initial triggering and guidance of the sprouting process via signaling through the endothelial-expressed tyrosine kinase VEGF receptor (VEGFR2) (Gerhardt *et al.*, 2003a; Geudens and Gerhardt, 2011). However, the cellular response to VEGF must be carefully regulated to guide the stereotypical patterning of vessels.

During sprout formation, angioblasts adopt two distinct cellular states – termed tip and stalk- which respond to external stimuli to promote and guide vessel growth (Gerhardt *et al.*, 2003b; Mattila and Lappalainen, 2008; Bayless and Johnson, 2011). The tip cell utilizes filopodia to scan the environment for attractive and repulsive cues that antagonistically control proliferation and migration (Pollard and Cooper, 2009; Adams and Eichmann, 2010b). In contrast, the trailing stalk cells have limited filopodia, and contribute to forming the vascular lumen and phalanx (Gerhardt *et al.*, 2003a; Carmeliet *et al.*, 2005). Tip and stalk cell identity is determined competitively during angiogenic sprout formation and is controlled by a complex feedback loop with the Delta-Notch lateral inhibition pathway and intersects with VEGF signaling. Notch signaling regulates the ratio of tip and stalk cells, where the Delta-Like 4 (Dll4) positive tip cells activate the Notch receptor in the trailing stalk cells (Hellström *et al*., 2007; High *et al*., 2008; Siekmann, Covassin, & Lawson, 2008). This lateral inhibition down-regulates VEGF receptor expression and limits talk cell responses to environmental VEGF (Bautch 2009; Bussmann *et al*., 2011; Wiley *et al*., 2011).

The vertebrate-specific secreted Class 3 Semaphorins (Sema3s) typically act as repulsive guidance cues to limit vessel growth (Banu *et al*., 2006; Liu *et al*., 2016; Ochsenbein *et al*., 2016). This has been well demonstrated in the evolutionary conserved and stereotypically patterned

intersegmental vessels that form in between the somites of the zebrafish trunk and begin sprouting at around 20 hpf. Vegf is normally expressed segmentally in the ventral-medial region of somites, adjacent to the notochord, while *sema3a* is expressed in a caudal gradient in the same somite. Paracrine signaling from Sema3a to its receptor Plexind1 in the endothelium acts to spatially restrict intersegmental vessels from entering the caudal region (Adams & Eichmann, 2010b; Lamont *et al*., 2009; Torres-Vázquez *et al*., 2004; Treps *et al*., 2013; Zhang *et al*., 2018, 2020). Interestingly, these instructive cues can be different depending on the species and tissue expression of ligands and receptors. For instance, in mouse Sema3e is the ligand of PlexinD1 and functions to guide intersomitic vessel growth (Gu *et al.*, 2005). However, during intersegmental vessel growth, *Sema3e* shows endothelial expression and acts as an autocrine pro-angiogenic factor to antagonize PlexinD1 function in fish (Lamont *et al.*, 2009). As an endothelial-specific receptor PlexinD1 serves an additional function to limit response to VEGF. PlexinD1 stimulation results in increased expressed of a soluble decoy VEGF receptor (sVEGFR2/*sFlt1*) decreasing the concentration of the VEGF signal around endothelial cells (Torres-Vázquez *et al.*, 2004; Zygmunt *et al.*, 2011; Carretero-Ortega *et al.*, 2019).

In both human and mouse, Sema3F is highly expressed by endothelial cells (He *et al*., 2018; Nakayama *et al*., 2015; Regano *et al*., 2017; Vanlandewijck *et al*., 2018; Yuan *et al*, 2018; Zhang *et al*., 2020) and studies demonstrate that exogenous SEMA3F regulates tumor vascularization and acts to inhibits angiogenesis and apoptosis of endothelial cells (Bielenberg *et al*., 2004; Staton *et al*., 2011; Zhang *et al*., 2020). Interestingly, murine models have demonstrated that Sema3F can function as a pro-angiogenic or anti-angiogenic cue in a context-dependent manner. For instance, Sema3F limits the aberrant growth of retinal vessels (Buehler *et al*., 2013; Sun *et al*., 2017), and we recently showed similar anti-angiogenic functions for *sema3fa* in zebrafish (Appendix). At the same time, Sema3F is pro-angiogenic in placental development in mice (Guttmann-Raviv *et al.*, 2007; Regano *et al.*, 2017). There is still a limited understanding of how an endothelial cell can receive the same signal yet coordinate different downstream molecular pathways driving angiogenic growth. Here we investigate the role of Sema3f in regulating VEGF-mediated angiogenic growth. We find that Sema3fb (but not sema3fa) is expressed within the major arterial vessels and its expression is necessary for guiding initial sprout migration in an EC autonomous manner. We show that Sema3fb signaling regulates the expression of a key set of

differentiation markers that control EC identity and migration in sprouting angiogenesis. Moreover, loss of function of Sema3fb promotes a VEGF-induced negative feedback mechanism to limit sprouting. Together these data reveal a new role for endothelial cells in modulating VEGF activity to ensure proper co-ordination of angiogenic sprouting.

2.3. Materials and Methods

2.3.1. Zebrafish strains and maintenance

All procedures were conducted in accordance with the University of Calgary Animal Care Committee (AC17-0189). CRISPR/Cas9 *sema3fb* zebrafish (Danio rerio) mutant lines, were previously described (Halabi, 2019). Briefly, genetic knock-outs were generated using the CRISPR/Cas9 system, with sgRNA targeting sema3fb exon 1 selected using CHOPCHOP (Montague *et al*., 2014), followed by the analysis of the secondary structure using Vienna RNAfold Prediction (rna.tbi.univie.ac.at). A single sgRNA template was generated using the 20 bp gene-specific oligonucleotide containing the SP6 (underlined) promoter sequence (5'GCATTTAGGTGACACTATAGAGAAGGACAAGAAGACCCGCGGTTTTAGAGCTAGAAATAGCAAG-3'). Template generation and transcription were carried in accordance with the protocol described in (Gagnon *et al*., 2014). Briefly, the gene-specific oligonucleotide was annealed with the Cas9 "constant" oligonucleotide, and single-stranded overhangs (underline) were filled in by T4 DNA polymerase (New England Biolabs) to form a double-stranded oligonucleotide (5'AAAAGCACCGACTCGGTGCCACTTTTTCAAGTTGATAACGGACTAGCCTTATTTTAACTTGCTATTTCTAGCTCTAAAAC-3'). The sgRNA template was then gel purified (120bp) and transcribed from using the Sp6 Maxi Kit (Ambion). Cas9 mRNA was transcribed from plasmid (Addgene plasmid #47322) using mMessage Machine T7 (Thermo Fischer).To generate knock-outs, 1-cell stage embryos were injected with a 1 nl mix of approximately 56-60 pg sgRNA and 190 pg Cas9 mRNA. Heterozygous F1 fish (sema3fb$^{+/\Delta 19bp}$ hereafter *sema3fb*$^{+/ca305}$) were outcrossed to TL fish. F2 heterozygous progeny were intercrossed to generate genotypes (wild type, heterozygous, homozygous mutant).

To generate endothelial-specific lines the *Tg(-6.5kdrl:mCherry)*^{ci5} and *Tg(fli1a:nEGFP)*^{y7} were crossed to homozygous mutant F2 s*ema3fb* $^{ca305/ca305}$ to generate heterozygote lines that label endothelial cytoplasm with mCherry and/or nuclear-localized EGFP, respectively (Roman *et al.*, 2002; Proulx, Lu and Sumanas, 2010). Embryos were collected within 10-minute intervals and incubated at 28.5°C in E3 embryo medium and staged in hours post-fertilization (hpf). Endogenous pigmentation was inhibited from 24 hpf by the addition of 0.003% 1-phenyl-2-thiourea (PTU, Sigma-Aldrich, St. Louis, MO) in E3 embryo medium. Embryos were screened at 6 hpf to remove any embryos that were delayed.

To genotype, tissue was collected from single 30 hpf embryos (following blinded imaging). Genomic DNA extraction was performed in 50µl of 50mM NaOH, boiled for 10 minutes and buffered with 1/10 volume of 100mM Tris-HCl pH 7.4, as described in Meeker et al., (2007) and amplified by PCR using the following primers around the mutational site as described by Halabi *et al* 2019, sema3fb forward (5'-ATTGCCCCACAAAATAACATTC-3') and sema3fb reverse (5'-GTCTACTCTGTGAATTTCCCGC-3')

2.3.2. Morpholino and construct injections

Morpholinos (MO) against the sema3fb start codon (sema3fb^{ATG}; ATG underlined) 5'-CATAGACTGTCCAAGAGCATGGTGC-3' and against the tnnt2a start codon (tnnt2a^{ATG}, ATG underlined) 5'- CATGTTTGCTCTGATCTGACACGCA – 3' were obtained from Gene Tools LLC (Corvallis, OR, USA). Morpholinos were injected into one-cell stage embryos within recommended dosage guidelines at 1ng/ embryo (Bill *et al.*, 2009; Bedell, Westcot and Ekker, 2011). For endothelial-specific expression, a Tol2 construct with Fli1ep promoter driving the expression of Lifeact-EGFP, *fli1^{ep}Lifeact-EGFP* was obtained from(Phng *et al*., 2013). One-cell stage embryos were injected with 20 ng/µl plasmid and 25 ng/µl transposase RNA.

2.3.3. Cell sorting, RNA Isolation, and RT-qPCR

For FACS analysis around ~200 24 hpf, *Tg(kdrl:mCherry)* embryos were collected for single-cell dissociation according to (Rougeot *et al.*, 2014). Briefly, embryos were washed once with calcium-free Ringers Solution and gently triturated 5–10 times before the dissociation solution was added and incubated in a 28.5°C water bath with shaking and periodic trituration for 20-30 min. The reaction was stopped with 10% Fetal Bovine Serum (FBS), centrifuged, and resuspended in Dulbecco's Phosphate-Buffered Saline (GE Healthcare Life Sciences, Logan, Utah, USA), centrifuged and the pellet resuspended in fresh resuspension solution (DPBS with 10%FBS). The single-cell suspension was filtered with 75 µm, followed by 35 µm filters. Cells were then sorted with a BD FACSAria III (BD Bioscience, San Jose, USA) and collected. Total RNA from FACS sorted cells was isolated using the miRNeasy Mini Kit (Qiagen). 500 ng of total RNA from each sample was reverse transcribed into cDNA using SuperScript III First-Strand Synthesis SuperMix (18080-400; Invitrogen) and the concentration determined. cDNA in a 5ng/ 10ul final reaction was used in a TaqMan Fast Advanced Master Mix (Thermo Fisher Scientific, Massachusetts, U.S).

Reactions were assayed using a QuantStudio6 Real-time system (Thermo Fisher Scientific). Zebrafish specific Taqman assays (Thermo Fisher Scientific) were used: vegfab (Cat# 4448892, Clone ID: Dr03072613_m1), kdrl(vegfr2) (4448892, Dr03432904_m1), dll4 (4448892,Dr03428646_m1), notch2 (4448892, Dr03436779_m1), jag1a (4448892, Dr03093490_m1), sflt1 (4331448, ADP47YD4) and normalized to β-actin (4448489, Dr03432610_m1). The ΔΔCt method was used to calculate the normalized relative expression level of a target gene.

2.3.4. Small molecule inhibition

The Vegfr2 inhibitor SU5416 (SIGMA #S8442) was prepared and used as described in (Covassin *et al.*, 2006; Stahlhut *et al.*, 2012; Carretero-Ortega *et al.*, 2019). Briefly, a 200 μM SU5416 stock solution in DMSO (Sigma #D8418) was dissolved in fish water to a final concentration of 0.2 μM SU5416 and 0.5 μM in 0.1% DMSO. Control (0.1% DMSO) treatments were also performed. Homozygous WT and homozygous *sema3fb*^{ca305} mutant embryos were manually dechorionated before receiving treatments using common solutions for both genotypes.

2.3.5. In situ hybridization and immunostaining

All embryos were fixed in 4% paraformaldehyde in PBS with 0.1% Tween-20 at 4°C overnight, followed by 100% methanol at −20°C. Digoxigenin (DIG)-labeled antisense RNA probes were used for in situ hybridization. Digoxigenin labeled RNA probes were synthesized as previously described (Thisse and Thisse, 2008). Probes were generated from plasmid templates containing a T3 or T7 RNA polymerase binding sequence on the reverse primer. Probes were generated from plasmid template (*sema3fa* - pCR4 with T7, linearized with PmeI) (*sema3fb* - pCR4 with T3, linearized with NotI) as previously described by Halabi *et al* 2019. Wholemount and section in situ hybridization were performed as described by (Thisse and Thisse, 2008) with some minor modifications: gradient changes in hybridization buffer were carried out at 70°C and 0.2 x SSC at 37°C and NBT/BCIP was used at a 2.5/3.5μl/ml ratio, respectively. For wholemount immunostaining embryo were permeabilized in 50:50 acetone/methanol for 20 minutes, rehydrated into PBT at RT, and blocked in 10% normal sheep serum (NSS)/PBST/1% triton, and incubated for at least 48 hours at 4°C in primary antibody. Laminin (1:400, Sigma-Aldrich, Missouri, United States) and mCherry (1:200, Developmental Studies Hybridoma Bank, Iowa

City, United States) were detected with mouse anti-mCherry antibody, (1:500, Clontech, Mountain View, California, USA) and detected with Alexafluor 555 or 488 secondary antibodies (1:500; Invitrogen), for 1 hour at RT in 5% NSS/PBST/0.1% triton.

2.3.6. Image acquisition and vessel measurements

For wholemount imaging, embryos were immobilized in 0.004% Tricaine (Sigma) and mounted in 0.8% low melt agarose on glass-bottom dishes (MatTek, Ashland, MA). Confocal images were collected on a Zeiss LSM 700 inverted microscope, processed in Zen Blue and are presented as maximal intensity projections, and analyzed using FIJI/ImageJ (Rasband, no date).

ISA length measurements were made with a segmented line tool along the vessel from the edge of DA to the leading edge of the spout. To calculate the % connected, each ISA connection to its neighboring sprout was counted and expressed as a percentage of the total number of ISA. Unless otherwise stated, at least 8 ISAs per embryo were measured. For ISA sprout diameter, 5 sprouts were measured at the boundary of the horizontal myoseptum. For EC nuclei spacing, 2 measurements were taken from the middle of each nucleus to its neighbor.

Total fluorescence (TF) was calculated using the formula: TF = Integrated Density—(Area X mean fluorescence of background area). Measurement area gated to 5 ISVs above the yolk extension.

2.3.7. Statistical Analysis

All data sets for heterozygote incross quantitation (qualitative scorings or absolute measurements) were analyzed blinded. Results are expressed as mean ± SD. All statistical analysis was performed using Prism 7 software (Graph Pad). Unpaired, nonparametric tests were used for all statistical tests, either the S.T-test with Welch’s correction for comparisons of two samples, or Two-Way ANOVA with a Kruskal-Wallis test for multiple comparisons

2.4. Results

2.4.1. sema3fb is expressed by developing blood vessels

As SEMA3F is highly expressed in both mouse and human endothelial cells, we asked whether *sema3f* is also expressed in zebrafish vasculature. The zebrafish genome contains duplicated orthologs of human SEMA3F - *sema3fa* and *sema3fb* (Yu and Moens, 2005). We previously reported that in the cardiovascular system, sema3fb has specific expression within cardiomyocytes during heart formation and promotes differentiation of the ventricle (Halabi, 2019). The stereotypic patterning of major trunk vessels in the zebrafish begins at around 20hpf when angioblasts (EC precursors) collectively migrate from the dorsal aorta (DA) and sprout laterally in between each pair of somites to form the ISAs. The ISAs then grow upwards and connect to form the dorsal longitudinal anastomosing vessel (DLAV) between 30-32hpf (Isogai *et al*, 2001). We found that *sema3fb* is expressed in the dorsal aorta at 26 hours post-fertilization (hpf) and in intersegmental vessels at 28 hpf and 30hpf (Figure 2.1A and Figure 2.2 A), similar to the endothelial expression patterns of Sema3e (Lamont *et al.*, 2009). In contrast, its homolog *sema3fa* is not expressed in vessels (Figure 2.2 A). The similar expression of Sema3f in murine, and human EC isolations and for *sema3fb* in zebrafish is supportive of a conserved role for Sema3f in endothelial cells.

2.4.2. Loss of sema3fb results in angiogenic deficits

We recently described the generation of a *sema3fb*^{305} CRISPR mutant with a 19bp deletion in exon1 which is predicted to produce premature truncations (32aa in length) within the 500aa SEMA domain that is necessary to elicit intracellular signaling (Tamagnone *et al*., 1999). (Halabi, 2019). RT-qPCR to detect relative transcript levels of mRNA isolated from 48 hpf wildtype and *sema3fb*^{305} embryos confirmed a reduction in sema3fb mRNA levels in the mutant as compared to wildtype (suggestive of nonsense-mediated decay (Hentze and Kulozik, 1999).To investigate the endogenous role of sema3fb in regulating vessel growth we crossed the *sema3fb*^{ca305} loss of function mutants to *Tg*(*kdrl:mCherry)*^{ci5} transgenic fish that fluorescently mark ECs to generate wild type, heterozygote, and mutant siblings. We analyzed angiogenic sprouting at 30 hpf a time when most ISAs are beginning to connect to form the DLAV (Figure 1B). We observed angiogenic deficits in both *sema3fb*$^{ca305/+}$ heterozygotes (Figure 2.1 D) and *sema3fb*^{ca305} homozygous mutants (Figure 2.1 E) when compared to their wild type siblings (Figure 1C). Specifically, we note a

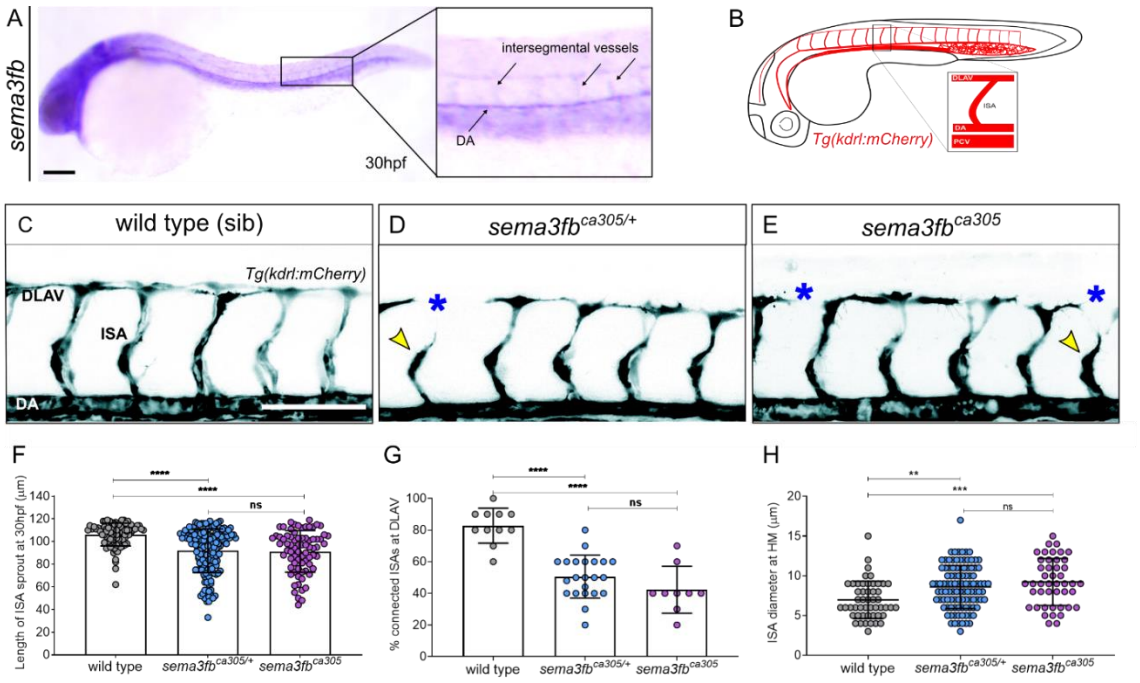

Figure 2.1: Endothelial-expressed *sema3fb* promotes endothelial cell sprouting

A) Lateral view of whole-mount in situ expression of *sema3fb* at 30hpf, inset: shows expression along the dorsal aorta (DA) and intersegmental arteries (ISAs). B) Schematic representation of the zebrafish vasculature. Inset: The ISAs sprouts from the dorsal aorta and typically connect to the Dorsal Longitudinal Anastomotic Vessel (DLAV) by 30hpf. C-E) Confocal lateral images of the trunk vasculature (black) of 30 hpf embryos. (C) wild type sibling (sib), (D) heterozygous *sema3fb*$^{ca305/+}$ and (E) homozygous *sema3fb*^{ca305} mutants . Angiogenesis gaps in DLAV (blue asterisks) and truncated ISA sprouts (yellow arrowhead) are noted. DLAV (Dorsal Longitudinal Anastomotic Vessel), DA (Dorsal Aorta), and PCV (Posterior Cardinal Vein). Anterior, left; dorsal, up. Scale bar, 100 µm. F) Quantification of ISA sprout length in 30 hpf embryos from DA. N= 3: Wild type sib (n =86 ISAs, 11 embryos, mean length of 106±10µm), heterozygous *sema3fb*$^{ca305/+}$ (n=163 ISAs, 22 embryos, mean length of 92±19µm), and homozygous *sema3fb*^{ca305} (=75 ISAs, 9 embryos, mean length of 91±18µm). 2-Way ANOVA Tukey's multiple comparisons test, ****p<0.0001. G) Percentage of ISA sprouts connected at DLAV in 30 hpf. N= 3: Wild type sib (n=11 embryos, 126 ISAs, mean 83% connected) , heterozygous *sema3fb*$^{ca305/+}$(n=22 embryos, 163 ISAs, mean 50% connected) and homozygous sema3fb^{ca305} (n=9 embryos, 75 ISAs, mean 42% connected). 2-Way ANOVA Tukey's multiple comparisons test, ****p<0.0001. H) Quantification of the cross-sectional diameter of ISA sprout at the

horizontal myoseptum (HM). N= 3: WT sib (n=86 ISAs, 11 embryos, mean diameter of 6.9±2µm), heterozygous *sema3fb*$^{ca305/+}$ (n=163 ISAs, 22 embryos, mean diameter of 8.5±2.7µm), and homozygous *sema3fb*^{ca305} (n=75 ISAs, 9 embryos, mean diameter of 9.2±2.9µm). 2-Way ANOVA Tukey's multiple comparisons test, **p<0.0016 and ***p=0.0002. Error bars = ±SD.

significant reduction in the average length of the ISA sprouts at 30 hpf from 106 μm in wild type to 91 μm in a heterozygote and 92 μm in homozygote mutant embryos (Figure 2.1 F). Second, the percentage of ISAs connected at the DLAV is reduced from 80% in wild type to 50% in heterozygotes and 40% in homozygote mutants (Figure 2.1 G). Lastly, sprouts have an increased diameter at the level of the horizontal myoseptum (HM) from 7 μm in wild type to 8.5-9 μm in heterozygotes and homozygote mutants (Figure 2.1 H). Together, these data suggest that Sema3fb normally promotes angiogenic sprouting and when it is lost, sprouts are shorter and wider.

We note that *sema3fb* mutation may function in a haploinsufficient manner since a losing single mutated allele of *sema3fb* results in highly penetrant vascular defects in the developing trunk. However, we cannot rule out that the ca305 allele acts dominant negatively. As a control, we validated that *sema3fb* morphants have a similar phenotype to *sema3fb* mutants, suggesting that this is a loss of function (haploinsufficient) phenotype, not a gain of function dominant-negative (Figure 2.2). We find that *sema3fa* is not expressed in trunk ECs (Figure 2.2 A). Furthermore, *sema3fa*^{ca304} mutants display normal sprouting and connections (Figure 2.2 B). Additionally, injection of antisense oligonucleotides that target *sema3fb* injected into the *sema3fa* mutant embryos results in no additional defects over *sema3fb*^{ca305} mutants and *sema3fb* morphants (note there is no quantification for *sema3fb*^{MO} alone due to limited embryo numbers). These results suggest that only one of the two sema3f orthologs, *sema3fb,* regulates angiogenic sprouting.

Migration of cells forming primary ISAs between 20-30hpf normally occurs independently of blood flow (Wang *et al.*, 2011; Karthik *et al.*, 2018). Since *sema3fb*^{ca305} mutants show reduced cardiac output (Halabi, 2019), we additionally asked whether the angiogenic deficits in mutants are a result of decreased flow at 30hpf. To block heart function, we injected a translation blocking morpholino against cardiac *troponin 2a* (*tnnt2aMO*) in wild type and *sema3fb* mutants. As expected, wild type ISA growth was unaffected by the loss of blood flow. Similarly, there was no significant difference in growth or connections in *sema3fb* mutants with no blood flow as compared to mutants with the flow (Figure 2.3). These data demonstrate that the angiogenic defects at the 30hpf stage in *sema3fb* mutants are independent of flow. We did note that uninjected *sema3fb*^{ca305} fish show a slight reduction in both the DA and post-cardinal vein (PCV) width (Figure 2.3 D-E), an effect was also seen in *tnnt2a* morphants, suggesting that the axial vessel diameter is sensitive to cardiac output. Taken together, these data indicate that *Sema3fb* controls angiogenesis growth in a cell-autonomous manner without affecting primary vessel formation.

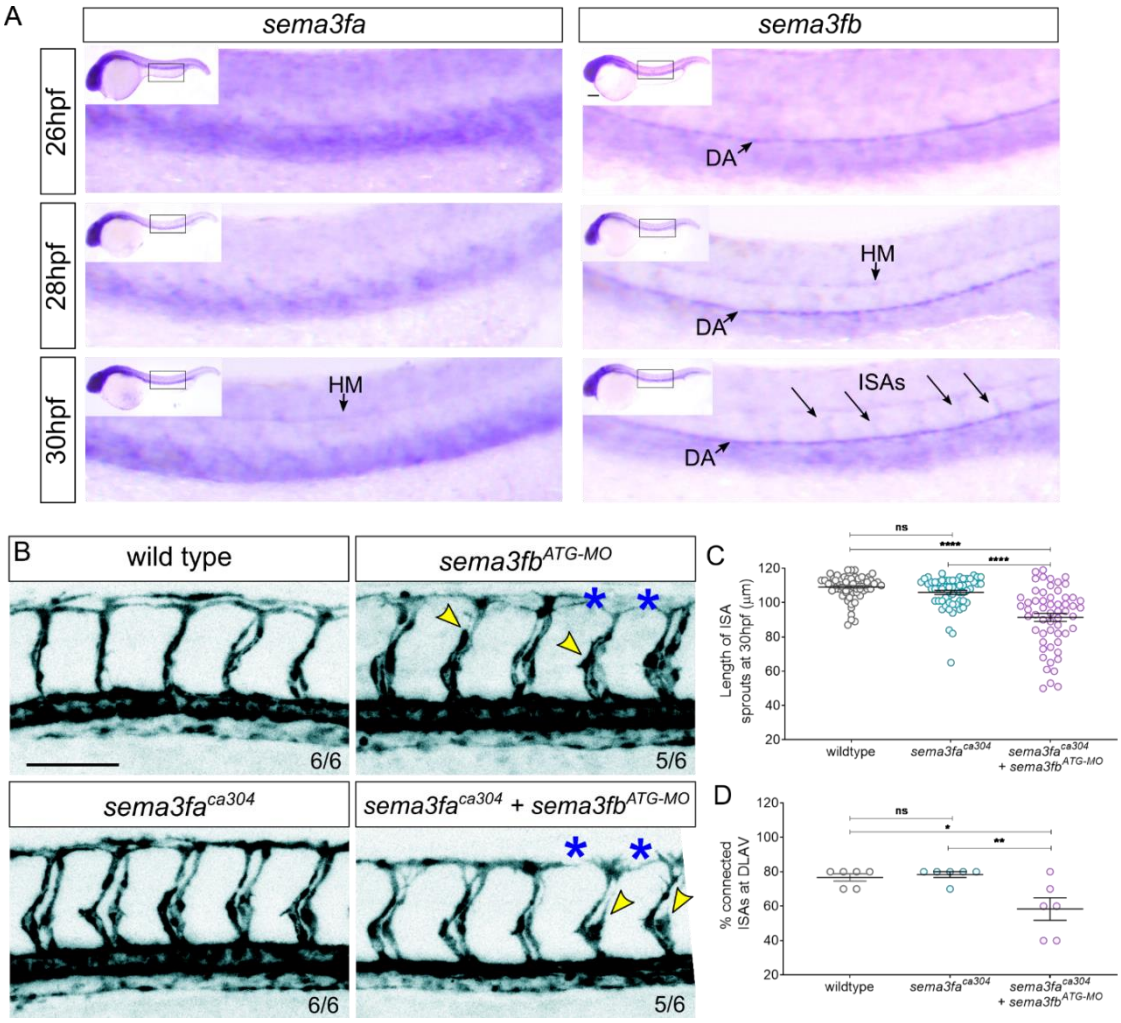

Figure 2.2: *sema3fa* mutants do not display angiogenic deficits

A) Lateral view of whole-mount ISH from 26-30hpf shows expression along the dorsal aorta (DA) and intersegmental arteries (ISAs) for *sema3fb* while *sema3fa* expression is restricted to the ventral somite. HM: Horizontal Myoseptum B) Lateral confocal images of the trunk vasculature (black) of 30 hpf embryos. B-D) Control wild type (WT) and homozygous *sema3fa*^{c3045} mutant embryos. C-E) WT and *sema3fa*^{ca304} *were* injected with 1ng *sema3fb*$^{ATG-MO}$.Scale bar, 100 µm. n/N = number of embryos with angiogenic defects/Total number of embryos. C) Length of ISA sprouts in 30 hpf embryos, N= 2, 6 embryos: WT (30 ISAs, mean length of 109±7µm), *sema3fa*^{ca304} (28 ISAs, mean of 106±9µm), and *sema3fa*^{ca304} + *sema3fb*^{MO} (30 ISAs, mean of 91±17µm), ****p<0.0001. D) Percentage of ISA sprouts connected at DLAV in 30 hpf embryos, N= 2: WT (30 ISAs, 6 embryos, mean 76±5% connected), *sema3fa*^{ca304} (28 ISAs, mean 78±4% connected), and *sema3fa*^{ca304} + *sema3fb*^{MO} (30 ISAs, mean 58±16% connected), p<0.001 Error bars = ±SD.

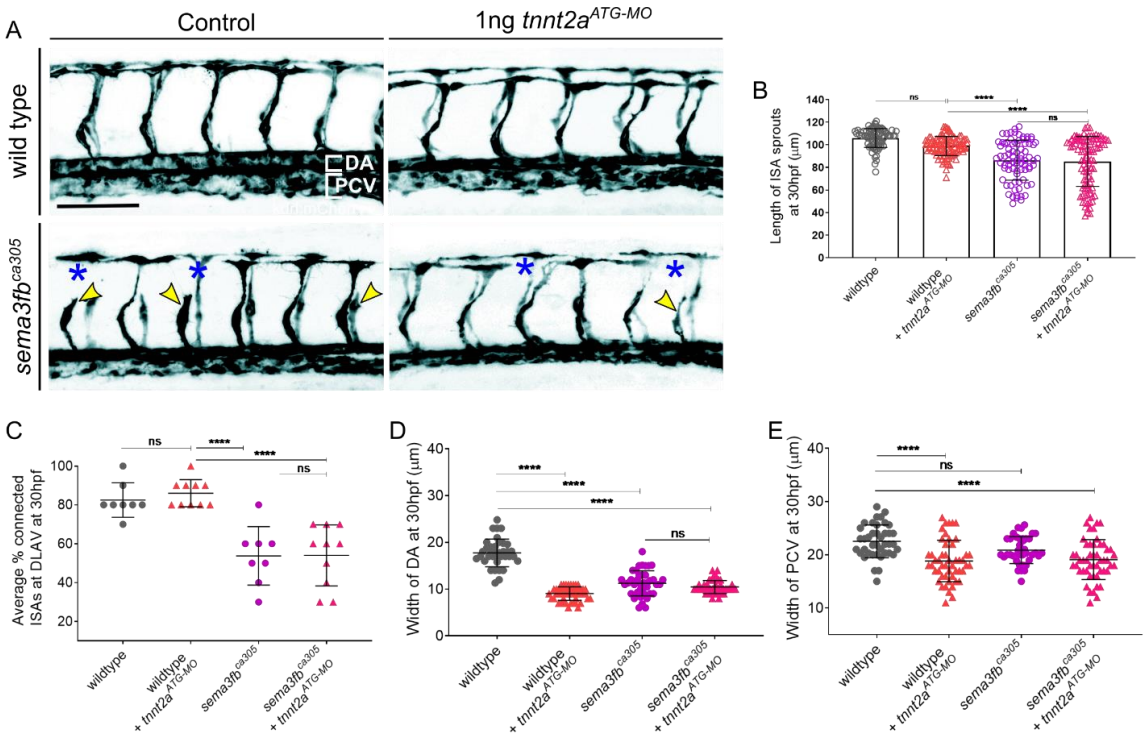

Figure 2.3: *sema3fb*^{ca305} angiogenic deficits are independent of blood flow

A) Confocal lateral images of the trunk vasculature (black) of blood flow stopped wild type sibling (WT) and *sema3fb*^{ca305} mutant *tnnt2*$^{ATG-MO}$ injected embryos. DLAV gaps (blue asterisks) and truncated ISAs sprouts (yellow arrowheads). Scale bar, 100µm. B) Length of ISA sprouts in 30 hpf embryos, N= 3: WT (80 ISAs, 8 embryos, mean length of 106±3µm), WT + *tnnt2a*$^{ATG-MO}$ (100 ISAs, 10 embryos, mean 98±8.4µm), *sema3fb*^{ca305} (80 ISAs, 8 embryos, mean 86±17µm), and *sema3fb*^{ca305} + *tnnt2a*$^{ATG-MO}$ (100 ISAs, 10 embryos, mean 85±22µm). C) Percentage of ISAs connected at DLAV in 30 hpf embryos, N= 3: WT (mean 82±9% connected), WT + *tnnt2a*$^{ATG-MO}$ (mean 86±7% connected), *sema3fb*^{ca340} (80 ISAs, 8 embryos, mean 54±15% connected), and *sema3fb*^{ca305} + *tnnt2a*$^{ATG-MO}$ (mean 54±16% connected). D) Quantification of width of DA in 30 hpf embryos, N= 3: WT (mean width of 18±3µm), WT + *tnnt2a*$^{ATG-MO}$ (mean 9±1µm), *sema3fb*^{ca305} (mean 11±3µm), and *sema3fb*^{ca305} + *tnnt2a*$^{ATG-MO}$ (mean 10±1µm).E) Quantification of width of PCV in 30 hpf embryos, N= 3: WT (mean width of 22±3µm), WT + *tnnt2a*$^{ATG-MO}$ (mean 19±4µm), *sema3fb*^{ca305} (mean 20±3µm), and *sema3fb*^{ca305} + *tnnt2a*$^{ATG-MO}$(mean 19±4µm). 2-Way ANOVA Tukey's multiple comparisons test, p=<0.001. Error bars = ±SD.

2.4.3. sema3fb mutant endothelial nuclear morphology is affected during sprouting

The finding that loss of *sema3fb* results in wider vessels(Figure 2.1 H) is interesting, as previous studies in zebrafish have linked changes in vessel diameter to increased EC proliferation (Roman *et al.*, 2002; Nicoli *et al.*, 2012; Lin *et al.*, 2013). To examine whether EC proliferation was impacted by loss of Sema3fb, we crossed *sema3fb*^{ca305} *Tg(kdrl:mCherry)* fish to the *Tg*(*fli1a:nEGFP)* line, which labels endothelial nuclei (Figure 2.4 A). ISAs sprout from the dorsal aorta through a stereotypic series of angioblast movements initiated by the migration of an angioblast tip cell from the DA followed by a trailing stalk cell. Once the leading angioblast reaches the HM, it typically divides and a single daughter cell migrates dorsally to form the DLAV (Childs., *et al.*, 2002; Lawson and Weinstein, 2002; Lamont *et al*., 2009). This process results in an average of 3-4 EC nuclei per sprout (Figure 2.4 A). We find that *sema3fb*^{ca305} mutants and heterozygotes have an identical number of ECs per vessel as wild type animals (Figure 2.4 B).

However, analysis of the distance between each EC nuclei reveals a significant decrease in the spacing between each EC nucleus (Figure 2.4 C). The reduced spacing gives the appearance of EC nuclei clumps, and their location below the horizontal myoseptum correlates with the increased width of ISAs. We also find that endothelial nuclei are significantly larger in mutants than in wild type controls (increased from an average of 49 μm^2 in wild type to 60 μm^2 in mutants, Figure 2.4 D). Similar increases are observed in *sema3fbMO* knockdown embryos, with an average nuclear area of 61 μm^2 (Figure 2.5 E). To whether spout direction was altered, we observed the position of sprouts with reference to laminin staining at the myotendinous junctions that separate somites. We found no significant changes in the sprout direction between *sema3fb* heterozygotes or homozygous mutants, and controls (Figure 2.5). Together, these results indicate that *sema3fb* promotes formation but is not important for the directional navigation of the sprout.

2.4.4. sema3fb mutants display persistent filopodia

As Sema3 pathways control actin dynamics (Gu *et al.*, 2003; Yazdani and Terman, 2006; Fantin *et al.*, 2011), we reasoned that angioblast migration defects might be accompanied by a change in filopodia activity. We injected wild type and *sema3fb*^{ca305} mutants with an endothelial-specific transgenic reporter, *fli1*^{ep}*Lifeact-EGFP* in which filamentous actin (F-actin), a major component of the cytoskeleton, is labeled with GFP to visualize filipodia in migrating ECs (Figure 2.6 A and Figure 2.7 A).

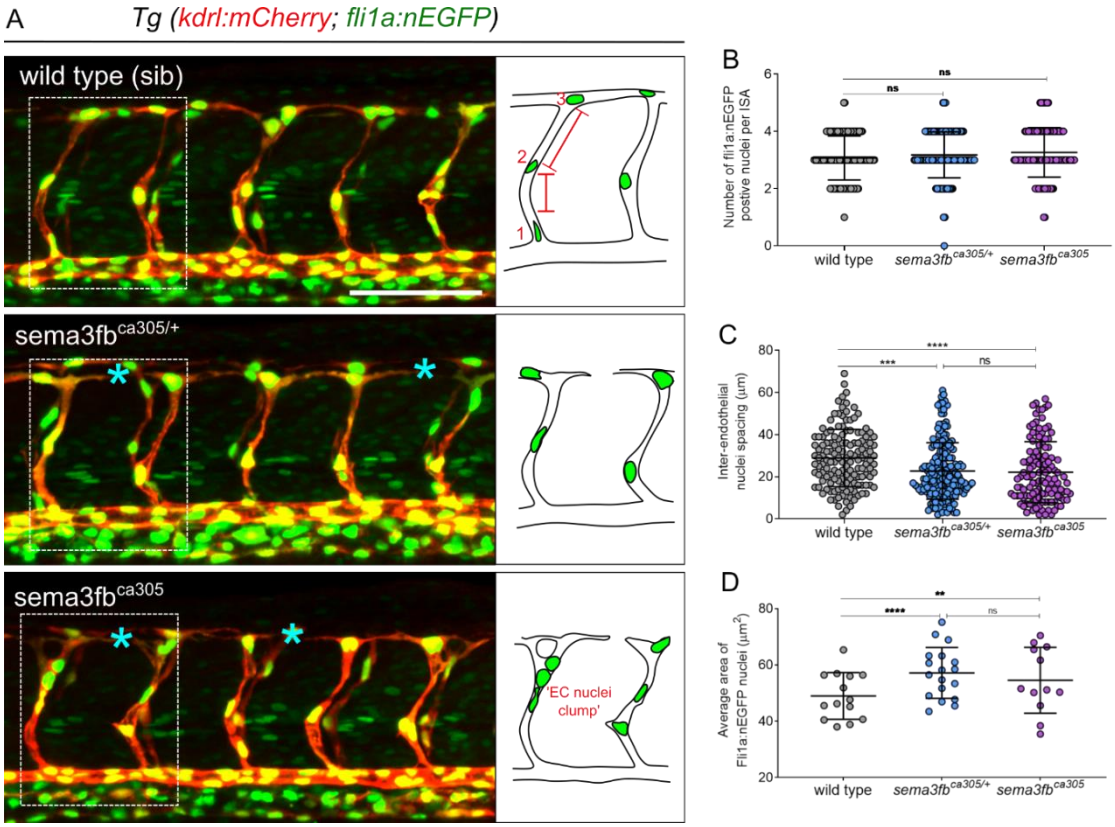

Figure 2.4: *sema3fb* mutants have enlarged endothelial nuclei size and variable spacing

A) Lateral confocal images of 30hpf double transgenic *Tg(kdrl:mCherry;fli1a:nEGFP)* endothelial cells (red) and nuclei (green). DLAV gaps (blue asterisks). Scale bar, 100 µm. Schematics show method for measuring distance between EC nuclei. B) Quantification of number of endothelial cell nuclei per ISAs in 30 hpf embryos, N= 3: wild type (WT) (138 ISAs, 14 embryos, mean of 3 nuclei/ISA), *sema3fb*$^{ca305/+}$ (190 ISAs, 19 embryos, mean of 3 nuclei/ISA), and *sema3fb*^{ca305} (110 ISAs, 11 embryos, mean of 3 nuclei/ISA). C) Quantification of inter-endothelial nuclei spacing per ISAs in 30 hpf embryos, N= 3: WT (mean of 28±13µm), *sema3fb*$^{ca305/+}$ (mean of 23±13µm), and *sema3fb*^{ca305} (mean of 22±14µm). 2-Way ANOVA Tukey's multiple comparisons test, ***p= 0.0002 and ****p<0.0001. Error bars = ±SD. D) Quantification of average area of endothelial cell nuclei per ISAs in 30 hpf embryos, N= 3: WT (mean 49±18µm^2), *sema3fb*$^{ca305/+}$ (mean 60±24 µm^2), and *sema3fb*^{ca305} (mean 56±23 µm^2). 2-Way ANOVA Tukey's multiple comparisons test,**p= 0.0069 and ****p<0.0001.

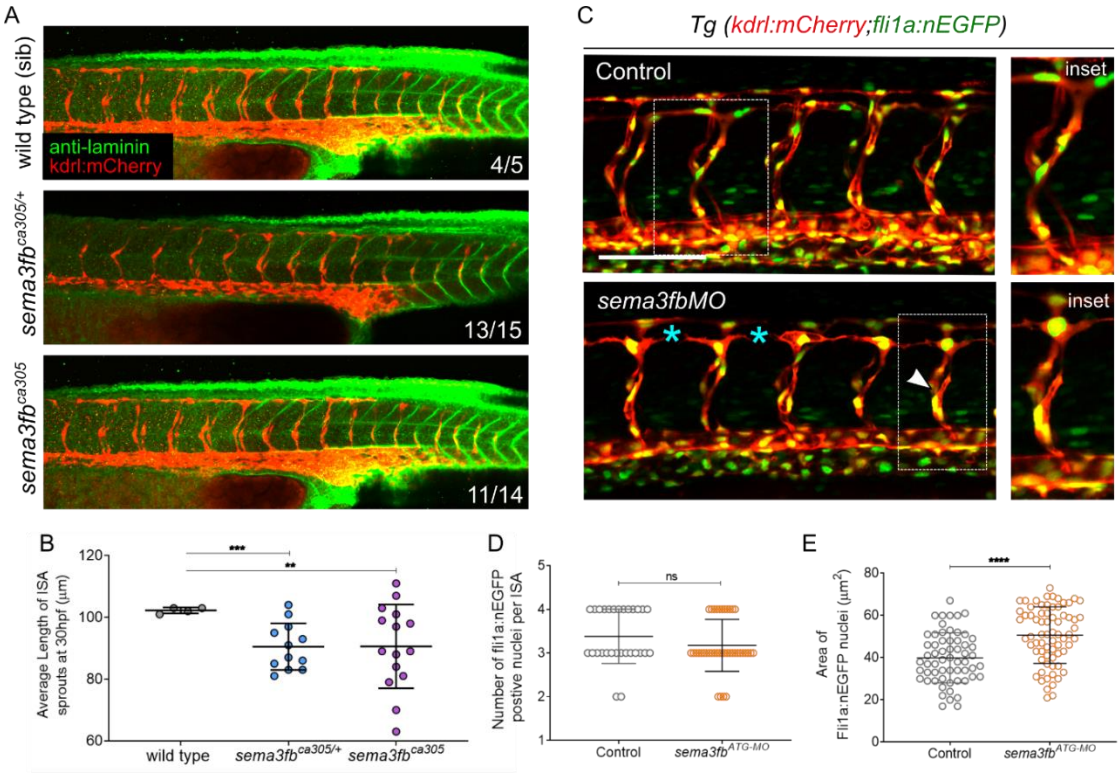

Figure 2.5: Loss of sema3fb does not alter sprout direction

A) Confocal lateral images of laminin stained embryos at 30hpf. *Tg(kdrl:mCherry)* vasculature (red) and laminin (green). Embryos derived from a heterozygous *sema3fb*$^{ca305/+}$ incross. B) Quantification of the length of ISA sprouts in 30 hpf embryos, N= 1: wild type (WT) (40 ISAs, 4 embryos, mean of 102±1µm^2), *sema3fb*$^{ca305/+}$ (120 ISAs, 12 embryos, mean of 90±8µm^2), and *sema3fb*^{ca305} (150 ISAs, 15 embryos, mean of 90±14µm^2). C) Lateral confocal images of double transgenic *Tg(kdrl:mCherry;fli1a:nEGFP)* vasculature (red) and endothelial cell nuclei (green). DLAV gaps (blue asterisks) and truncated ISAs sprouts (white arrowheads) are noted. Embryos derived from a heterozygous *sema3fb*$^{ca305/+}$ incross. Scale bar, 100 µm. D) Quantification of the number of endothelial cell nuclei per ISAs in 30 hpf embryos, N= 2: WT (6 embryos, mean of 3 nuclei/ISA), and *sema3fb*^{MO} (7 embryos, mean of 3 nuclei /ISA). Unpaired t-test with Welch's correction, p= 0.1714. E) Quantification of the average area of endothelial cell nuclei per ISAs in 30 hpf embryos, N= 3: WT (60 ISAs, 6 embryos, mean of 42±16µm^2), and *sema3fb*^{MO} (70 ISAs, 7 embryos, mean 61±19µm^2). Unpaired t-test with Welch's correction, ****p<0.0001. Error bars = ±SD

Time-lapse confocal imaging of individual ISA sprouts from 28-30 hpf revealed that wild type sprouts have highly dynamic filopodia that reduce over time as stalk cells lumenize and become quiescent (Figure 2.6 B). At 28hpf, wild type and *sema3fb* mutants have the same number of filopodia per ISA (average of 9 filopodia). By 29hpf *sema3fb* mutants have an increased number as compared to wild type (average of 7 in mutant vs 5 in wild type). By 30hpf, there is an average of 3 filopodia remaining in wild type, while *sema3fb* mutants have 8 filipodia present (Figure 2.6 B, C, and 2.7 B, C, D). These data suggest that *sema3fb* mutants fail to shut down filopodia formation at the appropriate time.

2.4.5. sema3fb mutants have increased VEGF receptor expression and activity

To investigate the molecular mechanisms at play when *sema3fb* is lost, we assayed gene expression on FACS-sorted *Tg(kdrl:mCherry) sema3fb* mutant and wildtype ECs. We then used RT-qPCR to analyze the gene expression of a key set of endothelial cell markers that regulate angiogenic sprouting. Tip cells are typically identified by higher expression of *vegfr2* and *dll4* whereas stalk cells express *notch2* and *jagged1a* (Figure 2.8 A).

Analysis of the isolated angioblasts revealed a 4.5-fold increase in *vegfr2/kdrl* and a 2.2 fold increase in *dll4* in *sema3fb* mutants as compared to controls. We found no significant difference in *vegfa* or the stalk cell markers *notch2* or *jagged1a* (Figure 2.8 B). As the transgenic *Tg(kdrl:mCherry)* reports the expression of *vegfr2*, we assayed fluorescence levels and found a significant increase in mCherry fluorescence *in vivo* in *sema3fb*^{ca305} mutants, confirming the qPCR findings of increased *kdrl* expression (Figure 2.8 C). While FACS isolation will include both tip and stalk cells, our data suggest that loss of *sema3fb* upregulates the expression of genes that typically mark tip cells.

We also investigated whether levels of the endothelial expressed *Vegfa* decoy receptor *soluble flt1 (sflt1)* are changed. Surprisingly we also found a significant 3-fold increase in the expression of *sflt1* in mutants as compared to controls (Figure 2.8 B). These data suggest the loss of *sema3fb* results in both upregulations of VEGF-pathway promoting (*dll4*) and -inhibiting genes (*sflt1*) in endothelial cells which disrupts EC migration.

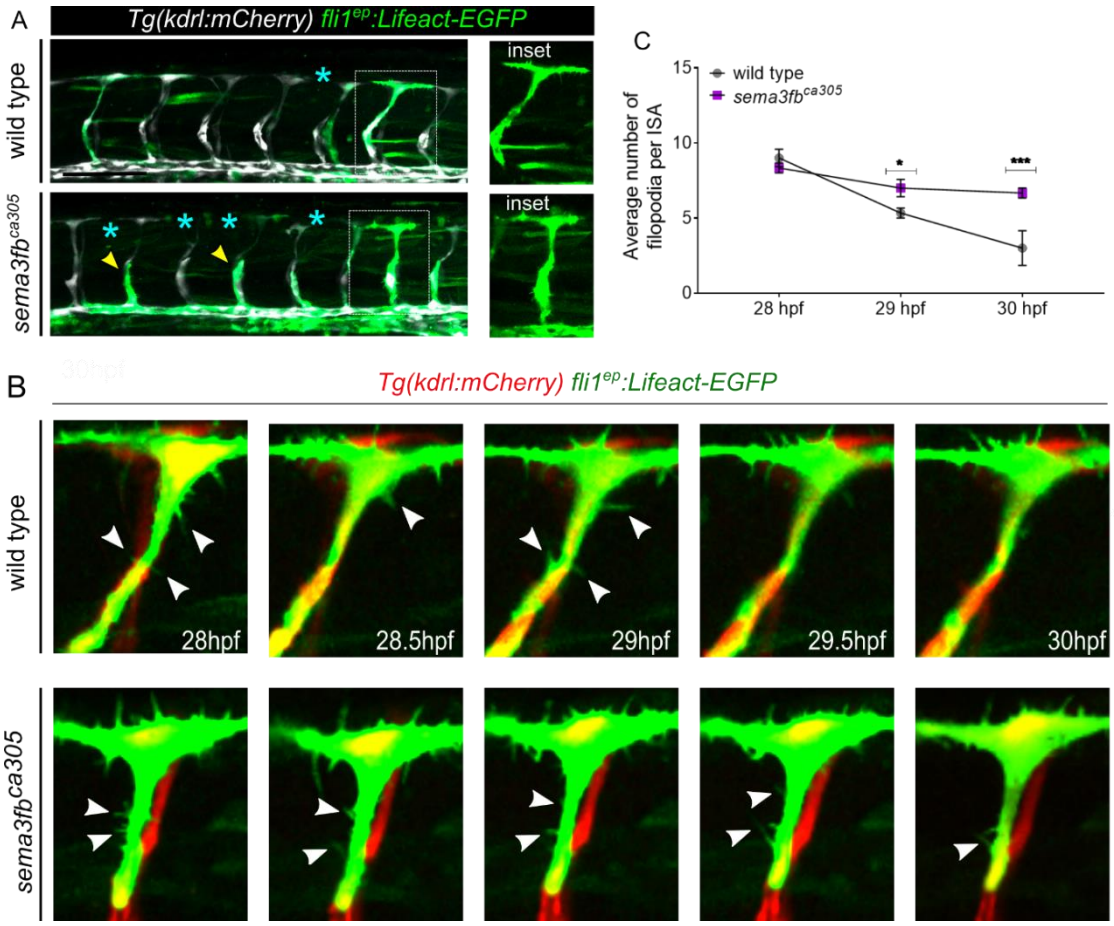

Figure 2.6: *sema3fb* mutants display aberrant and persistent filopodia

A) Lateral confocal images of the trunk vasculature with the mosaic endothelial expression of fli1^{ep}: Lifeact-EGFP highlighting actin in ISAs and DLAV of 30 hpf embryos, the vasculature of *Tg(kdrl:mCherry)* (white). DLAV gaps (blue asterisks) and truncated intersegmental artery (ISA) sprouts (yellow arrowheads). Insets show enlarged single ISAs with Lifeact-EGFP expression. Scale bar, 100 μm. B) Representative still images of mosaic Lifeact-EGFP (green) in an endothelial cell spanning the ISA and DLAV from 28-30hpf wildtype and *sema3fb*^{ca305} embryo time-lapse imaging. Vasculature of *Tg(kdrl:mCherry)* in red, white arrowheads indicate filopodia present along with the ISA sprout. C) Quantification of number Lifeact-EGFP positive filopodia on ISA from 28-30 hpf from embryos of the indicated genotypes. N= 3: WT (14 ISAs, 6 embryos, mean of 4 filipodia/ISA) and homozygous *sema3fb*^{ca305} (18 ISAs, 7 embryos, mean of 7 filipodia/ISA). Unpaired t-test with Welch's correction,***p=0.0002. Error bars = ±SD.

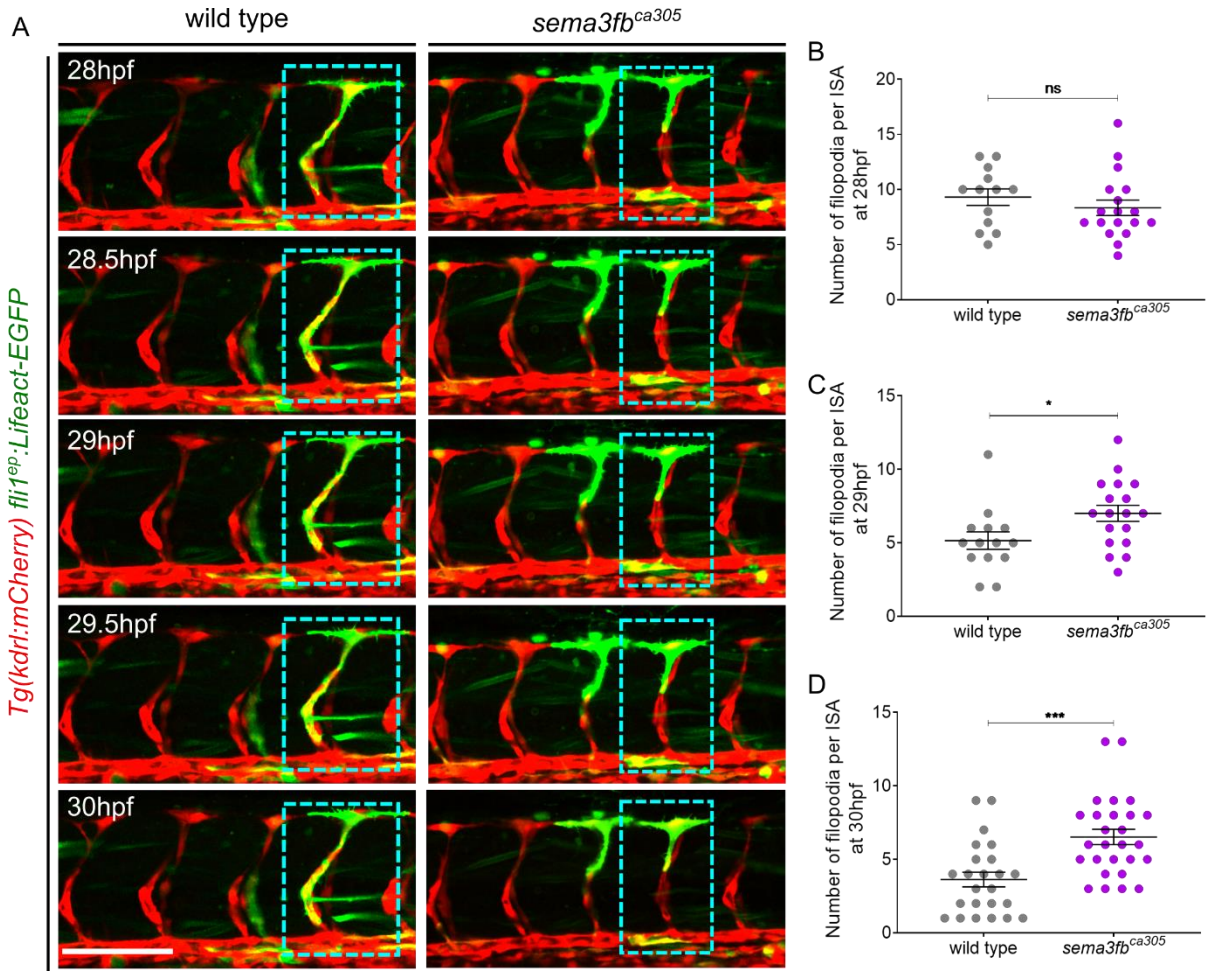

Figure 2.7: *sema3fb* mutants display aberrant and persistent filopodia

A) Representative still images of single-cell expression of fli1^{ep}: Lifeact-EGFP (green) in an endothelial cell spanning the ISA and DLAV from 28-30hpf wildtype and *sema3fb*^{ca305} embryo time-lapse imaging. B) Quantification of number Lifeact-EGFP positive filipodia on ISA at 28hpf from embryos of the indicated genotypes. Unpaired t-test, p=0.2192. C) Quantification of number Lifeact-EGFP positive filipodia on ISA at 29hpf from embryos of the indicated genotypes. Unpaired t-test, p= 0.0594. D) Quantification of number Lifeact-EGFP positive filipodia on ISA at 30hpf from embryos of the indicated genotypes. N= 3 for each quantification: WT (14 ISAs, 6 embryos, mean of 3 filipodia/ISA) and homozygous *sema3fb*^{ca305} (18 ISAs, 7 embryos, mean of 8 filipodia/ISA). Unpaired t-test, p=0.2192.

The upregulation *vegfr2* in *sema3fb* mutants is suggestive of enhanced Vegf pathway activation. To investigate whether the angiogenic defects in *sema3fb* mutants are dependent on increased Vegf activity, we treated wild type and *sema3fb* mutant embryos with SU5416, a selective inhibitor of the Vegfr2, from 20-30hpf. Previous studies in zebrafish report a dose of 0.5 μM SU5416 is an optimal concentration for disrupting ISA growth (Stahlhut *et al.*, 2012; Ochsenbein *et al.*, 2016; Carretero-Ortega *et al.*, 2019). While inhibitor-treated wild type embryos have significant disruption to sprout formation, inhibitor-treated *sema3fb* mutants do not show significant changes in sprout length. Sprouts are still able to form and grow to comparable lengths as the untreated control mutants, with an average length of 82 μm in both treated and untreated mutants (Figure 2.9).

At first glance, this result suggests that angiogenic deficits in *sema3fb* mutants may not result from increased Vegfr2 activity. However, we noted that loss of *sema3fb* also results in increased expression of *dll4*. We, therefore, reasoned that the optimal dose may drastically disrupt Vegf-dependant mechanisms of endothelial cell specification. Therefore, we lowered the SU4516 concentration to a sub-optimal (low-dose), which can induce minimal angiogenic deficits (Figure 2.8 D) (see Carretero-Ortega *et al*. 2019). We found that a low-dose treatment of wild type embryos with SU5416 from 20-30hpf resulted in a less drastic reduction in sprout length from 104 μm to 92 μm and a 60% decrease in the number of ISA connections to the DLAV, which is strikingly similar to the *sema3fb* mutants (Figure 2.8 D, E, and F). Conversely, the effect of the low-dose treatment significantly rescued *sema3fb* mutant defects, and restored sprout length to 94 μm and increased connections to the DLAV by roughly 20% (Figure 2.8 D-F). These additional tests indicate that slight reductions in *Vegfr2* activity attenuate *sema3fb* sprouting defects and suggest that *Sema3fb* functions via Vegf-dependant feedback within endothelial cells.

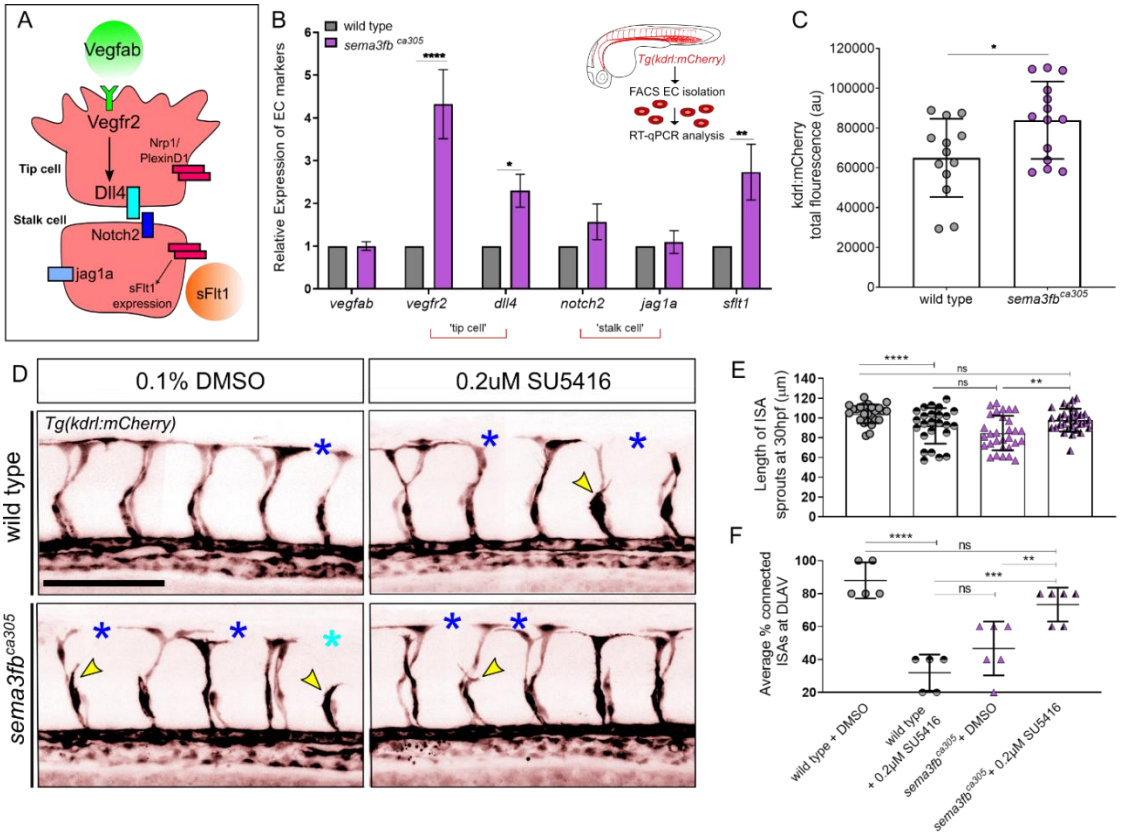

Figure 2.8: sema3fb mutants have increased VEGF receptor expression and activity

A) A model of signaling pathway activity of tip and stalk cell highlighting key genetic markers. B) RT-qPCR analysis of key endothelial 'tip' and 'stalk' markers in wildtype and *sema3fb*^{ca305} of FACS isolated *Tg(kdrl:mCherry)* ECs embryos at 26hpf (inset). N=2 biological replicates, 2-Way ANOVA Tukey's multiple comparisons test, *p= 0.0184, **p=0.0021, and ****p<0.0001. C) Quantification of total red fluorescent EC marker *Tg*(*kdrl:mCherry*) in wildtype and *sema3fb*^{ca305} ISAs at 30hpf. N=3: wildtype (13 embryos, 6500 a.u.) and *sema3fb*^{ca305} (14 embryos, 8400 a.u.). T-test with Welches correction, *p=0.0186, a.u. = arbitrary unit of intensity. D) Lateral confocal images of the trunk vasculature *Tg(kdrl:mCherry)* (black) of embryos treated with DMSO control or 0.2µM SU5416 from 20-30hpf. DLAV gaps (blue asterisks) and truncated ISA (yellow arrowheads). Scale bar, 100 µm. E) Length of ISA sprouts in treated 30 hpf embryos, N= 2: WT + DMSO (25 ISAs, 5 embryos, mean of 104±9µm), WT + 0.2 µM SU5416 (25 ISAs, 5 embryos, mean of 92±17µm), *sema3fb*^{ca305} + DMSO (30 ISAs, 6 embryos, mean of 85±17µm), and *sema3fb*^{ca305} + 0.2µm SU5416 (30 ISAs, 6 embryos, mean of 98±11µm). 2-Way ANOVA Tukey's, **p= 0.0039 and ****p<0.0001. F) Percentage of ISA sprouts connected at DLAV in treated 30

hpf embryos, N= 2: WT + DMSO (25 ISA-DLAV, 5 embryos, mean 88±11%), WT + 0.2µM SU5416 (25 ISA-DLAV, 5 embryos, mean 32±11%), *sema3fb*^{ca305} + DMSO (30 ISA-DLAV, 6 embryos, mean 46±16%), and *sema3fb*^{ca305} +0.2µm SU5416 (30 ISA-DLAV, 6 embryos, mean 73±10%). 2-Way ANOVA, **p= 0.0084 , ***p=0.0002 and ****p<0.0001.

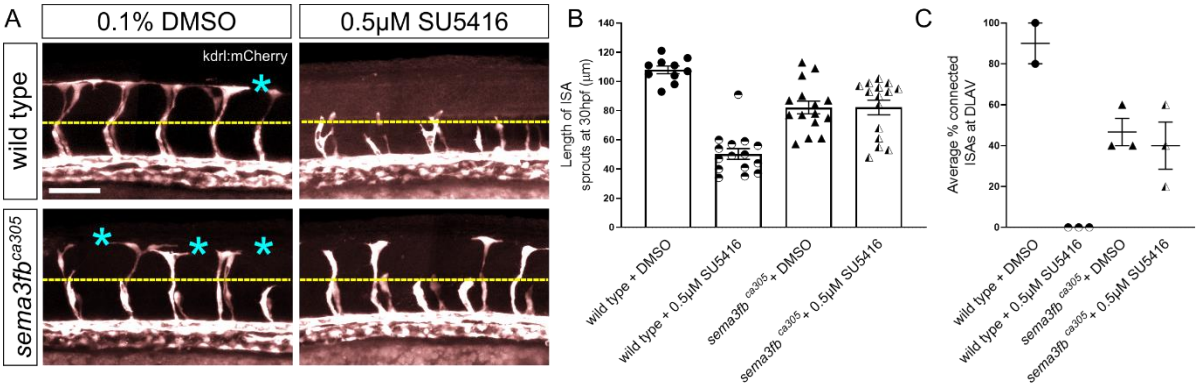

Figure 2.9: Interactions between VEGFR inhibitor and sprouting in *sema3fb* mutants

A and D) Lateral confocal images of the trunk vasculature *Tg(kdrl:mCherry)* (white) in embryos treated with 0.5µM SU5416 from 20hpf-30hpf. DLAV gaps (blue asterisks) and ISA truncated sprouts (yellow dashed line at the level of horizontal myoseptum, HM). Scale bar, 100 µm.

B) Quantification of length of ISA sprouts in 30 hpf embryos treated with 0.5µM SU5416, N= 1: WT + DMSO (25 ISAs, 5 embryos, mean of 107±8µm), WT + 0.5µM SU5416 (25 ISAs, 5 embryos, mean of 50±14µm), *sema3fb*^{ca305} + DMSO (30 ISAs, 6 embryos, mean of 82±17µm), and *sema3fb*^{ca305} +0.5µM SU5416 (30 ISAs, 6 embryos, mean of 82±19µm).

C) Percentage of ISA sprouts connected at DLAV in 30 hpf embryos treated with 0.5µM SU5416, N= 1: WT + DMSO (25 ISA-DLAV, 5 embryos, mean 78% of ISA-DLAV/embryo), WT + 0.5µM SU5416 (25 ISA-DLAV, 5 embryos, mean of 78%), *sema3fb*^{ca305} + DMSO (30 ISA-DLAV, 6 embryos, mean of 51%), and *sema3fb*^{ca305} + 0.5µM SU5416 (30 ISA-DLAV, 6 embryos, mean of 82±19%). Error bars = ±SD.

2.5. Discussion

As a secreted growth factor, VegfA plays a central role in the stimulation and control of angiogenesis, and its signaling through Vegfr2 is tightly regulated during embryonic development and homeostasis (Covassin *et al.*, 2006; Krueger *et al.*, 2011a). This control is exquisite, and the zebrafish model has uncovered many regulatory layers controlling Vegf pathway activity in endothelial cells (Lin *et al*., 2013; Nicoli *et al*., 2012a; Siekmann *et al*., 2008; Siekmann & Lawson, 2007). In the present study, we found that zebrafish *sema3fb* mRNA is expressed by developing trunk angioblasts. We found that Sema3fb signaling likely controls the expression of Vegfr2 in endothelial cells which in turn regulates Vegf-induced Dll4–Notch signaling, a key lateral inhibition pathway controlling endothelial cell identity. Sema3fb loss of function disrupts the morphology of ISA sprouts and leads to an uneven growth front, which can be restored by lowering Vegf activity in the mutant zebrafish. Therefore, our results suggest that Sema3fb may act in an autocrine loop with Vegf signaling to regulate sprouting angiogenesis (Figure 2.9).

Sema3F typically signals through Neuropilin receptors (Nrp1/2) to modulate migration in endothelial cell culture models (Guttmann-Raviv *et al.*, 2007; Guo *et al.*, 2013; Nakayama *et al.*, 2015). Interestingly this pathway can also antagonize Vegf-mediated migration as both Nrp1 and Nrp2 have additional functions as Vegf co-receptors that enhance migratory responses to Vegf signaling (Koch and Claesson-Welsh 2012).VEGF is a potent pro-angiogenic signal and activates many key pathways including the class I PI3-kinases (PI3k)/K-Akt pathway that controls endothelial physiology and regulates cellular growth, proliferation, migration (Abid *et al.*, 2004; Ruan and Kazlauskas, 2012). PI3Ks are lipid kinases that signal downstream of cell surface receptors to generate the lipid phosphatidylinositol-3,4,5-triphosphate, a second messenger that triggers signaling pathways such as those mediated by the serine/threonine kinase AKT and its substrates. PI3Kα, a class I PI3K isoform, is the only isoform required for endothelial-mediated vascular development (Graupera *et al.*, 2008). In our zebrafish *Sema3fb* knockout model the endothelial nuclear area is significantly increased. This result supports a role for Sema3F in controlling actin dynamics via PI3K where exogenous Sema3f inhibits PI3K activity and disrupts the mTOR-RhoA/GTPase axis that limits stress fiber formation and limits cell size (Nakayama *et al*. 2015).

In addition, we found that filopodia projections are persistent in *Sema3fb* mutants. This result is in line with the classical definition of Semaphorins as collapsins that regulate cytoskeletal rearrangements (Adams and Eichmann, 2010a; Treps *et al.*, 2013). Although filopodia appear to be dispensable for sprout initiation in zebrafish, the assembly of F-actin into filipodia influences the speed and direction of migration of ECs as well as their anastomosis to form a connected vessel bed (Phng *et al*., 2013; Wakayama *et al*. 2015). These processes are dependent on the activity of downstream effectors such as PI3Kα to promote cell motility and rearrangements during angiogenesis (Karar and Maity, 2011; Ruan and Kazlauskas, 2012; Angulo-Urarte *et al.*, 2018). Studies in mouse and zebrafish demonstrate that inhibition of PI3K results in dysregulation of actinomycin contractility, leading to failure of cell elongation, and increases in endothelial cell area (Angulo-Urarte *et al*., 2018; Graupera *et al*., 2008; Park *et al*., 2010). This presents an interesting paradigm, where PI3Kα activation is necessary to promote migration and cell elongation but excessive stimulation can also lead to the accumulation of fibers that halt migration. Indeed, the increased nuclear cell size may also be due to excessive Vegf stimulation and is consistent with VEGF dependent PI3K regulation of stress fiber accumulation which restricts nuclear elongation (Cole *et al*. 2010; Bhattacharya *et al*. 2009). Our data, therefore, suggest that Vegf and Sema3 signaling oppose each other to refine vessel growth. Negative feedback in response to pro-angiogenic signals is needed to promote proper cell rearrangements and limit vessel growth.

Vegf activity must be tightly regulated by endothelial cells to limit aberrant vessel sporting (Kim *et al*., 2011; Williams *et al*., 2006; Zarkada *et al*., 2015). Intriguingly, VEGF can also directly control the expression of Plexin-D1 in retinal murine models. In turn, the effects of Sema3e are also dependent upon a VEGF-induced feedback mechanism, in which Vegf directly controls levels of PlxnD1 to spatially restrict tip cell responses (Kim *et al*. 2011). Thus, the endothelial cell integrates responses between both pro- and anti-angiogenic molecules to carefully control vessel growth. Our *sema3fb* mutants display angiogenic deficits that are remarkably similar to those seen with Vegf inhibition alone, with disruption to sprout morphology and angiogenic ISA growth. We were, therefore, surprised to find increased expression of tip cell markers, *vegfr2,* and *dll4 in sema3fb* deficient angioblasts, which suggests that Vegf signaling may be upregulated in *sema3fb* mutants. Using a Vegfr2 inhibitor, we found that mild inhibition partially rescues the angiogenic

deficits in ISAs sprout growth. At higher doses, SU5416 completely disrupts EC migration in wild type but does not rescue the mutant phenotype suggesting that strong inhibition interferes with normal angiogenic growth signals. We noted an increase in the VEGF decoy sFlt1 in *sema3fb* mutants. sFlt1 mediates the anti-angiogenic effects of Sema3s in sprouting models. It also plays an important role in limiting EC response to Vegf ligands. Interestingly excessive VEGFR-2 stimulation can increase sFLT1 expression in human vascular ECs (Park *et al*. 2010). Our data suggest that *Sema3fb* acts in an autocrine manner to limit Vegf activity and promote appropriate vessel growth. Interestingly, as cell culture models have noted higher Sema3f expression on the leading edge of migrating ECs (Brambilla *et al*., 2000; Nasarre *et al*., 2003), further work could explore whether Sema3f is spatially restricted *in vivo* to control tip cell responses.

In this study, we provide evidence for Sema3fb to modulate Vegf-mediated angiogenic sprouting in zebrafish trunk vessels. A role for secreted Sema3s acting as both pro-and anti-angiogenic mediators is known, however to our knowledge this is the first work to suggest an autocrine role of Sema3f to modulate Vegf function *in vivo*. The Sema3f-Plexin-Nrp pathway is anti-angiogenic in many *in vitro* models of vessel growth, however, our data provides a unique role of Sema3f within the EC itself is to provide a negative signal to fine-tune the expression of genes necessary for its migration. The *sema3fb* mutant zebrafish is a novel model to understand the intrinsic molecular and cellular mechanisms that act in response to extrinsic environmental cues. Our work highlights that although cell culture systems are vital for studying cellular response pathways, it is equally important to understand how these pathways function in intact models. Importantly, we show that loss of a typically negative pathway promotes vessel growth by regulating endothelial cell responses to pro-angiogenic stimuli.

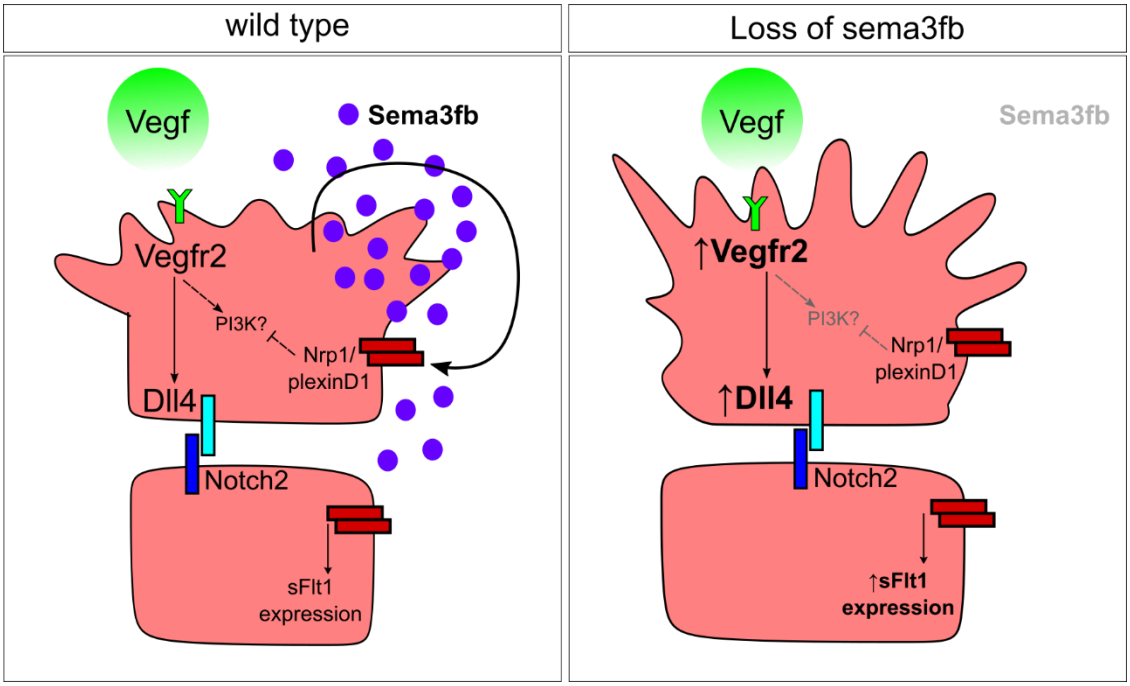

Figure 2.10: Proposed model of *sema3fb* action in sprouting vessels

Sema3fb is expressed by endothelial cells during angiogenic sprout formation and acts through auto-secretory feedback to suppress Vegfr2 expression to maintain endothelial cell dynamics via Dll4-Notch signaling. Loss of *sema3fb* leads to an increase in EC sprout size and *sflt1* expression, which suggests that the delayed migration also alters stalk cell dynamics. The changes in nuclear size and disrupted sprout formation indicate a possible role for *Sema3b* to oppose Vegf-mediated induction of PI3K signaling.

Chapter Three: MicroRNA26 attenuates vascular smooth muscle maturation via endothelial BMP signaling

This chapter is adapted from the publication: Charlene Watterston, Lei Zeng, Abidemi Onabadejo, Sarah J Childs. "MicroRNA26 attenuates vascular smooth muscle maturation via endothelial BMP signaling." PLoS genetics 15.5 (2019): e1008163.
DOI: : 10.1371/journal.pgen.1008163. eCollection 2019 May

3.1. Abstract

As small regulatory transcripts, microRNAs (miRs) act as genetic ‘fine-tuners’ of posttranscriptional events, and as genetic switches to promote phenotypic switching. The miR miR26a targets the BMP signaling effector, smad1. We show that loss of miR26a leads to hemorrhage (a loss of vascular stability) in vivo, suggesting altered vascular differentiation. Reduction in miR26a levels increases smad1 mRNA and phospho-Smad1 (pSmad1) levels. We show that increasing BMP signaling by overexpression of smad1 also leads to hemorrhage. Normalization of Smad1 levels through double knockdown of miR26a and smad1 rescues hemorrhage, suggesting a direct relationship between miR26a, smad1, and vascular stability. Using an in vivo BMP genetic reporter and pSmad1 staining, we show that the effect of miR26a on smooth muscle differentiation is non-autonomous; BMP signaling is active in embryonic endothelial cells, but not in smooth muscle cells. Nonetheless, increased BMP signaling due to loss of miR26a results in an increase in acta2-expressing smooth muscle cell numbers and promotes a differentiated smooth muscle morphology. Similarly, the forced expression of smad1 in endothelial cells leads to an increase in smooth muscle cell numbers and coverage. Furthermore, smooth muscle phenotypes caused by inhibition of the BMP pathway are rescued by loss of miR26a. Taken together, our data suggest that miR26a modulates BMP signaling in endothelial cells and indirectly promotes a differentiated smooth muscle phenotype. Our data highlights how crosstalk from BMP-responsive endothelium to smooth muscle is important for smooth muscle differentiation.

3.2. Introduction

Vascular smooth muscle cells (vSMCs) provide structural integrity to the vessel wall. Guided control of signaling cascades, including Platelet Derived Growth Factor (Pdgf), Notch, and Transforming Growth Factor-β/Bone morphogenic Protein (TGF-β/BMP) recruits and induces differentiation of perivascular mural cells (vSMCs and pericytes) to create a two-layered vessel wall with an internal endothelial cell lining and a muscle cell covering (Gaengel *et al*. 2009; Lamont *et al*., 2010; Liu *et al*., 2007). Once the vSMCs surround the vessel, they begin depositing extracellular matrix (ECM) proteins Laminin, Collagen IV, and Fibulins to support the vessel wall (Rensen *et al*., 2007). vSMCs then take on a mature phenotype that stabilizes the underlying endothelial cells through induction of quiescence, expression of junctional and attachment proteins, and expression of contractile proteins to provide myogenic tone (Lamont *et al*. 2010; David *et al*. 2008; Owens *et al*. 1996; Whitesell *et al*. 2014).vSMCs maintain phenotypic plasticity and can undergo a phenotypic switch from a quiescent contractile state to a proliferative synthetic state in response to cellular stimuli (Hendrix *et al.*, 2005; Rensen, Doevendans and Van Eys, 2007). Contractile vSMCs are defined by an elongated and thin 'spindle-shaped' morphology and low rates of proliferation. The expression of key differentiation markers such as smooth muscle (α)-actin (Acta2), smooth muscle β-myosin heavy chain (Myh11), and transgelin (Sm22α) allows vSMCs to perform their contractile function and provide vascular tone. In contrast, the immature synthetic vSMCs have reduced expression of contractile genes, produce ECM proteins, are highly proliferative, and have a rhomboid or rounded morphology (Lehoux *et al*., 2006; Mack & Owens, 1999; Miano *et al*., 1994; Owens *et al*., 2004).

Numerous studies have demonstrated that BMP signaling through Smad1 modulate vSMC plasticity (reviewed by Cai *et al*. 2012). Defective BMP signaling can affect both endothelial and vSMC cells (Benjamin *et al*., 1998; Beppu *et al*., 2000; El-Bizri *et al*., 2008; Lan *et al*., 2007; Li *et al*., 1996; Mishina *et al*., 1995; Roman *et al*., 2002; Torihashi *et al*., 2009). Aberrant vSMCs phenotype switching plays a critical role in the pathogenesis of vascular diseases, such as hereditary hemorrhagic telangiectasia (HHT) and pulmonary arterial hypertension (PAH). In canonical Smad-mediated BMP signaling, Smad1 is phosphorylated by the serine-threonine kinase activity of a type 1 BMP receptor (ACVRL1 (ALK1)/ BMPR1A, BMPR1B) allowing it to associate and dimerize with the co-mediator Smad4 and translocate to the nucleus to control gene

transcription. Murine homozygous null mutants for BMPR-1a (Activin like kinase 3, ALK3) or the type II receptor BMPR-2 (which is mutated in human patients with PAH) (Orvis *et al*., 2008; Paul *et al*., 2005) and their ligand Bmp4 or downstream co-Smad4 are embryonic lethal, and present with vascular deformities attributable to a loss of Smad1 mediated signaling (Sirard *et al.*, 1998). Mutations in ALK1 lead to HHT2, a disease characterized by arteriovenous malformations (AVMs) (McDonald *et al*., 2011). Deletion of Alk1 in mice leads to cranial hemorrhages, AVM-like fusion of micro-vessel plexi, dilation of large vessels, and reduced coverage of vessels by vSMCs (Park *et al.*, 2006). In fish, disruption of *Alk1* signaling results in pathological arterial enlargement and maladaptive responses to blood flow that generate AVMs. Potential vSMCs defects in this model have not been assessed (Corti *et al.*, 2011).

As small non-coding RNAs, microRNAs (miRs) regulate gene expression of key vSMC marker genes to control vSMC dynamics. (Albinsson *et al*., 2010; Ji *et al*., 2007; Xie *et al*. 2011; Zhang, 2010). A number of miRs have been identified as modulators of the vSMC phenotype *in vitro* and *in vivo,* including *miR-145, miR-21, miR-221, miR-222,* and *miR-146a* (Ali *et al*., 2015; Cordes *et al*., 2009; Rangrez *et al*., 2011; Sarkar *et al*., 2010; Sun *et al*., 2011; Wang *et al*., 2010; Xin *et al*., 2009; Xu *et al*., 2011; Zeng *et al*., 2009). We previously showed that miR-145 promotes visceral smooth muscle differentiation via controlling cross-talk between epithelial cells and smooth muscle (Zeng, Carter and Childs, 2009; Zeng and Childs, 2012). Here, we investigate the role of *microRNA26a* (*miR26a*) in regulating vSMC dynamics using the zebrafish model of vessel stabilization. *miR26a* regulates proliferation, migration, and differentiation of vSMCs and has been shown to target *smad1*, a key intracellular mediator of BMP signaling, in cultured vSMCs *in vitro* (Bai *et al.*, 2011; Leeper *et al.*, 2011; Icli, Dorbala and Feinberg, 2014; Yang *et al.*, 2017). *miR26a* expression is altered during abdominal aortic aneurysm (AAA) and neointimal lesion formation (Leeper *et al.*, 2011; Yang *et al.*, 2017). However, the role of *miR26a in vivo* in an intact animal in the context of developing vSMCs is largely unknown. Using a combination of genetic gain and loss of function methods to understand the role of *miR26a in vivo,* we show that *miR26a* acts within a BMP responsive pathway to fine-tune vSMC maturation via targeting *smad1*. Interestingly, we find that active BMP signaling and changes in Smad1 activation are observed within endothelium *in vivo,* and not in smooth muscle cells. Together the evidence suggests that *miR26a* plays a role in regulating blood vessel stabilization via a non-autonomous mechanism.

3.3. Materials and Methods

3.3.1. Zebrafish maintenance and husbandry

All animal procedures were approved by the University of Calgary Animal Care Committee (AC17-0189). Zebrafish (Danio rerio) embryos were collected and incubated at 28.5 °C in E3 embryo medium and staged in hours post-fertilization (hpf) or days post fertilization (dpf). Endogenous pigmentation was inhibited from 24 hpf by the addition of 0.003% 1-phenyl-2-thiourea (PTU, Sigma-Aldrich) in E3 embryo medium. The fluorescent transgenic endothelial mCherry-expressing Tg(kdrl:mCherry)ci5, GFP-expressing Tg(kdrl:EGFP)la116 report endothelial expression and Tg(fli1a:nEGFP)y7 (Roman *et al*. 2002) reports EGFP cDNA fused to a nuclear localization sequence in endothelial nuclei. Tg(acta2:GFP)ca7 and Tg(acta2:mCherry)ca8 report smooth muscle expression (Whitesell *et al*. 2014). BMP-reporter fish Tg(BRE-AAVmlp: EGFP)mw29 [BRE: EGFP] report active BMP signaling (Collery and Link 2011).

3.3.2. Morpholino knockdown, CRISPRi, and mRNA overexpression

Both MO and mimic were injected into one- to four-cell stage embryos within recommended dosage guidelines (Bill *et al.*, 2009; Schulte-Merker and Stainier, 2014). Injected doses were 1ng/embryo for *miR26a* MO, Scrambled (Scr.) control, *miR26a,* and *smad1* MO. Morpholinos (MO) were obtained from Gene Tools LLC Corvallis, OR, USA. *mir-26a* MO blocks the mature microRNA (5 AGCCTATCC*TG*GATTACT*TG*AAC-3’), *miR26a* Scrambled control has 6bp mismatch (5’-ACCGTATCG*TG*CATTACTTCAAC-3’), and *smad1* MO blocks Smad1 translation (5’-AGGAAAAGAG*TG*AGG*TG*ACATTCAT-3’) (McReynolds *et al.*, 2007). For rescue experiments, embryos were first injected with *miR26a* MO and then *smad1* MO. To control for non-specific neural cell death that occurs from nonspecific activation of p53 with morpholinos, a standard p53 MO was co-injected with high dose morpholino to establish a dosage curve. Hsa *miR26a* miRIDIAN mimic was obtained from Dharmacon (Chicago IL) and injected in a dose of 3ng/ embryo. For CRISPRi mediated knockdown of *miR26a,* sgRNA were designed using CHOPCHOP (Montague *et al.*, 2014; Labun *et al.*, 2016) to target the seed sequence of *miR26a* family members, to reduce *miR26a* processing. *MiR26a-1, miR26a-2, miR26a-3,* are independent genes located on different chromosomes. *miR26b* differs by one nucleotide. To generate sgRNA we followed a method established by (Narayanan *et al.*, 2016). 10 μmol of forward primer and 50

μmol of a universal reverse primer (IDT Oligos, Iowa) were annealed and filled in (Montague *et al.*, 2014), purified (Qiagen PCR purification kit) and *in vitro* transcribed (T7 mMessage machine, Ambion)

F:(5'TAATACGACTCACTATAGGATCCTGGATTACTTGAACCAGTTTTAGAGCTAGAA-3′)

R:(5′AAAAGCACCGACTCGGTGCCACTTTTTCAAGTTGATAACGGACTAGCCTTATTTTAACTTGCTATTTCTAGCTCTAAAAC-3′)

Zebrafish codon-optimized dCas9 plasmid (Rossi *et al.*, 2015) was linearized with XbaI and *in vitro* transcribed using Ambion Maxi Kit (Life Technologies Inc., Burlington, ON), and RNA purified using an RNeasy Mini Kit (Qiagen). Zebrafish embryos at the one-cell stage were injected with 200pg of a solution containing 75 ng/μl of sgRNA with 150 ng/μl of Cas9 mRNA. For overexpression of *smad1*, mRNA was *in vitro* transcribed as described (McReynolds *et al*. 2007; gift from Todd Evans Lab) using mMessage mMachine (Life Technologies Inc., Burlington, ON). 40pg of mRNA was injected per embryo at the 1 cell stage

3.3.3. Plasmid construction

For endothelial-specific overexpression, *smad1* was amplified from zebrafish cDNA using primers that incorporate attb1/b2 recombination sites

(5'GGGGACAAGTTTGTACAAAAAAGCAGGCTTCACCATGAATGTCACCTCACTCTTTTCC-3') and

(3'GGGGACCACTTTGTACAAGAAAGCTGGGTGCTAGGACACTGAAGAAATGGGGT-5') and inserted into pDONR221 to create a pME-*smad1* vector. Three-way Tol2 gateway cloning (Kwan *et al.*, 2007) was used to insert *smad1* downstream of the *kdrla* promoter to achieve a TolCG2:*kdrla:smad1* vector. One-cell stage zebrafish embryos were injected with a solution consisting of 5-20 ng/μl *kdrla-smad1* plasmid and 50 ng/μl transposase mRNA.

For the *in vivo* sensor test, *smad1* 3′UTR forward and reverse oligos (IDT, Iowa) were designed incorporating BamHI and Bsrg1 sites using the prediction software TargetScan (Lewis, Burge and Bartel, 2005) for miR26 targets within the 3'UTR of zebrafish *smad1 (*underlined).

(5'GCGTGTACACCGGATGACTAGAGGGTTAGGTTGTGTACTACTTGAAGGCAGTTTGTTAGGGTGGGGGTCATCGAATCTGGCTGAAGAGTCCTCAGTTTTCAGCCCGTGAGAATCTGGAAGATACTTGACAACTCTGTGGCCGGATCCATA-3') and

(3’TATGGATCCGGCCACAGAGTTGTCAAGTATCTTCCAGATTCTCACGGGCTGAAAA
CTGAGGACTCTTCAGCCAGATTCGATGACCCCCACCCTAACAAACTGCCTTCAAGTA
GTACACAACCTAACCCTCTAGTCATCCGGTGTACACGC-5’). Oligos were digested and ligated into the p3E-polyA vector. This construct was then recombined into pDestTol2pA2 by Gateway cloning to achieve a CMV-SP6 promoter upstream of EGFP: *smad1* 3′UTR: EGFP or a control EGFP: p3E-polyA 3′UTR. Sensor mRNA and mCherry mRNA were in vitro transcribed from the pCS2 Gateway compatible vector (39) by using the mMessage Machine SP6 kit (Ambion). One-cell zebrafish embryos were injected with 150 pg sensor mRNA and 100 pg mCherry mRNA. When applicable, *miR26a* MO or miRNA mimic were added. Live embryos were imaged with an identical exposure time at 24 hpf (n = 10/group). The average pixel intensity for fluorescence was measured as described (17).

3.3.4. Cell sorting, RNA Isolation, and RT-qPCR

For FACS analysis ~200 embryos were collected from 4 dpf Tg(acta2: EGFP;kdrl:mCherry) fish. Embryos were anesthetized with 0.4% Tricaine (Sigma) and heads dissected and pooled. Single-cell dissociation was performed according to Rougeot *et al*. 2014. Briefly dissected embryo heads were washed once with calcium-free Ringers Solution and gently triturated 5-10 times before dissociation solution was added and incubated in a 28.5°C water bath with shaking and periodic trituration for 45min. The reaction was stopped, centrifuged, and resuspended in Dulbecco’s Phosphate-Buffered Saline (GIBCO), centrifuged and resuspended in fresh resuspension solution. The single-cell suspension was filtered with 75 µm, followed by 35 µm filters. Cells were then sorted with a BD FACSAria III (BD Bioscience, San Jose, USA) and collected. Total RNA from 48hpf whole embryos, 4dpf dissected embryo heads or FACS sorted cells was isolated using the miRNeasy Mini Kit (Qiagen). For microRNA RT-qPCR, 5ng of total RNA from each sample was reverse transcribed using the miRCURY LNA™ Universal RT cDNA Synthesis Kit and expression assayed using the miRCURY LNA™ Universal RT microRNA PCR System (Qiagen). For miRNA expression primers were ordered for
miR26a-5p (MIMAT0000082, Target sequence: UUCAAGUAAUCCAGGAUAGGCU), and, expression levels normalized to that of miR-103a-3p
(MIMAT0000425, Target sequence: CAGUGCAAUGUUAAAAGGGCAU)

For gene expression, zebrafish specific Taqman assays were used: smad1 (Cat# 4351372, Clone ID: Dr03144278_m1), acta2 (4331182, Dr03088509_mH), myh11a (444889, Dr03141711_m1), pdgfrβ (4441114, ARKA4GC), pdgfba (4441114, ARWCXGT), nothch3 (4448892, Dr03432970_m1) and normalized to β-actin (4448489, Dr03432610_m1). 500 ng of total RNA from each sample was reverse transcribed into cDNA using and assayed using according to manufacturer's protocols in a 5ng/10ul final reaction using TaqMan™ Fast Advanced Master Mix (Thermo Fischer). Reactions were assayed using a QuantStudio6 Real-time system (Thermo Scientific). The ΔΔCt method was used to calculate the normalized relative expression level of a target gene from triplicate measurements. Experiments were repeated independently at least three times unless stated otherwise.

3.3.5. Small molecule inhibition

K02288 was used at a dose of 15μM (SML1307, Sigma). DSMO (D8418, Sigma) was used as a vehicle and control. Drug stocks were heated for 20min at 65C and then diluted in E3 embryo medium. Drug or control was applied to the media from 52hpf until 4dpf. Embryos were grown at 28.5C in the dark until imaging, and drug changed once.

3.3.6. In situ hybridization and Immunostaining

All embryos were fixed in 4% paraformaldehyde in PBS with 0.1% Tween-20 at 4 °C overnight, followed by 100% methanol at −20 °C. Digoxigenin (DIG)-labeled antisense RNA probes were used for in situ hybridization. Probes for *smad1* (construct described by (McReynolds *et al.*, 2007)) *sm22a, acta2, myh11a* were synthesized from PCR fragments previously described (Georgijevic *et al.*, 2007; Whitesell *et al.*, 2014). Probes were synthesized by using SP6 or T7 RNA polymerase (Roche). *miR26a* double-DIG-labeled LNA probe was obtained from Exiqon. In situ hybridization was performed as described using a Biolane HTI robot (Holle and Huttner AG, Tubingen, Germany). For microRNA in situ hybridization, a double-DIG-labeled Locked Nucleic Acid (LNA) probe (Exiqon, Copenhagen, Denmark) was used to detect the mature miR26a in whole-mount embryos as recommended by the manufacturer with the modification that hybridization was at 54 °C. For whole-mount immunostaining, an antigen retrieval protocol optimized from (Lopez-Rios, 2012) was used. Briefly, embryos are hydrated into PBST, washed twice with 15 mM Tris–HCl pH 9.5, 150 mM EDTA and then heated in 15 M Tris–HCl pH 9.5, 150 mM EDTA at 70˚C

for 15 minutes. Embryos are then washed 3 times in PBST at room temperature and incubated in 10% normal sheep serum in PBST with 1% triton block and incubated for at least 48 hours at 4˚C in primary antibody. Phospho-SMAD1/5/9 (pSMAD1/5/9) was detected with Rabbit anti-Phospho-Smad1 (Ser463/465)/Smad5 (Ser463/465)/Smad9 (Ser426/428) (1:400; Cell Signaling Technology), GFP was detected with mouse anti-GFP antibody, JL8 (1:500, Clontech) and detected with Alexafluor 647 or 488 secondary antibodies for 1 hour at room temp in 5% normal sheep serum/PBST with 0.1% triton (1:500;Invitrogen).

3.3.7. Imaging and data analysis

For imaging, embryos were immobilized in 0.004% Tricaine (Sigma) and mounted in 0.8% low melt agarose on glass-bottom dishes (MatTek, Ashland, MA). Confocal images were collected on a Zeiss LSM 700 inverted microscope. Image stacks were processed in Zen Blue and are presented as maximal intensity projections and analyzed using FIJI/ImageJ (Rasband, W.S., ImageJ, U. S. National Institutes of Health, Bethesda, Maryland, USA, https://imagej.nih.gov/ij/, 1997-2018). For cell counts, images were converted to 16-bit using ImageJ, and the threshold adjusted to allow counting of cells over a region of the VA from the anterior bulbous arteriosus (BA) to the most anterior pharyngeal arch arteries (PAA).

To measure intensity, total cell fluorescence (CTCF) was calculated using the formula: CTCF = Integrated Density - (Area of selected cell X Mean fluorescence of background readings). The area for measurement was gated by tracing the aorta from bulbous where the bulbous arteriosus merges with the ventral aorta to the distal tip of the ventral aorta or the bifurcation point of the ventral aorta using the free form drawing tool, whichever was shorter (Isogai, Horiguchi and Weinstein, 2001).

For measurement of vSMC cell heights, measurements were made from the endothelial *kdrla*: EGFP expression to the highest point of the vSMC. 8 measurements were taken for each sample where possible. Ventral head measurements were taken from the ventral aorta and the aortic arch arteries. Measurements represent mean vessel diameter ± standard deviation in micrometers.

3.3.8. Statistical analysis.

Distribution of data points are expressed as mean ± standard error of the mean (S.E.M.), or as the relative proportion of 100% as mentioned in the appropriate legends. Depending on the number of the groups and independent factors, student's t-tests, one-way or two-way analyses of variance (ANOVA) with non-parametric tests were used as indicated in the figures. Two treatment groups were compared using Student's t-test, using Welch's correction. Three or more treatment groups were compared by one- or two-way ANOVA followed by post hoc analysis adjusted with a least significant-difference correction for multiple comparisons using GraphPad Prism version 7.00 (La Jolla California USA). Results were classed as significant as follows: *$P < 0.05$, **$P < 0.01$, and ***$P < 0.001$.

3.4. Results

3.4.1. miR26a is expressed in developing blood vessels

miR26a targets *smad1* and thereby directly regulates BMP signaling (Leeper *et al.*, 2011; Ali *et al.*, 2015) (Figure 3.1 A). To observe the spatial gene expression pattern of *miR26a* in developing embryos we used *in situ* hybridization. At 48hpf, *miR26a* has a ubiquitous expression pattern (Figure 3.1 B-B'), however by 4dpf expression becomes enriched in the ventral head of the embryo, with strong expression in the pharyngeal region, bulbus arteriosus, and ventral aorta (Figure 3.1 C). *miR26a* is expressed in and around the blood vessel endothelium where it could potentially play a role modulating BMP signaling in blood vessels (compare to *kdrl: GFP* stain; Figure 3.1 C', inset).

In order to further analyze the cell-specific expression of *miR26a,* we used fluorescent-activated cell sorting (FACS) to isolate $EGFP^{+ve}$ vSMCs and $mCherry^{+ve}$ endothelial cells from 4dpf *Tg(acta2:EGFP;kdrl:mCherry)* embryos. In keeping with the *in situ* hybridization data, RT-qPCR showed that *miR26a* is indeed expressed in both cell types, although it is not significantly enriched in endothelial cells (Figure 3.2 B). FACS sorting efficiently separated vSMCs and endothelial cells; we find that *acta2: $EGFP^{+ve}$* vSMCs cells have an average 37.4-fold enrichment in *acta2* expression, and minimal expression of *alk1* or *smad1* when compared to *kdrl: mCherry* endothelial cells. However, *smad1* is 14-fold enriched, and *acvrl1* is 3.5-fold enriched in *$mCherry^{+ve}$* endothelial cells while there is nearly no expression of *acta2* (Figure 3.2 C). Thus a *miR26a* target, *smad1* is enriched in endothelial cells.

3.4.2. BMP signaling is active in the aorta endothelium

We next tested the relationship between *mir26a* expression and activated BMP signaling using an *in vivo* reporter of Smad1/5 activity. *Tg(BRE:EGFP]* transgenic fish encodes EGFP driven by an upstream *Bmp Response Element (BRE)* that contains multiple short Smad-binding sites from the *inhibitor of differentiation-1 (id1)* promoter, a major transcriptional target of canonical Bmp/Smad1 signaling (Collery and Link, 2011; Laux, Febbo and Roman, 2011). We crossed *Tg(BRE:EGFP]* to endothelial *Tg*(*kdrl*:mCherry*)* or vSMC *Tg(acta2:mCherry)* lines to observe BMP activation in endothelial and vSMCs, respectively (Figure 3.1 D and G). We use the 4dpf time point as vSMC cells first differentiate and begin to express the mature marker *acta2* between 3 and 4dpf (Georgijevic *et al.*, 2007; Whitesell *et al.*, 2014).

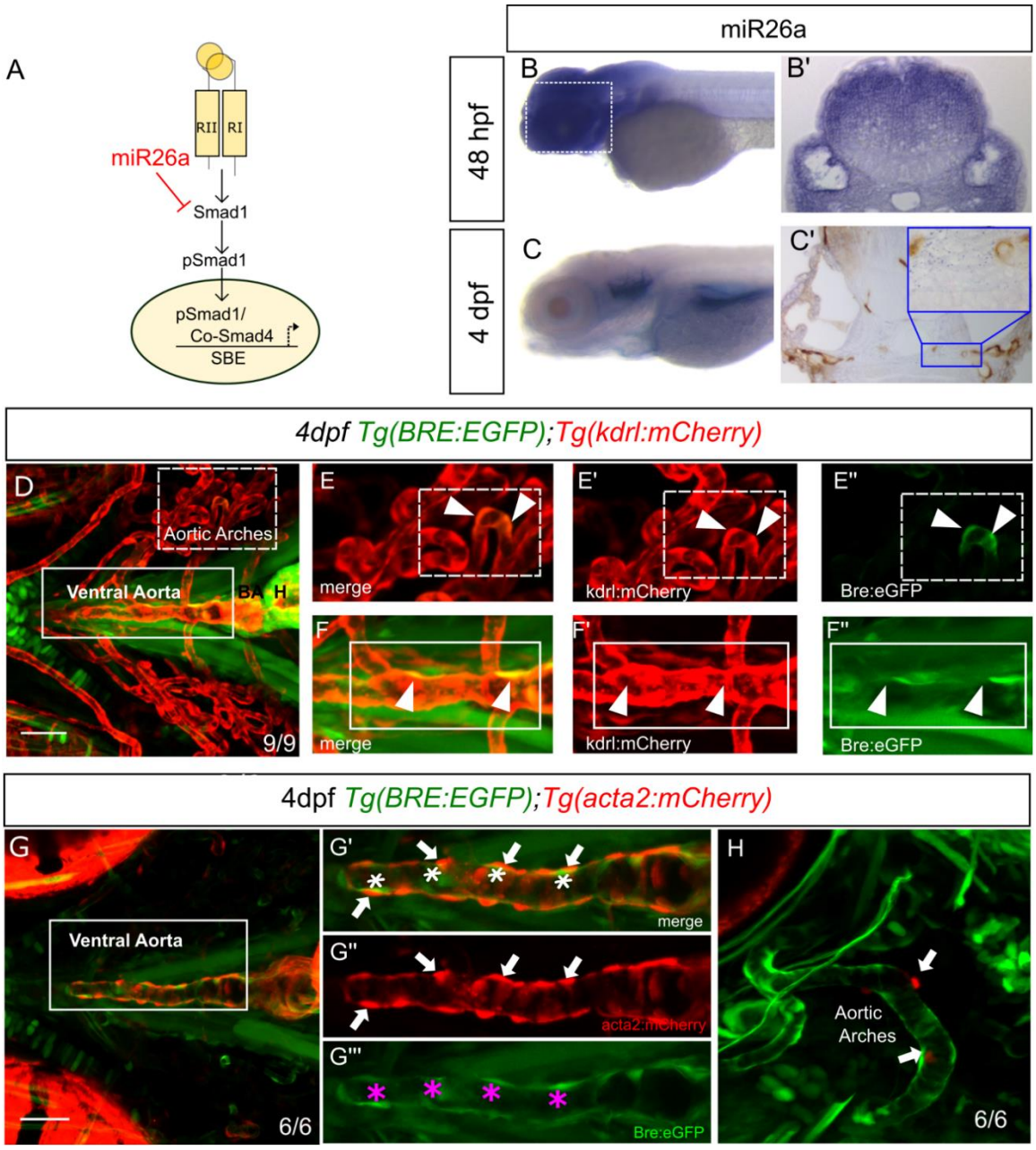

Figure 3.1: miR26a is expressed in blood vessels; endothelial cells have active BMP signaling.

A) Model of how *miR26a* controls BMP signaling via direct targeting of *smad1*. B) Lateral view of whole-mount in situ expression of *miR26a* at 2dpf shows ubiquitous expression pattern, with strong expression in the ventral head of the embryo. B') Cross-section of the head at 48 hpf. C) At 4dpf *miR26a* is expressed in the pharyngeal arches, bulbous arteriosus, and ventral aorta. C') Cross-section of the head showing miR26a expression in blood vessels (purple; punctate stain)

compared with endothelial stain (brown; kdrl:GFP transgenic). Inset is an enlargement of image in C'. D) Ventral view of the pharyngeal region of a 4 dpf double transgenic *Tg(BRE:EGFP);Tg(kdrl:mCherry)* embryo shows BRE:EGFP (green) expression within endothelial cells in aortic arches (red, white arrowheads in E'-E''') and ventral aorta (red, white arrowheads F'-F'''). G-H) Ventral and lateral views of a 4 dpf double transgenic *Tg(BRE:EGFP); Tg(acta2:mCherry)* zebrafish shows that *acta2* positive cells are in direct contact with BMP-responsive endothelial cells but do not express BRE:EGFP. Scale bar= 50μm. n/N = number of embryos /Total number of embryos. microRNA26 ISH in B-C was performed by Lei Zeng

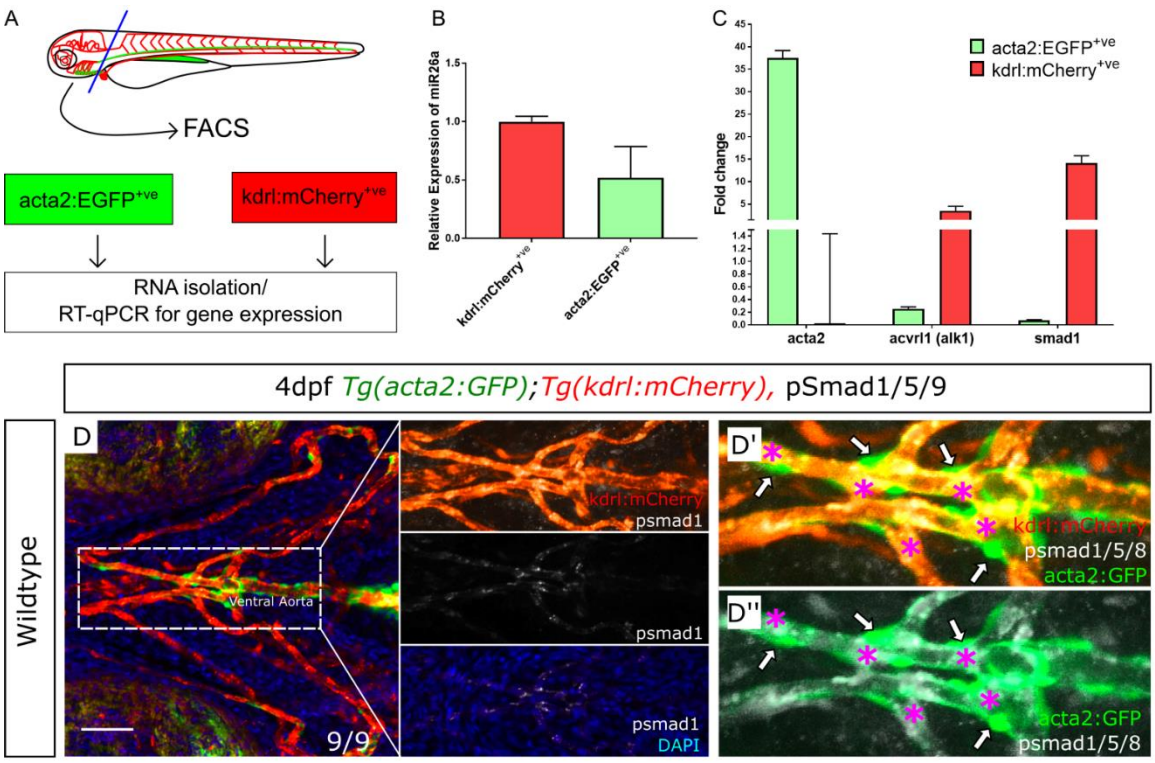

Figure 3.2: p*Smad1* is observed in endothelial cells

A) Schematic of FACS sorting strategy for acta2:EGFP+ and kdrl:mCherry+ cells from 4dpf Tg(acta2:EGFP;kdrl:mCherry) dissected embryo heads. B) Expression level of *miR26a* in acta2:EGFP+ and kdrl:mCherry+ isolated by FACS (n=2). C) Expression level of *smad1*, *acvrl (alk1)* and *acta2* in acta2:EGFP+ and kdrl:mCherry+ isolated by FACS (n=2). RT-qPCR analysis of values represents mean ± SEM, n= biological replicates. D) Wholemount immunohistochemistry of pSmad1/5/9 in Tg(*acta2*:EGFP)^{ca7}; Tg(kdrl:mCherry)^{ci5} shows nuclear staining of pSmad1 in endothelial cells. B-B)' pSmad 1/5/9 is observed in endothelium (red) but not smooth muscle (green) of the hyoid artery and afferent branchial arches. Magenta asterisk indicates pSmad1/5/9 stain; arrows indicate smooth muscle cells. Scale bar= 50µm. n/N = number of embryos/Total number of embryos.

Surprisingly, although miR26a has been implicated in controlling Smad1 regulated vSMC dynamics directly, we found that transgenic *BRE:EGFP* signals are restricted to the endothelium of the vessel wall and have co-localized expression with *kdrl:mCherry* (Figure 3.1 E-E' and F-F'). The *acta2:mCherry*-positive vSMCs lie directly adjacent to *BRE:EGFP*-expressing cells, with no detectable expression of *BRE:EGFP* in vSMCs on the ventral aorta or in pharyngeal aortic arch arteries (Figure 3.1 G-G", H, both ventral and lateral projections are shown). Similarly, *acta2:mCherry*-positive cells are closely associated with pSmad1-positive endothelial cells but do not show pSmad1 staining (Figure 3.2 Fig D). Together, our data suggest that in early development, *miR26a* and *smad1* are expressed within endothelial cells where BMP signaling is also active, as visualized by two methods of detection.

3.4.3. Loss of miR26a leads to upregulation of smad1 mRNA

The highly conserved miR-26 family constitutes *miR26a-1, miR26a-2, miR26a-3,* and *miR26b* (Bai *et al.*, 2011) as identified by their seed sequences and accessory sequence. In zebrafish and humans, *miR26a-1, miR26a-2,* and *miR26a-3* have the same mature sequence and only differ from the mature *miR-26b* sequence by two nucleotides (Griffiths-Jones *et al*., 2008; Icli *et al*., 2014).

To investigate the role of *miR26a* in vascular development *in vivo,* we knocked down *miR26a* using an antisense morpholino that targets the mature miRNA seed sequence of all three *miR26a* isoforms. A 6bp mismatch scrambled control morpholino was used as a control. 1ng doses of morpholino were used, as suggested by current guidelines (Bill *et al.*, 2009; Bedell, Westcot and Ekker, 2011). In parallel, we designed a second genetic knockdown approach using CRISPR interference (CRISPRi) (Long *et al.*, 2015) to target the pri-miR hairpin structure using the complementary sequence to the mature miRNA (Figure 3.3 A). RT-qPCR shows a 26% (0.74±0.65) reduction in miR26a following *miR26a* MO knockdown and 34% (0.65±0.10) reduction of *miR26a* using CRISPRi (Figure 3.3 B, C) confirming that both knockdown methods result in decreased *miR26a* expression. *smad1* is a demonstrated target of *miR26a in vitro*(Leeper *et al.*, 2011; Ali *et al.*, 2015). In support of *smad1* being a *miR26a* target *in vivo, miR26a* knockdown results in increased *smad1* expression in 2dpf and 4dpf injected embryos as compared to controls by in situ hybridization (Figure 3.3 D) and resulted in an average 1.6-fold and 1.8-fold increase by RT-qPCR, respectively (Figure 3.3 E and F).

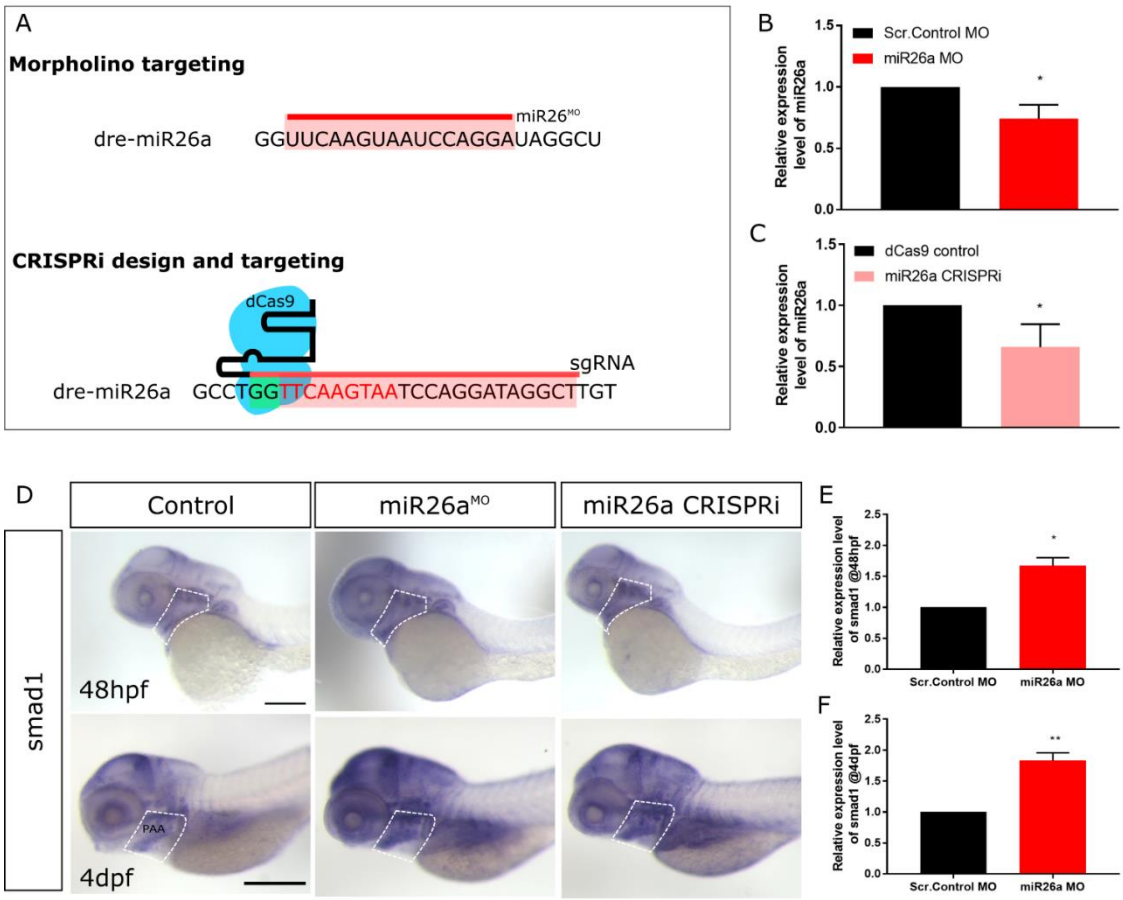

Figure 3.3: *miR26a* knockdown increases *smad1* expression.

A) Schematic of miR26a transient knockdown methods. B and C) Relative expression level of *miR26a* in morpholino and CRISPRi injected embryos at 48hpf (n=3). D) Whole-mount in situ hybridization staining for *smad1* at 48hpf and 4 dpf shows increased expression of *smad1* in *miR26a* knockdown embryos particularly in the ventral aorta, aortic arches, and pharyngeal region (dotted outline). Scale bar= 200µm. E) Relative expression of *smad1* in 48 hpf morphants is increased compared to control embryos (n=3). F) Relative expression of *smad1* in 4dpf *miR26a* morphants is increased compared to control embryos (n=4). RT-qPCR data show the mean ± SEM, Student's two-tailed t-test *$p < 0.05$, n, number of biological replicates.

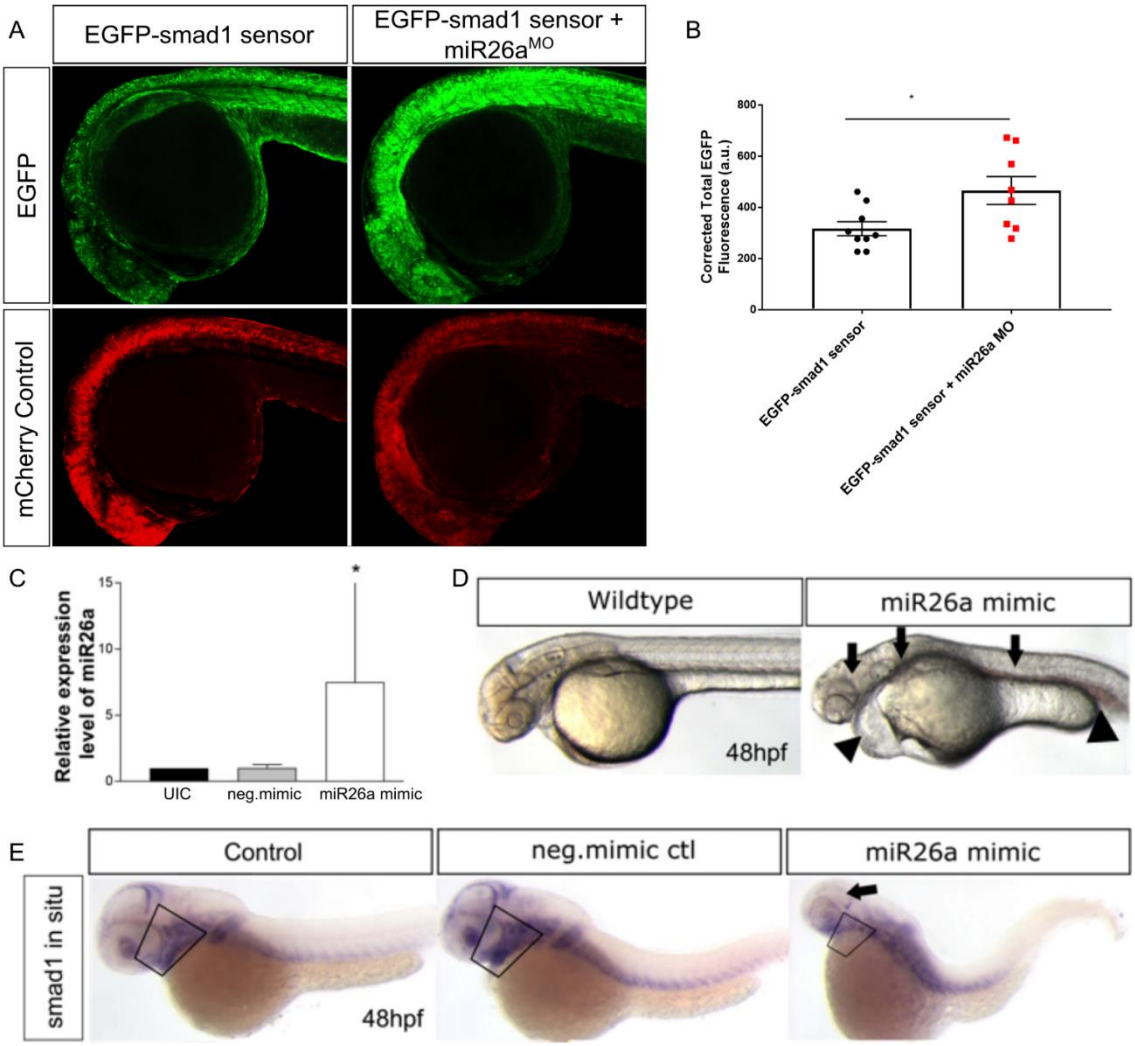

Figure 3.4: *miR26a* overexpression decreases *smad1* expression

A) EGFP:*smad1* sensor assay. B) Quantification of EGFP fluorescence compared to controls. Student's two-tailed t-test *p=0.05, N=3, total of 9 embryos per group, Error bars = SEM, Scale bar= 50µm. C) RT-qPCR of relative expression of *miR26a* in *miR26a*-mimic injected embryos at 2dpf. Values are means of 3 replicates and normalized to *miR122*; Unpaired t-test, *p<0.01 as compared to control; Error Bars = SD. D) *miR26a* mimic injected embryo with mild dorsalization phenotype, heart edema (arrowhead), dorsal axis defects (arrows), and poor circulation (arrowhead at tail) at 2dpf. E) Whole-mount in situ hybridization staining for *smad1* at 48hpf in uninjected control, negative control mimic and *miR26a* injected embryos. There is decreased expression of *smad1* in miR26a mimic injected embryos (boxes and arrow). microRNA26 mimic and ISH in C-E were performed by Lei Zeng

To further determine whether *miR26a* can regulate smad1 expression *in vivo*, we designed a sensor assay and fused the *smad1* 3′UTR to EGFP (*EGFP: smad1pA*) and injected it with an internal mCherry control into single-cell zebrafish embryos in the presence or absence of a *miR26a* morpholino. When fluorescence levels were examined at 24hpf, injections of *EGFP: smad1pA* sensor mRNA alone resulted in high EGFP expression; however, this fluorescence was enhanced by over 65% by co-injection of miR26a morpholino (Figure 3.4 Fig A, B). At 4dpf, upregulation of *smad1* in *miR26a* morphants and CRISPRi knockdown embryos is more prominent in the ventral pharyngeal region, with staining in the ventral aorta, aortic arches, and bulbous arteriosus (Figure 3.3 D, highlighted areas), similar to where *miR26a* is expressed most strongly (Figure 3.1 B-C).

In a complementary approach, we injected a *miR26a* mimic to overexpress *miR26a* and observe an increase in *miR26a* expression by RT-qPCR (Figure 3.4 Fig C), and a marked reduction of *smad1* expression in the ventral pharyngeal region by in situ hybridization (Figure 3.4 Fig E). Overexpression of *miR26a* results in mildly dorsalized embryos by 48hpf with pericardial edema, dorsal axis defects, and poor circulation (Figure 3.4 Fig D), suggesting overexpression of *miR26a* disrupts the BMP pathway that patterns early embryonic axes.

3.4.4. Loss of miR26a leads to increased phosphor- Smad1 in endothelium

We next tested whether the increased expression of *smad1* mRNA in *miR26a* knockdown embryos leads to enhanced Smad1 phosphorylation. Wildtype immunostaining showed pSmad1/5/9 is high in endothelium but not in vSMCs (Figure 3.2 Fig D-D’’). *miR26a* knockdown embryos do not show any significant difference in endothelial cell number as compared to controls, using endothelial nuclear transgenic lines (*Tg(fli1a:nEGFP; kdrl:mCherry);* Figure 3.5 A-D, and Figure 3.6). However, there is a significant 20% increase in pSmad1 positive/ *fli1a:nEGFP* nuclei in *miR26a* knockdown embryos as compared to controls, with an average of 60±3.1% and 64.9±3.9% in *miR26a* morphants (Figure 3.5 B-B’’ and F) and CRISPRi embryos (Figure 3.5 D-D’’ and G), respectively as compared to 41±2.9 and 46±6.5% in controls.

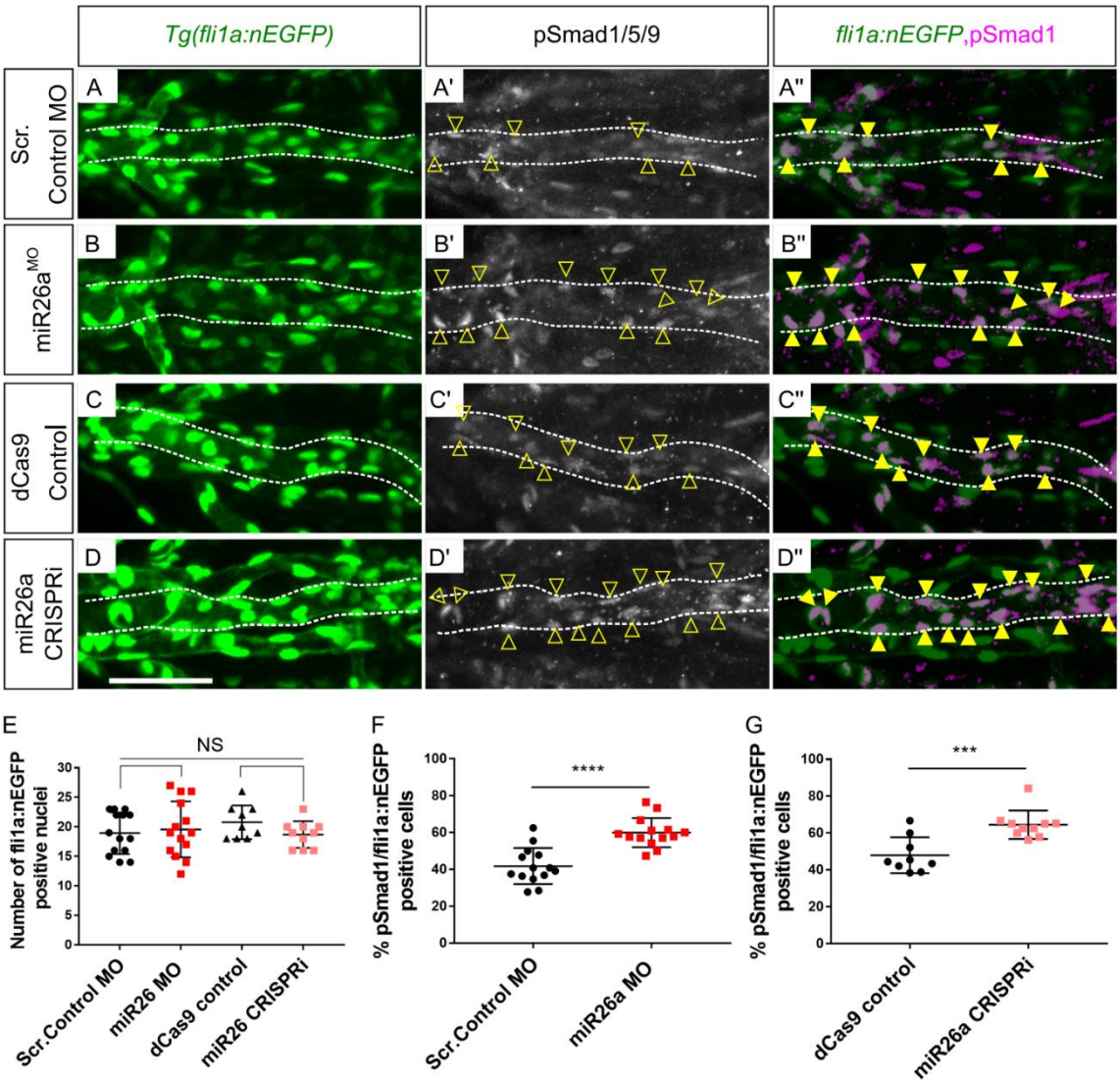

Figure 3.5: *miR26a* knockdown embryos have increased endothelial pSmad1. Ventral view confocal projections of the 4dpf ventral aorta (dotted outline). Endothelial nuclei (*fli1a:nEGFP*; A-D, arrowheads) and pSmad1/5/9 (pSmad1,white E-H) and overlay (magenta, I-L) in 4dpf Scr. Control (A,E,I), *miR26a* MO (B,F,J), dCas9 control (C,G,K) and *miR26a* CRISPRi (D,H,L) embryos. Yellow arrowheads indicate double positive pSmad1 + *fli1a:nEGFP* nuclei in the ventral aorta. M) Total number of *fli1a:nEGFP* nuclei in the ventral aorta. N and O) Percentage of double pSmad1; *fli1a:nEGFP* positive nuclei in *miR26a* morphants and miR26a CRISPRi embryos. N=3: Scr.MO n =14, miR26a MO n=14, dCas9 cont n=9 and *miR26a* CRISPRi n=10. Student's two-tailed t-test, $p<0.0001$ as compared to WT, error bars = SD. Scale bar: 50μm

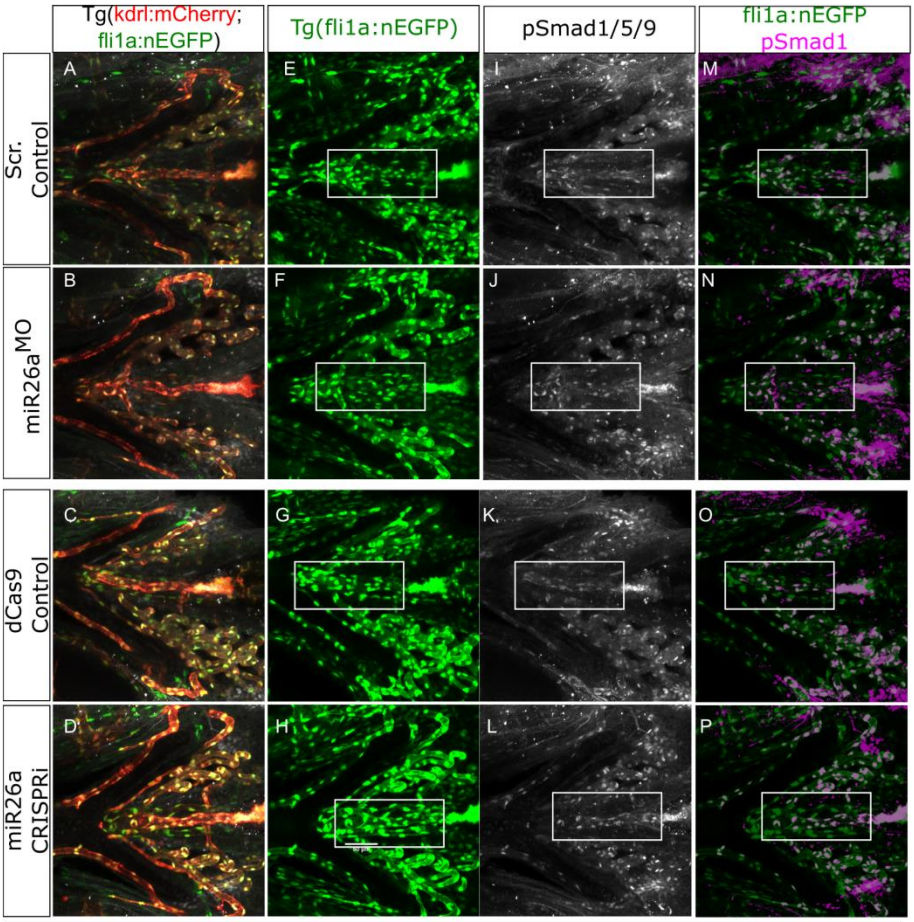

Q

	Number of fli1a:nEGFP positive cells			Percentage of pSmad1/fli1a:nEGFP positive cells	
	Scr. Control	miR26a MO		Scr. Control	miR26a MO
Trial 1	19	20	Trial 1	40.33	57.71
Trial 2	20	16	Trial 2	39.66	59.59
Trial 3	19	21	Trial 3	45.67	63.79
Average	18.97	18.93	Average	41.67	60.36
SD	0.47	2.61	SD	2.91	3.11

R

	Number of fli1a:nEGFP positive cells			Percentage of pSmad1/fli1a:nEGFP positive cells	
	dCas9 Control	miR26a CRISPRi		dCas9 Control	miR26a CRISPRi
Trial 1	21	18	Trial 1	43.78	68.90
Trial 2	20	20	Trial 2	42.27	61.09
Trial 3	22	18	Trial 3	54.33	64.72
Average	20.64	18.61	Average	46.79	64.90
SD	1.05	0.79	SD	6.57	3.91

Figure 3.6: miR26a knockdown embryos have increased endothelial p*Smad1*.

Ventral confocal projections of 4dpf Tg(*kdrl:mCherry; fli1a:nEGFP* ventral aorta (dotted outline,A-D). E-H) pSmad1/5/9 (white I-L) and overlay (magenta, M-P) Q) Average number of fli1a:nEGFP nuclei. R) Average percentage pSmad1/fli1a:nEGFP double positive nuclei. Scale bar: 50 μm

3.4.5. Increased levels of smad1 lead to vascular stability defects

Loss of *miR26a* leads to compromised vessel integrity at 2dpf. *miR26a* morphants have an average 13±2% hemorrhage (Figure 3.7 B and D) and CRISPRi embryos have an average 15±1% hemorrhage (Figure 3.7 C and D) as compared to 2-3% rate of the controls. The phenotype is dose-dependent as higher doses of morpholino lead to an increase in hemorrhage to 40% and a 1.8-fold reduction in *miR26a* expression (Figure 3.8 C, D). As *smad1* overexpression has not been previously connected to vascular stability defects, we next tested whether overexpressed *smad1* could lead to hemorrhage. Injection of *smad1* mRNA into single-cell stage embryos resulted in a significantly higher hemorrhage rate of 12±0.9% in injected embryos as compared to uninjected controls (Figure 3.7 4E-F, I). Further, as *miR26a* knockdown leads to increased *smad1* levels, we predicted that reduction in *smad1* would rescue hemorrhage in *miR26a* knockdown embryos. Double knockdown by co-injection of *smad1* (McReynolds *et al.*, 2007) and *miR26a* morpholinos reduced hemorrhage rates to below 5±0.8% (Figure 3.7 H, top embryo, and Figure 3.7 I). Of note, *smad1* MO alone did not result in hemorrhage; however, it did result in a range of phenotypes associated with *smad1* knockdown including dorsal-ventral axis defects and hydrocephalus as previously reported (McReynolds *et al.*, 2007). *smad1* knockdown led to an average a 77±8.6% of embryos with a mild (V1) ventralized defect and 12±17% with a more severe (V2) phenotype (Figure 3.7 G - I). Both defects were reduced in double knockdown embryos (Figure 3.7 G and H, bottom). Thus, reducing *miR26a* or increasing *smad1 in vivo* leads to a loss of vascular stability.

3.4.6. Loss of miR26a leads to increased numbers of acta2-positive vSMCs and upregulation of pathways involved in endothelial-vSMC crosstalk

To demonstrate the functional consequences of increased endothelial BMP signaling on vSMCs, we next investigated vSMC investment on the ventral aorta and pharyngeal arch arteries of *Tg(BRE:EGFP;acta2:mCherry)* embryos in *miR26a* knockdown embryos. This assay allowed us to make three key observations. Firstly, *BRE:EGFP* signal intensity is enhanced in *miR26a* morphants (Figure 3.9 A', B' and C), which correlates with the increased pSmad1 staining we observed in endothelial nuclei of knockdown embryos (Figure 3.5). Secondly, the number of *acta2:mCherry* positive cells along the ventral aorta and pharyngeal arch arteries (PAA) is increased in *miR26a* morphants (33.8±1.6 in controls vs 47.22±2.2 in *miR26a* knockdown, Figure 3.9 A', B' and D).

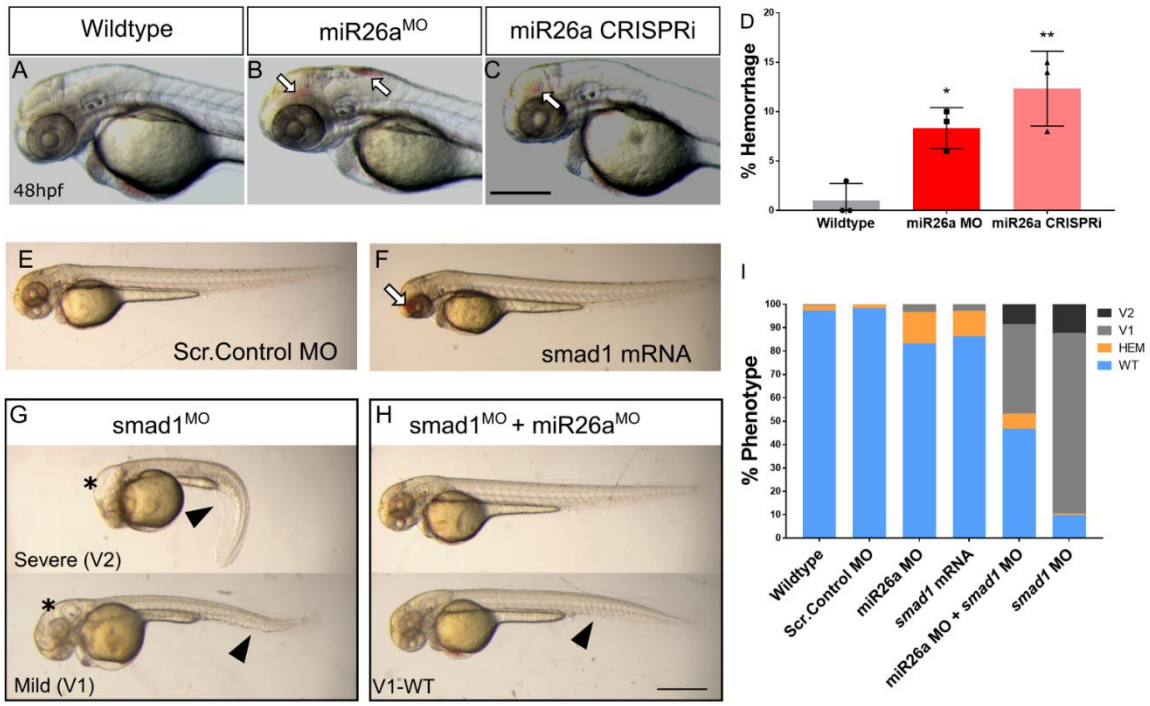

Figure 3.7: Increased levels of *smad1* result in defects in the vascular system and body axis.

A-C) Representative 2dpf *miR26a* knockdown embryos with hemorrhage, as indicated by arrows. D) Quantification of average rates of hemorrhage. (Error bars = SD Unpaired t test, *miR26a* MO *p<0.01 and mi26 CRISPRi **p<0.001 as compared to WT, N=3, Wildtype =224, miR26a MO = 124, miR26a CRISPRi =180). E-F) Representative morphology with *smad1* overexpression. G-I) *miR26a* and *smad1* double knockdown experiments. G) Representative 2dpf *smad1* MO embryos with mild (V1) and severe (V2) ventralization phenotypes, Asterix indicate cranial edema. H) Representative 2dpf double *miR26a* and *smad1* knockdown embryos with rescued hemorrhage and mild (V1-WT) ventralization phenotypes. I) Quantification of observed phenotypes double knockdown experiments (N=4, total n wildtype=193, Scr. Control MO = 157, *smad1* MO = 175, *smad1* mRNA = 95, miR26a MO =190, and miR26a MO + *smad1* MO = 190. One Way ANOVA of hemorrhage phenotype; Wildtype/Scr. Control MO vs. *miR26a*MO p=0.0001 Wildtype/Scr. Control vs. *SMAD1* mRNA p=0.0001 *miR26a* MO vs. miR26a MO+ *SMAD1* MO p<0.0001 ; of V1 phenotype: Wildtype/Scr. MO; vs. *SMAD1* MO p<0.0001 vs. miR26a MO+ *SMAD1* MO p<0.0001. Error Bars = SEM. Scale bar= 500µm. This experimental design was conceptualized by Abidemi Onabadejo, with my further analysis of the ventralization defects.

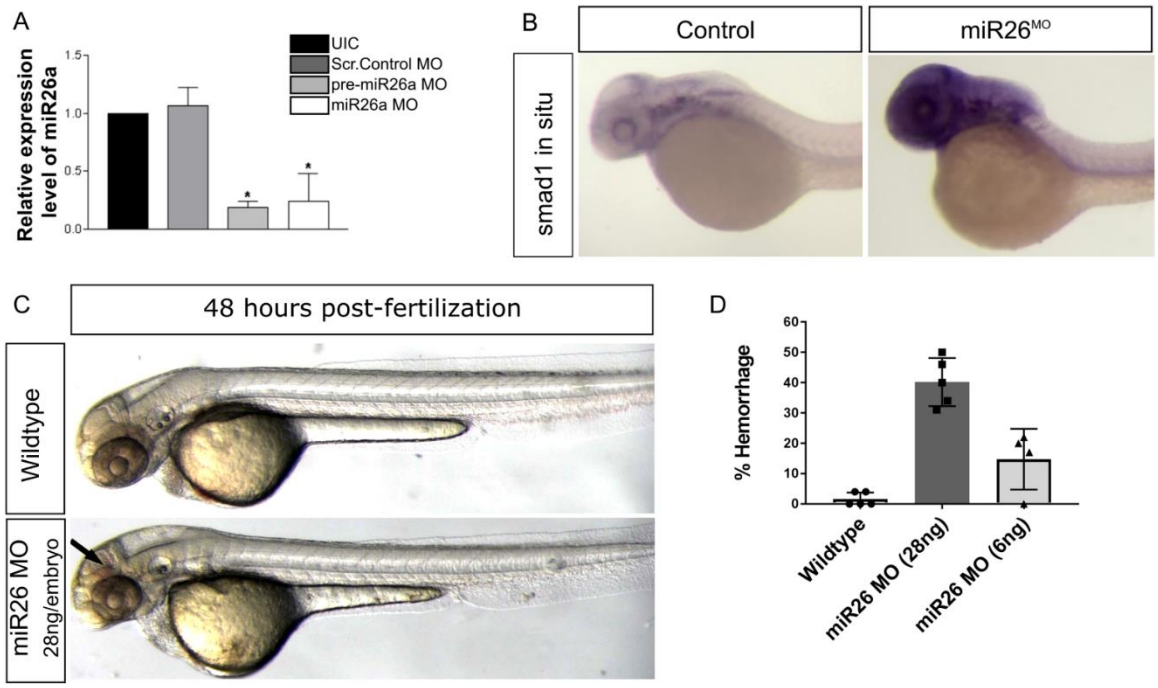

Figure 3.8: *miR26a* morpholino results in a dose-dependent increase in hemorrhage and *smad1*

A) RT-qPCR of relative expression of *miR26a* in *miR26a* MO at 2dpf injected at 28ng/embryos, values are means of 3 replicates and normalized to *miR122*, n=3: UIC vs. Neg. CTL. MO (Scr.Control MO) p = 0.16. UIC vs. Pre-miR26a MO: p <.0001. UIC vs. miR-26a mature MO: p = 0.0002. RT-qPCR analysis of values represents mean ± SEM, n=2 biological replicates. B) Whole-mount in situ hybridization staining for *smad1* at 48hpf shows increased expression of *smad1* at a higher dose of *miR26a* MO. C) Representative images of wildtype (uninjected) and high dose *miR26a* morpholino-injected embryos showing normal body axis, but with hemorrhage and mild hydrocephalus. E) Average rates of hemorrhage for *miR26a* MO at 28ng/ embryo and 6ng/ embryo (Student's two-tailed t-test, ****p<0.0001 as compared to WT, Error Bars = SEM. N= 5, n total *miR26a* MO 28ng = 488, 6ng= 501 and Wildtype = 535). qPCR data in A was performed and analyzed by Lei Zeng.

Thirdly, the increase in *acta2* positive cell number is accompanied by a change in cell morphology in *miR26a* knockdown embryos (Figure 3.9 E-G). Thirdly, the increase in *acta2* positive cell number is accompanied by a change in cell morphology in *miR26a* knockdown embryos (Figure 3.9 E-G). In control embryos, *acta2* positive cells have a rounded, punctate morphology, and 'sit' high on the vessel wall with an average height of 4.5±0.4 μm, above the underlying endothelium. In *miR26a* morphants, vSMCs have a significantly reduced vSMC height of 3.4 ± 0.1μm, and appear flattened and more closely apposed to the endothelium when compared to control embryo vSMCs. These data suggest that loss of *miR26a* results in increased vSMC coverage along blood vessels and a shift to a differentiated morphology.

In parallel, we quantitated gene expression for vSMC differentiation genes. RT-qPCR using isolated embryonic head mRNA at 4dpf showed a 1.7-fold increase in *acta2* and a 1.8-fold increase in *myh11a* mRNA in *miR26a* morphants (Figure 3.9 5H). Further, using in situ hybridization, we found that *miR26a* morphants have increased expression of *acta2* and *myh11a* in the pharyngeal region (Figure 3.10 A-D), similar to the location of increased *smad1* staining (Fig 3.3 D). Conversely by 4dpf, *miR26a* mimic injected embryos had reduction in *acta2* and *sm22* expression by in situ hybridization (Figure 3.10 E-J).

The Bmp/ Notch3/ Pdgf signaling axis is an important regulator of vSMC proliferation and subsequent differentiation. We found that the vSMC notch receptor *notch3* has a 2.0-fold increase in *miR26a* morphants (Figure 3.9 5 H). Furthermore, the endothelial expressed ligand *pdgfba* and its mural cell receptor *pdgfr*β, had a 3.6 and 2.0-fold increase, respectively, in *miR26a* morphants as compared to controls. This suggests that increased vSMC numbers could potentially arise from enhanced proliferation via activation of the Pdgfrβ pathway downstream of Smad1 activation. Increases in *acta2, myh11,* and *notch3* may therefore reflect increased cell numbers in addition to increased vSMC differentiation.

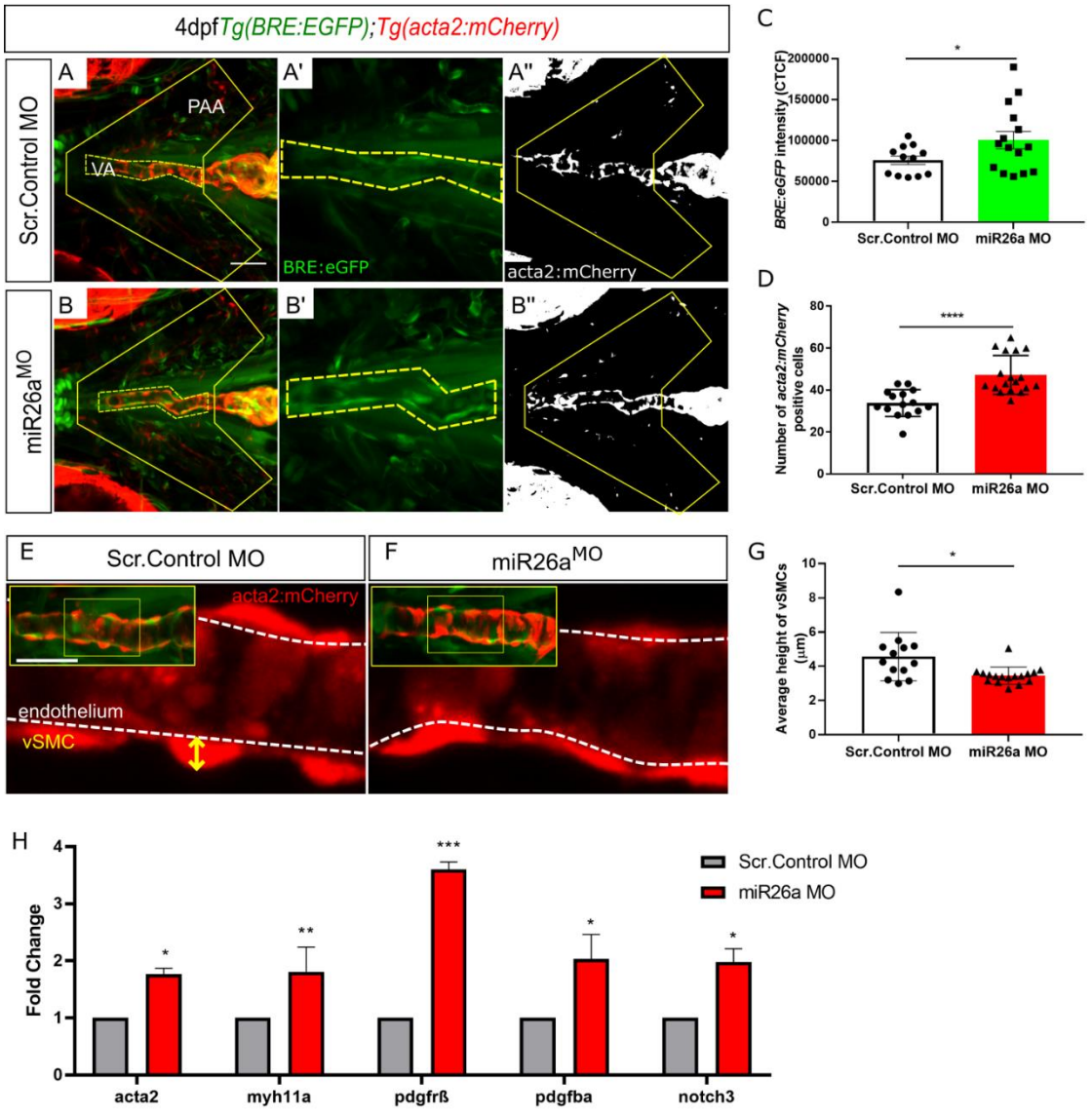

Figure 3.9: Loss of *miR26a* leads to increased expression of vSMC genes and *acta2* positive vSMCs.

A-B) Representative ventral views of 4 dpf *Tg(BRE:EGFP); Tg(acta2:mCherry)* embryos. Scr. Control embryos (A-A'') and *miR26a* morphant embryos (B-B'') showing qualitative upregulation of *BRE:EGFP* in the ventral aorta (VA) and pharyngeal arch arteries (PAA). C) Quantification of green fluorescent marker (*BRE:EGFP*) along the VA, taken from the highlighted yellow region in A' and B', and represented as corrected total cell fluorescence (CTCF) (N=3, miR26a MO = 15, Scr. Control = 12, Unpaired t-test, ****p<0.0001 as compared to control, error bars = SEM). D) Quantification of *acta2* positive cell number on VA and PAAs, within the area outlined in A'' and

B’’. Number of *acta2* positive cells is significantly increased in *miR26a* morphants (N=3, miR26a MO = 18, Scr. Control = 15, Unpaired t-test, ****p<0.0001 as compared to control, error bars = SEM). E and F) Measurement of vSMC height (yellow axis) from the endothelium (white dashed line). Representative images of ventral aorta (from insets), Scr. Control (E) and *miR26a* morphants (F). G) Quantification of average vessel heights along length of VA (N= 3, miR26a MO = 18, Scr. Control = 13, Student's two-tailed t-test, ****p<0.0001 as compared to control, error bars = SEM). H) RT-qPCR quantification of vSMC differentiation genes in injected controls and *miR26a* morphants (n=3). RT-qPCR data show the mean ± SEM, Student's two-tailed t-test *p < 0.05, n, number of biological replicates.

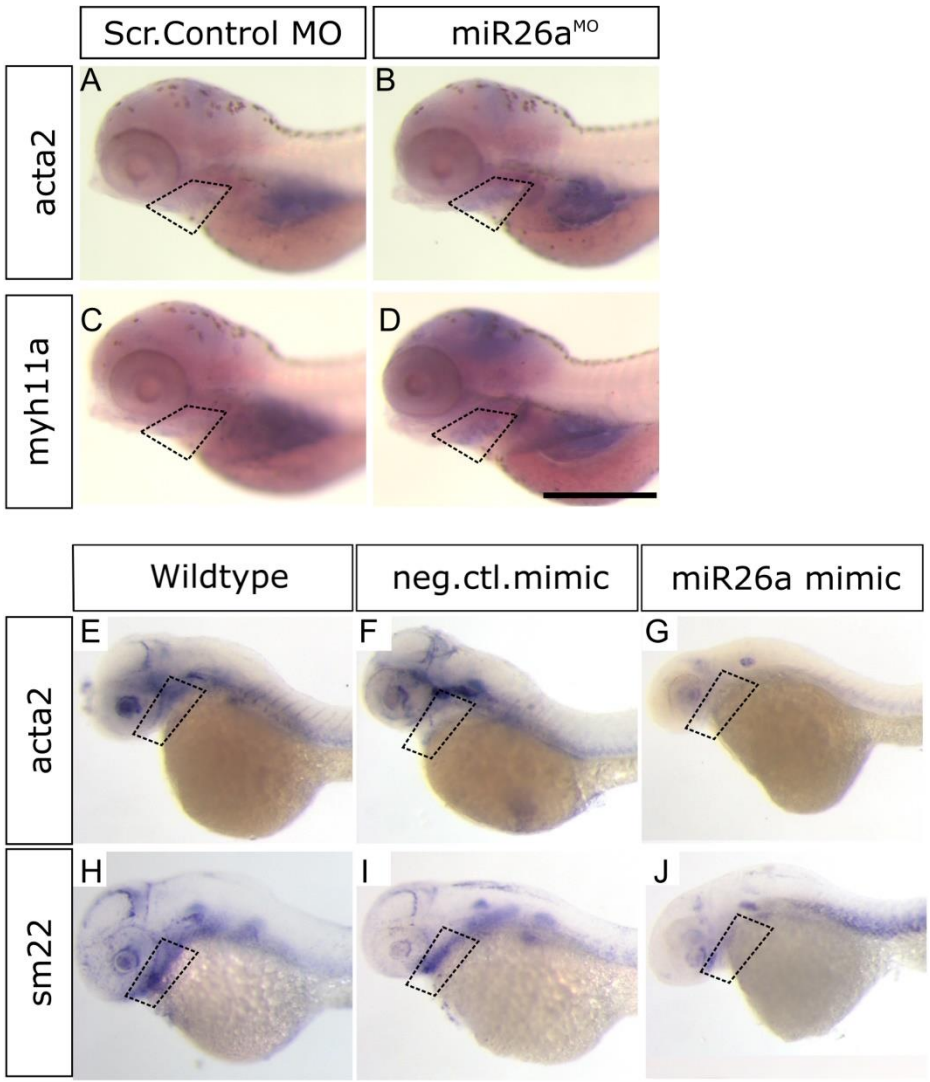

Figure 3.10: Changes in vascular smooth muscle marker gene expression in *miR26a* morphant and mimic embryos.

A-D) Whole-mount in situ hybridization staining for *acta2* and *myh11a* at 4 dpf shows increased expression in *miR26a* knockdown embryos in the aortic arches and pharyngeal region. E-J) Whole-mount in situ hybridization staining for *acta2* and *sm22α* at 4 dpf shows decreased expression in *miR26a* mimic injected embryos. microRNA26 mimic injections and ISH in E-J were performed by Lei Zeng

3.4.7. Endothelial overexpression of smad1 promotes vSMC differentiation

To demonstrate that endothelial *smad1* expression in endothelial cells promotes vSMC differentiation, we expressed *smad1* under an endothelial promoter in a transposon vector (TolCG2:*kdrl:smad1*, hereafter *smad1*^{ECOE}; Figure 3.11 A). The vector and transposase or transposase alone control were injected into *Tg(BRE:EGFP;acta2:mCherry)* embryos and scored at 2dpf and 4dpf. At 2dpf, 10% of smad1^{ECOE} embryos hemorrhage, similar to the increased hemorrhage observed in mirR26 knockdown and global *smad1* mRNA overexpression (Figure 3.7). Higher doses of the vector result in significant cranial and pericardial edemas (Figure 3.12 A and B). At 4dpf, RT-qPCR of *smad1*^{ECOE} embryos shows a 1.9-fold increase in *smad1* and 1.4-fold increase in the BMP responsive gene *id1* expression as compared to control (Figure 3.11 B). Similarly, *BRE:EGFP* fluorescence is also increased in *smad1*^{ECOE} embryos by 30% as compared to controls (Figure 3.11 C", D", F). Together, the data show that activation of Smad1 was significantly increased in *smad1* injected embryos. *smad1*^{ECOE} embryos do not show a change in the length of the ventral aorta, however, the *BRE:EGFP* signal extends further along the ventral aorta (Figure 3.11 C", D'' and G). The total number of *acta2:mCherry* positive vSMCs along the ventral aorta in *smad1*^{ECOE} embryos was significantly increased from 15±0.6 in controls to an average 24±1.4 cells (Figure 3.11 C', D' and E). The percent vSMC coverage of the ventral aorta is also increased by 20% with an average of 80 ± 2.05% in *smad1*^{ECOE} as opposed to 65.3±2.1% in controls (Figure 3.11 C', D' and H). Our data suggest that the upregulation of *smad1* in endothelial cells is sufficient to increase vSMC number and coverage of the ventral aorta at 4dpf.

3.4.8. BMP inhibition rescues the effect of on vSMC differentiation after miR26a knockdown

Our results showed that *miR26a* knockdown leads to an increased number of *acta2* positive vSMCs on the ventral aorta and upregulation of Smad1 activation in the endothelium. To further investigate the interplay between BMP signaling in endothelial cells and vSMC differentiation, we tested whether the increase in vSMC number and differentiation after the loss of *miR26a* could be reversed by blocking endothelial BMP signaling. K02288 is a selective and potent small-molecule inhibitor of BMP signaling that blocks Smad1 phosphorylation by type I receptor Activin like kinase 1 (Alk1) and Alk2 (Sanvitale *et al.*, 2013; Kerr *et al.*, 2015). We show that *alk1* expression is enriched in endothelial cells at this developmental stage, but not vSMCs (Figure 3.2).

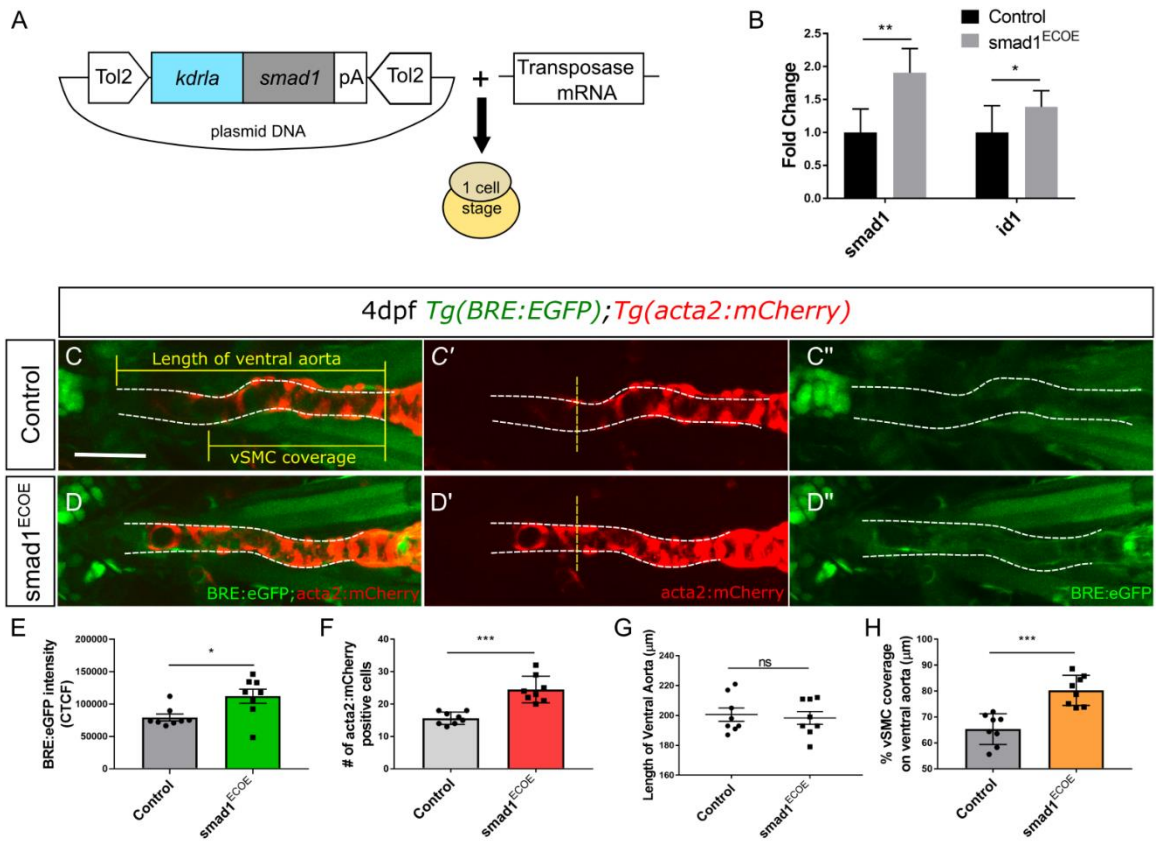

Figure 3.11: *smad1* overexpression in endothelial cells results in increased vSMC coverage.

A) Vector construct for overexpression of *smad1* under the endothelial cell promoter *kdrla*. B) RT-qPCR fold change in *smad1* and *id-1* expression levels in endothelial-specific *smad1* overexpressing embryos (*smad1*^{ECOE}) embryos (n=3). mean ± SEM. C – D) Representative orthogonal projections of ventral views of 4 dpf Tg(BRE:EGFP); Tg(*acta2*:mCherry) embryos. Control embryos (C-C'') and *smad1*^{ECOE} embryos (D-D'') showing endothelial *BRE:EGFP* and vSMC *acta2:mCherry* expression in the ventral aorta (VA) and pharyngeal arch arteries (PAA). E) Quantification of *acta2* positive cell number on VA, within the area outlined in C and D. Number of *acta2* positive cells, is significantly increased in *smad1*^{ECOE} embryos. F) Quantification of green fluorescent marker (*BRE:EGFP*) along the VA, highlighted within the yellow region in C'' and D'', as corrected total cell fluorescence (CTCF). G) length of VA, within the area outlined in C and D. H) Percent vSMC coverage of ventral aorta. N=3, *smad1*^{ECOE} embryos n= 8, Control n= 8, Student's two-tailed t-test, $p<0.01$. Error bars = SEM, Scale bar= 50µm

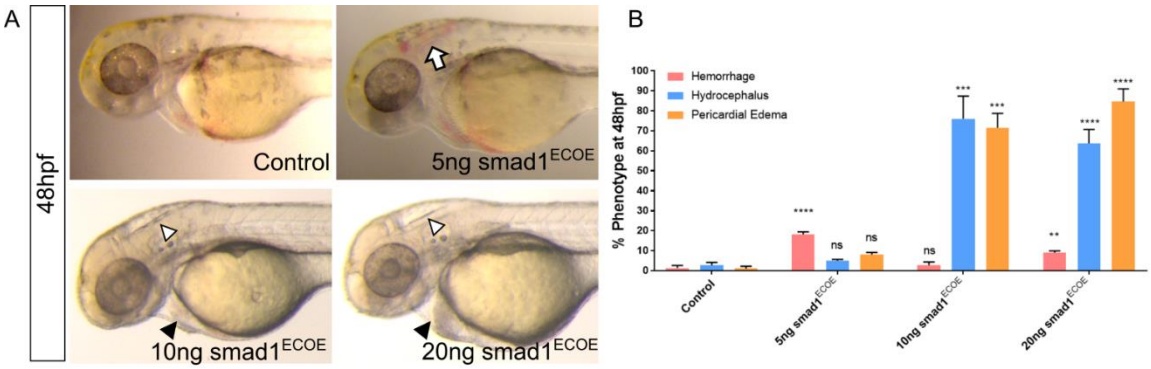

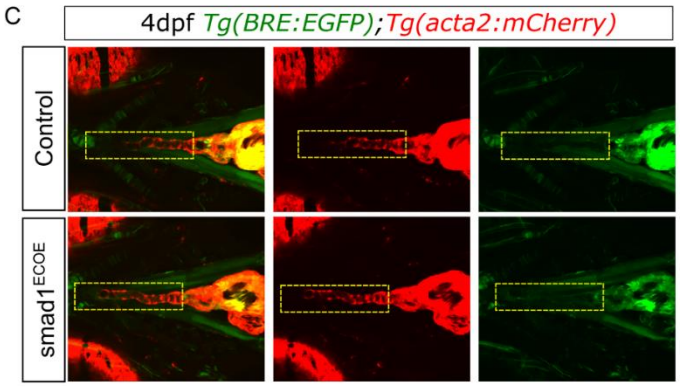

D

# of acta2:mCherry cells	Control	smad1-ECOE
Trial 1	15	25
Trial 2	16	26
Trial 3	15	23
Mean ± SEM	15.63 ± 0.6797, n=8	24.5 ± 1.452, n=8

BRE:EGFP intensity	Control	smad1-ECOE
Trial 1	91953	99825
Trial 2	73828	133031
Trial 3	68758	99490
Mean ± SEM	79357 ± 5251, n=8	112193 ± 10895, n=8

	Control		smad1-ECOE	
	Length of VA	% acta2 coverage	Length of VA	% acta2 coverage
Trial 1	202	61.55	204	81.25
Trial 2	200	68.24	201	79.21
Trial 3	199	66.65	186	80.44
Mean ± SEM	200.6 ± 4.44, n=8	65.33 ± 2.104, n=8	198.4 ± 4.28, n=8	80.28 ± 2.052, n=8

Figure 3.12: Higher doses of the Smad1 expression vector result in significant cranial hemorrhage and pericardial edemas

A) Phenotypes observed at 48hpf with increasing doses of *smad1*^{ECOE}. B) Quantification of phenotypes, Student's two-tailed t-test **-****p=0.005-0.00005 as compared to control. Error Bars = SEM. N= 3, n total smad1^{-ECOE} 5ng =60, 10ng=61, 20ng=63 and control = 72. C) Ventral view confocal projections of the 4dpf ventral aorta of Tg(BRE:EGFP) embryos. Q) Average number of acta2:mCherry cells, BRE intensity and vSMC coverage.

We selected a time point for drug application when the endothelium of the major blood vessels is patterned (Isogai, Horiguchi and Weinstein, 2001), but when vSMC coverage of the ventral aorta and PAA is only starting (Whitesell *et al.*, 2014). *Tg(acta2:EGFP;kdrl:mCherry)* embryos were treated with 15μM K02288 from 52hpf to 4dpf. As expected, *miR26a* morphant and *miR26a* CRISPRi treated embryos have significantly more vSMCs than wild type embryos (Figure 3.13 B-B', C-C', and G). Wildtype embryos treated with K02288 show a 62% reduction in the total average number *acta2:EGFP* positive cells compared to vehicle control alone (Figure 3.13 A', D', and G. 29±1 to 11±3). In *miR26a* knockdown embryos (Figure 3.13 B'-C'), the effects of K02288 were rescued; *miR26a* morphants had a non-significant 17% reduction in vSMC numbers (35±5 to 29±5) and *miR26a* CRISPRi embryos had a non-significant 11% reduction from 39±1 to 34±3 (Figure 3.13 E'-F' and G). We also found that BMP inhibition not only affects vSMC number but also reduces ventral aorta length by 55% in K02288 treated wildtype embryos, from an average 159±2.08 μm to 77±19.5 μm (Figure 3.13 A, D and H). However *miR26a* morphants treated with K02288 are rescued and have a ventral aorta length not significantly different than wildtype. *miR26a* CRISPRi embryos showed a smaller rescue and had a 20% decrease in length when treated (Figure 3.13 B-C and E-F, 177±8.6 to 136±5.6). Of note, there was no statistical difference in ventral aorta length between *miR26a* knockdown and control embryos, which supports our finding that endothelial cell number is not affected by the loss of *miR26a.*

We next tested whether pSmad1 levels are rescued in K02288 treated *miR26a* knockdown embryos as compared to controls (Figure 3.13 I-L). Using the endothelial nuclear marker *fli1a:nEGFP,* we confirmed that there was no significant difference in endothelial cell number between untreated control and *miR26a* morphants (Figure 3.13 M). In control embryos, treatment with K02288 (Figure 3.13 I-I' and J-J') significantly reduced the number *fli1a:nEGFP* positive cells to 16± 0.2, which is 20% less than controls. Similarly, the proportion of pSmad1 positive/*nEGFP* nuclei also decreased from 43±1% to 28±2% (Figure 3.13 N). Although K02288 treated miR26a morphants have a slight reduction in the total number *fli1a:nEGFP* positive cells (Fig 7 M), there is no significant decrease in the proportion of pSmad1 positive/*fli1a:nEGFP* nuclei (Figure 3.13, K-K', L-L' and N), and they remain similar to untreated controls. Taken together, our results further suggest that the endothelial cell is a critical site of Smad1-mediated BMP signaling, and blocking its activation can significantly affect vSMC coverage.

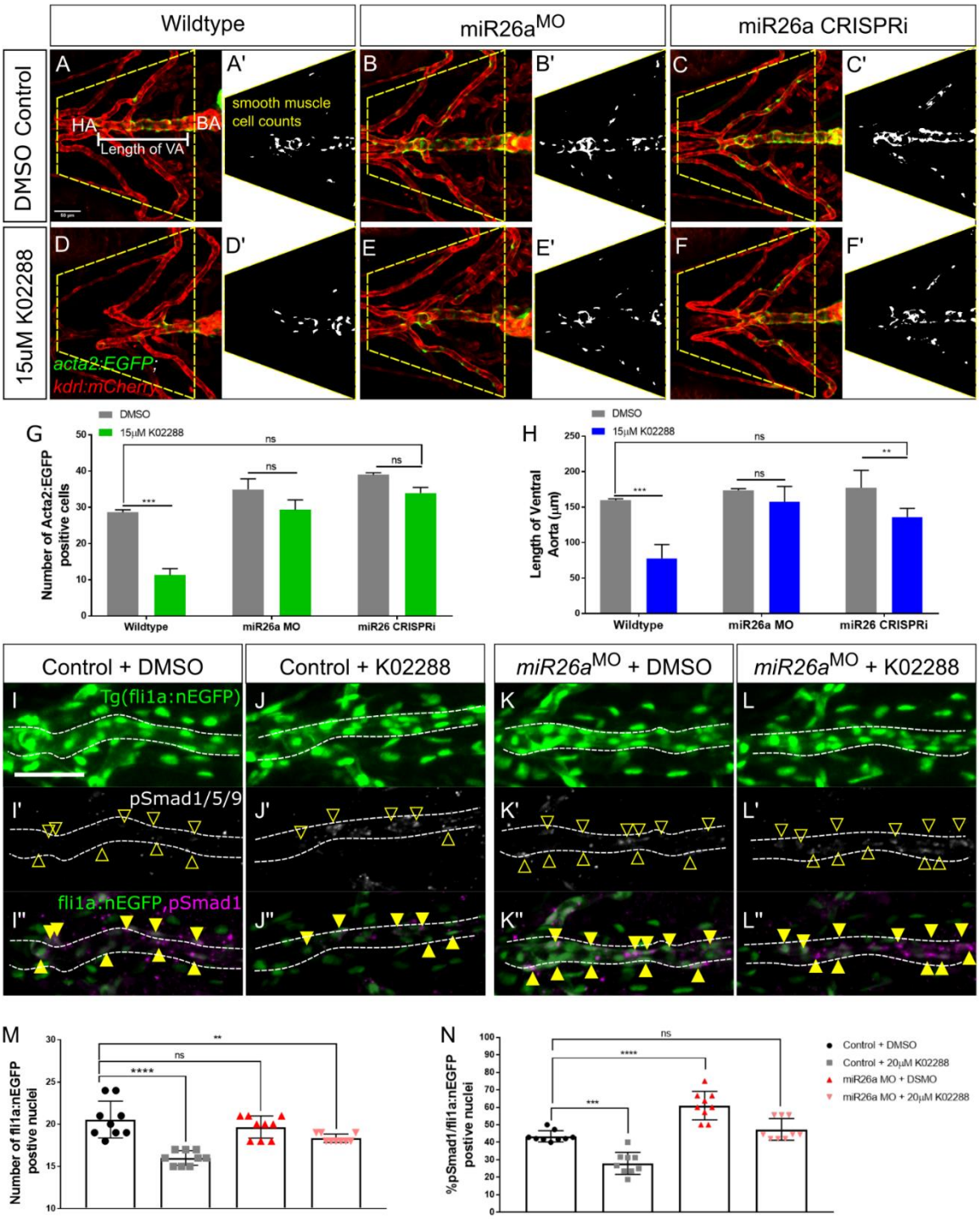

Figure 3.13: *miR26a* controls vSMC differentiation via *smad1*-mediated BMP signaling.

Ventral aorta showing endothelial (red) and smooth muscle (green) cells in miR26a morphants or CRISPRi- injected embryos treated with vehicle control (DMSO) or 15μM K02288 from 52 hpf to 4 dpf. A-C) DMSO-treated vehicle control embryos D-F) K02288 treated control embryos. (A, D), *miR26a* morphant (B, E), *miR26a* CRISPRi knockdown (C, F). A'-F' are threshold adjusted

images of *acta2*-EGFP expression. G) Quantification of *acta2* positive cell number on VA and PAAs, within the area outlined in A and B. Number of *acta2* positive cells is significantly reduced in K02288 treated embryos as compared to DMSO control. There is no significant decrease in *miR26a* knockdown embryos (two Way ANOVA, N=3,miR26a MO = 15, Wildtype = 15, Unpaired t-test, ****p<0.0001 as compared to control, error bars = SEM. H) Quantification of the length of VA, within the area outlined in A and B. Length of VA is significantly reduced in K02288 treated embryos as compared to DMSO control. There is no significant decrease in *miR26a* knockdown embryos (Two Way ANOVA, N=3, miR26a MO = 15, Scr.Control = 15, Unpaired t-test, ****p<0.0001 as compared to control, error bars = SEM. VA= ventral aorta, HA = hyoid artery, BA= bulbous arteriosus. (N= 3, 8-9 embryos per treatment group. One Way ANOVA, p=0.001-0.0001***-****. Scale bar= 50µm. I-L) pSmad1/5/9 staining in K02288 treated embryos. Endothelial nuclei (*fli1a:nEGFP*; I-L, arrowheads) and p*Smad1*/5/9 (pSmad1, white I'-L') and overlay (magenta, I''-L'') in 4dpf Scr. Control and *miR26a* morphants. Solid yellow arrowheads in I''-L'' indicate pSmad1 + *fli1a:nEGFP* double-positive nuclei in the ventral aorta. M) Quantification of the total number of *fli1a:nEGFP* nuclei in the ventral aorta. N and O) Quantification of the percent pSmad1; *fli1a:nEGFP* double-positive nuclei in *miR26a* morphants and *miR26a* CRISPRi embryos. N=3 experiments, total embryos Scr. Control MO = 9, miR26a MO =9. One Way ANOVA, p=0.001-0.0001***-****. Scale bar= 50µm.

3.5. Discussion

Compromised structural vascular integrity, vessel weakening and rupture (hemorrhage) can result from aberrant BMP signaling (Dzau *et al*., 2002; Milewicz *et al*., 2010; Nebbioso *et al*., 2012). Hemorrhage ultimately results from weak endothelial junctions, however defects in mural cell coverage (attachment and ECM secretion) are implicated in the pathological progression of vascular diseases. We show that the endothelium of the ventral aorta in zebrafish has activated pSmad1 at 4dpf, but that pSmad1 is not detectable in mural cells. At a stage when mature vSMC are normally present, embryos with loss of *miR26a* have upregulation of pSmad1, increased vSMC coverage, and a change in vSMC morphology, with no observable changes in the number or morphology of the pSmad1-expressing endothelial cells. We show that inhibition of BMP signaling reduces both vSMC coverage and the length of the ventral aorta while dual *miR26a* knockdown and BMP receptor inhibition leads to a rescue such that animals maintain normal vSMC number, length of the ventral aorta, and vSMC coverage. We, therefore, suggest that *miR26a* modulates BMP signaling in endothelial cells to control vSMC differentiation via a paracrine mechanism potentially involving Notch and/or Pdgfrβ signaling (Figure 3.14).

We propose that *miR26a*, therefore, functions *in vivo* to fine-tune endothelial signals to the vSMCs. Studies in cultured vSMC have suggested that *miR26a* controls Smad1-mediated BMP signaling within vSMCs to modulate their phenotype (Albinsson *et al.*, 2010). However, these studies do not address whether the levels of pathway activation *in vitro* are relevant to tissues *in vivo*. Additionally, data collected from *in vitro* culture systems do not address the role of cell to cell communication (autonomous and non-autonomous signaling) that is critical *in vivo* (Gaengel *et al*., 2009a; Owens *et al*., 2004). We, therefore, sought to use an *in vivo* model of vascular development with intact tissue and cellular contexts to assess how the loss of *miR26a* and subsequent increases can affect vSMC coverage. We have multiple lines of evidence that suggest that endothelial pSmad1 levels correlate with increased vSMC coverage of blood vessels. Our use of BMP-reporter transgenic fish reveals that during normal development, and under physiological conditions, vSMCs directly contact BRE and pSmad1 positive endothelial cells but have undetectable BRE or pSmad1 signal themselves.

In parallel to the loss of *miR26a* resulting in a subsequent increase in *smad1* and vSMC coverage, we also demonstrated that endothelial-specific overexpression of *smad1* (smad1^{ECOE}) results in increased vSMC coverage. Our data therefore inversely complement the murine knockout models of HHT that have noted reduced vSMC coverage when endothelial Smad1 signaling is reduced. Of note, endothelial-specific knockdown of Alk1 or Smad4 leads to a reduction of αSMA/Acta2 coverage on larger arterial vessels. Interestingly, there is a context-dependent shift in vSMC coverage in these studies, as ectopic expression of vSMCs is seen on venous and capillary vessel beds (Ola *et al.*, 2018). This hypervascularization was presumed to be in response to increased flow from AVM affected vessels into finer retinal vessels. Similar shifts are seen when BMP9/10 blocking antibodies are used (Ola *et al.*, 2016). Our study did not address changes in vSMC coverage in venous beds, but it would be interesting to see if overexpression of *smad1* leads to increased vSMC coverage across both arterial and venous vessel beds.

Our data suggest that the normal function of *miR26a* is to reduce Smad1 protein activation within the endothelium, and indirectly inhibit vSMC differentiation in early development. Treatment with K02288, a potent ALK1/2 inhibitor, significantly reduced both *acta2*-positive vSMC coverage and reduced the length of the ventral aorta. These effects could be rescued by the loss of *miR26a*. Thus, we suggest that enhanced Smad1 activation in these embryos compensates for receptor inhibition. ALK1, ALK2, and ALK3 are expressed in both endothelial and vSMCs (Mishina *et al.*, 1995; Benjamin, Hemo and Keshet, 1998; Beppu *et al.*, 2000; Roman *et al.*, 2002; Lan *et al.*, 2007), however in zebrafish *Alk1* is highly expressed in the endothelium at 36hpf (Laux, Febbo and Roman, 2011). *Violet beauregarde (vbg^{ft09e}) alk1* loss of function zebrafish mutants develop striking cranial vessel abnormalities by 2dpf due to increased endothelial cell proliferation (Roman *et al.*, 2002). *vbg^{ft09e}* are also unable to limit the diameter of arteries carrying increasing flow from the heart (Corti *et al.*, 2011). Based on our data involving indirect control by endothelial signaling, we would predict there is an additional defect in vSMC recruitment in Alk1 mutants, although this remains to be tested.

Endothelial and mural cells signal through several paracrine pathways to stabilize vessels (Mack, 2011; Winkler, Bell and Zlokovic, 2011). BMP signaling in endothelial cells activates an axis of BMP/ Notch3/ Pdgf signaling to promote the expression of contractile vSMCs genes such

as Acta2 and Myh11a in *in vitro* co-culture systems (Tachida *et al.*, 2017). Specifically, BMP9 signaling via endothelial cells induces NOTCH3 in vSMCs, which in turn induces expression of Pdgfrβ and maintains the proper response to Pdgf ligands (Lindahl *et al.*, 1997; Benjamin, Hemo and Keshet, 1998). There is evidence that mouse MiR26a is modulated by Pdgf-BB signaling (Yang *et al.*, 2017). For instance, neointimal hyperplasia results in elevated levels of Pdgfbb associated with the upregulation of miR26a and accumulation and proliferation of vSMC at sites of injury. Furthermore, the treatment of primary mouse aortic vSMCs with miR26a mimic drives cells to a synthetic vSMC state (Yang *et al.*, 2017). We found that *notch3, pdgfrβ,* and contractile vSMC markers were significantly increased in *miR26a* knockdown embryos, suggesting that increases in endothelial Smad1 in zebrafish may be transmitted to vSMCs through a BMP/ Notch3/ Pdgf signaling axis. Pdgf ligands are primarily released by endothelial cells, and we observe an increase in *pdgfba* in *miR26a* morphants, providing a potential mechanism by which active BMP signaling in endothelium can recruit and induce vSMC differentiation via paracrine non-autonomous signaling pathways.

While we found increased differentiation of vSMCs at the later stage 4 dpf time point, at 2dpf loss of *miR26a* results in hemorrhage. The 2dpf to 4dpf window is a common window for vascular instability phenotypes to emerge in zebrafish (Liu *et al.*, 2007; High *et al.*, 2008; Montero-Balaguer *et al.*, 2009; Zheng *et al.*, 2010). BMP signaling is initiated in endothelium at this time point and perturbations can affect endothelial cell junction development (Winkler, Bell and Zlokovic, 2011). We have previously shown mural cells present around vessels by 2dpf, although they are mesenchymal and immature (Liu *et al.*, 2007). These cells express *pdgfrβ* but have no expression of mature vSMC markers (Ando *et al.*, 2016), suggesting the 48hpf time point represents a critical window for vascular mural cell attachment to endothelium and differentiation to a mature phenotype. It is paradoxical then that we see increased maturation of vSMCs at 4dpf when *mir26a* is reduced. We suggest that the altered receptor and ligand expression in *miR26a* morphants may promote morphological change towards maturation, but may not regulate all aspects of maturation, leading to destabilization. For instance, aberrant ECM deposition would not be visible in our assays and could lead to vascular instability at the earlier time points (Winkler, Bell and Zlokovic, 2011).

As critical modulators of vascular cell function and with roles in cell differentiation, contraction, migration, proliferation, and apoptosis, miRs are attractive targets of therapeutic treatments aimed at modulating the vSMC phenotypic switch. Specific to TGF-β/BMP signaling, the *miR-145/143* family has direct involvement in SMC differentiation by repressing the Klf4 to induce a contractile morphology and reduced rates of proliferation (Cordes *et al.*, 2009). *miR-21* controls vSMC differentiation through cross-talk with *miR-143/-145* (Sarkar *et al.*, 2010) and by mediating TGF-β/BMP induction to promote *miR-21* cleavage to its mature form and a more contractile phenotype (Fig 5). *miR26a* is unique in this group in that it represses smooth muscle differentiation, likely via paracrine signaling from endothelial cells. As drug delivery to the endothelium is relatively straightforward, modulation of *miR26a* might be therapeutically useful for post-transcriptional control of key genes involved in vSMC phenotypic switching.

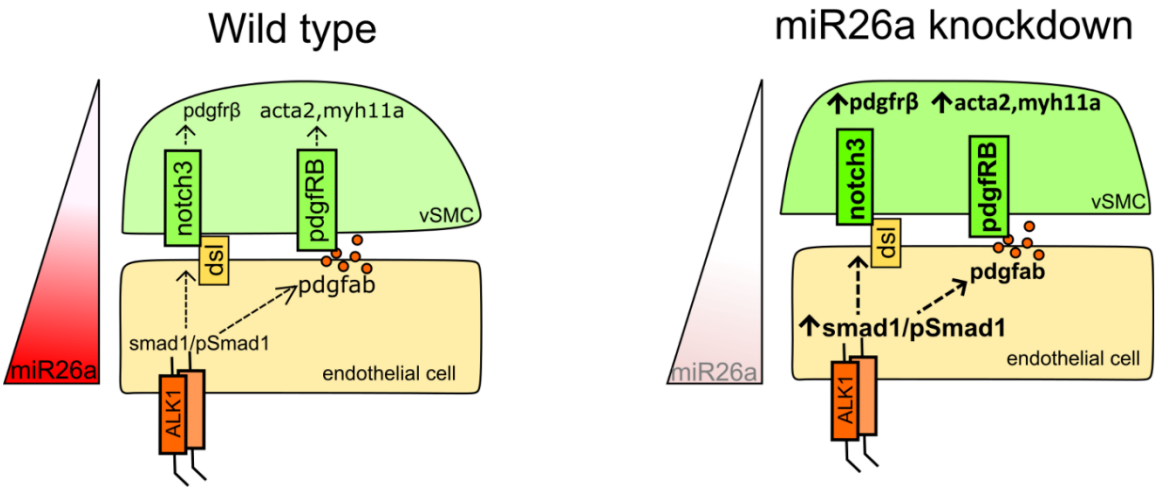

Figure 3.14: Mechanistic model by which *miR26a* modulates BMP signaling to promote vSMC differentiation via interactions with endothelial cells

miR26a modulates vascular stability by directly targeting *smad1*. At developmental stages when smooth muscle appears, the endothelium has active BMP signaling. Loss of *miR26a* results in increased BMP signaling in endothelial cells where *smad1* becomes phosphorylated. Increased pSmad1 in endothelial cells leads to increased differentiation (*acta2* expression) and increased vSMC cell number while blocking BMP signaling leads to a decrease of both. (Dashed arrows indicated the indirect effect on vSMC marker expression and cell number)

Chapter Four: General Discussion

In this thesis, I explored different aspects of endothelial cell communication. Cellular signaling can be simplified to a linear pathway of communication e.g. the input stimuli/ligand binds to a receiver/receptor and transmits the signal within the cell. This allows the cell to receive information from the extracellular environment and to respond with the appropriate action. The positive responses to stimuli are often balanced by negative regulators which are generally considered to limit cell responses. My work has highlighted that negative regulators play an important role in enhancing cell-signaling control to fine-tune vessel development. In Chapter 2, I report the role of a Sema3 in regulating angiogenic vessel growth. I find that the expression of *sema3fb* in developing trunk vasculature is necessary for the appropriate formation of angiogenic sprouts. In Chapter 3, I provide evidence for the role of microRNA26a (miR26a) in controlling smooth muscle coverage of vessels. I demonstrate a non-autonomous role for miR26 in regulating vSMC coverage via its endothelial expressed target gene *smad1*. Together these data present roles for endothelial cells to utilize negative signals to carefully modulate vessel growth and later vessel maturation. In this chapter, I will discuss my findings, and future experiments to answer questions which stem from my work.

4.1. Sema3fb as a regulator of angiogenesis

My work in Chapter 2 highlights a role for negative regulation in promoting angiogenic vessel growth. I showed that loss of *Sema3fb* results in defective ISA spout formation characterized by shorter and wider sprouts which fail to make connections to neighboring sprouts. Additionally, the increased endothelial nuclei size and presence of persistent filipodia is suggestive of a migration defect. It is intriguing that loss of a factor that typically produces negative signals results in delayed angiogenic growth, rather than overgrowth. There is evidence of both positive and negative signals from Sema3s to promote appropriate vessel growth by balancing receptor and ligand expression (Kim *et al*., 2011). One surprising finding was that despite having increased *vegfr2*, *sema3fb* deficient embryos had defective sprout formation. The same analysis also revealed increased *sflt1* a potent negative regulator of angiogenesis. Thus, both positive and negative signals are induced by the loss of the same factor.

The finding of a delayed migration and disrupted sprout formation despite a significant increase in *vegfr2* and *dll4* is interesting as it suggests that multiple inputs into the pathway are integrated during vessel formation. Gain and loss of function phenotypes that are similar have been seen with other signaling events in vascular development. EC-specific expression of an activated form of Notch-4 driven by the flk1-promoter led to embryonic lethality with abnormal vessel structure which is similar to the phenotype seen in Notch-1- and Notch-1/Notch-4-deficient mice (Uyttendaele *et al.*, 2001). The similar vascular phenotypes for both transgenic (gain-of-function) and knockout mice (loss-of-function) have been attributed to a balance of appropriate Notch protein abundance to promote tip specification. Interestingly, although there is an increase in tip cell marker expression, the disrupted sprout migration would argue that the anti-angiogenic *sflt1* dominates over the pro-angiogenic *vegfr2/dll4* signals. However, as there are currently no antibodies or staining methods to distinguish between the cell types in zebrafish, I am unable to conclude whether there is an increase in the number of tip cells or change in stalk cells.

As both Sema3fb and sFlt1 are expressed by endothelial cells it suggests a disruption to the local vessel environment may be responsible for the angiogenic defects. Typically, the expression of sFlt1 is important in shaping the vessel environment by acting as a Vegfa antagonist to limit ligand availability (Krueger *et al.*, 2011b; Pang *et al.*, 2013; Failla, Carbo and Morea, 2018). It would be interesting to investigate the effects of sfl1 in sema3fb mutants. Going forward, utilizing sFlt1 morpholino knockdown in mutants would test whether changes in *sflt1* could rescue the angiogenic defects. Detecting *sflt1* mRNA expression via ISH would also be interesting. Therefore, future work should be directed at exploring whether the increase in *sflt1* is responsible for disrupting ISA growth. One simple approach could be to design an endothelial-specific construct to knockdown sFlt1. For example, a tissue-specific CRISPR construct could prove helpful in showing its importance in causing the delayed spout formation in *sema3fb* mutants. However, knockdown of sFlt1 early in development is embryologically lethal and attributed to impaired vascularization (Krueger *et al.*, 2011a). In that case, a conditional expression construct could prove useful, for example, an endothelial-specific Inducible-Cre recombination construct would allow timed control of sFlt1 knockout in endothelial cells.

As a soluble growth factor, VegfA is capable of diffusing across the tissue to establish a gradient that directs vessel growth (Koch & Claesson-Welsh, 2012). qPCR analysis in Sema3fb mutants showed upregulation of *vegfr2* but did not address possible changes in its ligand in the local environment. Interestingly several Semas function as proangiogenic factors to enhance Vegf secretion from adjacent cells (reviewed in Capparuccia and Tamagnone 2009). For example, activated macrophages release Vegfa at the site of an injury to increase vessel growth and promote the circulation of wound healing factors. These pro-angiogenic signals are often capitalized on in tumor vascularization models, for example, increased expression of membrane-bound Sema6A by endothelial cells can attract NRP or plexinD1-expressing macrophages to provide Vegfa (Segarra *et al.*, 2012). Recent evidence demonstrated membrane-bound ligand Sema4a is expressed by macrophages. Upon recruitment, MMPs in the extracellular environment cleave Sema4a to a soluble form which can then bind to the plexinD1 receptor and trigger the release of Vegfa (Meda *et al.*, 2012). These examples highlight that high levels of Vegf as necessary for pathological vessel overgrowth and this is modulated by some Semas. Sema3F acts in an opposing manner to these other semaphorins. There is limited evidence of SEM3F expression by immune cells (Plant *et al.*, 2020), however, SEMA3F can mediate the expression of VEGF from cancer cells to limit vascularization and also repels NRP expressing cells away from tumors (Zhang *et al*., 2020). It would be interesting to assay whether macrophages play a role in establishing Vegfa gradients during zebrafish angiogenesis. To investigate this, I would use neutral red, a vital dye that is phagocytosed by microglia and macrophages, and makes them visible under light microscopy, to analyze whether macrophage recruitment to blood vessels is affected. Together with vegfa expression, this could show whether proangiogenic gradients are affected by the loss of *sema3fb.*

Early studies in zebrafish and mice demonstrated that Sema3e repulsive guidance is achieved via endothelial PlexnD1 expression, and loss of either Sema3e or plexinD1 results in drastic vessel overgrowth (Torres-Vázquez *et al.*, 2004; Gu *et al.*, 2005). However, the spatial restriction of Sema-PlexinD1 is also important in regulating the EC response, for example, Sema3E–Plexin-D1 signaling is spatially controlled by VEGF through its regulation of Plexin-D1 to limit the response to tip cells (Kim *et al*. 2011). While I have no protein localization data, the known functions of secreted Sema3f argue that the proteins are localized to the vessel growth front. For instance, in endothelial cell migration assays, SEMA3F is expressed on the leading edge of an

endothelial cell, and this polarized expression limits migration in response to VEGF (Nakayama *et al.*, 2015, 2018). Of note, no commercially available antibody exists for zebrafish Sema3fb. Making our own antibody to Sema3fb to detect its expression would be very useful to determine its spatial localization. Importantly, as the expression of both ligands and receptors by the same cell is suggestive of autonomous regulation, antibody staining could also prove useful in visualizing the idea of Sema3F functioning in an autocrine fashion via Nrp1. Unpublished endothelial cell-specific RNAseq data from our lab (Whitesell, 2018) identified *nrp1b, plxnd1,* and *plxnb3* transcript enrichment at 5 dpf. Although the role of the *nrp1b* receptor in Sema3fb-dependent angiogenic growth has not been verified, it's expression in ECs does suggest Nrp1b could canonically interpret Sema3f signaling to limit the cytoskeletal rearrangements necessary for cell migration.

Finally, the examination of endothelial nuclei and filopodial extensions in *sema3fb* mutants revealed an increase in nuclear size and the presence of persistent filipodia. These are consistent with perturbations to Vegf signaling which results in the accumulation of stress fibers that interfere with cell elongation (Cole *et al.*, 2010). Also, as Sema3F functions to regulate stress fiber formation cell culture (Nakayama *et al.*, 2015), my data argues *sema3fb* serves a similar function *in vivo*. However, the analysis was limited by the mosaic expression of the *Fli^{ep}:LifeACT* construct.

Going forward, generation of stable *sema3fb* heterozygote: *Fli^{ep}:LifeACT* transgenic lines would enable assays in siblings with equivalent fluorescent expression. An alternative would be to stain for F-actin using Phalloidin on fixed embryos. Although this would indiscriminately stain all cells, immunostaining embryos that express both cytoplasmic and nuclear fluorescence in endothelial cells, such as the Tg(Fli^{y7}:nEGFP; kdrl:mCherry) line, could highlight stress fiber formation. Of interest, my data suggests that P13Ka activity may be upregulated in response to increased Vegf signaling. A recent study showed that zebrafish embryos treated with a PI3Kα -specific inhibitor, GDC-0326, also display ISA sprouting defects attributed to a decrease in f-actin assembly (Angulo-Urarte *et al.*, 2018). As discussed in Chapter 2, excess F-actin can also disrupt vessel growth, and it would be interesting to test if PI3Kα inhibition could rescue the angiogenic defects *sema3fb* mutants.

4.2. Sema3F as a regulator of vessel growth

In this thesis, I have presented my work on understanding and characterizing an autocrine role for *sema3fb* in regulating angiogenic growth. However, there is possible genetic compensation with *sema3fa*. I collaborated with Dr. Sarah McFarlane's lab to characterize a paracrine role for *sema3fa* in retinal vascularization (Appendix; Halabi *et al* 2019). We demonstrated that *sema3fa* expression in the retinal environment is necessary to restrict blood vessel growth from the choroid into the zebrafish retina. Interestingly, within the eye, there is a transient expression *sema3fb* in the temporal retina at 18 hpf but it diminishes after this time (Halabi, 2019). This shared expression argues for potential genetic compensation to modulate phenotypes at earlier time points and is currently under further investigation by Dr. Sarah McFarlane.

Vessel development can be either dependent or independent of blood flow; blood flow results in changes to cell-signaling mechanisms that remodel vessels (Bussmann *et al*., 2011; Ghaffari *et al*., 2017; Xu & Cleaver, 2011). Halabi *et al*. characterized the Sema3fb mutant and showed that homozygous loss of function results in impaired cardiac function by 48hpf (Halabi, 2019). For this reason, my assays focused on vessel growth during 26-30 hpf – a time when most ISAs have branched from the DA and have formed connections at the DLAV independently of blood flow. Within the developing trunk vasculature, I found that *sema3fa* and *sema3fb* have non-overlapping expression patterns which allowed me to distinguish the role of *sema3fb* in angiogenic growth. In support of this, I showed that *sema3fa* mutants do not show angiogenic defects in ISA formation, and argued against genetic compensation in this vessel bed. There also appeared to be expression of *sema3fb* within the CVP which is also forming during this time. I did note that the CVP in *sema3fb* mutant embryos appears enlarged by 30 hpf and appeared to persist until at least 48hpf, however, these defects are most likely a result of decreased blood flow. There is no detectable eye vessel phenotype in sema3fb mutants.

In addition as the vessel infiltration assays used to characterize *sema3fa* mutants were carried out at a time when vessel growth is dependent on blood flow (Liao *et al.*, 1997; Dhakal *et al.*, 2015), I did not assess a role for *sema3fb* in regulating retinal vessel growth. Future work to establish a double homozygote line to fully elucidate the function of both *sema3f* homologs in vivo could provide important information on how the two homologs function together, however, these studies would be impacted by the *sema3fb* cardiac defects. To characterization the expression of

both genes throughout vessel development, I would make use of our transgenic lines to perform micro-dissections of different vessel beds, such as retinal, brain, and trunk vessels, and assay the expression of both *sema3fb* and *sema3fa* in endothelial cells through FACS sorting as described in Chapter 2. Going forward it will also be important to address the fact that *sema3fb*^{ca305} CRISPR mutants are a global knockout, meaning that all the cells which normally express *sema3fb* are affected including non-endothelial cells. Characterizing the expression of *sema3fb* in different vessel beds, it would be beneficial to generate endothelial-specific loss or gain of function mutants to bypass the cardiac defect which limited my characterization assays. I have assumed in this thesis that the *sema3fb*^{ca305} mutation is a loss of function mutation with haploinsufficiency. However, to rule out that the mutation might be a dominant-negative, it will also be important to confirm that endothelial-specific expression of the mutant *sema3fb* does not impair vessel growth.

4.3. microRNA26a as a regulator of mural cell recruitment

My work in chapter 3 highlighted the importance of cellular cross-talk in maintaining smooth muscle coverage. I investigated the role of *mir-26a* and its target *smad1*, a mediator of BMP signaling, in regulating vSMC maturation. These early steps of vascular maturation have not been examined *in vivo* before due to this process occurring in utero in mammals. I demonstrated that when mural cells associate with the endothelium, they lack expression of pSmad1 and do not show evidence of BMP activity as measured by a reporter. Using a combination of genetic manipulation and inhibitor treatment, I demonstrated that changes in endothelial *smad1* influenced vSMC coverage *in vivo* in a non-cell-autonomous manner.

The effects of changes in Smad1 in the endothelium to influence mural cell maturation warrants further investigation. Specifically, it would be interesting to ask whether *miR26a* has an earlier role in promoting vSMC recruitment and differentiation. In my work, I used our *acta2* (smooth muscle actin) transgenic line to characterize changes in vSMC coverage and gene expression. I assayed embryos at 4dpf, which is the earliest time when *acta2* expressing cells associate with a larger vessel such as the ventral aorta. However, my analysis of vSMCs isolated from *miR26a* morphants revealed an increase in expression of *pdgfrβ* which is a key factor in guiding mural cell migration in response to endothelial stimuli. Our lab has recently created and characterized a *foxc1b* transgenic line and we have generated Pdgfrβ transgenic lines that mark

mural cells that associate with vessels before the expression of *acta2*. Characterization of these lines revealed that, while *foxc1b* is co-expressed in the *acta2* positive vSMCs that associate with large diameter vessels in the brain, it is not co-expressed in capillaries where Pdgfrβ positive pericytes are located (Whitesell *et al.*, 2019). It would, therefore, be interesting to see the effects of *mir26a* and *smad1* in regulating these other subsets of mural cells *in vivo*. Assaying the expression of *foxc1b* and *pdgfrβ* transgenic zebrafish at 2 dpf through 4 dpf will allow further characterization to capture changes in early mural cell association through to the onset of vSMC marker expression. The differing expression patterns described by Whitesell *et al*.2019 will also guide the study of additional vessel beds such as the brain and retinal vasculature and could reveal organ-specific and arterio-venous specific changes in vSMC coverage.

Another important finding which warrants further investigation is whether the increased vSMC coverage correlates to increased contractile function. Alterations in the BMP pathways that control vSMC maturation can result in hypertensive disorders characterized by excess vSMC coverage (Laurent *et al*., 2009; Johnson *et al*., 2012; Lagna *et al*., 2007). Recently, our lab demonstrated both pericyte- and vSMC-covered vessels regulate their diameter in early development in response to contractile agonists (Bahrami and Childs, 2020). Using *miR26a* knockdown or endothelial *smad1* overexpression to increased contractile gene expression, zebrafish embryos could be treated with similar contractile agonists to test the contractile responses. Also, as smooth muscle coverage in the embryonic brain occurs later than vessels in the ventral head, (Chen *et al*., 2017), these experiments could be repeated in the brain with contractile agonists in *acta2, pdgfrβ,* and *foxc1b* transgenic zebrafish. Together these experiments would allow an understanding of the functional consequence of increased mural cell coverage on regulating embryonic blood flow and potentially directing mural cell recruitment.

4.4. microRNA26a as a regulator of endothelial cells

During normal blood vessel development, context-dependent functions of TGF-β/BMP influence both endothelial and smooth muscle cell differentiation. As discussed in Chapter 1, cell-specific knockout or loss-of-function mutations demonstrated that loss of BMP signaling in either cell type results in vessel malformations. Although my work in Chapter 3 focuses on the effects of BMP

signaling via Smad1 mediating cell cross-talk, a potential avenue for future work could be to understand the role of *mir26a* to regulate smad1-dependant signaling within endothelial cells.

One unexplored phenotype is the loss of vascular stability in early stages, where *mir26a* knockdown results in a hemorrhage phenotype. This phenotype warrants further investigation to understand how an increase in Smad1 could result in hemorrhage. Generally, BMP signaling induces endothelial cell quiescence and maintains the expression of inter-endothelial cell junctions to regulate vascular permeability. In HHT disease models, downregulation of Alk1 signaling causes severe hemorrhaging, often as a result of vessel distension during angiogenesis (Cunha *et al*., 2017). However, enhanced BMP signaling can have diverse effects. For example, BMP stimulation induces hyper-permeabilization of human endothelial cells through internalization via Src-dependent phosphorylation of VE-cadherin. This loosens cell-cell contacts and weakens the endothelial lining of the vessel. Additional genes regulated by Alk1 such as the pro-migratory factors Cxcr4 and Dll4, that are expressed by endothelial tip cells, also regulate angiogenic growth (Chen *et al*., 2013; Van Meeteren *et al*., 2012). In cultured human ECs, BMP9/ALK1 signaling downregulates CXCR4 and induces Connexin 40 (CX40, a component of gap junctions) which limits vessel sprouting but increase vessel permeability (Gkatzis *et al.*, 2016). It would, therefore, be interesting to determine whether disruption of cell contacts accounts for the hemorrhage phenotype observed in *mir26a* knockdown embryos. Assaying the expression of the VE-Cadherin using an antibody or measuring mRNA levels of *cxcr4/cxcl12* in 48 hpf embryos could determine if hemorrhage can be attributed to changes in endothelial migration and/ or vascular permeability.

An interesting link between BMP-induced signaling and vessel growth is the interaction between canonical Smad signaling and Notch to influence tip/stalk cell determination of endothelial cells during angiogenesis (Ten Dijke, Miyazono and Heldin, 2000; Ten Dijke, Goumans and Pardali, 2008; Larrivée *et al.*, 2012). For example, Larrivée *et al*. showed that Alk1-dependent Smad1/5 signaling collaborated with Notch to induce expression of Hey1 and Hey2 in stalk cells, which limits the response of stalk cells to Vegf. Moya *et al*. used the endothelium-specific Tie2-Cre mice crossed with floxed Smad1 and Smad5 to demonstrate that Smad1 and Notch collaborate to regulate tip/stalk cell selection in endothelial cells (Moya *et al.*, 2012). In zebrafish, disruption of *acvrl1* or *bmp10/bmp10-like* upregulates *cxcr4a* and *dll4* expression and contributes to vessel

overgrowth (Corti *et al.*, 2011; Laux *et al.*, 2013). As discussed above, in Chapter 3 I assessed the effects of *miR26a* on vSMC maturation. In line with the experiments above, measuring the endothelial expression of *notch* target genes, such as *dll4, hey1, hes1, and jag1* may also help us understand how *miR26a* can influence initial vessel growth and later stabilization through mural cell recruitment.

4.5. Importance of negative signaling in vascular development and disease

During development, negative-feedback mechanisms can act to limit the strength, duration, and/or range of growth factor signaling to fine-tune cellular responses. Current treatments for vascular disorders are based on knowledge of the cell signaling pathways that control vessel growth. As such the treatment options usually rely on targeted inhibition or restoration of pathways to limit vessel growth. The idea of limiting vessel growth by reducing Vegf in the local environment has led to the development of numerous disease models, drug development, and clinical trials for disorders where vessel overgrowth contributes to disease pathologies. However as anti-VEGF therapy has shown varying success, and is limited in its effectiveness (Cui & Lu, 2018; Eelen *et al*., 2020), it calls into question the additional pathways which limit vessel invasion and whether these may be better targets to design treatment options.

Sema3s are attractive therapeutic targets for pathological angiogenesis and efforts to produce effective treatments to restore normal tissue function have focused on two main strategies; 1) to deliver a soluble anti-angiogenic Sema to limit vascularization and 2) to use small molecules such as blocking antibodies and antagonist peptides to inhibit the pro-angiogenic sema-receptor complexes (reviewed in Serini *et al*. 2013). Sema3A and E have been explored for therapies due to their anti-angiogenic potential in limiting vessel environments. Angiogenic tumor models suggest the success of exogenous delivery of Sema3A or Sema3E is in part due to blocking the pro-angiogenic activity of Sema4A or Sema4D through competitive binding(Moriya *et al.*, 2010; Casazza *et al.*, 2011). Indeed, treatment options that directly target and block the action of pro-angiogenic Semas have demonstrated this idea. For example, Sema4D blocking antibodies and NRP-1 peptides have successfully reduced vessel density both in vitro and in vivo studies(Kong *et al.*, 2010; Fisher *et al.*, 2016). However, although studies suggest Sema3s could be potential therapeutic agents to regulate angiogenesis, difficulties can be encountered in targeting specific

tissues in more complex disease models (reviewed in Iragavarapu-Charyulu *et al*., 2020). For example, Sema3s can either promote or inhibit angiogenesis depending on the receptor they engage with, whether it is a transmembrane or a secreted molecule, and which signaling pathways are activated. As I have highlighted in my work, tissue-specific combinations of receptor and ligand expression are also important in regulating the environmental response. It will, therefore, be crucial to consider how all these factors function *in vivo* to design effective treatments.

Current treatments that aim to limit vessel growth have also explored targeting Bmp signaling to regulating vessel growth. Interestingly Bmp9/10 signaling antagonizes Vegf mediated endothelial cell migration to promote tube formation (Park *et al*., 2012; Van Meeteren *et al*., 2012). Preclinical mouse studies determined Vegf neutralization prevents the formation of AVMs and improves bleeding. While current trials are investigating dual treatment with Vegf inhibitors and drugs to increase Alk1 expression to restore vascular function (reviewed in Cunha *et al*. 2017). The current therapeutic options for PAH are focused on the reversal of the proliferation of vascular cells to relieve vessel constriction. In keeping with the idea of cellular crosstalk, restoration of endothelial BMP signaling could be a promising alternative to drug treatments to limit vessel growth and prevent vSMC proliferation (reviewed in Orriols *et al*., 2017).

With their role in regulating vSMC maturation, microRNAs also present an attractive model for treating vascular disorders. miR-based therapeutics have mainly focus on restoring miRNA expression levels via two main approaches; 1) overexpression of downregulated miRNAs and 2) suppression of upregulated miRNAs. Oligonucleotides serve as promising tools to either mimic the endogenous miRNA or suppress the mature miRNA by sequence complementarity and have been modified to improve clinical applications. For example, cholesterol conjugation enhances circulation time, serum stability, and cellular uptake. (Zhou *et al*. 2018; Chamorro-Jorganes *et al*., 2013; Lindow and Kauppinen 2012; Ozcan *et al*. 2015). In vascular repair models, an interesting option to improve stabilization and efficiency are adeno-associated viruses (AAVs) as delivery vehicles (Bish *et al*., 2008). Santulli *et al*. 2014 demonstrate that an AAV containing miR126-3p target sites (commonly termed a microRNA sponge) inhibits vSMC proliferation and prevents restenosis. As miR126 is an endothelial-specific miRNA this study provided an efficient tool for gene transfer and targeted delivery of miRNA-based therapeutics to modulate cell crosstalk

(Santulli *et al.*, 2014). Other miRNA-based studies have focused on exosomes as delivery vehicles. For example, Zhang *et al*. 2010 transfected phagocytic THP-1 cells with anti-miR150 oligonucleotides to produce a conditioned media enriched with oligo-bearing exosomes. Exogenous incubation with this media reduced endothelial cell migration, demonstrating the use of exosomes as a feasible delivery method (Zhang *et al*., 2010). Due to their natural role in miRNA secretion and shuttling between different tissues, exosomes also serve to facilitate communication between cells (Stoorvogel, 2012; Feinberg, 2014; Sahoo and Losordo, 2014; Gray *et al.*, 2015). Of particular interest to my work, Wang *et al* 2019, showed that glioma stem cells (GSCs)-derived exosomes containing miR26a could exert pro-angiogenic effects on human brain microvascular endothelial cells (HBMECs) via PTEN and subsequent PI3K/Akt downregulation (Wang *et al*., 2019). Intriguingly, as exosomal membranes contain proteins with binding affinity to specific receptors on the surface of recipient cells they offer further potential to selectively target cell types. However, further studies would be necessary to optimize their quality and characterization for targeted delivery to reduce the potential for cytotoxicity and low efficiency due to inappropriate tissue uptake *in vivo* (Rooij and Olson, 2012). Furthermore, questions on the specificity of miRNA action will have to be fully addressed in vivo. I found that *miR26a* functions as an endothelial regulator of vSMC differentiation, but its endothelial actions still need further investigation. Therefore, when investigating the effects of miRNA therapeutics on vessel growth, it will be critical to examine their effects on both endothelial cell and vSMC functions in intact models

4.6. Concluding Remarks

My work highlights that endothelial cells are an important integration hub for the signals that control vessel growth, and are continually exposed to extrinsic factors, which in turn regulate their intrinsic properties. In later life, angiogenesis is limited to physiological causes, such as wound healing or pathologies that impair the balance between angiogenic inhibitors and activators. Both newly formed and pathological vessels are augmented by the recruitment of smooth muscle cells. Dysregulation of smooth muscle cells is often associated with changes in vascular permeability and can result in breakage (hemorrhages) and subsequent damage to surrounding tissues. As both microRNAs and Semaphorins are currently under investigation as therapeutics that aim to modulate vascular dynamics, my work will contribute to the understanding of the endothelial-specific delivery strategies needed to promote appropriate vessel growth and stabilization

References

Abid, M. R. *et al.* (2004) 'Vascular Endothelial Growth Factor Activates PI3K/Akt/Forkhead Signaling in Endothelial Cells'. doi: 10.1161/01.ATV.0000110502.10593.06.

Acevedo, L. M., Weis, S. M. and Cheresh, D. A. (2008) 'Robo4 counteracts VEGF signaling', *Nature Medicine*, pp. 372–373. doi: 10.1038/nm0408-372.

Adams, R. H. and Alitalo, K. (2007) 'Molecular regulation of angiogenesis and lymphangiogenesis', *Nature Reviews Molecular Cell Biology*. Nat Rev Mol Cell Biol, pp. 464–478. doi: 10.1038/nrm2183.

Adams, R. H. and Eichmann, A. (2010a) 'Axon guidance molecules in vascular patterning.', *Cold Spring Harbor perspectives in biology*. Cold Spring Harbor Laboratory Press, p. a001875. doi: 10.1101/cshperspect.a001875.

Adams, R. H. and Eichmann, A. (2010b) 'Axon guidance molecules in vascular patterning.', *Cold Spring Harbor perspectives in biology*. Cold Spring Harb Perspect Biol. doi: 10.1101/cshperspect.a001875.

Albinsson, S. *et al.* (2010) 'miRNAs are necessary for vascular smooth muscle growth, differentiation and function', *Arterioscler Thromb Vasc Biol*, 30(6), pp. 1118–1126. doi: 10.1161/atvbaha.109.200873.

Ali, S. S. *et al.* (2015) 'Pathological microRNAs in acute cardiovascular diseases and microRNA therapeutics', *Journal of Acute Disease*. doi: 10.1016/j.joad.2015.08.001.

Alliot, F. *et al.* (1999) 'Pericytes and periendothelial cells of brain parenchyma vessels co-express aminopeptidase N, aminopeptidase A, and nestin', *Journal of Neuroscience Research*. John Wiley & Sons, Ltd, 58(3), pp. 367–378. doi: 10.1002/(SICI)1097-4547(19991101)58:3<367::AID-JNR2>3.0.CO;2-T.

Anderson, L. M. and Gibbons, G. H. (2007) 'Notch: a mastermind of vascular morphogenesis.', *The Journal of clinical investigation*, 117(2), pp. 299–302. doi: 10.1172/JCI31288.

Ando, K. *et al.* (2016) 'Clarification of mural cell coverage of vascular endothelial cells by live imaging of zebrafish', *Development (Cambridge, England)*, pp. 1328–1339. doi: 10.1242/dev.132654.

Angulo-Urarte, A. *et al.* (2018) 'Endothelial cell rearrangements during vascular patterning require PI3-kinase-mediated inhibition of actomyosin contractility', *Nature Communications*. Nature Publishing Group, 9(1), pp. 1–16. doi: 10.1038/s41467-018-07172-3.

Armulik, A., Genové, G. and Betsholtz, C. (2011) 'Pericytes: Developmental, Physiological, and Pathological Perspectives, Problems, and Promises', *Developmental Cell*. Cell Press, pp. 193–215. doi: 10.1016/j.devcel.2011.07.001.

Avagyan, S. and Zon, L. I. (2016) 'Fish to Learn: Insights into Blood Development and Blood Disorders from Zebrafish Hematopoiesis.', *Human gene therapy*. Mary Ann Liebert Inc., 27(4), pp. 287–94. doi: 10.1089/hum.2016.024.

Bahary, N. *et al.* (2007) 'Duplicate VegfA genes and orthologues of the KDR receptor tyrosine kinase family mediate vascular development in the zebrafish', *Blood*. The American Society of Hematology, 110(10), pp. 3627–3636. doi: 10.1182/blood-2006-04-016378.

Bahrami, N. and Childs, S. J. (2020) 'Development of vascular regulation in the zebrafish embryo', *Development*. Oxford University Press for The Company of Biologists Limited, 147(10), pp. 1–12. doi: 10.1242/dev.183061.

Bai, Y. *et al.* (2011) 'Circulating microRNA-26a: potential predictors and therapeutic targets for non-hypertensive intracerebral hemorrhage', *Med Hypotheses*. 2011/07/19, 77(4), pp. 488–490.

doi: 10.1016/j.mehy.2011.06.017.
Baldessari, D. and Mione, M. (2008) 'How to create the vascular tree? (Latest) help from the zebrafish', *Pharmacology and Therapeutics*. Pharmacol Ther, pp. 206–230. doi: 10.1016/j.pharmthera.2008.02.010.
BANG, C., FIEDLER, J. and THUM, T. (2012) 'Cardiovascular Importance of the MicroRNA-23/27/24 Family', *Microcirculation*. John Wiley & Sons, Ltd, 19(3), pp. 208–214. doi: 10.1111/j.1549-8719.2011.00153.x.
Banu, N. *et al.* (2006) 'Semaphorin 3C regulates endothelial cell function by increasing integrin activity', *The FASEB Journal*. Wiley, 20(12), pp. 2150–2152. doi: 10.1096/fj.05-5698fje.
Bartel, D. P. (2004) 'MicroRNAs: Genomics, Biogenesis, Mechanism, and Function', *Cell*, 116(2), pp. 281–297. doi: http://dx.doi.org/10.1016/S0092-8674(04)00045-5.
Bautch, V. L. (2009) 'Endothelial Cells Form a Phalanx to Block Tumor Metastasis', *Cell*. Cell, pp. 810–812. doi: 10.1016/j.cell.2009.02.021.
Bayless, K. J. and Johnson, G. A. (2011) 'Role of the Cytoskeleton in Formation and Maintenance of Angiogenic Sprouts', *Journal of Vascular Research*. Karger Publishers, 48(5), pp. 369–385. doi: 10.1159/000324751.
Bedell, V. M., Westcot, S. E. and Ekker, S. C. (2011) 'Lessons from morpholino-based screening in zebrafish', *Brief Funct Genomics*. 2011/07/13, 10(4), pp. 181–188. doi: 10.1093/bfgp/elr021.
Benjamin, L. E., Hemo, I. and Keshet, E. (1998) 'A plasticity window for blood vessel remodelling is defined by pericyte coverage of the preformed endothelial network and is regulated by PDGF-B and VEGF', *Development*. The Company of Biologists Limited, 125(9), pp. 1591–1598.
Beppu, H. *et al.* (2000) 'BMP type II receptor is required for gastrulation and early development of mouse embryos.', *Developmental biology*, 221(1), pp. 249–58. doi: 10.1006/dbio.2000.9670.
Betz, C. *et al.* (2016) 'Cell behaviors and dynamics during angiogenesis', *Development (Cambridge)*. Company of Biologists Ltd, pp. 2249–2260. doi: 10.1242/dev.135616.
Bielenberg, D. R. *et al.* (2004) 'Semaphorin 3F, a chemorepulsant for endothelial cells, induces a poorly vascularized, encapsulated, nonmetastatic tumor phenotype', *Journal of Clinical Investigation*. The American Society for Clinical Investigation, 114(9), pp. 1260–1271. doi: 10.1172/JCI21378.
Bill, B. R. *et al.* (2009) 'A primer for morpholino use in zebrafish', *Zebrafish*. Mary Ann Liebert, Inc. 140 Huguenot Street, 3rd Floor New Rochelle, NY 10801 USA, 6(1), pp. 69–77.
Bish, L. T. *et al.* (2008) 'Adeno-associated virus (AAV) serotype 9 provides global cardiac gene transfer superior to AAV1, AAV6, AAV7, and AAV8 in the mouse and rat', *Human Gene Therapy*. Mary Ann Liebert, Inc. 140 Huguenot Street, 3rd Floor New Rochelle, NY 10801 USA , 19(12), pp. 1359–1368. doi: 10.1089/hum.2008.123.
Bonauer, A. *et al.* (2009) 'MicroRNA-92a controls angiogenesis and functional recovery of ischemic tissues in Mice', *Science*. American Association for the Advancement of Science, 324(5935), pp. 1710–1713. doi: 10.1126/science.1174381.
Brambilla, E. *et al.* (2000) 'Semaphorin SEMA3F localization in malignant human lung and cell lines: A suggested role in cell adhesion and cell migration', *American Journal of Pathology*. American Society for Investigative Pathology Inc., 156(3), pp. 939–950. doi: 10.1016/S0002-9440(10)64962-0.
Brose, K. and Tessier-Lavigne, M. (2000) 'Slit proteins: Key regulators of axon guidance, axonal branching, and cell migration', *Current Opinion in Neurobiology*. Current Biology Ltd, pp. 95–102. doi: 10.1016/S0959-4388(99)00066-5.
Buehler, A. *et al.* (2013) 'Semaphorin 3F forms an anti-angiogenic barrier in outer retina', *FEBS*

Letters. No longer published by Elsevier, 587(11), pp. 1650–1655. doi: 10.1016/j.febslet.2013.04.008.
Bussmann, J. *et al.* (2008) 'Zebrafish VEGF receptors: A guideline to nomenclature', *PLoS Genetics*, 4(5), pp. e1000064–e1000064. doi: 10.1371/journal.pgen.1000064.
Bussmann, J. *et al.* (2010) 'Arteries provide essential guidance cues for lymphatic endothelial cells in the zebrafish trunk', *Development*. Oxford University Press for The Company of Biologists Limited, 137(16), pp. 2653–2657. doi: 10.1242/dev.048207.
Bussmann, J., Wolfe, S. A. and Siekmann, A. F. (2011) 'Arterial-venous network formation during brain vascularization involves hemodynamic regulation of chemokine signaling', *Development*. Development, 138(9), pp. 1717–1726. doi: 10.1242/dev.059881.
Cai, J. *et al.* (2012) 'BMP signaling in vascular diseases', *FEBS Letters*. No longer published by Elsevier, 586(14), pp. 1993–2002. doi: 10.1016/J.FEBSLET.2012.04.030.
Capparuccia, L. and Tamagnone, L. (2009) 'Semaphorin signaling in cancer cells and in cells of the tumor microenvironment - Two sides of a coin', *Journal of Cell Science*. The Company of Biologists Ltd, 122(11), pp. 1723–1736. doi: 10.1242/jcs.030197.
Carmeliet, P. (2003a) 'Angiogenesis in health and disease', *Nature Medicine*. Nature Publishing Group, pp. 653–660. doi: 10.1038/nm0603-653.
Carmeliet, P. (2003b) 'Blood vessels and nerves: Common signals, pathways and diseases', *Nature Reviews Genetics*, pp. 710–720. doi: 10.1038/nrg1158.
Carmeliet, P. and Tessier-Lavigne, M. (2005) 'Common mechanisms of nerve and blood vessel wiring', *Nature*. Nature Publishing Group, pp. 193–200. doi: 10.1038/nature03875.
Carretero-Ortega, J. *et al.* (2019) 'GIPC proteins negatively modulate Plexind1 signaling during vascular development', *eLife*. eLife Sciences Publications Ltd, 8. doi: 10.7554/eLife.30454.
Casazza, A. *et al.* (2011) 'Systemic and targeted delivery of semaphorin 3A inhibits tumor angiogenesis and progression in mouse tumor models', *Arteriosclerosis, Thrombosis, and Vascular Biology*, 31(4), pp. 741–749. doi: 10.1161/ATVBAHA.110.211920.
Chamorro-Jorganes, A. *et al.* (2011) 'MicroRNA-16 and MicroRNA-424 regulate cell-autonomous angiogenic functions in endothelial cells via targeting vascular endothelial growth factor receptor-2 and fibroblast growth factor receptor-1', *Arteriosclerosis, Thrombosis, and Vascular Biology*. Lippincott Williams & WilkinsHagerstown, MD, 31(11), pp. 2595–2606. doi: 10.1161/ATVBAHA.111.236521.
Chamorro-Jorganes, A., Araldi, E. and Suárez, Y. (2013) 'MicroRNAs as pharmacological targets in endothelial cell function and dysfunction', *Pharmacological Research*. Academic Press, pp. 15–27. doi: 10.1016/j.phrs.2013.04.002.
Chen, Hao *et al.* (2013) 'Context-dependent signaling defines roles of BMP9 and BMP10 in embryonic and postnatal development', *Proceedings of the National Academy of Sciences of the United States of America*, 110(29), pp. 11887–11892. doi: 10.1073/pnas.1306074110.
Chen, S. *et al.* (2006) 'RhoA modulates Smad signaling during transforming growth factor-β-induced smooth muscle differentiation', *Journal of Biological Chemistry*. ASBMB, 281(3), pp. 1765–1770.
Chen, W. *et al.* (2019) 'The endothelial tip-stalk cell selection and shuffling during angiogenesis', *Journal of Cell Communication and Signaling*. Springer Netherlands, pp. 291–301. doi: 10.1007/s12079-019-00511-z.
Chen, Z. *et al.* (2018) 'MicroRNA-125b Affects Vascular Smooth Muscle Cell Function by Targeting Serum Response Factor', *Cellular Physiology and Biochemistry*. S. Karger AG, 46(4), pp. 1566–1580. doi: 10.1159/000489203.

Childs, S., Chen, J. N., *et al.* (2002) 'Patterning of angiogenesis in the zebrafish embryo', *Development*, pp. 973–982.
Childs, S., Chen, J.-N., *et al.* (2002) 'Patterning of angiogenesis in the zebrafish embryo', *Development*, 129(4), pp. 973 LP – 982.
Chu, G. C. *et al.* (2004) 'Differential requirements for Smad4 in TGFbeta-dependent patterning of the early mouse embryo', *Development*, 131. doi: 10.1242/dev.01248.
Clark, C. R. *et al.* (2016) 'Common pathways regulate type III TGFβ receptor-dependent cell invasion in epicardial and endocardial cells.', *Cellular signalling*. doi: 10.1016/j.cellsig.2016.03.004.
Clements, R. T. *et al.* (2005) 'RhoA and Rho-kinase dependent and independent signals mediate TGF-β-induced pulmonary endothelial cytoskeletal reorganization and permeability', *American Journal of Physiology - Lung Cellular and Molecular Physiology*. Am J Physiol Lung Cell Mol Physiol, 288(2 32-2). doi: 10.1152/ajplung.00213.2004.
Cole, C. L. *et al.* (2010) 'Synthetic heparan sulfate oligosaccharides inhibit endothelial cell functions essential for angiogenesis', *PLoS ONE*. Public Library of Science, 5(7), pp. 1–15. doi: 10.1371/journal.pone.0011644.
Collery, R. F. and Link, B. A. (2011) 'Dynamic Smad-mediated BMP signaling revealed through transgenic zebrafish', *Developmental dynamics : an official publication of the American Association of Anatomists*, pp. 712–722. doi: 10.1002/dvdy.22567.
Conde, J. and Artzi, N. (2015) 'Are RNAi and miRNA therapeutics truly dead?', *Trends in biotechnology*, 33(3), pp. 141–4. doi: 10.1016/j.tibtech.2014.12.005.
Cordes, K. R. *et al.* (2009) 'miR-145 and miR-143 regulate smooth muscle cell fate and plasticity', *Nature*. Nature Publishing Group, 460(7256), pp. 705–710.
Corti, P. *et al.* (2011) 'Interaction between alk1 and blood flow in the development of arteriovenous malformations', *Development*, 138(8), pp. 1573–1582.
Covassin, L. D. *et al.* (2006) 'Distinct genetic interactions between multiple Vegf receptors are required for development of different blood vessel types in zebrafish', *Proceedings of the National Academy of Sciences of the United States of America*, 103(17), pp. 6554–6559. doi: 10.1073/pnas.0506886103.
Covassin, L. D. *et al.* (2009) 'A genetic screen for vascular mutants in zebrafish reveals dynamic roles for Vegf/Plcg1 signaling during artery development', *Developmental Biology*. Academic Press Inc., 329(2), pp. 212–226. doi: 10.1016/j.ydbio.2009.02.031.
Cui, C. and Lu, H. (2018) 'Clinical observations on the use of new anti-VEGF drug, conbercept, in age-related macular degeneration therapy: A meta-analysis', *Clinical Interventions in Aging*. Dove Medical Press Ltd., 13, pp. 51–62. doi: 10.2147/CIA.S151225.
Cunha, S. I. *et al.* (2017) 'Deregulated TGF-β/BMP signaling in vascular malformations', *Circulation Research*. Lippincott Williams and Wilkins, 121(8), pp. 981–999. doi: 10.1161/CIRCRESAHA.117.309930.
David, L. *et al.* (2008) 'Bone morphogenetic protein-9 is a circulating vascular quiescence factor', *Circ Res*, 102. doi: 10.1161/CIRCRESAHA.107.165530.
David, L., Feige, J. J. and Bailly, S. (2009) 'Emerging role of bone morphogenetic proteins in angiogenesis', *Cytokine and Growth Factor Reviews*. Elsevier BV, pp. 203–212. doi: 10.1016/j.cytogfr.2009.05.001.
Davidson, A. J. and Zon, L. I. (2004) 'The "definitive" (and 'primitive') guide to zebrafish hematopoiesis', *Oncogene*. Oncogene, pp. 7233–7246. doi: 10.1038/sj.onc.1207943.
Davis-Dusenbery, B. N., Wu, C. and Hata, A. (2011) 'Micromanaging vascular smooth muscle

cell differentiation and phenotypic modulation', *Arterioscler Thromb Vasc Biol*. 2011/10/21, 31(11), pp. 2370–2377. doi: 10.1161/atvbaha.111.226670.
Davis, B. N. *et al.* (2009) 'Induction of microRNA-221 by platelet-derived growth factor signaling is critical for modulation of vascular smooth muscle phenotype.', *The Journal of biological chemistry*, 284(6), pp. 3728–38. doi: 10.1074/jbc.M808788200.
Davis, B. N. *et al.* (2010) 'Smad proteins bind a conserved RNA sequence to promote microRNA maturation by Drosha', *Molecular cell*. Elsevier, 39(3), pp. 373–384.
Davis, G. E. *et al.* (2011) 'Molecular basis for endothelial lumen formation and tubulogenesis during vasculogenesis and angiogenic sprouting.', *International review of cell and molecular biology*. Elsevier Inc., 288, pp. 101–65. doi: 10.1016/B978-0-12-386041-5.00003-0.
Davis, G. E. *et al.* (2013) 'Control of vascular tube morphogenesis and maturation in 3D extracellular matrices by endothelial cells and pericytes', *Methods in Molecular Biology*. Humana Press Inc., 1066, pp. 17–28. doi: 10.1007/978-1-62703-604-7_2.
Dekker, R. J. *et al.* (2002) 'Prolonged fluid shear stress induces a distinct set of endothelial cell genes, most specifically lung Krüppel-like factor (KLF2)', *Blood*. American Society of Hematology, 100(5), pp. 1689–1698. doi: 10.1182/blood-2002-01-0046.
Dekker, R. J. *et al.* (2005) 'Endothelial KLF2 links local arterial shear stress levels to the expression of vascular tone-regulating genes', *American Journal of Pathology*. American Society for Investigative Pathology Inc., 167(2), pp. 609–618. doi: 10.1016/S0002-9440(10)63002-7.
Deng, Z. *et al.* (2000) 'Familial primary pulmonary hypertension (Gene PPH1) is caused by mutations in the bone morphogenetic protein receptor–II gene', *The American Journal of Human Genetics*. Elsevier, 67(3), pp. 737–744.
Dhakal, S. *et al.* (2015) 'Abnormal retinal development in Cloche mutant zebrafish', *Developmental Dynamics*. John Wiley and Sons Inc., 244(11), pp. 1439–1455. doi: 10.1002/dvdy.24322.
Díaz-Flores, L. *et al.* (2009) 'Pericytes. Morphofunction, interactions and pathology in a quiescent and activated mesenchymal cell niche', *Histology and Histopathology*. Histol Histopathol, pp. 909–969. doi: 10.14670/HH-24.909.
Ten Dijke, P., Goumans, M. J. and Pardali, E. (2008) 'Endoglin in angiogenesis and vascular diseases', *Angiogenesis*. Springer, pp. 79–89. doi: 10.1007/s10456-008-9101-9.
Ten Dijke, P., Miyazono, K. and Heldin, C. H. (2000) 'Signaling inputs converge on nuclear effectors in TGF-β signaling', *Trends in Biochemical Sciences*. Elsevier, pp. 64–70. doi: 10.1016/S0968-0004(99)01519-4.
Domenga, V. *et al.* (2004) 'Notch3 is required for arterial identity and maturation of vascular smooth muscle cells', *Genes and Development*. Genes Dev, 18(22), pp. 2730–2735. doi: 10.1101/gad.308904.
Dooley, K. and Zon, L. I. (2000) 'Zebrafish: a model system for the study of human disease', *Current opinion in genetics & development*, 10(3), pp. 252–256.
Dzau, V. J., Braun-Dullaeus, R. C. and Sedding, D. G. (2002) 'Vascular proliferation and atherosclerosis: new perspectives and therapeutic strategies', *Nat Med*, 8(11), pp. 1249–1256.
Eblaghie, M. C. *et al.* (2006) 'Evidence that autocrine signaling through Bmpr1a regulates the proliferation, survival and morphogenetic behavior of distal lung epithelial cells', *Dev Biol*, 291. doi: 10.1016/j.ydbio.2005.12.006.
Eelen, G. *et al.* (2020) 'Basic and Therapeutic Aspects of Angiogenesis Updated', *Circulation Research*. Lippincott Williams & WilkinsHagerstown, MD, 127(2), pp. 310–329. doi: 10.1161/CIRCRESAHA.120.316851.

El-Bizri, N. *et al.* (2008) 'SM22α-Targeted Deletion of Bone Morphogenetic Protein Receptor IA in Mice Impairs Cardiac and Vascular Development and Influences Organogenesis', *Development (Cambridge, England)*, pp. 2981–2991. doi: 10.1242/dev.017863.
Endo-Takahashi, Y. *et al.* (2014) 'Systemic delivery of miR-126 by miRNA-loaded Bubble liposomes for the treatment of hindlimb ischemia', *Scientific reports*. Nature Publishing Group, 4.
Failla, C. M., Carbo, M. and Morea, V. (2018) 'Positive and negative regulation of angiogenesis by soluble vascular endothelial growth factor receptor-1', *International Journal of Molecular Sciences*. MDPI AG. doi: 10.3390/ijms19051306.
Fang, Y., Wu, D. and Birukov, K. G. (2019) 'Mechanosensing and Mechanoregulation of Endothelial Cell Functions.', *Comprehensive Physiology*. Wiley-Blackwell Publishing Ltd, 9(2), pp. 873–904. doi: 10.1002/cphy.c180020.
Fantin, A. *et al.* (2011) 'The cytoplasmic domain of neuropilin 1 is dispensable for angiogenesis, but promotes the spatial separation of retinal arteries and veins', *Development*. Oxford University Press for The Company of Biologists Limited, 138(19), pp. 4185–4191. doi: 10.1242/dev.070037.
Fantin, A. *et al.* (2013) 'NRP1 acts cell autonomously in endothelium to promote tip cell function during sprouting angiogenesis', *Blood*. American Society of Hematology, 121(12), pp. 2352–2362. doi: 10.1182/blood-2012-05-424713.
Fantin, A. *et al.* (2015) 'NRP1 Regulates CDC42 Activation to Promote Filopodia Formation in Endothelial Tip Cells', *Cell Reports*. Elsevier, 11(10), pp. 1577–1590. doi: 10.1016/j.celrep.2015.05.018.
Feinberg, M. W. (2014) 'Healing the injured vessel wall using microRNA-facilitated gene delivery', *Journal of Clinical Investigation*. American Society for Clinical Investigation, pp. 3694–3697. doi: 10.1172/JCI77509.
Fernández-Klett, F. *et al.* (2010) 'Pericytes in capillaries are contractile in vivo, but arterioles mediate functional hyperemia in the mouse brain.', *Proceedings of the National Academy of Sciences of the United States of America*, 107(51), pp. 22290–5. doi: 10.1073/pnas.1011321108.
Fernández-Klett, F. and Priller, J. (2015) 'Diverse functions of pericytes in cerebral blood flow regulation and ischemia', *Journal of Cerebral Blood Flow and Metabolism*. Nature Publishing Group, pp. 883–887. doi: 10.1038/jcbfm.2015.60.
Ferrara, N. (2002) 'VEGF and the quest for tumour angiogenesis factors', *Nature Reviews Cancer*. Nat Rev Cancer, pp. 795–803. doi: 10.1038/nrc909.
Fischer, C., Schneider, M. and Carmeliet, P. (2006) 'Principles and Therapeutic Implications of Angiogenesis, Vasculogenesis and Arteriogenesis', in *The Vascular Endothelium II*. Springer Berlin Heidelberg, pp. 157–212. doi: 10.1007/3-540-36028-x_6.
Fish, Jason E *et al.* (2008) 'miR-126 regulates angiogenic signaling and vascular integrity', *Developmental cell*. Elsevier, 15(2), pp. 272–284.
Fish, Jason E. *et al.* (2008) 'miR-126 Regulates Angiogenic Signaling and Vascular Integrity', *Developmental Cell*. Cell Press, 15(2), pp. 272–284. doi: 10.1016/j.devcel.2008.07.008.
Fisher, T. L. *et al.* (2016) 'Saturation monitoring of VX15/2503, a novel semaphorin 4D-specific antibody, in clinical trials', *Cytometry Part B - Clinical Cytometry*. John Wiley and Sons Inc., 90(2), pp. 199–208. doi: 10.1002/cyto.b.21338.
Fishman, M. C. (2000) 'gridlock, an HLH gene required for assembly of the aorta in zebrafish', *Science*. Science, 287(5459), pp. 1820–1824. doi: 10.1126/science.287.5459.1820.
Fjose, A. and Zhao, X.-F. (2010) 'Exploring microRNA functions in zebrafish', *New Biotechnology*, 27(3), pp. 250–255. doi: http://dx.doi.org/10.1016/j.nbt.2010.02.017.
Fouquet, B. *et al.* (1997) 'Vessel patterning in the embryo of the zebrafish: Guidance by

notochord', *Developmental Biology*. Academic Press Inc., 183(1), pp. 37–48. doi: 10.1006/dbio.1996.8495.
Frank, D. B. *et al.* (2005) 'Bone morphogenetic protein 4 promotes pulmonary vascular remodeling in hypoxic pulmonary hypertension', *Circulation research*. Am Heart Assoc, 97(5), pp. 496–504.
Gaengel, K. *et al.* (2009a) 'Endothelial-mural cell signaling in vascular development and angiogenesis', *Arteriosclerosis, Thrombosis, and Vascular Biology*. Lippincott Williams & Wilkins, pp. 630–638. doi: 10.1161/ATVBAHA.107.161521.
Gaengel, K. *et al.* (2009b) 'Endothelial-mural cell signaling in vascular development and angiogenesis', *Arteriosclerosis, thrombosis, and vascular biology*. Am Heart Assoc, 29(5), pp. 630–638.
Gammill, L. S. *et al.* (2006) 'Guidance of trunk neural crest migration reguires neuropilin 2/semaphorin 3F signaling', *Development*, 133(1), pp. 99–106. doi: 10.1242/dev.02187.
Gammill, L. S., Gonzalez, C. and Bronner-Fraser, M. (2007) 'Neuropilin 2/semaphorin 3F signaling is essential for cranial neural crest migration and trigeminal ganglion condensation', *Developmental Neurobiology*. Dev Neurobiol, 67(1), pp. 47–56. doi: 10.1002/dneu.20326.
Gay, C. M., Zygmunt, T. and Torres-Vázquez, J. (2011) 'Diverse functions for the semaphorin receptor PlexinD1 in development and disease', *Developmental Biology*. Academic Press Inc., pp. 1–19. doi: 10.1016/j.ydbio.2010.09.008.
Georgijevic, S. *et al.* (2007) 'Spatiotemporal expression of smooth muscle markers in developing zebrafish gut', *Developmental Dynamics*. Wiley Online Library, 236(6), pp. 1623–1632.
Gerhardt, H. *et al.* (2003a) 'VEGF guides angiogenic sprouting utilizing endothelial tip cell filopodia', *Journal of Cell Biology*, 161(6), pp. 1163–1177. doi: 10.1083/jcb.200302047.
Gerhardt, H. *et al.* (2003b) 'VEGF guides angiogenic sprouting utilizing endothelial tip cell filopodia', *Journal of Cell Biology*. The Rockefeller University Press, 161(6), pp. 1163–1177. doi: 10.1083/jcb.200302047.
Gerhardt, H. and Betsholtz, C. (2003) 'Endothelial-pericyte interactions in angiogenesis', *Cell and Tissue Research*, pp. 15–23. doi: 10.1007/s00441-003-0745-x.
Gessler, M. *et al.* (2002) 'Mouse gridlock: No aortic coarctation or deficiency, but fatal cardiac defects in Hey2 -/- mice', *Current Biology*. Elsevier, 12(18), pp. 1601–1604. doi: 10.1016/S0960-9822(02)01150-8.
Geudens, I. and Gerhardt, O. (2011) 'Coordinating cell behaviour during blood vessel formation', *Development*. Development, pp. 4569–4583. doi: 10.1242/dev.062323.
Ghaffari, S., Leask, R. L. and Jones, E. A. V. (2017) 'Blood flow can signal during angiogenesis not only through mechanotransduction, but also by affecting growth factor distribution', *Angiogenesis*. Springer Netherlands, 20(3), pp. 373–384. doi: 10.1007/s10456-017-9553-x.
Gimenez, F. *et al.* (2015) 'Robo 4 counteracts angiogenesis in herpetic stromal keratitis', *PLoS ONE*. Public Library of Science, 10(12). doi: 10.1371/journal.pone.0141925.
Gkatzis, K. *et al.* (2016) 'Interaction between ALK1 Signaling and Connexin40 in the Development of Arteriovenous Malformations', *Arteriosclerosis, Thrombosis, and Vascular Biology*. Lippincott Williams and Wilkins, 36(4), pp. 707–717. doi: 10.1161/ATVBAHA.115.306719.
Gore, A. V *et al.* (2012) 'Vascular development in the zebrafish', *Cold Spring Harbor perspectives in medicine*. Cold Spring Harbor Laboratory Press, 2(5), p. a006684.
Goumans, M. J. and Mummery, C. (2000) 'Functional analysis of the TGFbeta receptor/Smad pathway through gene ablation in mice.', *The International journal of developmental biology*.

SPAIN, 44(3), pp. 253–265.
Graupera, M. *et al.* (2008) 'Angiogenesis selectively requires the p110α isoform of PI3K to control endothelial cell migration', *Nature*. Nature Publishing Group, 453(7195), pp. 662–666. doi: 10.1038/nature06892.
Gray, W. D. *et al.* (2015) 'Identification of therapeutic covariant microRNA clusters in hypoxia-treated cardiac progenitor cell exosomes using systems biology', *Circulation Research*. Lippincott Williams and Wilkins, 116(2), pp. 255–263. doi: 10.1161/CIRCRESAHA.116.304360.
Griffiths-Jones, S. *et al.* (2008) 'miRBase: tools for microRNA genomics', *Nucleic acids research*. Oxford Univ Press, 36(suppl 1), pp. D154–D158.
Gu, C. *et al.* (2003) 'Neuropilin-1 conveys semaphorin and VEGF signaling during neural and cardiovascular development', *Developmental Cell*. Cell Press, 5(1), pp. 45–57. doi: 10.1016/S1534-5807(03)00169-2.
Gu, C. *et al.* (2005) 'Semaphorin 3E and plexin-D1 control vascular pattern independently of neuropilins', *Science*. American Association for the Advancement of Science, 307(5707), pp. 265–268. doi: 10.1126/science.1105416.
Guo, H. F. *et al.* (2013) 'Mechanistic basis for the potent anti-angiogenic activity of Semaphorin 3f', *Biochemistry*. American Chemical Society, 52(43), pp. 7551–7558. doi: 10.1021/bi401034q.
Guttmann-Raviv, N. *et al.* (2007) 'Semaphorin-3A and semaphorin-3F work together to repel endothelial cells and to inhibit their survival by induction of apoptosis', *Journal of Biological Chemistry*, 282(36), pp. 26294–26305. doi: 10.1074/jbc.M609711200.
Halabi, R. (2019) *Semaphorin3f as a Spatial Regulator of Embryogenesis*. Cumming School of Medicine.
Hall, C. N. *et al.* (2014) 'Capillary pericytes regulate cerebral blood flow in health and disease', *Nature*. Nature Publishing Group, 508(1), pp. 55–60. doi: 10.1038/nature13165.
Ham, O. *et al.* (2017) 'Small molecule-mediated induction of miR-9 suppressed vascular smooth muscle cell proliferation and neointima formation after balloon injury', *Oncotarget*. Impact Journals LLC, 8(55), pp. 93360–93372. doi: 10.18632/oncotarget.21382.
Harris, T. A. *et al.* (2010) 'Ets-1 and Ets-2 regulate the expression of MicroRNA-126 in endothelial cells', *Arteriosclerosis, Thrombosis, and Vascular Biology*. Lippincott Williams & Wilkins, 30(10), pp. 1990–1997. doi: 10.1161/ATVBAHA.110.211706.
Hartmann, D. A. *et al.* (2015) 'Pericyte structure and distribution in the cerebral cortex revealed by high-resolution imaging of transgenic mice', *Neurophotonics*. SPIE-Intl Soc Optical Eng, 2(4), p. 041402. doi: 10.1117/1.nph.2.4.041402.
He, L. *et al.* (2018) 'Data descriptor: Single-cell RNA sequencing of mouse brain and lung vascular and vessel-associated cell types', *Scientific Data*. Nature Publishing Groups, 5(1), pp. 1–11. doi: 10.1038/sdata.2018.160.
Hellström, M. *et al.* (1999) 'Role of PDGF-B and PDGFR-beta in recruitment of vascular smooth muscle cells and pericytes during embryonic blood vessel formation in the mouse.', *Development (Cambridge, England)*. England, 126(14), pp. 3047–3055.
Hellström, M. *et al.* (2001) 'Lack of pericytes leads to endothelial hyperplasia and abnormal vascular morphogenesis', *Journal of Cell Biology*. Rockefeller University Press, 152(3), pp. 543–553. doi: 10.1083/jcb.153.3.543.
Hellström, M. *et al.* (2007) 'Dll4 signalling through Notch1 regulates formation of tip cells during angiogenesis', *Nature*. Nature Publishing Group, 445(7129), pp. 776–780. doi: 10.1038/nature05571.
Hendrix, J. A. *et al.* (2005) '5′ CArG degeneracy in smooth muscle α-actin is required for injury-

induced gene suppression in vivo', *Journal of Clinical Investigation*, pp. 418–427. doi: 10.1172/JCI200522648.
Herbert, S. P. and Stainier, D. Y. R. (2011) 'Molecular control of endothelial cell behaviour during blood vessel morphogenesis', *Nature Reviews Molecular Cell Biology*. Nat Rev Mol Cell Biol, pp. 551–564. doi: 10.1038/nrm3176.
Herzog, B. *et al.* (2011) 'VEGF binding to NRP1 is essential for VEGF stimulation of endothelial cell migration, complex formation between NRP1 and VEGFR2, and signaling via FAK Tyr407 phosphorylation', *Molecular Biology of the Cell*, 22(15), pp. 2766–2776. doi: 10.1091/mbc.E09-12-1061.
High, F. A. *et al.* (2007) 'An essential role for Notch in neural crest during cardiovascular development and smooth muscle differentiation', *Journal of Clinical Investigation*. J Clin Invest, 117(2), pp. 353–363. doi: 10.1172/JCI30070.
High, F. A. *et al.* (2008) 'Endothelial expression of the Notch ligand Jagged1 is required for vascular smooth muscle development', *Proceedings of the National Academy of Sciences*, 105(6), pp. 1955 LP – 1959.
Hill, R. A. *et al.* (2015) 'Regional Blood Flow in the Normal and Ischemic Brain Is Controlled by Arteriolar Smooth Muscle Cell Contractility and Not by Capillary Pericytes.', *Neuron*. Cell Press, 87(1), pp. 95–110. doi: 10.1016/j.neuron.2015.06.001.
Hirschi, K. K. *et al.* (1999) 'Endothelial Cells Modulate the Proliferation of Mural Cell Precursors via Platelet-Derived Growth Factor-BB and Heterotypic Cell Contact', *Circulation Research*. Lippincott Williams and Wilkins, 84(3), pp. 298–305. doi: 10.1161/01.RES.84.3.298.
Hisano, Y. *et al.* (2015) 'Comprehensive analysis of sphingosine-1-phosphate receptor mutants during zebrafish embryogenesis', *Genes to Cells*. Blackwell Publishing Ltd, 20(8), pp. 647–658. doi: 10.1111/gtc.12259.
Hogan, B. M. and Schulte-Merker, S. (2017) 'How to Plumb a Pisces: Understanding Vascular Development and Disease Using Zebrafish Embryos', *Developmental Cell*. doi: 10.1016/j.devcel.2017.08.015.
Hungerford, J. E. *et al.* (1996) 'Development of the aortic vessel wall as defined by vascular smooth muscle and extracellular matrix markers', *Dev Biol*, 178(2), pp. 375–392.
Huppert, S. S. *et al.* (2000) 'Embryonic lethality in mice homozygous for a processing-deficient allele of Notch1', *Nature*. Nature Publishing Group, 405(6789), pp. 966–970. doi: 10.1038/35016111.
Icli, B., Dorbala, P. and Feinberg, M. W. (2014) 'An emerging role for the miR-26 family in cardiovascular disease', *Trends in cardiovascular medicine*. Elsevier, 24(6), pp. 241–248.
Intengan, H. D. and Schiffrin, E. L. (2001) 'Vascular remodeling in hypertension roles of apoptosis, inflammation, and fibrosis', *Hypertension*. Am Heart Assoc, 38(3), pp. 581–587.
Iragavarapu-Charyulu, V., Wojcikiewicz, E. and Urdaneta, A. (2020) 'Semaphorins in Angiogenesis and Autoimmune Diseases: Therapeutic Targets?', *Frontiers in Immunology*. Frontiers Media S.A., p. 346. doi: 10.3389/fimmu.2020.00346.
Iso, T., Hamamori, Y. and Kedes, L. (2003) 'Notch signaling in vascular development', *Arteriosclerosis, Thrombosis, and Vascular Biology*. Arterioscler Thromb Vasc Biol, pp. 543–553. doi: 10.1161/01.ATV.0000060892.81529.8F.
Isogai, S. *et al.* (2003) 'Angiogenic network formation in the developing vertebrate trunk', *Development*. Development, 130(21), pp. 5281–5290. doi: 10.1242/dev.00733.
Isogai, S., Horiguchi, M. and Weinstein, B. M. (2001) 'The Vascular Anatomy of the Developing Zebrafish: An Atlas of Embryonic and Early Larval Development', *Developmental Biology*,

230(2), pp. 278–301. doi: http://dx.doi.org/10.1006/dbio.2000.9995.
Ji, R. *et al.* (2007) 'MicroRNA expression signature and antisense-mediated depletion reveal an essential role of MicroRNA in vascular neointimal lesion formation', *Circ Res*. 2007/05/05, 100(11), pp. 1579–1588. doi: 10.1161/circresaha.106.141986.
Johnson, J. A. *et al.* (2012) 'Cytoskeletal defects in Bmpr2-associated pulmonary arterial hypertension', *American Journal of Physiology - Lung Cellular and Molecular Physiology*, 302(5), pp. L474–L484.
Jones, C. A. *et al.* (2009) 'Slit2-Robo4 signalling promotes vascular stability by blocking Arf6 activity', *Nature Cell Biology*, 11(11), pp. 1325–1331. doi: 10.1038/ncb1976.
Joutel, A. *et al.* (1996) 'Notch3 mutations in CADASIL, a hereditary adult-onset condition causing stroke and dementia', *Nature*. Geo/. Soc. Am, 383(6602), pp. 707–710. doi: 10.1038/383707a0.
Kangsamaksin, T. *et al.* (2015) 'NOTCH decoys that selectively block DLL/NOTCH or JAG/NOTCH disrupt angiogenesis by unique mechanisms to inhibit tumor growth', *Cancer Discovery*. American Association for Cancer Research Inc., 5(2), pp. 182–197. doi: 10.1158/2159-8290.CD-14-0650.
Karar, J. and Maity, A. (2011) 'PI3K/AKT/mTOR Pathway in Angiogenesis', *Frontiers in Molecular Neuroscience*. Frontiers Media SA, 4. doi: 10.3389/fnmol.2011.00051.
Karthik, S. *et al.* (2018) 'Synergistic interaction of sprouting and intussusceptive angiogenesis during zebrafish caudal vein plexus development', *Scientific Reports*. Nature Publishing Group, 8(1), pp. 1–15. doi: 10.1038/s41598-018-27791-6.
Kerr, G. *et al.* (2015) 'A small molecule targeting ALK1 prevents Notch cooperativity and inhibits functional angiogenesis', *Angiogenesis*, 18(2), pp. 209–217. doi: 10.1007/s10456-014-9457-y.
Kim, J. *et al.* (2011) 'Semaphorin 3E-plexin-d1 signaling regulates VEGF function in developmental angiogenesis via a feedback mechanism', *Genes and Development*. Cold Spring Harbor Laboratory Press, 25(13), pp. 1399–1411. doi: 10.1101/gad.2042011.
Kim, J. D. *et al.* (2012) 'Context-Dependent Proangiogenic Function of Bone Morphogenetic Protein Signaling Is Mediated by Disabled Homolog 2', *Developmental Cell*. Dev Cell, 23(2), pp. 441–448. doi: 10.1016/j.devcel.2012.07.007.
Koch, A. W. *et al.* (2011) 'Robo4 Maintains Vessel Integrity and Inhibits Angiogenesis by Interacting with UNC5B', *Developmental Cell*, 20(1), pp. 33–46. doi: 10.1016/j.devcel.2010.12.001.
Koch, S. and Claesson-Welsh, L. (2012) 'Signal transduction by vascular endothelial growth factor receptors', *Cold Spring Harbor Perspectives in Medicine*. Cold Spring Harbor Laboratory Press, p. a006502. doi: 10.1101/cshperspect.a006502.
Koh, W. *et al.* (2008) 'In vitro three dimensional collagen matrix models of endothelial lumen formation during vasculogenesis and angiogenesis', *Methods in enzymology*. Elsevier, 443, pp. 83–101.
Kong, J. S. *et al.* (2010) 'Anti-neuropilin-1 peptide inhibition of synoviocyte survival, angiogenesis, and experimental arthritis', *Arthritis and Rheumatism*, 62(1), pp. 179–190. doi: 10.1002/art.27243.
Korchynskyi, O. and ten Dijke, P. (2002) 'Identification and functional characterization of distinct critically important bone morphogenetic protein-specific response elements in the Id1 promoter.', *The Journal of biological chemistry*, 277(7), pp. 4883–91. doi: 10.1074/jbc.M111023200.
Krebs, L. T. *et al.* (2000) 'Notch signaling is essential for vascular morphogenesis in mice', *Genes and Development*. Cold Spring Harbor Laboratory Press, 14(11), pp. 1343–1352. doi: 10.1101/gad.14.11.1343.

Krueger, J. *et al.* (2011a) 'Flt1 acts as a negative regulator of tip cell formation and branching morphogenesis in the zebrafish embryo', *Development*. Development, 138(10), pp. 2111–2120. doi: 10.1242/dev.063933.
Krueger, J. *et al.* (2011b) 'Flt1 acts as a negative regulator of tip cell formation and branching morphogenesis in the zebrafish embryo', *Development*, 138(10), pp. 2111–2120. doi: 10.1242/dev.063933.
Kuehbacher, A. *et al.* (2007) 'Role of Dicer and Drosha for endothelial microRNA expression and angiogenesis', *Circulation Research*. Lippincott Williams & Wilkins, 101(1), pp. 59–68. doi: 10.1161/CIRCRESAHA.107.153916.
Kuijper, S., Turner, C. J. and Adams, R. H. (2007) 'Regulation of angiogenesis by Eph-ephrin interactions.', *Trends in cardiovascular medicine*, 17(5), pp. 145–51. doi: 10.1016/j.tcm.2007.03.003.
Kullander, K. and Klein, R. (2002) 'Mechanisms and functions of Eph and ephrin signalling', *Nature Reviews Molecular Cell Biology*. Nat Rev Mol Cell Biol, pp. 475–486. doi: 10.1038/nrm856.
Kusy, S. *et al.* (2005) 'Promoter characterization of Semaphorin SEMA3F, a tumor suppressor gene', *Biochimica et Biophysica Acta - Gene Structure and Expression*. Elsevier, 1730(1), pp. 66–76. doi: 10.1016/j.bbaexp.2005.05.008.
Kwan, K. M. *et al.* (2007) 'The Tol2kit: A multisite gateway-based construction kit for Tol2 transposon transgenesis constructs', *Developmental Dynamics*. John Wiley & Sons, Ltd, 236(11), pp. 3088–3099. doi: 10.1002/dvdy.21343.
Kye, W. P. *et al.* (2004) 'The axonal attractant Netrin-1 is an angiogenic factor', *Proceedings of the National Academy of Sciences of the United States of America*. Proc Natl Acad Sci U S A, 101(46), pp. 16210–16215. doi: 10.1073/pnas.0405984101.
Labun, K. *et al.* (2016) 'CHOPCHOP v2: a web tool for the next generation of CRISPR genome engineering', *Nucleic acids research*. Oxford Univ Press, p. gkw398.
Lagna, G. *et al.* (2007) 'Control of phenotypic plasticity of smooth muscle cells by bone morphogenetic protein signaling through the myocardin-related transcription factors.', *The Journal of biological chemistry*, 282(51), pp. 37244–55. doi: 10.1074/jbc.M708137200.
Lamont, R. E. *et al.* (2010) 'Hedgehog signaling via angiopoietin1 is required for developmental vascular stability', *Mechanisms of development*. Elsevier, 127(3), pp. 159–168.
Lamont, R. E., Lamont, E. J. and Childs, S. J. (2009) 'Antagonistic interactions among Plexins regulate the timing of intersegmental vessel formation', *Developmental Biology*. Academic Press Inc., 331(2), pp. 199–209. doi: 10.1016/j.ydbio.2009.04.037.
Lan, Y. *et al.* (2007) 'Essential role of endothelial Smad4 in vascular remodeling and integrity', *Molecular and cellular biology*. Am Soc Microbiol, 27(21), pp. 7683–7692.
Larrivée, B. *et al.* (2012) 'ALK1 Signaling Inhibits Angiogenesis by Cooperating with the Notch Pathway', *Developmental Cell*. Elsevier, 22(3), pp. 489–500. doi: 10.1016/j.devcel.2012.02.005.
Laux, D. W. *et al.* (2013) 'Circulating Bmp10 acts through endothelial Alk1 to mediate flow-dependent arterial quiescence', *Development (Cambridge)*. Company of Biologists, 140(16), pp. 3403–3412. doi: 10.1242/dev.095307.
Laux, D. W., Febbo, J. A. and Roman, B. L. (2011) 'Dynamic analysis of BMP-responsive smad activity in live zebrafish embryos', *Developmental Dynamics*. Wiley-Liss, Inc., 240(3), pp. 682–694. doi: 10.1002/dvdy.22558.
Lawson, N. D. and Weinstein, B. M. (2002) 'In vivo imaging of embryonic vascular development using transgenic zebrafish', *Developmental Biology*, 248(2), pp. 307–318.

Leeper, N. J. *et al.* (2011) 'MicroRNA-26a is a novel regulator of vascular smooth muscle cell function', *Journal of cellular physiology*. Wiley Online Library, 226(4), pp. 1035–1043.
Lehoux, S., Castier, Y. and Tedgui, A. (2006) 'Molecular mechanisms of the vascular responses to haemodynamic forces', *Journal of internal medicine*. Wiley Online Library, 259(4), pp. 381–392.
Lewis, B. P., Burge, C. B. and Bartel, D. P. (2005) 'Conserved seed pairing, often flanked by adenosines, indicates that thousands of human genes are microRNA targets', *cell*. Elsevier, 120(1), pp. 15–20.
Li, L. *et al.* (1996) 'Expression of the SM22alpha promoter in transgenic mice provides evidence for distinct transcriptional regulatory programs in vascular and visceral smooth muscle cells.', *The Journal of cell biology*. Rockefeller Univ Press, 132(5), pp. 849–859.
Li, Linheng *et al.* (1997) 'Alagille syndrome is caused by mutations in human Jagged1, which encodes a ligand for notch1', *Nature Genetics*. Nature Publishing Group, 16(3), pp. 243–251. doi: 10.1038/ng0797-243.
Li, Li *et al.* (1997) 'Evidence for Serum Response Factor-Mediated Regulatory Networks GoverningSM22αTranscription in Smooth, Skeletal, and Cardiac Muscle Cells', *Developmental biology*. Elsevier, 187(2), pp. 311–321.
Li, M. *et al.* (2018) 'Endothelial–Vascular Smooth Muscle Cells Interactions in Atherosclerosis', *Frontiers in Cardiovascular Medicine*. Frontiers Media S.A. doi: 10.3389/fcvm.2018.00151.
Liao, W. *et al.* (1997) 'The zebrafish gene cloche acts upstream of a flk-1 homologue to regulate endothelial cell differentiation', *Development*, 124(2), pp. 381–389.
Lin, C.-Y. *et al.* (2013) 'ARTICLE miR-1 and miR-206 target different genes to have opposing roles during angiogenesis in zebrafish embryos', *Nature Communications*, 4. doi: 10.1038/ncomms3829.
Lindahl, P. *et al.* (1997) 'Pericyte loss and microaneurysm formation in PDGF-B-deficient mice', *Science*. American Association for the Advancement of Science, 277(5323), pp. 242–245.
Lindblom, P. *et al.* (2003) 'Endothelial PDGF-B retention is required for proper investment of pericytes in the microvessel wall', *Genes and Development*, 17(15), pp. 1835–1840. doi: 10.1101/gad.266803.
Lindow, M. and Kauppinen, S. (2012) 'Discovering the first microRNA-targeted drug.', *The Journal of cell biology*, 199(3), pp. 407–12. doi: 10.1083/jcb.201208082.
Liu, H., Kennard, S. and Lilly, B. (2009) 'NOTCH3 expression is induced in mural cells through an autoregulatory loop that requires Endothelial-expressed JAGGED1', *Circulation Research*. Circ Res, 104(4), pp. 466–475. doi: 10.1161/CIRCRESAHA.108.184846.
Liu, J. *et al.* (2007) 'A βPix–Pak2a signaling pathway regulates cerebral vascular stability in zebrafish', *Proceedings of the National Academy of Sciences*. National Acad Sciences, 104(35), pp. 13990–13995.
Liu, J. *et al.* (2010) *Notch signaling in the regulation of stem cell self-renewal and differentiation, Current Topics in Developmental Biology*. Curr Top Dev Biol. doi: 10.1016/S0070-2153(10)92012-7.
Liu, X. *et al.* (2016) 'Semaphorin 3G Provides a Repulsive Guidance Cue to Lymphatic Endothelial Cells via Neuropilin-2/PlexinD1', *Cell Reports*. Elsevier B.V., 17(9), pp. 2299–2311. doi: 10.1016/j.celrep.2016.11.008.
Long, L. *et al.* (2015) 'Regulation of transcriptionally active genes via the catalytically inactive Cas9 in C. elegans and D. rerio.', *Cell research*, 25(5), p. 638.
Lopez-Rios, J. (2012) 'Sensing BMP Pathway Activity by Immune Detection of Phosphorylated

R-Smad Proteins in Mouse Embryonic Kidney', in Michos, O. (ed.) *Kidney Development: Methods and Protocols*. Totowa, NJ: Humana Press, pp. 267–273. doi: 10.1007/978-1-61779-851-1_24.
Lu, X. *et al.* (2004) 'The netrin receptor UNC5B mediates guidance events controlling morphogenesis of the vascular system', *Nature*. Nature, 432(7014), pp. 179–186. doi: 10.1038/nature03080.
Mack, C. P. (2011) 'Signaling Mechanisms That Regulate Smooth Muscle Cell Differentiation', *Arteriosclerosis, thrombosis, and vascular biology*, pp. 1495–1505. doi: 10.1161/ATVBAHA.110.221135.
Mack, C. P. and Owens, G. K. (1999) 'Regulation of smooth muscle α-actin expression in vivo is dependent on CArG elements within the 5′ and first intron promoter regions', *Circulation Research*. Am Heart Assoc, 84(7), pp. 852–861.
Mahmoud, M. *et al.* (2010) 'Pathogenesis of arteriovenous malformations in the absence of endoglin', *Circulation research*. Am Heart Assoc, 106(8), pp. 1425–1433.
Manabe, I. and Owens, G. K. (2001) 'The smooth muscle myosin heavy chain gene exhibits smooth muscle subtype-selective modular regulation in vivo', *Journal of Biological Chemistry*. ASBMB, 276(42), pp. 39076–39087.
Massagué, J. and Wotton, D. (2000) 'Transcriptional control by the TGF-β/Smad signaling system', *The EMBO Journal*, 19(8), pp. 1745–1754.
Mattila, P. K. and Lappalainen, P. (2008) 'Filopodia: Molecular architecture and cellular functions', *Nature Reviews Molecular Cell Biology*. Nature Publishing Group, pp. 446–454. doi: 10.1038/nrm2406.
McDonald, J., Bayrak-Toydemir, P. and Pyeritz, R. E. (2011) 'Hereditary hemorrhagic telangiectasia: An overview of diagnosis, management, and pathogenesis', *Genetics In Medicine*. The American College of Medical Genetics, 13, p. 607.
McReynolds, L. J. *et al.* (2007) 'Smad1 and Smad5 differentially regulate embryonic hematopoiesis', *Blood*. Washington, DC, pp. 3881–3890. doi: 10.1182/blood-2007-04-085753.
Meda, C. *et al.* (2012) 'Semaphorin 4A Exerts a Proangiogenic Effect by Enhancing Vascular Endothelial Growth Factor-A Expression in Macrophages', *The Journal of Immunology*. The American Association of Immunologists, 188(8), pp. 4081–4092. doi: 10.4049/jimmunol.1101435.
Van Meeteren, L. A. *et al.* (2012) 'Anti-human activin receptor-like kinase 1 (ALK1) antibody attenuates bone morphogenetic protein 9 (BMP9)-induced ALK1 signaling and interferes with endothelial cell sprouting', *Journal of Biological Chemistry*. J Biol Chem, 287(22), pp. 18551–18561. doi: 10.1074/jbc.M111.338103.
Miano, J. M. *et al.* (1994) 'Smooth muscle myosin heavy chain exclusively marks the smooth muscle lineage during mouse embryogenesis.', *Circulation research*. Am Heart Assoc, 75(5), pp. 803–812.
Miano, J. M. *et al.* (2000) 'Serum response factor-dependent regulation of the smooth muscle calponin gene', *Journal of Biological Chemistry*. ASBMB, 275(13), pp. 9814–9822.
Milewicz, Dianna M. *et al.* (2010) 'De novo ACTA2 mutation causes a novel syndrome of multisystemic smooth muscle dysfunction', *American Journal of Medical Genetics Part A*, 152A(10), pp. 2437–2443. doi: 10.1002/ajmg.a.33657.
Milewicz, Dianna M *et al.* (2010) 'Genetic variants promoting smooth muscle cell proliferation can result in diffuse and diverse vascular diseases: evidence for a hyperplastic vasculomyopathy', *Genetics IN Medicine*, 12(4), pp. 196–203.

Mishina, Y. *et al.* (1995) 'Bmpr encodes a type I bone morphogenetic protein receptor that is essential for gastrulation during mouse embryogenesis.', *Genes & development*. UNITED STATES, 9(24), pp. 3027–3037.
Montague, T. G. *et al.* (2014) 'CHOPCHOP: a CRISPR/Cas9 and TALEN web tool for genome editing', *Nucleic acids research*. Oxford Univ Press, p. gku410.
Montero-Balaguer, M. *et al.* (2009) 'Stable Vascular Connections and Remodeling Require Full Expression of VE-Cadherin in Zebrafish Embryos', *PLOS ONE*. Public Library of Science, 4(6), p. e5772.
Moriya, J. *et al.* (2010) 'Inhibition of semaphorin as a novel strategy for therapeutic angiogenesis', *Circulation Research*, 106(2), pp. 391–398. doi: 10.1161/CIRCRESAHA.109.210815.
Moya, I. M. *et al.* (2012) 'Stalk Cell Phenotype Depends on Integration of Notch and Smad1/5 Signaling Cascades', *Developmental Cell*. Europe PMC Funders, 22(3), pp. 501–514. doi: 10.1016/j.devcel.2012.01.007.
Nakaoka, T. *et al.* (1997) 'Inhibition of rat vascular smooth muscle proliferation in vitro and in vivo by bone morphogenetic protein-2.', *Journal of Clinical Investigation*. American Society for Clinical Investigation, 100(11), p. 2824.
Nakayama, H. *et al.* (2015) 'Regulation of mTOR signaling by semaphorin 3F-neuropilin 2 interactions in vitro and in vivo', *Scientific Reports*. Nature Publishing Group, 5(1), pp. 1–14. doi: 10.1038/srep11789.
Nakayama, H. *et al.* (2018) 'Semaphorin 3F and netrin-1: The novel function as a regulator of tumor microenvironment', *Frontiers in Physiology*. Frontiers Media S.A. doi: 10.3389/fphys.2018.01662.
Narayanan, A. *et al.* (2016) 'In vivo mutagenesis of miRNA gene families using a scalable multiplexed CRISPR/Cas9 nuclease system', *Scientific Reports*. The Author(s), 6, p. 32386.
Nasarre, P. *et al.* (2003) 'Semaphorin SEMA3F and VEGF have opposing effects on cell attachment and spreading', *Neoplasia*. Neoplasia Press, 5(1), pp. 83–92. doi: 10.1016/s1476-5586(03)80020-9.
Nayak, L., Lin, Z. and Jain, M. K. (2011) '"go with the flow": How Krüppel-like factor 2 regulates the vasoprotective effects of shear stress', *Antioxidants and Redox Signaling*. Mary Ann Liebert, Inc. 140 Huguenot Street, 3rd Floor New Rochelle, NY 10801 USA , pp. 1449–1461. doi: 10.1089/ars.2010.3647.
Nebbioso, A. *et al.* (2012) 'Trials with "epigenetic" drugs: an update.', *Molecular oncology*. Elsevier, 6(6), pp. 657–82. doi: 10.1016/j.molonc.2012.09.004.
Nicoli, S. *et al.* (2010) 'MicroRNA-mediated integration of haemodynamics and Vegf signalling during angiogenesis', *Nature*. Nature Publishing Group, 464(7292), pp. 1196–1200. doi: 10.1038/nature08889.
Nicoli, S., Knyphausen, C.-P., *et al.* (2012) 'miR-221 is required for endothelial tip cell behaviors during vascular development.', *Developmental cell*, 22(2), pp. 418–29. doi: 10.1016/j.devcel.2012.01.008.
Nicoli, S., Knyphausen, C. P., *et al.* (2012) 'MiR-221 Is Required for Endothelial Tip Cell Behaviors during Vascular Development', *Developmental Cell*. Cell Press, 22(2), pp. 418–429. doi: 10.1016/j.devcel.2012.01.008.
Ochsenbein, A. M. *et al.* (2016) 'Endothelial cell-derived semaphorin 3A inhibits filopodia formation by blood vascular tip cells', *Development (Cambridge)*. Company of Biologists Ltd, 143(4), pp. 589–594. doi: 10.1242/dev.127670.
Oh, W. J. and Gu, C. (2013) 'The role and mechanism-of-action of Sema3E and Plexin-D1 in

vascular and neural development', *Seminars in Cell and Developmental Biology*. Elsevier Ltd, pp. 156–162. doi: 10.1016/j.semcdb.2012.12.001.
Ola, R. *et al.* (2016) 'PI3 kinase inhibition improves vascular malformations in mouse models of hereditary haemorrhagic telangiectasia', *Nature Communications*. The Author(s), 7, p. 13650.
Ola, R. *et al.* (2018) 'SMAD4 Prevents Flow Induced Arteriovenous Malformations by Inhibiting Casein Kinase 2', *Circulation*, 138(21), pp. 2379–2394. doi: 10.1161/CIRCULATIONAHA.118.033842.
Orlidge, A. and D'Amore, P. A. (1987) 'Inhibition of capillary endothelial cell growth by pericytes and smooth muscle cells', *Journal of Cell Biology*. J Cell Biol, 105(3), pp. 1455–1462. doi: 10.1083/jcb.105.3.1455.
Orriols, M., Gomez-Puerto, M. C. and Ten Dijke, P. (2017) 'BMP type II receptor as a therapeutic target in pulmonary arterial hypertension', *Cellular and Molecular Life Sciences*. Birkhauser Verlag AG, pp. 1–17. doi: 10.1007/s00018-017-2510-4.
Orvis, G. D. *et al.* (2008) 'Functional redundancy of tgf-Beta family type I receptors and receptor-smads in mediating anti-mullerian hormone-induced mullerian duct regression in the mouse', *Biol Reprod*, 78. doi: 10.1095/biolreprod.107.066605.
Owens, G. K. (1995) 'Regulation of differentiation of vascular smooth muscle cells', *Physiol Rev*, 75(3), pp. 487–517.
Owens, G. K., Kumar, M. S. and Wamhoff, B. R. (2004) 'Molecular regulation of vascular smooth muscle cell differentiation in development and disease.', *Physiological reviews*, 84(3), pp. 767–801. doi: 10.1152/physrev.00041.2003.
Owens, G. K., Vernon, S. M. and Madsen, C. S. (1996) 'Molecular regulation of smooth muscle cell differentiation.', *Journal of hypertension. Supplement: official journal of the International Society of Hypertension*, 14(5), pp. S55-64.
Ozcan, G. *et al.* (2015) 'Preclinical and clinical development of siRNA-based therapeutics.', *Advanced drug delivery reviews*, 87, pp. 108–19. doi: 10.1016/j.addr.2015.01.007.
Pan, Y. *et al.* (2011) 'Conditional deletion of Dicer in vascular smooth muscle cells leads to the developmental delay and embryonic mortality', *Biochemical and biophysical research communications*. Elsevier, 408(3), pp. 369–374.
Pang, L. *et al.* (2013) 'An Increase in Vascular Endothelial Growth Factor (VEGF) and VEGF Soluble Receptor-1 (sFlt-1) Are Associated with Early Recurrent Spontaneous Abortion', *PLoS ONE*. PLoS One, 8(9). doi: 10.1371/journal.pone.0075759.
Park, C. *et al.* (2006) 'Bone morphogenetic protein receptor 1A signaling is dispensable for hematopoietic development but essential for vessel and atrioventricular endocardial cushion formation', *Development*, 133. doi: 10.1242/dev.02499.
Park, J. E. S. *et al.* (2012) 'BMP-9 induced endothelial cell tubule formation and inhibition of migration involves Smad1 driven endothelin-1 production', *PLoS ONE*, 7(1). doi: 10.1371/journal.pone.0030075.
Park, J. K. *et al.* (2010) 'Inhibition of the PI3K-Akt Pathway Suppresses sFlt1 Expression in Human Placental Hypoxia Models In Vitro', *Placenta*. W.B. Saunders, 31(7), pp. 621–629. doi: 10.1016/J.PLACENTA.2010.04.009.
Pascoe, H. G., Wang, Y. and Zhang, X. (2015) 'Structural mechanisms of plexin signaling', *Progress in Biophysics and Molecular Biology*. Elsevier Ltd, pp. 161–168. doi: 10.1016/j.pbiomolbio.2015.03.006.
Paul, B. Y. *et al.* (2005) 'Bone morphogenetic protein (BMP) type II receptor deletion reveals BMP ligand-specific gain of signaling in pulmonary artery smooth muscle cells', *Journal of*

Biological Chemistry. ASBMB, 280(26), pp. 24443–24450.
Phng, L. K., Stanchi, F. and Gerhardt, H. (2013) 'Filopodia are dispensable for endothelial tip cell guidance', *Development (Cambridge)*. Oxford University Press for The Company of Biologists Limited, 140(19), pp. 4031–4040. doi: 10.1242/dev.097352.
Pitulescu, M. E. and Adams, R. H. (2010) 'Eph/ephrin molecules - A hub for signaling and endocytosis', *Genes and Development*. Genes Dev, pp. 2480–2492. doi: 10.1101/gad.1973910.
Plant, T. *et al.* (2020) 'Semaphorin 3F signaling actively retains neutrophils at sites of inflammation', *Journal of Clinical Investigation*. American Society for Clinical Investigation, 130(6), pp. 3221–3237. doi: 10.1172/JCI130834.
Pollard, T. D. and Cooper, J. A. (2009) 'Actin, a central player in cell shape and movement', *Science*. American Association for the Advancement of Science, pp. 1208–1212. doi: 10.1126/science.1175862.
Proulx, K., Lu, A. and Sumanas, S. (2010) 'Cranial vasculature in zebrafish forms by angioblast cluster-derived angiogenesis', *Developmental Biology*. Academic Press Inc., 348(1), pp. 34–46. doi: 10.1016/j.ydbio.2010.08.036.
Ramasamy, S. K., Kusumbe, A. P. and Adams, R. H. (2015) 'Regulation of tissue morphogenesis by endothelial cell-derived signals', *Trends in Cell Biology*. Elsevier Ltd, pp. 148–157. doi: 10.1016/j.tcb.2014.11.007.
Rangrez, A. Y. *et al.* (2011) 'MiR-143 and miR-145 molecular keys to switch the phenotype of vascular smooth muscle cells', *Circulation: Cardiovascular Genetics*. Am Heart Assoc, 4(2), pp. 197–205.
Rasband, W. . (no date) 'ImageJ'. U. S. National Institutes of Health, Bethesda, Maryland, USA.
Regano, D. *et al.* (2017) 'Sema3F (Semaphorin 3F) Selectively Drives an Extraembryonic Proangiogenic Program.', *Arteriosclerosis, thrombosis, and vascular biology*. Lippincott Williams and Wilkins, 37(9), pp. 1710–1721. doi: 10.1161/ATVBAHA.117.308226.
Rensen, S. S. M., Doevendans, P. and Van Eys, G. (2007) 'Regulation and characteristics of vascular smooth muscle cell phenotypic diversity', *Netherlands Heart Journal*. Springer, 15(3), pp. 100–108.
Roman, B. L. *et al.* (2002) 'Disruption of acvrl1 increases endothelial cell number in zebrafish cranial vessels', *Development*, 129(12), pp. 3009–3019.
Rossi, A. *et al.* (2015) 'Genetic compensation induced by deleterious mutations but not gene knockdowns', *Nature*. Nature Publishing Group, a division of Macmillan Publishers Limited. All Rights Reserved., 524, p. 230.
Rougeot, J. *et al.* (2014) 'RNA sequencing of FACS-sorted immune cell populations from zebrafish infection models to identify cell specific responses to intracellular pathogens', *Methods in Molecular Biology*. Humana Press Inc., 1197, pp. 261–274. doi: 10.1007/978-1-4939-1261-2_15.
Ruan, G. X. and Kazlauskas, A. (2012) 'VEGF-A engages at least three tyrosine kinases to activate PI3K/Akt', *Cell Cycle*. Taylor and Francis Inc., pp. 2047–2048. doi: 10.4161/cc.20535.
Sahoo, S. and Losordo, D. W. (2014) 'Exosomes and cardiac repair after myocardial infarction', *Circulation Research*. Lippincott Williams and Wilkins, pp. 333–344. doi: 10.1161/CIRCRESAHA.114.300639.
Sakurai, A., Doci, C. and Gutkind, J. S. (2012) 'Semaphorin signaling in angiogenesis, lymphangiogenesis and cancer', *Cell Research*. Nature Publishing Group, pp. 23–32. doi: 10.1038/cr.2011.198.
Santoro, M. M., Pesce, G. and Stainier, D. Y. (2009) 'Characterization of vascular mural cells

during zebrafish development', *Mechanisms of development*. Elsevier, 126(8), pp. 638–649.
Santulli, G. *et al.* (2014) 'A selective microRNA-based strategy inhibits restenosis while preserving endothelial function', *Journal of Clinical Investigation*. American Society for Clinical Investigation, 124(9), pp. 4102–4114. doi: 10.1172/JCI76069.
Sanvitale, C. E. *et al.* (2013) 'A New Class of Small Molecule Inhibitor of BMP Signaling', *PLoS ONE*. Public Library of Science, 8(4), p. e62721.
Sarkar, J. *et al.* (2010) 'MicroRNA-21 plays a role in hypoxia-mediated pulmonary artery smooth muscle cell proliferation and migration', *American Journal of Physiology-Lung Cellular and Molecular Physiology*. Am Physiological Soc, 299(6), pp. L861–L871.
Sawamiphak, S. *et al.* (2010) 'Ephrin-B2 regulates VEGFR2 function in developmental and tumour angiogenesis', *Nature*. Nature, 465(7297), pp. 487–491. doi: 10.1038/nature08995.
Schulte-Merker, S. and Stainier, D. Y. R. (2014) 'Out with the old, in with the new: reassessing morpholino knockdowns in light of genome editing technology', *Development*. The Company of Biologists Limited, 141(16), pp. 3103–3104.
Segarra, M. *et al.* (2012) 'Semaphorin 6A regulates angiogenesis by modulating VEGF signaling', *Blood*. American Society of Hematology, 120(19), pp. 4104–4115. doi: 10.1182/blood-2012-02-410076.
Serini, G. *et al.* (2013) 'Class 3 semaphorins: Physiological vascular normalizing agents for anti-cancer therapy', *Journal of Internal Medicine*, pp. 138–155. doi: 10.1111/joim.12017.
Sheldon, H. *et al.* (2009) ' Active involvement of Robo1 and Robo4 in filopodia formation and endothelial cell motility mediated via WASP and other actin nucleation-promoting factors ', *The FASEB Journal*. Wiley, 23(2), pp. 513–522. doi: 10.1096/fj.07-098269.
Siekmann, A. F., Covassin, L. and Lawson, N. D. (2008) 'Modulation of VEGF signalling output by the Notch pathway', *BioEssays*. John Wiley & Sons, Ltd, 30(4), pp. 303–313. doi: 10.1002/bies.20736.
Siekmann, A. F. and Lawson, N. D. (2007) 'Notch signalling limits angiogenic cell behaviour in developing zebrafish arteries', *Nature*. Nature Publishing Group, 445(7129), pp. 781–784. doi: 10.1038/nature05577.
Sirard, C. *et al.* (1998) 'The tumor suppressor gene Smad4/Dpc4 is required for gastrulation and later for anterior development of the mouse embryo.', *Genes & development*. UNITED STATES, 12(1), pp. 107–119.
De Smet, F. *et al.* (2009) 'Mechanisms of vessel branching: Filopodia on endothelial tip cells lead the way', *Arteriosclerosis, Thrombosis, and Vascular Biology*. Lippincott Williams & Wilkins, pp. 639–649. doi: 10.1161/ATVBAHA.109.185165.
Somlyo, A. P. and Somlyo, A. V (2003) 'Ca2+ sensitivity of smooth muscle and nonmuscle myosin II: modulated by G proteins, kinases, and myosin phosphatase', *Physiological reviews*. Am Physiological Soc, 83(4), pp. 1325–1358.
Srinivasan, S. *et al.* (2003) 'A mouse model for hereditary hemorrhagic telangiectasia (HHT) type 2', *Human Molecular Genetics*. Oxford Univ Press, 12(5), pp. 473–482.
Stahlhut, C. *et al.* (2012) 'miR-1 and miR-206 regulate angiogenesis by modulating VegfA expression in zebrafish', *Development (Cambridge)*. Oxford University Press for The Company of Biologists Limited, 139(23), pp. 4356–4364. doi: 10.1242/dev.083774.
Stainier, D. Y. R. *et al.* (1996) 'Mutations affecting the formation and function of the cardiovascular system in the zebrafish embryo', *Development*, 123, pp. 285–292. doi: 10.5167/uzh-237.
Staton, C. A. *et al.* (2011) 'Expression of class 3 semaphorins and their receptors in human breast

neoplasia', *Histopathology*. doi: 10.1111/j.1365-2559.2011.03922.x.
Stoorvogel, W. (2012) 'Functional transfer of microRNA by exosomes', *Blood*. American Society of Hematology, pp. 646–648. doi: 10.1182/blood-2011-11-389478.
Stratman, A. N. *et al.* (2010) 'Endothelial-derived PDGF-BB and HB-EGF coordinately regulate pericyte recruitment during vasculogenic tube assembly and stabilization', *Blood*, 116(22), pp. 4720–4730. doi: 10.1182/blood-2010-05-286872.
Stratman, A. N. *et al.* (2019) 'A Molecular Pathway for Arterial-Specific Association of Vascular Smooth Muscle Cells', *bioRxiv*. Cold Spring Harbor Laboratory, p. 2019.12.27.889782. doi: 10.1101/2019.12.27.889782.
Stratman, A. N. and Davis, G. E. (2012) 'Endothelial cell-pericyte interactions stimulate basement membrane matrix assembly: Influence on vascular tube remodeling, maturation, and stabilization', in *Microscopy and Microanalysis*. NIH Public Access, pp. 68–80. doi: 10.1017/S1431927611012402.
Suárez, Y. *et al.* (2007) 'Dicer dependent microRNAs regulate gene expression and functions in human endothelial cells', *Circulation Research*. Circ Res, 100(8), pp. 1164–1173. doi: 10.1161/01.RES.0000265065.26744.17.
Suchting, S. *et al.* (2005) 'Soluble Robo4 receptor inhibits in vivo angiogenesis and endothelial cell migration.', *FASEB journal : official publication of the Federation of American Societies for Experimental Biology*. Wiley, 19(1), pp. 121–3. doi: 10.1096/fj.04-1991fje.
Sun, H. *et al.* (2006) 'Rho and ROCK signaling in VEGF-induced microvascular endothelial hyperpermeability.', *Microcirculation (New York, N.Y.: 1994)*, 13(3), pp. 237–47. doi: 10.1080/10739680600556944.
Sun, S. *et al.* (2011) 'miR-146a and Krüppel-like factor 4 form a feedback loop to participate in vascular smooth muscle cell proliferation', *EMBO reports*. EMBO Press, 12(1), pp. 56–62.
Sun, Y. *et al.* (2017) 'Sema3f Protects Against Subretinal Neovascularization In Vivo', *EBioMedicine*. Elsevier B.V., 18, pp. 281–287. doi: 10.1016/j.ebiom.2017.03.026.
Tachida, Y. *et al.* (2017) 'Mutual interaction between endothelial cells and mural cells enhances BMP9 signaling in endothelial cells', *Biology Open*, 6(3), pp. 370 LP – 380. doi: 10.1242/bio.020503.
Tamagnone, L. *et al.* (1999) 'Plexins are a large family of receptors for transmembrane, secreted, and GPI-anchored semaphorins in vertebrates', *Cell*. Cell Press, 99(1), pp. 71–80. doi: 10.1016/S0092-8674(00)80063-X.
Tammela, T. *et al.* (2008) 'Blocking VEGFR-3 suppresses angiogenic sprouting and vascular network formation', *Nature*. Nature, 454(7204), pp. 656–660. doi: 10.1038/nature07083.
Thisse, C. and Thisse, B. (2008) 'High-resolution in situ hybridization to whole-mount zebrafish embryos', *Nature Protocols*. Nat Protoc, 3(1), pp. 59–69. doi: 10.1038/nprot.2007.514.
Tomasek, J. J. *et al.* (2005) 'Regulation of α-Smooth Muscle Actin Expression in Granulation Tissue Myofibroblasts Is Dependent on the Intronic CArG Element and the Transforming Growth Factor-β1 Control Element', *The American Journal of Pathology*, pp. 1343–1351.
Torihashi, S. *et al.* (2009) 'The expression and crucial roles of BMP signaling in development of smooth muscle progenitor cells in the mouse embryonic gut.', *Differentiation; research in biological diversity*, 77(3), pp. 277–89. doi: 10.1016/j.diff.2008.10.003.
Torres-Vázquez, J. *et al.* (2004) 'Semaphorin-plexin signaling guides patterning of the developing vasculature', *Developmental Cell*. Dev Cell, 7(1), pp. 117–123. doi: 10.1016/j.devcel.2004.06.008.
Treps, L., Le Guelte, A. and Gavard, J. (2013) 'Emerging roles of Semaphorins in the regulation

of epithelial and endothelial junctions', *Tissue Barriers*. Informa UK Limited, 1(1), p. e23272. doi: 10.4161/tisb.23272.
Uyttendaele, H. *et al.* (2001) 'Vascular patterning defects associated with expression of activated Notch4 in embryonic endothelium', *Proceedings of the National Academy of Sciences of the United States of America*. National Academy of Sciences, 98(10), pp. 5643–5648. doi: 10.1073/pnas.091584598.
Vanlandewijck, M. *et al.* (2018) 'A molecular atlas of cell types and zonation in the brain vasculature', *Nature*. Nature Publishing Group, 554(7693), pp. 475–480. doi: 10.1038/nature25739.
Vidigal, J. A. and Ventura, A. (2014) 'The biological functions of miRNAs: lessons from in vivo studies', *Trends in Cell Biology*, 25(3), pp. 137–147. doi: 10.1016/j.tcb.2014.11.004.
Wakayama, Y. *et al.* (2015) 'Cdc42 mediates Bmp - Induced sprouting angiogenesis through Fmnl3-driven assembly of endothelial filopodia in zebrafish', *Developmental Cell*. Cell Press, 32(1), pp. 109–122. doi: 10.1016/j.devcel.2014.11.024.
Walker, E. J. *et al.* (2011) 'Arteriovenous malformation in the adult mouse brain resembling the human disease', *Annals of Neurology*. Wiley Subscription Services, Inc., A Wiley Company, 69(6), pp. 954–962. doi: 10.1002/ana.22348.
Wang, D. and Atanasov, A. G. (2019) 'The microRNAs regulating vascular smooth muscle cell proliferation: A minireview', *International Journal of Molecular Sciences*. MDPI AG. doi: 10.3390/ijms20020324.
Wang, J. *et al.* (2010) 'Serum miR-146a and miR-223 as potential new biomarkers for sepsis', *Biochemical and biophysical research communications*. Elsevier, 394(1), pp. 184–188.
Wang, L. *et al.* (2011) 'Ablood flow-dependent klf2a-NO signaling cascade is required for stabilization of hematopoietic stem cell programming in zebrafish embryos', *Blood*, 118(15), pp. 4102–4110. doi: 10.1182/blood-2011-05-353235.
Wang, R. N. *et al.* (2014) 'Bone Morphogenetic Protein (BMP) signaling in development and human diseases.', *Genes & Diseases*, 1(1), pp. 87–105. doi: 10.1016/j.gendis.2014.07.005.
Wang, Y. *et al.* (2010) 'Ephrin-B2 controls VEGF-induced angiogenesis and lymphangiogenesis', *Nature*. Nature, 465(7297), pp. 483–486. doi: 10.1038/nature09002.
Wang, Z. *et al.* (2003) 'Myocardin is a master regulator of smooth muscle gene expression', *Proceedings of the National Academy of Sciences of the United States of America*, pp. 7129–7134. doi: 10.1073/pnas.1232341100.
Wang, Z. F. *et al.* (2019) 'Glioma stem cells-derived exosomal miR-26a promotes angiogenesis of microvessel endothelial cells in glioma', *Journal of Experimental and Clinical Cancer Research*. BioMed Central Ltd., 38(1), p. 201. doi: 10.1186/s13046-019-1181-4.
Wei, C.-Y. *et al.* (2014) 'Transcriptional factors smad1 and smad9 act redundantly to mediate zebrafish ventral specification downstream of smad5.', *The Journal of biological chemistry*. American Society for Biochemistry and Molecular Biology, 289(10), pp. 6604–18. doi: 10.1074/jbc.M114.549758.
Whitesell, T. R. *et al.* (2014) 'An ?-Smooth Muscle Actin (acta2/?sma) Zebrafish Transgenic Line Marking Vascular Mural Cells and Visceral Smooth Muscle Cells', *PLoS ONE*. Public Library of Science, 9(3), p. e90590.
Whitesell, T. R. *et al.* (2019) 'foxc1 is required for embryonic head vascular smooth muscle differentiation in zebrafish', *Developmental Biology*. Elsevier Inc., 453(1), pp. 34–47. doi: 10.1016/j.ydbio.2019.06.005.
Wiens, K. M. *et al.* (2010) 'Platelet-derived growth factor receptor β is critical for zebrafish

intersegmental vessel formation', *PLoS ONE*. Public Library of Science, 5(6). doi: 10.1371/journal.pone.0011324.
Wiley, D. M. *et al.* (2011) 'Distinct signalling pathways regulate sprouting angiogenesis from the dorsal aorta and the axial vein', *Nat Cell Biol*. Nature Publishing Group, a division of Macmillan Publishers Limited. All Rights Reserved., 13(6), pp. 686–692.
Williams, C. K. *et al.* (2006) 'Up-regulation of the Notch ligand Delta-like 4 inhibits VEGF-induced endothelial cell function', *Blood*. The American Society of Hematology, 107(3), pp. 931–939. doi: 10.1182/blood-2005-03-1000.
Wilson, B. D. *et al.* (2006) 'Netrins promote developmental and therapeutic angiogenesis.', *Science (New York, N.Y.)*, 313(5787), pp. 640–4. doi: 10.1126/science.1124704.
Winkler, E. A., Bell, R. D. and Zlokovic, B. V. (2011) 'Lack of Smad or Notch Leads to a Fatal Game of Brain Pericyte Hopscotch', *Developmental Cell*. Cell Press, 20(3), pp. 279–280. doi: 10.1016/J.DEVCEL.2011.03.002.
Xie, C., Zhang, J. and Chen, Y. E. (2011) 'MicroRNA and vascular smooth muscle cells', *Vitam Horm*. 2011/12/01, 87, pp. 321–339. doi: 10.1016/b978-0-12-386015-6.00034-2.
Xin, M. *et al.* (2009) 'MicroRNAs miR-143 and miR-145 modulate cytoskeletal dynamics and responsiveness of smooth muscle cells to injury', *Genes & Development* .
Xu, C. *et al.* (2014) 'Arteries are formed by vein-derived endothelial tip cells', *Nature Communications*. Nature Publishing Group, 5(1), pp. 1–11. doi: 10.1038/ncomms6758.
Xu, J. *et al.* (2011) 'Circulating MicroRNAs, miR-21, miR-122, and miR-223, in patients with hepatocellular carcinoma or chronic hepatitis', *Molecular carcinogenesis*. Wiley Online Library, 50(2), pp. 136–142.
Xu, K. and Cleaver, O. (2011) 'Tubulogenesis during blood vessel formation', *Seminars in Cell and Developmental Biology*. Elsevier Ltd, pp. 993–1004. doi: 10.1016/j.semcdb.2011.05.001.
Yamaguchi, T. P. *et al.* (1993) 'Flk-1, an fit-related receptor tyrosine kinase is an early marker for endothelial cell precursors', *Development*. The Company of Biologists Ltd, 118(2), pp. 489–498.
Yang, X. *et al.* (2017) 'MiR-26a contributes to the PDGF-BB-induced phenotypic switch of vascular smooth muscle cells by suppressing Smad1', *Oncotarget*, pp. 75844–75853. doi: 10.18632/oncotarget.17998.
Yazdani, U. and Terman, J. R. (2006) 'The semaphorins', *Genome Biology*. BioMed Central, pp. 1–14. doi: 10.1186/gb-2006-7-3-211.
Yokota, Y. *et al.* (2015) 'Endothelial Ca2+ oscillations reflect VEGFR signaling-regulated angiogenic capacity in vivo', *eLife*. eLife Sciences Publications Ltd, 4(NOVEMBER2015). doi: 10.7554/eLife.08817.
Yoshida, T., Gan, Q. and Owens, G. K. (2008) 'Krüppel-like factor 4, Elk-1, and histone deacetylases cooperatively suppress smooth muscle cell differentiation markers in response to oxidized phospholipids', *American Journal of Physiology-Cell Physiology*. Am Physiological Soc, 295(5), pp. C1175–C1182.
Yu, H. H. and Moens, C. B. (2005) 'Semaphorin signaling guides cranial neural crest cell migration in zebrafish', *Developmental Biology*. Academic Press Inc., 280(2), pp. 373–385. doi: 10.1016/j.ydbio.2005.01.029.
Yuan, H. S. H., Katyal, S. and Anderson, J. E. (2018) 'A mechanism for semaphorin-induced apoptosis: DNA damage of endothelial and myogenic cells in primary cultures from skeletal muscle', *Oncotarget*. Impact Journals LLC, 9(32), pp. 22618–22630. doi: 10.18632/oncotarget.25200.
Yuan, S.-M. and Jing, H. (2010) 'Cardiac pathologies in relation to Smad-dependent pathways',

Interactive cardiovascular and thoracic surgery, 11(4), pp. 455–460.
Zarkada, G. *et al.* (2015) 'VEGFR3 does not sustain retinal angiogenesis without VEGFR2', *Proceedings of the National Academy of Sciences of the United States of America*. National Academy of Sciences, 112(3), pp. 761–766. doi: 10.1073/pnas.1423278112.
Zeng, L., Carter, A. D. and Childs, S. J. (2009) 'miR-145 directs intestinal maturation in zebrafish', *Proceedings of the National Academy of Sciences* , 106(42), pp. 17793–17798. doi: 10.1073/pnas.0903693106.
Zeng, L. and Childs, S. J. (2012) 'The smooth muscle microRNA miR-145 regulates gut epithelial development via a paracrine mechanism', *Developmental Biology*, 367(2), pp. 178–186. doi: 10.1016/j.ydbio.2012.05.009.
Zhang, C. (2010) 'MicroRNAs in vascular biology and vascular disease', *Journal of cardiovascular translational research*. Springer, 3(3), pp. 235–240.
Zhang, H. *et al.* (2018) 'Understanding netrins and semaphorins in mature endothelial cell biology', *Pharmacological Research*. Academic Press, pp. 1–10. doi: 10.1016/j.phrs.2018.09.015.
Zhang, H. *et al.* (2020) 'Endothelial Semaphorin 3F Maintains Endothelial Barrier Function and Inhibits Monocyte Migration', *International Journal of Molecular Sciences*. MDPI AG, 21(4), p. 1471. doi: 10.3390/ijms21041471.
Zhang, Y. *et al.* (2010) 'Secreted Monocytic miR-150 Enhances Targeted Endothelial Cell Migration', *Molecular Cell*. Cell Press, 39(1), pp. 133–144. doi: 10.1016/j.molcel.2010.06.010.
Zheng, X. *et al.* (2010) 'CCM3 signaling through sterile 20–like kinases plays an essential role during zebrafish cardiovascular development and cerebral cavernous malformations', *The Journal of Clinical Investigation*. The American Society for Clinical Investigation, 120(8), pp. 2795–2804. doi: 10.1172/JCI39679.
Zhong, T. P. *et al.* (2001) 'Gridlock signalling pathway fashions the first embryonic artery.', *Nature*, 414(6860), pp. 216–20. doi: 10.1038/35102599.
Zhou, Q. *et al.* (2011) 'Regulation of angiogenesis and choroidal neovascularization by members of microRNA-23~27~24 clusters', *Proceedings of the National Academy of Sciences of the United States of America*. National Academy of Sciences, 108(20), pp. 8287–8292. doi: 10.1073/pnas.1105254108.
Zhou, S. S. *et al.* (2018) 'MiRNAS in cardiovascular diseases: Potential biomarkers, therapeutic targets and challenges review-article', *Acta Pharmacologica Sinica*. Nature Publishing Group, pp. 1073–1084. doi: 10.1038/aps.2018.30.
Zygmunt, T. *et al.* (2011) 'Semaphorin-PlexinD1 Signaling Limits Angiogenic Potential via the VEGF Decoy Receptor sFlt1', *Developmental Cell*. Cell Press, 21(2), pp. 301–314. doi: 10.1016/j.devcel.2011.06.033.

Appendix

Semaphorin 3f controls ocular vascularization from the embryo through to the adult

Halabi, R.[1,3], Watterston, C.[2], Mori-Kreiner, R[1,3]., Childs, S.[2,5], McFarlane, S[3,4,5].

1) Graduate Program in Neuroscience, University of Calgary
2) Department of Biochemistry and Molecular Biology, University of Calgary, 3330 Hospital Dr., NW, Calgary, AB, T2N 4N1
3) Department of Cell Biology and Anatomy, University of Calgary, 3330 Hospital Dr., NW, Calgary, AB, T2N 4N1
4) Hotchkiss Brain Institute, University of Calgary
5) Alberta Children's Hospital Research Institute, University of Calgary

Acknowledgements: The authors would like to thank Mrs. C. Hehr and Dr. G.E. Bertolesi for technical assistance. R.H. was supported by a T. Chen Fong Hotchkiss Brain Institute studentship, and by a studentship from Alberta Innovates-Health Solutions. This work was supported by the Bright focus Foundation to SM, and by project grants from the Canadian Institutes of Health Research to SJC and SM.

Commercial Relationships Disclosures: None

Word Count: recommends 3500 or fewer (excluding title page, legends and references); text double spaced, lines numbered

Abstract:

Purpose: Pathological angiogenesis in the eye is implicated in several diseases that result in vision loss, including age related macular degeneration and diabetic retinopathy. The limits of current disease therapies have created the need to identify and characterize new anti-angiogenics. Here, we use the zebrafish model to investigate the secreted chemorepellent Semaphorin3fa (Sema3fa) as an endogenous anti-angiogenic in the eye.

Methods: We generated a CRISPR/Cas9 sema3fa zebrafish mutant line, sema3faca304/304. We assessed the retinal and choroidal vasculature in both larval and adult wild type and sema3fa mutant zebrafish.

Results: We find sema3fa mRNA is expressed by the ciliary marginal zone, neural retina and RPE of zebrafish larvae, as choroidal vascularization emerges and the hyaloid/retinal vasculature is remodelled. The hyaloid vessels of sema3fa mutants develop appropriately, but during the larval period fail to remodel to the simplified network of wild type fish, and, in the adult, exhibit a denser network of capillaries in the retinal periphery than seen in wild type. The choroid vasculature was also defective in sema3fa mutants, in that it developed precociously, and aberrant, leaky sprouts were present in the normally avascular outer retina of both sema3faca304/304 larvae and adult fish.

Conclusions: These data point to Sema3fa as key in preventing pathologic vascularization of the retina, and highlight the RPE's role in providing a molecular barrier to maintain an avascular retina. Further, we provide a new experimentally accessible, disease relevant model for studying CNV resulting from changes in the RPE-mediated environment as opposed to endothelial cell dysfunction.

Introduction:

The retina is a highly metabolic structure of the central nervous system, with the highest energy demand coming from photoreceptors and the retinal pigment epithelium (RPE) (Country, 2017). Vascularization of the eye during development aims to match neural activity with metabolic demand, by providing the appropriate number and distribution of vessels to supply nutrients and oxygen. The underlying molecular signaling that regulates this process for the eye, however, is poorly understood.

The embryonic retina becomes perfused by two vessel beds – the hyaloid and choroidal vasculatures (Campochiaro, 2015). The hyaloid, or retinal, vasculature consists of an intra-retinal plexus that vascularizes the inner portion of the retina. In contrast, the photoreceptors of the avascular back of the retina are supported by nutrients and oxygen that diffuse from a dense plexus of fenestrated choroidal vessels across the RPE. Avascularity of the outer retina prevents light from being absorbed by hemoglobin containing blood cells (Campochiaro, 2015; Saint-Geniez and D'Amore, 2004). In retinal diseases such as retinopathy of prematurity, diabetic retinopathy, and the wet form of Age-Related Macular Degeneration (AMD), blood vessels grow aberrantly within the retina, which can result in serious vision loss (Lim et al., 2012). One approach to identify what goes wrong in the regulatory processes that normally prevent vessel growth in the adult retina, is to understand the molecular mechanisms that control the initial establishment of the vessel networks of the eye during embryonic development.

Often, the vessels that grow aberrantly within the neural retina in vascular retinal diseases are weak and leaky, and give rise to pathology. This is true of choroidal retinopathies, which include the wet form of AMD (Saint-Geniez and D'Amore, 2004), where there is pathological angiogenesis of the outer retina from the choroid. In this process, termed choroid neovascularization (CNV) (Baffi et al., 2000; Spilsbury et al., 2000), vessels enter the subretinal space as a result of increased expression of the key angiogenic Vascular Endothelial Growth Factor (VEGF) and tears to the extracellular matrix rich Bruch's membrane. In wet AMD, the infiltrating vessels can leak, which results in macular edemas and detachment of either the RPE or retina, and functional vision loss. anti-VEGF therapy is the only current treatment available for wet AMD, but is somewhat limited in its effectiveness (Cui and Lu, 2018). Aberrant growth of normally quiescent vessels also underlies the pathology of the inner retina that manifests in proliferative diabetic retinopathy, venous occlusion, and retinopathy of prematurity (Saint-Geniez and

D'Amore, 2004). Here, regions of ischemic retina trigger neovascularization to allow for reperfusion of the tissue, a process that, similar to the choroidal retinopathies, is VEGF or hypoxia driven. Understanding the etiology of diseases that impact the vasculature supporting the inner and the outer retina will aid in exploring new therapeutic avenues.

The molecular mechanisms that normally limit vessel outgrowth in the embryonic and adult eye are poorly understood. In addition to VEGF, dysregulation of secreted Semaphorin 3 (SEMA3) signaling molecules appears to control vessel growth during retinal disease. For instance, reduced transcript levels for the chemorepellent SEMA3F are found in RPE isolates from patients with wet AMD, and exogenous SEMA3F is a powerful anti-angiogenic in in vitro and in vivo mouse models of CNV (Buehler et al., 2013; Sun et al., 2017). These studies raise the interesting possibility of an endogenous role for SEMA3F as an anti-angiogenic secreted from the RPE that prevents the erroneous invasion of choroidal vessels into the outer retina.

The zebrafish retina is nourished by choroid and hyaloid vessels, but intraretinal plexi do not form (Alvarez et al., 2007) as they do in mouse and primates (Fruttiger, 2007; Provis, 2001). Thus, the zebrafish neural retina is normally avascular, which makes it an excellent model for the study of molecular regulators of vascular retinopathies. Here, we generate a sema3fa zebrafish mutant by CRISPR/Cas9 gene editing technology (Hwang et al., 2013) to show that Sema3fa, expressed both by the RPE and the neural retina, regulates the growth of blood vessels that metabolically support the inner and outer regions of the larval and adult eye. In larvae, loss of Sema3fa causes overgrowth of the intraocular hyaloid vasculature, and aberrant retinal infiltration of leaky blood vessels from the choroid. These phenotypes persist in the adult, arguing for an ongoing role for Sema3fa in limiting vessel growth through the lifetime of the fish. Of note, the sema3fa mutant zebrafish is the first model of vascular retinopathy that arises from retina-associated changes in the signaling environment of the blood vessels, and not from genetic manipulations of the blood vessels or artificially-induced vascularization.

Results:

sema3fa is expressed by the RPE in development and adulthood

Previous reports in mouse found SEMA3F expressed by the RPE and the outer nuclear layer of the photoreceptors (Buehler et al., 2013; Sun et al., 2017). As such, we asked if sema3fa was expressed by the zebrafish RPE from 24 hours post fertilization (hpf), when pigmentation first appears in the RPE (Cechmanek and McFarlane, 2017), to larval stages, when the retina becomes functional, and into adulthood. The RPE expressed sema3fa at 72 hpf (data not shown) as the retinal layers form, and maintained this expression through larval stages (7 days post-fertilization (dpf)) (Fig. 1A,B) and into the adult (Fig. 1C). The similar expression of SEMA3F in the mouse, human and zebrafish RPE are supportive of a conserved role (Buehler et al., 2013).

To investigate an endogenous role for Sema3fa in regulating the two vessel beds of the eye, we used CRISPR/Cas9 gene editing technology (Hwang et al., 2013) to generate a sema3fa loss of function mutant, by using three sgRNAs to target exon 1 (Figure 1E). A single founder was produced with a two base pair (bp) deletion, which was predicted to generate a protein size of 76 amino acids (aa) due to a premature truncation within the 500 aa SEMA domain (Figure 1F) that is necessary to elicit intracellular signaling (Tamagnone et al., 1999). RT-qPCR to detect relative transcript levels of mRNA isolated from 48 hpf wild type and homozygous mutant embryos indicated a reduction in sema3fa mRNA levels in the mutant as compared to wild type (Figure 1D), suggestive of nonsense mediated mRNA decay. Further, Western blot analysis revealed that Sema3f protein was absent in sema3faca304 mutants, indicating that we generated a sema3fa null mutant (Figure 1G). No differences were found in either head-to-tail body length (Figure 1H,I), or the ratios of lateral eye to body size (Figure 1J) in embryos of the different genotypes from 36–72 hpf. These data suggest no gross abnormalities in the development of sema3fa mutant embryos or their eyes.

Sema3fa refines and limits retinal vessel branching in the larvae and adult

In order to directly investigate eye vessel growth in an environment that lacked Sema3fa, we outcrossed a female sema3fa homozygous mutant to a male Tg(kdrl:mCherry), in which all endothelial cells are labelled by mCherry (Proulx et al., 2010). Resulting heterozygotes were raised to adulthood, and then incrossed to generate wildtype and homozygous mutant lines. All

subsequent analyses were performed on a mix of embryos generated from either heterozygous incross matings, or from the established monogenic transgenic lines.

The hyaloid vessel enters the eye and branches to form a network of vessels covering the posterior aspect of the lens (Alvarez et al., 2007; Hartsock et al., 2014; Isogai et al., 2001; Saint-Geniez and D'Amore, 2004). Beginning at 15 days post fertilization (dpf), the hyaloid detaches from the lens, adheres to the inner limiting membrane, and forms the adult retinal vasculature (Alvarez et al., 2007). In mouse, the hyaloid vessel instead regresses completely and regrows to form the retinal vasculature through an angiogenic program (Saint-Geniez and D'Amore, 2004). Entry of the hyaloid vessel into the retina was unaffected in the sema3fa mutants as assessed by confocal live-imaging at 24 hpf (Figure 2A,B) (Hartsock et al., 2014). Additionally, at 72 hpf the branched hyaloid network around the lens formed normally in mutant (N=1, n=4/4) and wildtype (N=1, n=4/4) embryos (Figure 2C,D). Thus, Sema3fa appears to have no role in the establishment of the vasculature of the early retina.

In zebrafish, between 4-5 dpf retinal vessel complexity is reduced markedly by a refinement process where extraneous connections are retracted (Hartsock et al., 2014). Given the expression of sema3fa in the CMZ and nuclear layers of the 72 hpf retina, close to the hyaloid vessel bed, we asked whether vessel refinement was affected by the loss of Sema3fa. From confocal projections of live embryos at 4 dpf, we observed that in 91% of wild type (N=4, n=10/11) embryos the hyaloid network had refined to a simplified stereotypic pattern (Figure 2E,E',G), all of the heterozygous (N=1, n=2/2) and homozygous (N=4, n=12/12) sema3fa-/- (Figure 2F,F',G) larvae retained complex hyaloid vessel networks, with interconnections throughout the plexus. These data support a role for Sema3fa in embryonic hyaloid vasculature development.

To determine if patterning of the hyaloid network continued to be impacted by the absence of Sema3fa, we assessed the vasculature of the retinas of wild type and mutant adults. Because the hyaloid network comes to adhere to the inner limiting membrane of the retina (Alvarez et al., 2007), the state of complexity of the vessel network was readily visualized in retinal flat mounts of transgenic sema3fa+/+ and sema3fa-/- 5-month-old adult Tg(kdrl:mcherry) fish (Figure 3A,B). We measured three parameters of vessel growth; primary vessel length (Figure 3C), as measured from the optic nerve head to the first branching event, primary vessel width (Figure 3D), and capillary spacing in the retinal periphery (Figure 3G) (Bozic et al., 2018). Primary vessel length

was significantly shorter (N=2, n=6, p=0.0016) (Figure 3C), and the width of these vessels significantly thinner (N=2, n=6, p=0.0078) in mutants as compared to wild types (N=2, n=6 vessel length; N=1, n=6 vessel width) (Figure 3D). Finally, capillaries in the retinal periphery (Figure 3E,F), where arterial capillaries anastomose with circumferential vein capillaries (Cao et al., 2008), were spaced more closely in the mutant (48.0± 1.6 μm; N=1, n=4, p<0.0001) as compared to in wild type retinas (92.7 ± 2.3 μm; N=1, n=4) (Figure 3G). Interestingly, more intercapillary connections and sprouts (Figure 3H) were also apparent in the mutants as compared to the wild types (Figure 3E,F, arrowheads). These data support a role for Sema3fa in the patterning of the hyaloid and retinal vasculature throughout life.

The choroid plexus undergoes neovascularization in sema3fa mutant retina

The choroid plexus surrounds the back of the retina, and nourishes the RPE and outer retina (Alvarez et al., 2007; Isogai et al., 2001; Saint-Geniez and D'Amore, 2004). In zebrafish, formation of this plexus is first observed at the back of the eye by 5.75 dpf (van Rooijen et al., 2010). At this time point, and through to the adult, sema3fa was expressed in the RPE underlying the choroid plexus (Figure 1B,C). Thus, we asked if the adjacent choroidal vessel network was impacted by the loss of Sema3fa. With live imaging of 6 dpf wild type and mutant Tg(kdrl:mCherry) embryos, we found that sema3fa-/- embryos exhibited a choroid plexus (N=1, n=3/3) before the network was observed in wild type embryos (N=1, n=0/3). Because the presence of the choroid plexus was somewhat variable at 6 dpf in wild type, we used 7 dpf for quantitation, when most wild type larvae exhibit a choroid plexus. While a nascent choroid plexus was present in 88% of wild type embryos (N=6, n=15/17, Figure 4A), the plexi were overgrown or advanced in 69% of heterozygous (N=4, n=9/13, Figure 4B) and 71% of homozygous (N=6, n=12/17, Figure 4C) sema3fa embryos. These data suggest that precocious choroid plexus growth occurs when Sema3fa signals are removed from the retina.

sema3fa -/- orbital vasculature is leaky

Since the overgrowth of the choroid plexus occurs over top of the RPE, we asked if the physiologic avascularity of the retina was compromised. In order to label the retinal and choroid vasculatures, we performed fluorescent angiography by using a 2,000,000 MW rhodamine-dextran, a molecule normally too large to pass through any vessel wall (van Rooijen et al., 2010). We injected the hearts of 7 and 9 dpf wild type and mutant embryos with the rhodamine-dextran,

fixed the embryos 24 hours post injection, and cryostat-sectioned retinas for analysis using the confocal microscope (Figure 4D-O). Vessels were detected within the outer nuclear layer in all of the 8 (N=2, n=4/4) and 10 (N=3, n=10/10) (arrowheads Figure 4I,O) dpf mutant larvae, but none of the wild type larvae (N=2, n=4/4 for 8 dpf; N=2, n=10/10 for 10 dpf) (Figure 4F,L). Of note, dextran accumulated throughout the nuclear layers of the retina in all of the 8 dpf (N=2, n=4/4) and most of the 10 dpf (N=3, n=8/10) (Figure 4H,M-O) mutant larvae, but was largely absent from the nuclear layers of the wild type counterparts (N=2, n=4/4 for 8 dpf; N=3, n=9/10 10 dpf) (Figure 4E-F,K-L). Taken together, these data indicate that in the absence of Sema3fa, blood vessels invade the normally avascular outer retina and leak into the neural retina proper. While there was no increase in TUNEL-positive dying cells in the retinas lacking Sema3fa (Figure 4Q), we did find instances where the retinal cellular architecture appeared disrupted by penetrating pathologic vessels (Figure 4R,S).

To address whether the entry of leaky vessels into the eye was solely a larval phenotype, we analyzed in retinal sections the extent of vessel infiltration into wild type and mutant adult (5 months) Tg(kdrl:mCherry) outer retinas (Figure 5). mCherry positive cells were present in 75% (N=1, n=3/4, Figure 5D-F) of the mutants and none of the wild type siblings (N=1, n=4, Figure 5A-C). To determine whether the vessels remained leaky in the adult, we injected the fluorescent angiography dye into aged (12 month) adult non-transgenic wild type and mutant fish. Dextran was present within the nuclear layers of the retina (Figure 5H) in 60% of homozygous mutants (N=1, n=3/5) and none of the wildtype siblings (N=1, n=3, Figure 5G), indicating that in the mutants the ectopic vessels remain leaky.

Sema3fa functions as an endogenous anti-angiogenic that prevents CNV

Increased expression of VEGF is thought to drive CNV development in AMD (Baffi et al., 2000; Spilsbury et al., 2000), as anti-VEGF therapy limits disease progression (Cui and Lu, 2018). In zebrafish, Vegfa is a potent endothelial cell mitogen necessary for vascular development (Coultas et al., 2005), promotes hypoxia driven angiogenesis (Thomas, 1996), and drives retinal and choroidal vascularization (Cheung et al., 2014). As such, we asked whether the sema3fa mutant CNV phenotype was due to an upregulation of vegfa expression in the outer retina. Zebrafish have a duplicated vegfa, with vegfaa and vegfab isoforms (Bahary et al., 2007). By ISH, neither isoform

was expressed at significant levels in wild type or mutant larval eyes (data not shown). We confirmed these data by RT-qPCR of cDNA from eyes isolated from 5 dpf fish, showing that neither vegfaa nor vegfab isoforms were upregulated in sema3faca304 eyes as compared to wild type (Figure 4P). These data suggest that vessel infiltration into the neural retina is not due to an increase in vegfa expression.

A disruption in the continuity of the RPE would provide a conduit for blood vessel sprouts from the choroid plexus to enter the neural retina (Ersoz et al., 2017). To analyze whether the RPE was intact in sema3fa mutant fish, we first looked at histological sections stained by hematoxylin and eosin at 72 hpf (data not shown) and 8 dpf (Figure 6A,B). Loss of Sema3fa caused no obvious disruption or thinning of the RPE (Figure 6A,B), and the epithelium appeared to exhibit the appropriate morphology and polarity, with apical microvilli present in both the wild type and sema3faca304 retinas (Figure 6A',B') (N=3, n=9 at 72 hpf for both genotypes, N=2, n=10 at 8 dpf for both genotypes). We also immunolabelled with the Zpr2 antibody, which labels mature RPE (Zou et al., 2008), and found Zpr2 immunostaining was indistinguishable between wild type (N=2, n=9) and mutant (N=2, n=9) retinas (Figure 6C,D). The outer limiting membrane (OLM), which consists of junctions between the Muller glia and the inner segment of the photoreceptors, contributes to the outer blood-retinal barrier (Omri et al., 2010). The OLM was investigated with ZO-1 that marks adhesion junctions between photoreceptors and Muller glia (Figure 6E,F), and phalloidin, that labels F-actin (Figure 6G,H) (Krock and Perkins, 2014). Punctate ZO-1 and uninterrupted F-actin labeling of the OLM was observed in both genotypes. Ultimately these results support the idea that the ectopic retinal entry of blood vessels with the loss of Sema3fa likely arises from the loss of an endogenous anti-angiogenic, rather than an underlying RPE dysfunction.

Discussion:

Here we demonstrate the necessity of Sema3f to control the growth of the vasculature of the eye from the embryo to the adult: Sema3f maintains the physiologic avascularity of the outer retina, and limits the extent of the retinal vascular network. Interestingly, while we find that both the retinal and choroid vasculature of the eye are disrupted with the loss of Sema3fa, the impact of Sema3fa loss is different in the two beds. With Sema3fa loss we find that the embryonic intraocular vasculature fails to undergo its normal refinement, while the extraocular vasculature grows precociously in the embryo, and leaky vessels infiltrate into the larval neural retina that persist into the adult. This work provides sema3fa knockout zebrafish as a novel model to be used to understand the cellular and molecular mechanisms of choroidal retinopathies that arise from an environmental change in the outer retina, and to test novel anti-angiogenics via high throughput drug screening.

Both intra and extra-ocular vascular beds are affected significantly in the sema3fa mutant embryo and adults. Based on our data, we propose a model whereby spatially localized Sema3fa signalling negatively controls vascular growth (Figure 6I,J). We suggest that Sema3fa secreted from the RPE inhibits choroid vessel sprouting (Figure 6I), while Sema3fa from the neurons of the inner neural retina and/or progenitors of the CMZ refine a simple hyaloid vasculature, and then maintain a patterned retinal vessel network (Figure 6J). In support, sema3fa mRNA is expressed by the RPE, inner nuclear layers and CMZ in the larval and adult zebrafish retina. Moreover, with Sema3fa loss the choroid vessels grow both precociously and inappropriately through the RPE and into the outer retina, while hyaloid/retinal vessel refinement is impaired and the retinal vasculature is more extensive. We propose that Sema3fa works in a direct paracrine manner via Nrp1b on endothelial cells of the orbital vasculature. In support of a role for Sema3f as an anti-angiogenic in the eye, AAV-mediated expression of SEMA3F in mouse models inhibits sprouting from retinal and choroidal vessels (Buehler et al., 2013; Sun et al., 2017). The initial analysis of the Sema3f null mouse did not report vascular abnormalities (Sahay et al., 2003), but further analysis is likely warranted. Interestingly, SEMA3F may function in a tissue specific manner. Our work in fish, and that with exogenous SEMA3F in mouse (Buehler et al., 2013; Sun et al., 2017), indicates that SEMA3F inhibits eye vessel growth, however, it appears to act in a pro-angiogenic fashion in the mouse placenta (Kessler et al., 2004; Regano et al., 2017).

The sema3fa mutant vessel phenotypes could arise through a number of means, including increased endothelial cell proliferation, increased stability of vessels, and/or failure to block pro-angiogenic cellular guidance. VEGF might be important in this regard. VEGFA binds to FLK-1 and via Src kinases and MAPK promotes endothelial cell proliferation (Mahabeleshwar et al., 2007; Soldi et al., 1999; Werdich and Penn, 2005; West et al., 2012), and Müller glia-derived VEGF contributes to pathologic neovascularization in the mouse retina (Bai et al., 2009). Yet, we find that vegfaa and vegfab are expressed at low levels in both wild type and mutant larval retinas, arguing that retinal Vegf does not drive the overgrowth of the choroid plexus and presence of infiltrating vessels in the mutants. Interestingly, Sema3f signals through Nrp2 to inhibit Vegf-induced proliferation of endothelial cells of cultured human umbilical vein endothelial cells (Kessler et al., 2004), suggesting that Sema3fa may limit choroid vessel sprouting by a similar block of Vegf-induced proliferation.

Cells, including endothelial cells, are guided by a mix of repulsive and attractive extrinsic signals. VEGF is one such pro-angiogenic attractive signal (Chauvet et al., 2013). Interestingly, while pro-angiogenic regulators have an endogenous physiological role in attracting vessels, anti-angiogenic pathways appear relevant only in a pathological scenario (Serini and Tamagnone, 2015). Here we argue for an endogenous role for Sema3fa signalling in maintaining vessel quiescence in vivo, whereby loss of the anti-angiogenic Sema3fa removes the “brakes” on vessel growth and permits vessels to wander into the retina.

In mice and humans, choroidal vessels that invade the neural retina are generally immature and lack proper tight-junctions and smooth muscle/pericyte coverage, and are therefore prone to leakage (Törnquist et al., 1990). Leakage and subsequent fluid accumulation in the macula of the human retina accelerates vision loss in wet AMD (Saint-Geniez and D’Amore, 2004). Leakage is likely due to disruption of the blood-retina barrier (BRB) between the vasculature and retina. The BRB is maintained via tight junctions between both RPE cells, which prevent passage of substances, and endothelial cells. Disruption of these junctions results in vascular leakage and subsequent edema (Bharadwaj et al., 2013). The nearly 100% penetrance of vascular leakage (though no obvious edema was present) in sema3fa mutants suggests a disruption to the BRB.

Leakiness may be attributed directly to the loss of Sema3fa, or may reflect the small size of the capillaries that navigate into the subretinal space. Interestingly, while ectopic blood vessels are present in the retina throughout the lifetime of the mutants, we find no evidence of retinal detachments. Potentially, the regenerative capacity of zebrafish can correct the insult.

Dysregulation of crosstalk between the neural retina and the inner retinal vasculature is recognized as a major contributor to the pathogenesis of vascular retinopathies (Sun et al., 2017b). In the absence of Sema3fa, the adult retinal vasculature was more dense in the mutant as compared to wild type. In mammals, the retinal vasculature is thought to associate with an astrocyte scaffold that influences branching pattern in a VEGF-dependent manner (Fruttiger, 2007; Scott et al., 2010). Interestingly, no astrocytic scaffold has been identified in zebrafish. It is possible, however, that Müller glia still play some role in vascular patterning in teleosts, in that the glial end feet form intimate connections with the endothelium following vascular dissection (Alvarez et al., 2007). Potentially Sema3f provides an opposing mechanism to that of Vegf in patterning the retinal vasculature, so as to prevent overgrowth. A model for Sema3fa function is that through repellent mechanisms it spaces out and calms retinal vessel growth along the inner limiting membrane (Figure 6J). Secreted Sema3fa would most likely come from the closest sources, which include from cells of the retinal ganglion cell layer and/or cmz progenitors. One interesting idea is that Müller glia, whose cell bodies reside in the inner nuclear layer, secrete Sema3fa preferentially from their end feet in contact with the inner limiting membrane and overlying endothelium.

Here we provide evidence that Sema3fa establishes and maintains physiologic avascularity of the zebrafish retina through the life time of the fish. A role for secreted Sema3s in mediating blood vessel dynamics is known (Sakurai et al., 2012). To the best of our knowledge, however, we show for the first time that the loss of an anti-angiogenic molecular barrier makes the RPE receptive to blood vessel infiltration in the absence of any further insults. The robustness of the sema3fa mutant zebrafish model in mitigating eye vessel pathology argues convincingly for its continued use for understanding the underlying cellular and molecular events that control the growth of the vessel networks that support eye function.

Figure Legends:

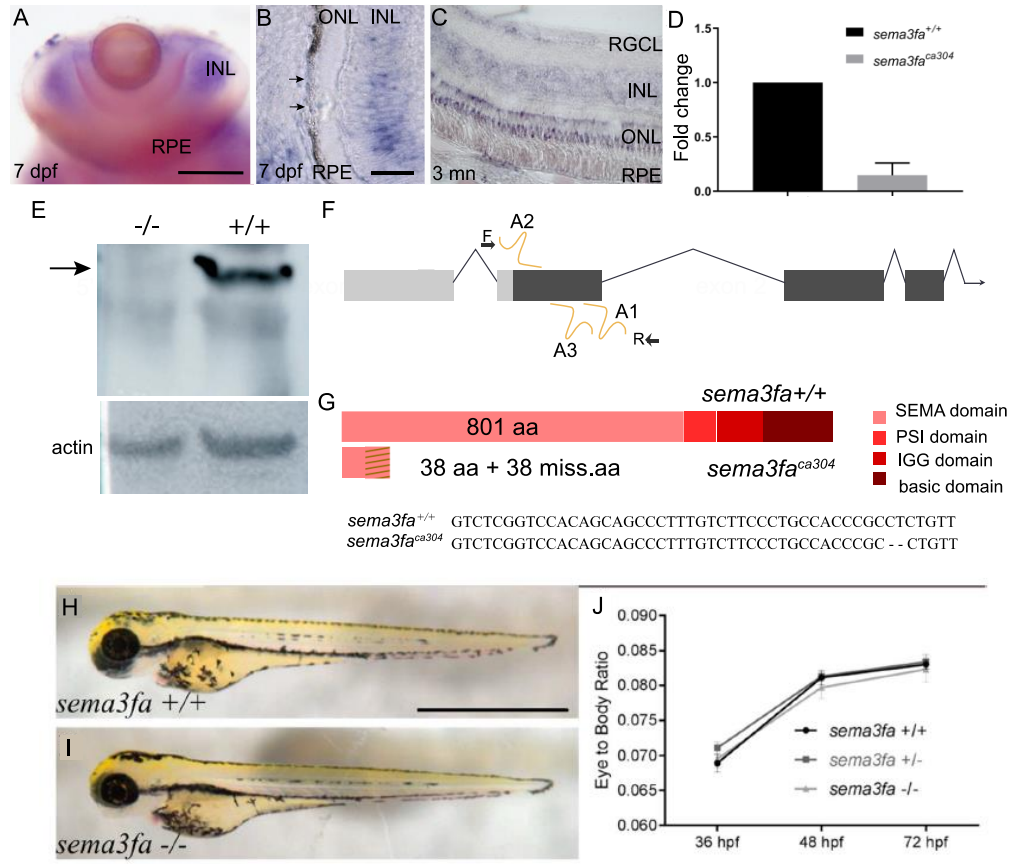

Figure 1: *sema3fa* is expressed by the RPE of larval and adult retinas. A-C) *sema3fa* RNA ISH of whole mount (A) and retinal sections (B-C). ISH signal is detected in the RPE during development and into adulthood. In larval retina (7 dpf), *sema3fa* is also expressed in the inner nuclear layer and ciliary marginal zone, while in the adult (3 months), *sema3fa* is expressed within all retinal layers. cmz, ciliary marginal zone; INL, inner nuclear layer; ONL, outer nuclear layer; RGC, retinal ganglion cell layer; RPE, retinal pigment epithelium. Scale bar: 100 µm in A, 50 µm B-C. **D)** RT-qPCR of *sema3fa* mRNA levels in wild type and *sema3fb*^{ca304} embryos at 48 hpf suggest nonsense mediated decay of mRNA transcript (N=2). Error bar represents standard error of the mean (SEM). **E)** Western blot of protein isolated from 72 hpf wild type and *sema3fa*^{ca304} mutant fish processed with a custom-made antibody against zebrafish Sema3fa. The antibody recognizes a protein of the appropriate size for Sema3fa in wild

type fish, which is absent in the mutants. Loading control is ß-actin. **F)** Chromosomal overview of the *sema3fa* locus targeted by CRISPR/Cas9 mutagenesis to exon 1 (guide RNA: A1-3) and primers used to identify the mutation. UTR: untranslated region; F: forward primer; R: reverse primer. **G)** Schematic representation of wild type and premature stop codon mutant proteins. *sema3fa*^{ca304} fish have a 2 bp deletion (dashes) to produce a predicted product of 76 aa. Dashes represent missense amino acids (miss.aa). **H-I)** Lateral views of 72 hpf wild type (H) and *sema3fa*^{ca304} (I) fish. **J)** The ratio of the anterior-posterior body length and eye width, measured along the antero-posterior axis, at 36, 48 and 72 hpf, arguing that there is no gross abnormalities in body or eye growth in the *sema3fa*^{ca304} fish.

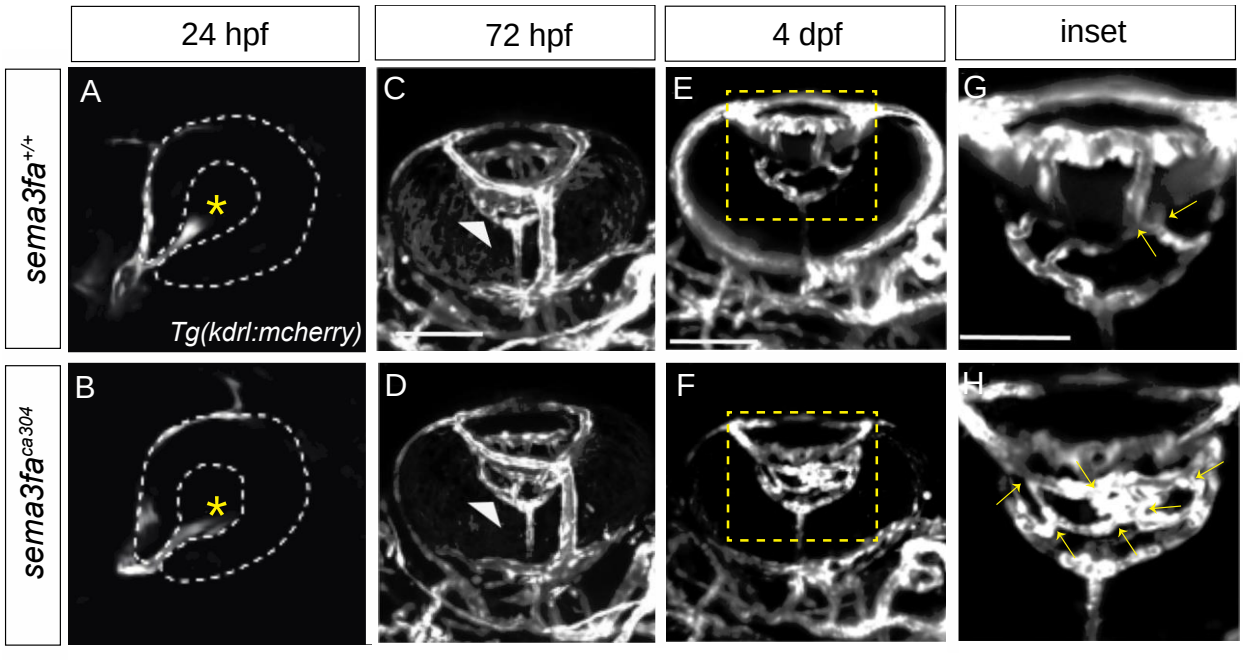

Figure 2: Sema3fa is required to refine and limit retinal vessel branching in the larval eye. Live imaging of *Tg(kdrl:mCherry)* wild type (A,C,E,C') and *sema3fa*^{ca304} (B,D,F,F') eyes during retinal intraocular vascular development acquired by confocal microscopy. **A-B)** In lateral views of wild type (A, N=1, n=3/3) and *sema3fa*^{ca304} (N=1, 4/4) *Tg(kdrl:mCherry)* embryos, the hyaloid artery (endothelial cells labelled by mCherry) makes contact with the lens (asterisk) of the retina by 24 hpf. **C-D)** Maximal projections of stacks of ventral views of wild type (C, N=1, n=4/4) and *sema3fa*^{ca304} (D, N=1, n=4/4) embryos reveals that the hyaloid artery (arrowhead) forms a vascular plexus network around the lens by 72 hpf. **E-F)** The intraocular hyaloid vessel (orange chevron) undergoes remodelling between 4-5 dpf to simplify the network (Hartsock et al., 2014). At 4 dpf, the numbers of vessel crossovers (arrows) are increased in *sema3fa*^{ca304} (F, N=4, n=12) embryos as compared to wild type siblings (E, N=4, n=11). Magnification of boxed regions (E,F) of hyaloid vasculature shown in E',F'. Scale bar: 100 μm; 50 μm for E'F.

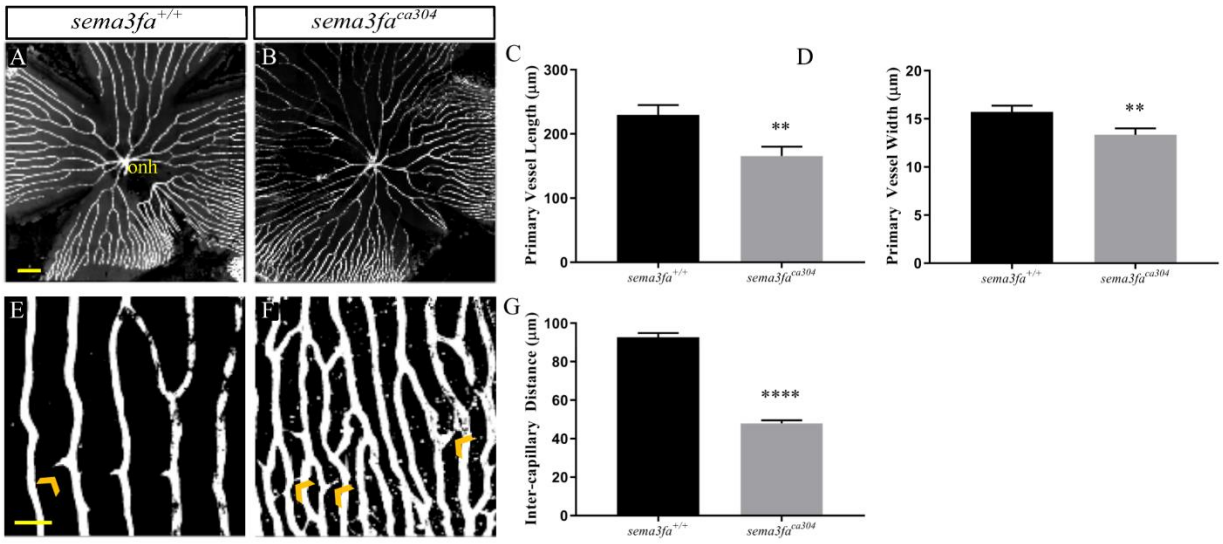

Figure 3: Increased vascularization of the retina is observed into adulthood. Retinal flat mounts of *Tg(kdrl:mCherry)* wild type siblings (A) and *sema3fa*^{ca304} (B) 5 month fish. **C)** Primary vessel length as measured from the optic nerve head (onh) to the first branching event is significantly shorter in mutants (N=2, n=6, **p=0.0016) as compared to wild type siblings (N=2, n=6). **D)** The average width of the primary vessels is reduced significantly in mutants (N=2, n=6, **p=0.0078) as compared to wild type (N=2, n=6). **E-F)** Capillaries furthest from the optic nerve head (onh) in the peripheral retina (E,F). A greater number of tip cell interconnections between capillaries are present in mutant retina (yellow chevrons). **G)** Measurement of the intercapillary distance shows that mutant capillaries are less far apart (N=1, n=4 flat mounts, ****p<0.0001) as compared to wild type (N=1, n=4 flat mounts). Error bars represent standard error of the mean SEM). Statistics represent the non-parametric Mann-Whitney U test. Scale bar: 200 µm (A) and 50 µm (E).

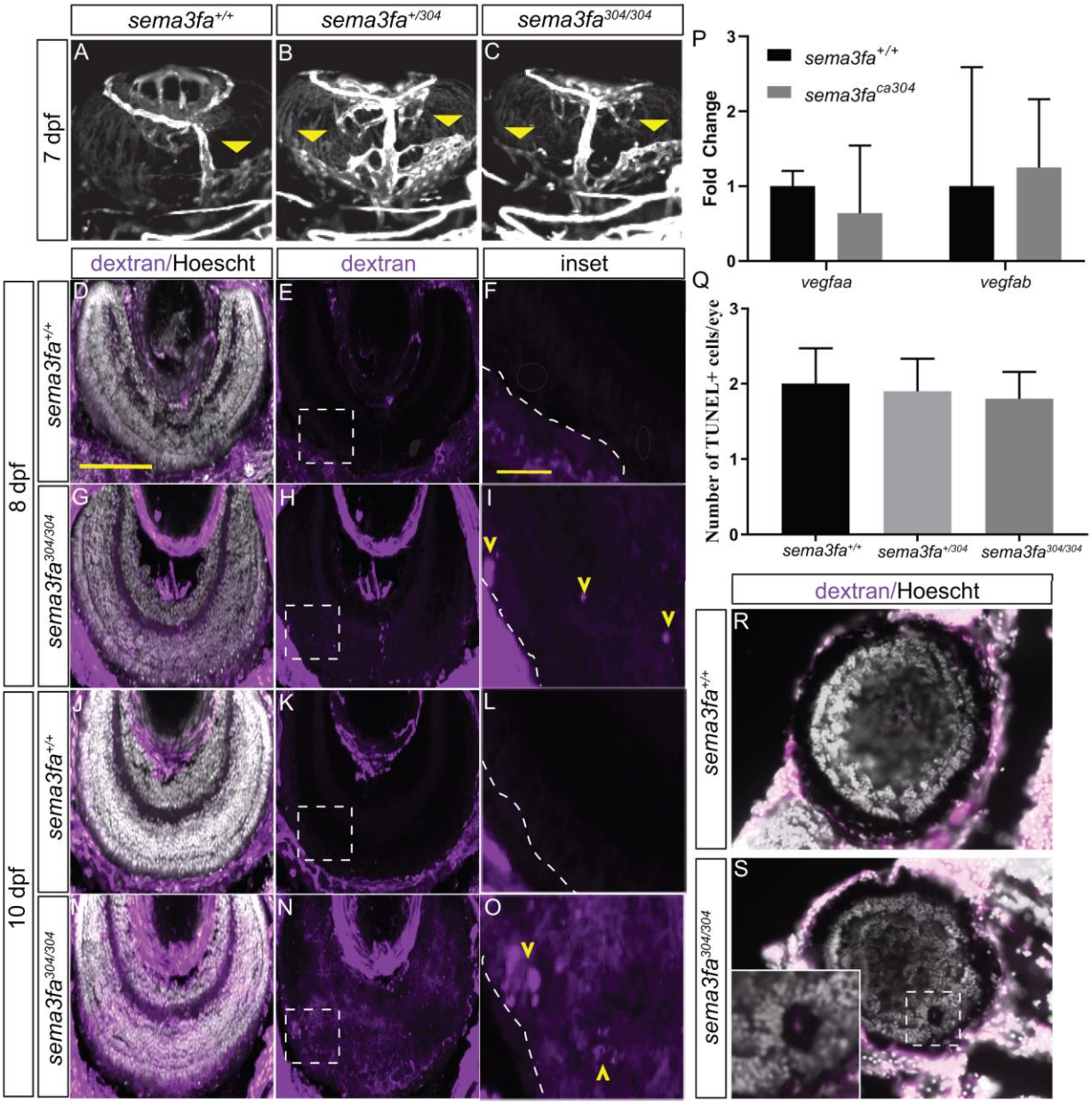

Figure 4: *sema3fa* deficient embryos present with leaky vessels within the outer retina. A-C) Maximal projections of z-stacks of live imaged *Tg(kdrl:mCherry)* embryos imaged from a ventral view on a confocal microscope. In 7 dpf wild type (A, N=6, n=17) larvae the extraocular choroid plexus (yellow arrowhead) has begun to branch over the back of the retina. Heterozygous (B, N=4, n=13) and homozygous (C, N=6, n=17) *semafa*^{ca304} eyes exhibit a dramatic increase in the choroid vasculature as compared to wild type siblings. Scale bar: 100 μm. **D-O)** Sema3fa deficiency permits entry of leaky vessels into the neural retina. Thick (40 μm) cryosections through the eyes

of embryos injected at 7 dpf (E-J) or 9 dpf (K-P) with 2,000,000 MW rhodamine dextran and fixed 24 hours later. Sections are counterstained with nuclear label (Hoechst). Blood vessels (yellow arrowheads) infiltrate aberrantly into the outer retina of homozygous embryos at 8 dpf (J, N=2, n=4/4)) and 10 dpf (P, N=3, n=10/10), but are not present in wild type embryos (G, N=2, n=0/4; M, N=3, n=0/10). Dextran is present in the neural retina at 10 dpf in homozygous mutant eyes (O, N=3, n=8/10), but is essentially absent from wild type (L, N=3, n=1/10) eyes. Dashed line represents boundary between the RPE and neural retina. Boxed areas in F,I,J,O are shown magnified in G,J,M,P. Scale bar: 100 μm and of inset 20 μm. **P)** RT-qPCR for *vegfaa* and *vegfab* performed on mRNA isolated from wild type and *semafa*^{ca304} 4 dpf eyes. Error bars are s.e.m. **Q)** Similar average numbers of TUNEL+ apoptotic cells in whole mount heterozygous (N=2, n=10, p>0.99) and homozygote (N=2, n=10, p>0.99) eyes as compared to wild type sibling eyes (N=2, n=10) at 7 dpf. **R-S)** The peripheral retina of a wild type (R) and *semafa*^{ca304} (S) embryo (10pf), where in the mutant penetrating pathologic vessels appear to contribute to a disruption in retinal cellular architecture.

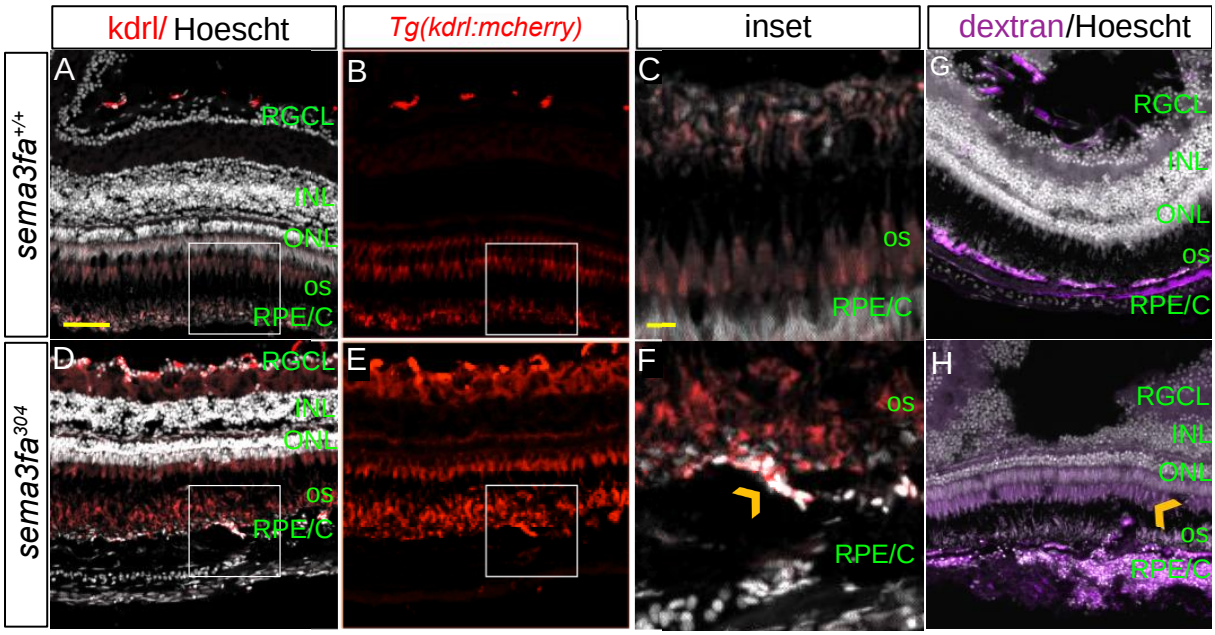

Figure 5: Vessel infiltration persists in the adult *sema3fa* mutant retina. A-H) Cryosections made through the retinas of *Tg(kdrl:mCherry) sema3fa* wild type (A-C) and mutant (D-F) 5 month old siblings. Nuclei are labelled by Hoechst (white). In the majority of *semafa*^{ca304} eyes (n=3/4), but in none of the wild type retinas (n=4), a blood vessel in the area of the photoreceptor outer segments (os) was detected. **G-H)** One-year old adult *sema3fa*+/+ (G) and *sema3fa*-/- (H) fish were injected with 2,000,000 MW rhodamine dextran (purple) and fixed 4 hours later. Thick (40 µm) eye cryosections counterstained with nuclear label (Hoechst) reveal leakage of dye (purple, yellow chevron) is also present in the neural retina of *semafa*^{ca304} fish (N=1, n=3/5, H), but not wild type siblings (G, N=1, n=3). inl: inner nuclear layer; onl: outer nuclear layer; RGC: retinal ganglion cell layer; RPE/C: retinal pigment epithelium/choroid. Scale bar: 50 µm. Scale bar of inset: 10 µm.

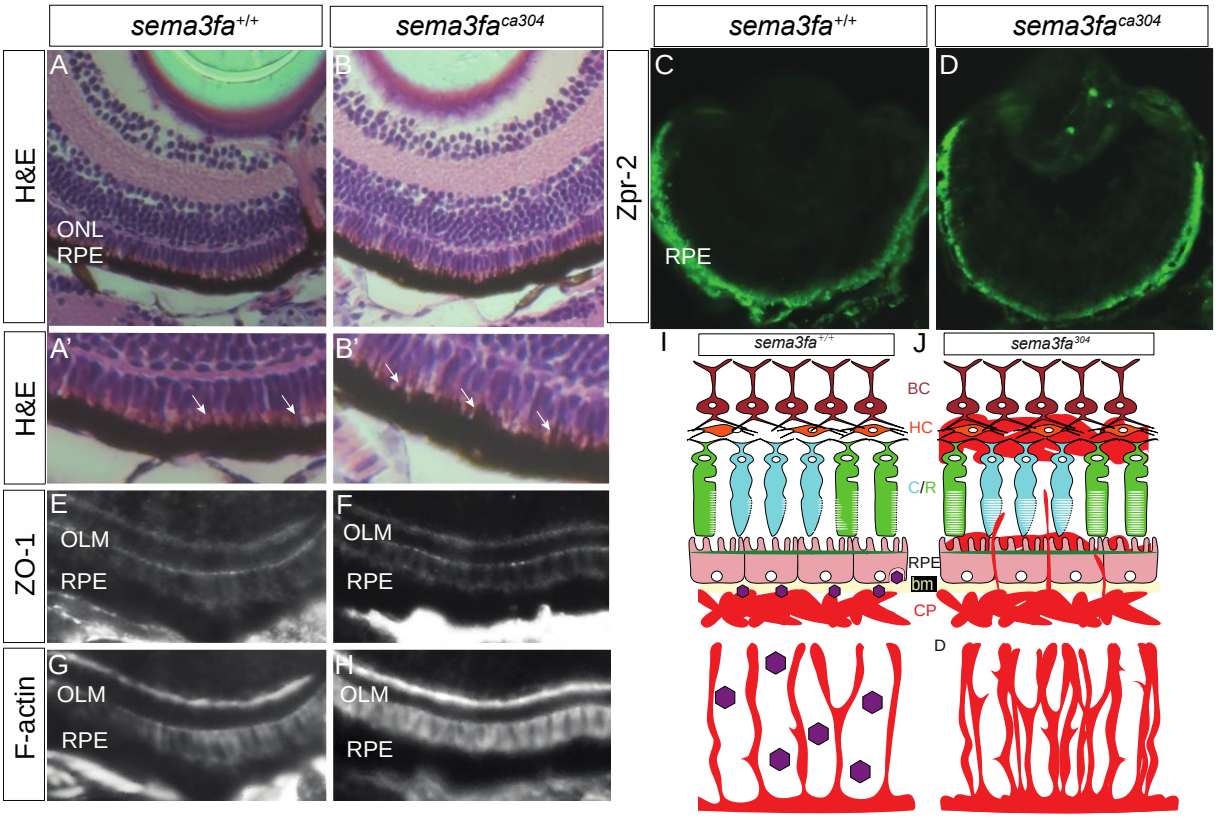

Figure 6: The RPE and the outer limiting membrane are not obviously disrupted with the loss of Sema3fa. A-B) Transverse sections of 8 dpf wild type (N=2, n=) and *sema3fa*^{ca304} (N=2, n=) mutant retinas labelled with haematoxylin and eosin. A higher power view of the RPE isshown in A' and B'. No obvious gaps are seen in the RPE, and apical microvilli (arrows) are evident in both genotypes. **C-D)** Immunolabeling of the RPE with the Zpr2 antibody is comparable in wild type (N=1, n=4) and mutant (N=1, n=4) retinas. **E-H)** No obvious disruption of the outer limiting membrane, as stained with antibodies for the adhesive junction protein ZO-1 (N=1; *sema3fa*$^{+/+}$, n=6; *sema3fa*^{ca304} n=6) and phalloidin that labels F-actin (N=2; *sema3fa*$^{+/+}$, n=12; *sema3fa*^{ca304} n=12). **I-J)** Working model of roles for Sema3fa in regulating vascularization of the neural retina. **I)** In wild type, the choroid plexus (CP) remains outside of the RPE and Bruch's membrane (bm) through the release of Sema3fa (purple hexagon) by the RPE. If Sema3fa signaling is perturbed, vessels pass through the RPE and leak into the nuclear layers containing the cone and rod (C/R) photoreceptors, horizontal cells (HC) and bipolar cells (BC). **J)** In the hyaloid/retinal vascular bed, Sema3fa (purple hexagon) maintains spacing and reduces the density of blood vessel networks in wild type retinas. In the absence of Sema3fa, blood vessels overgrow and attempt to make aberrant connections with each other.

References:

Alvarez, Y., Cederlund, M.L., Cottell, D.C., Bill, B.R., Ekker, S.C., Torres-Vazquez, J., Weinstein, B.M., Hyde, D.R., Vihtelic, T.S., Kennedy, B.N., 2007. Genetic determinants of hyaloid and retinal vasculature in zebrafish. BMC Developmental Biology. https://doi.org/10.1186/1471-213X-7-114

Baffi, J., Byrnes, G., Chan, C.C., Csaky, K.G., 2000. Choroidal neovascularization in the rat induced by adenovirus mediated expression of vascular endothelial growth factor. Investigative Ophthalmology and Visual Science.

Bahary, N., Goishi, K., Stuckenholz, C., Weber, G., LeBlanc, J., Schafer, C.A., Berman, S.S., Klagsbrun, M., Zon, L.I., 2007. Duplicate VegfA genes and orthologues of the KDR receptor tyrosine kinase family mediate vascular development in the zebrafish. Blood. https://doi.org/10.1182/blood-2006-04-016378

Bai, Y., Ma, J.X., Guo, J., Wang, J., Zhu, M., Chen, Y., Le, Y.Z., 2009. Müller cell-derived VEGF is a significant contributor to retinal neovascularization. Journal of Pathology. https://doi.org/10.1002/path.2611

Bharadwaj, A.S., Appukuttan, B., Wilmarth, P.A., Pan, Y., Stempel, A.J., Chipps, T.J., Benedetti, E.E., Zamora, D.O., Choi, D., David, L.L., Smith, J.R., 2013. Role of the retinal vascular endothelial cell in ocular disease.

Bozic, I., Li, X., Tao, Y., 2018. Quantitative biometry of zebrafish retinal vasculature using optical coherence tomographic angiography. Biomed Opt Express 9, 1244–1255. https://doi.org/10.1364/BOE.9.001244

Buehler, A., Sitaras, N., Favret, S., Bucher, F., Berger, S., Pielen, A., Joyal, J.-S., Juan, A.M., Martin, G., Schlunck, G., Agostini, H.T., Klagsbrun, M., Smith, L.E.H., Sapieha, P., Stahl, A., 2013. Semaphorin 3F forms an anti-angiogenic barrier in outer retina. FEBS Lett. 587, 1650–1655. https://doi.org/10.1016/j.febslet.2013.04.008

Campochiaro, P.A., 2015. Molecular pathogenesis of retinal and choroidal vascular diseases.

Cechmanek, P.B., McFarlane, S., 2017. Retinal pigment epithelium expansion around the neural retina occurs in two separate phases with distinct mechanisms. Dev. Dyn. 246, 598–609. https://doi.org/10.1002/dvdy.24525

Chauvet, S., Burk, K., Mann, F., 2013. Navigation rules for vessels and neurons: cooperative signaling between VEGF and neural guidance cues. Cell. Mol. Life Sci. 70, 1685–1703. https://doi.org/10.1007/s00018-013-1278-4

Cheung, N., Wong, I.Y., Wong, T.Y., 2014. Ocular anti-VEGF therapy for diabetic retinopathy: Overview of clinical efficacy and evolving applications. Diabetes Care. https://doi.org/10.2337/dc13-1990

Coultas, L., Chawengsaksophak, K., Rossant, J., 2005. Endothelial cells and VEGF in vascular development.

Country, M.W., 2017. Retinal metabolism: A comparative look at energetics in the retina.

Cui, C., Lu, H., 2018. Clinical observations on the use of new anti-VEGF drug, conbercept, in age-related macular degeneration therapy: A meta-analysis. Clinical Interventions in Aging. https://doi.org/10.2147/CIA.S151225

Ersoz, M.G., Karacorlu, M., Arf, S., Sayman Muslubas, I., Hocaoglu, M., 2017. Retinal pigment epithelium tears: Classification, pathogenesis, predictors, and management.

Fruttiger, M., 2007. Development of the retinal vasculature. Angiogenesis. https://doi.org/10.1007/s10456-007-9065-1

Hartsock, A., Lee, C., Arnold, V., Gross, J.M., 2014. In vivo analysis of hyaloid vasculature morphogenesis in zebrafish: A role for the lens in maturation and maintenance of the hyaloid. Dev. Biol. 394, 327–339. https://doi.org/10.1016/j.ydbio.2014.07.024

Hwang, W.Y., Fu, Y., Reyon, D., Maeder, M.L., Tsai, S.Q., Sander, J.D., Peterson, R.T., Yeh, J.-R.J., Joung, J.K., 2013. Efficient genome editing in zebrafish using a CRISPR-Cas system. Nat. Biotechnol. 31, 227–229. https://doi.org/10.1038/nbt.2501

Isogai, S., Horiguchi, M., Weinstein, B.M., 2001. The vascular anatomy of the developing zebrafish: an atlas of embryonic and early larval development. Dev. Biol. 230, 278–301. https://doi.org/10.1006/dbio.2000.9995

Kessler, O., Shraga-Heled, N., Lange, T., Gutmann-Raviv, N., Sabo, E., Baruch, L., Machluf, M., Neufeld, G., 2004. Semaphorin-3F is an inhibitor of tumor angiogenesis. Cancer Res. 64, 1008–1015.

Krock, B.L., Perkins, B.D., 2014. The Par-PrkC polarity complex is required for cilia growth in zebrafish photoreceptors. PLoS ONE 9, e104661. https://doi.org/10.1371/journal.pone.0104661

Lim, L.S., Mitchell, P., Seddon, J.M., Holz, F.G., Wong, T.Y., 2012. Age-related macular degeneration. Lancet 379, 1728–1738. https://doi.org/10.1016/S0140-6736(12)60282-7

Mahabeleshwar, G.H., Feng, W., Reddy, K., Plow, E.F., Byzova, T.V., 2007. Mechanisms of integrin-vascular endothelial growth factor receptor cross-activation in angiogenesis. Circulation Research. https://doi.org/10.1161/CIRCRESAHA.107.155655

Omri, S., Omri, B., Savoldelli, M., Jonet, L., Thillaye-Goldenberg, B., Thuret, G., Gain, P., Jeanny, J.C., Crisanti, P., Behar-Cohen, F., 2010. The outer limiting membrane (OLM) revisited: clinical implications. Clin Ophthalmol 4, 183–195. https://doi.org/10.2147/opth.s5901

Proulx, K., Lu, A., Sumanas, S., 2010. Cranial vasculature in zebrafish forms by angioblast cluster-derived angiogenesis. Developmental Biology. https://doi.org/10.1016/j.ydbio.2010.08.036

Provis, J.M., 2001. Development of the primate retinal vasculature.

Regano, D., Visintin, A., Clapero, F., Bussolino, F., Valdembri, D., Maione, F., Serini, G., Giraudo, E., 2017. Sema3F (Semaphorin 3F) Selectively Drives an Extraembryonic Proangiogenic Program. Arteriosclerosis, Thrombosis, and Vascular Biology. https://doi.org/10.1161/ATVBAHA.117.308226

Sahay, A., Molliver, M.E., Ginty, D.D., Kolodkin, A.L., 2003. Semaphorin 3F is critical for development of limbic system circuitry and is required in neurons for selective CNS axon guidance events. Journal of Neuroscience. https://doi.org/10.1523/jneurosci.23-17-06671.2003

Saint-Geniez, M., D'Amore, P.A., 2004. Development and pathology of the hyaloid, choroidal and retinal vasculature.

Sakurai, A., Doci, C., Gutkind, J.S., 2012. Semaphorin signaling in angiogenesis, lymphangiogenesis and cancer.

Scott, A., Powner, M.B., Gandhi, P., Clarkin, C., Gutmann, D.H., Johnson, R.S., Ferrara, N., Fruttiger, M., 2010. Astrocyte-derived vascular endothelial growth factor stabilizes vessels in the developing retinal vasculature. PLoS ONE. https://doi.org/10.1371/journal.pone.0011863

Serini, G., Tamagnone, L., 2015. Bad vessels beware! Semaphorins will sort you out! EMBO Molecular Medicine. https://doi.org/10.15252/emmm.201505551

Soldi, R., Mitola, S., Strasly, M., Defilippi, P., Tarone, G., Bussolino, F., 1999. Role of α(v)β3 integrin in the activation of vascular endothelial growth factor receptor-2. EMBO Journal. https://doi.org/10.1093/emboj/18.4.882

Spilsbury, K., Garrett, K.L., Shen, W.Y., Constable, I.J., Rakoczy, P.E., 2000. Overexpression of vascular endothelial growth factor (VEGF) in the retinal pigment epithelium leads to the development of choroidal neovascularization. American Journal of Pathology. https://doi.org/10.1016/S0002-9440(10)64525-7

Sun, Y., Liegl, R., Gong, Y., Bühler, A., Cakir, B., Meng, S.S., Burnim, S.B., Liu, C.H., Reuer, T., Zhang, P., Walz, J.M., Ludwig, F., Lange, C., Agostini, H., Böhringer, D., Schlunck, G., Smith, L.E.H., Stahl, A., 2017. Sema3f Protects Against Subretinal Neovascularization In Vivo. EBioMedicine. https://doi.org/10.1016/j.ebiom.2017.03.026

Tamagnone, L., Artigiani, S., Chen, H., He, Z., Ming, G.L., Song, H.J., Chedotal, A., Winberg, M.L., Goodman, C.S., Poo, M.M., Tessier-Lavigne, M., Comoglio, P.M., 1999. Plexins are a large family of receptors for transmembrane, secreted, and GPI-anchored semaphorins in vertebrates. Cell. https://doi.org/10.1016/S0092-8674(00)80063-X

Thomas, K.A., 1996. Vascular endothelial growth factor, a potent and selective angiogenic agent.

Törnquist, P., Alm, A., Bill, A., 1990. Permeability of ocular vessels and transport across the blood-retinal-barrier. Eye (Lond) 4 (Pt 2), 303–309. https://doi.org/10.1038/eye.1990.41

van Rooijen, E., Voest, E.E., Logister, I., Bussmann, J., Korving, J., van Eeden, F.J., Giles, R.H., Schulte-Merker, S., 2010. von Hippel-Lindau tumor suppressor mutants faithfully model pathological hypoxia-driven angiogenesis and vascular retinopathies in zebrafish. Dis Model Mech 3, 343–353. https://doi.org/10.1242/dmm.004036

Werdich, X.Q., Penn, J.S., 2005. Src, Fyn and Yes play differential roles in VEGF-mediated endothelial cell events. Angiogenesis. https://doi.org/10.1007/s10456-005-9021-x

West, X.Z., Meller, N., Malinin, N.L., Deshmukh, L., Meller, J., Mahabeleshwar, G.H., Weber, M.E., Kerr, B.A., Vinogradova, O., Byzova, T.V., 2012. Integrin β 3 crosstalk with VEGFR accommodating tyrosine phosphorylation as a regulatory switch. PLoS ONE 7, e31071. https://doi.org/10.1371/journal.pone.0031071

Zou, J., Lathrop, K.L., Sun, M., Wei, X., 2008. Intact retinal pigment epithelium maintained by Nok is essential for retinal epithelial polarity and cellular patterning in zebrafish. J. Neurosci. 28, 13684–13695. https://doi.org/10.1523/JNEUROSCI.4333-08.2008